DEVELOPMENT AND CHARACTERIZATION OF LOW COST COMPOSITE FROM SUGARCANE BAGASSE WASTE

A THESIS SUBMITTED IN PARTIAL FULFILMENT OF THE REQUIREMENT FOR THE DEGREE OF

Doctor of Philosophy

in

Mechanical Engineering

By

Punyapriya Mishra

Department of Mechanical Engineering
National Institute of Technology
Rourkela -769 008 (India)
May-2011

DEVELOPMENT AND CHARACTERIZATION OF LOW COST COMPOSITE FROM SUGARCANE BAGASSE WASTE

A THESIS SUBMITTED IN PARTIAL FULFILMENT OF THE REQUIREMENT FOR THE DEGREE OF

Doctor of Philosophy

in

Mechanical Engineering

Submitted to

National Institute of Technology, Rourkela

(Deemed University)

By

Punyapriya Mishra

Under the supervision of

Dr. Samir Kumar Acharya

Department of Mechanical Engineering
National Institute of Technology
Rourkela -769 008 (India)
May-2011

Dedicated to

My Father-in-Law

Late Dr. Niranjan Debata

National Institute of Technology
Rourkela-769008 (Orissa), INDIA

CERTIFICATE

This is to certify that the thesis entitled "**Development and Characterization of low cost composite from Sugarcane Bagasse waste"** submitted to the National Institute of Technology, Rourkela (Deemed University) by Punyapriya Mishra, Roll No. 507-ME-011 for the award of the Degree of Doctor of Philosophy in Mechanical Engineering is a record of bonafide research work carried out by her under my supervision and guidance. The results presented in this thesis has not been, to the best of my knowledge, submitted to any other University or Institute for the award of any degree or diploma.

The thesis, in my opinion, has reached the standards fulfilling the requirement for the award of the degree of **Doctor of Philosophy** in accordance with regulations of the Institute.

Date: - 20th -May-2011

(Dr. S. K. Acharya)
Associate Professor
Mechanical Engineering Department

ACKNOWLEDGEMENT

It is with a feeling of great pleasure that I would like to express my most sincere heartfelt gratitude to Dr.S.K.Acharya, Associate Professor, Department of Mechanical Engineering, NIT, Rourkela for suggesting the topic for my thesis report and for his ready and able guidance throughout the course of my preparing the report. I am greatly indebted to him for his constructive suggestions and criticism from time to time during the course of progress of my work.

I express my sincere thanks to Prof. R.K.Sahoo, Head of the Department of Mechanical Engineering, NIT, Rourkela for providing me the necessary facilities in the department.

I also express my thanks to Dr. S. C. Mishra of Metallurgical and Materials Engineering Department for helping in the micro structural study in his department.

I thankful to Sri Rajesh Pattnayak for his co-operation in experimental work. I am also thankful to all the staff members of the Department of Mechanical Engineering and to all my well wishers for their inspiration and help.

This work is also the outcome of the blessing guidance and support of my father Mr. D.N.Mishra, my mother Dr. R.L.Dubey & my mother-in-law Mrs. Giribala Debata. This work could have been a distant dream if I did not get the moral encouragement and help from my husband, Ar. N.R.Debata. He equally shared my success and failures with me. My son Debaditya sacrificed many of his pleasant dreams for me. This thesis is the outcome of the sincere prayers and dedicated support of my family.

Finally, I wish to acknowledge the support given to me by Dr. D.K.Tripathy, Vice-Chancellor, VSSUT, Burla and all the staff members of the Department of Mechanical Engineering, VSSUT, Burla.

Date: - 20th-May-2011 **(Punyapriya Mishra)**

ABSTRACT

Environmental awareness today motivates the researchers, worldwide on the studies of natural fiber reinforced polymer composite and cost effective option to synthetic fiber reinforced composites. The availability of natural fibers and ease of manufacturing have tempted researchers to try locally available inexpensive fibers and to study their feasibility of reinforcement purposes and to what extent they satisfy the required specifications of good reinforced polymer composite for different applications. With low cost and high specific mechanical properties, natural fiber represents a good renewable and biodegradable alternative to the most common synthetic reinforcement, i.e. glass fiber. Despite the interest and environmental appeal of natural fibers, there use is limited to non-bearing applications, due to their lower strength compared with synthetic fiber reinforced polymer composite. The stiffness and strength shortcomings of biocomposites can be overcome by structural configurations and better arrangement in a sense of placing the fibers in specific locations for highest strength performance. Accordingly extensive studies on preparation and properties of polymer matrix composite (PMC) replacing the synthetic fiber with natural fiber like Jute, Sisal, Pineapple, Bamboo and Kenaf were carried out. These plant fibers have many advantages over glass fiber or carbon fiber like renewable, environmental friendly, low cost, lightweight and high specific mechanical performance.

Large varieties of sugar cane grow abundantly in many parts of India. Bagasse is considered to be a by-product of the milling process after production of sugar. Bagasse (fibrous residue) is essentially a waste product that causes mills to incur additional disposal costs. Bagasse is mainly used as a burning raw material in the sugar cane mill furnaces. The low caloric power of bagasse makes this a low efficiency process. Also, the sugar cane mill management encounters problems regarding regulations of “clean air” from the Environmental Protection Agency, due to the quality of the smoke released in the atmosphere. Presently 85% of bagasse production is burnt. Even so, there is an excess of bagasse. Usually this excess is deposited on empty fields altering the landscape.

With increasing emphasis on fuel efficiency, it is expected that bagasse based composites may enjoy wider applications in automobiles and railway coaches & buses for public transport system. There also exist an excellent opportunity in fabricating bagasse

based composites towards a wide array of applications in building and construction industry. Value added novel applications of bagasse based composites would not go in a long way in improving the quality of life of people engaged in bagasse cultivation, but would also ensure international market for cheaper substitution. Against this back ground the present research work has been undertaken with an objective to explore the use of natural fiber Bagasse as a reinforcement material in epoxy base.

The work presented in this dissertation involves investigation of two distinct problems of natural fiber composites:

i. A study of favourable mechanical properties of Bagasse fiber in thermosetting matrix composite.

ii. An experimental investigation of tribological potential of Bagasse fiber reinforced composite.

To study the mechanical properties of the composite, different volume fractions of fiber have been taken. These fibers were randomly distributed in the matrix. Usual hand-lay-up technique has been adopted for manufacturing the composite. To find out the critical fiber length Single fiber Pull-out test has been carried out. To have a good compatibility between the fiber and matrix, chemical modification of fibers such as Acetone and Alkali treatments has been carried out. It was found that alkali treated fiber composite exhibits favourable strength and stiffness in comparison to acetone treatments. Moisture absorption behaviour of both treated and untreated fiber composite was also carried out.

For studying the tribo-potential of Bagasse fiber, different wear tests like abrasive wear test (multi-pass condition) on Pin-on-Disc wear testing machine, two body abrasion wear test (Single pass condition) by Two-body abrasion wear tester and Solid particle erosion behaviour by Air jet erosion test rig, have been carried out. All these tests have been carried out as per ASTM standard. The abrasive wear test results shows that the wear rate of pure epoxy reduces significantly with the addition of Bagasse fiber up to 20 vol%. The wear anisotropy of the composite studied with Two-body abrasion tester shows wear characteristics follow the following the trends: $W_{NO} < W_{APO} < W_{PO}$. The solid particle erosion test clearly indicates that the composite behaviour is brittle in nature.

Two different mathematical models have been developed to predict the abrasive wear and erosive wear of Bagasse fiber reinforced epoxy composite separately under various testing conditions by using Response Surface Methodology (RSM). The full factorial design experimentation has been intended to model the abrasive and erosive wear response. These two different second order regression equations for abrasive wear rate (Δw) and erosion rate (E_R) have been evaluated after implementation of Analysis of variance (ANOVA) at 95% confidence level. To have an assessment of pure error and model fitting error, some of the experimental trials are replicated in both the cases and the adequacy of the models is also investigated by the examination of residuals. The mathematical models which are developed to predict the abrasive and erosive wear characteristics has been found to be statistically valid and sound within the range of the factors.

There are other fabrication techniques available like injection moulding, compression moulding and extrusion, where the volume fraction of reinforcement can be increased. In addition there are other chemical methods by which the fiber surface modification can be done. This work can be further extended to those techniques. However the results reported here can act as a starting point for both industrial designer and researchers to design and develop polymer matrix composite components using Bagasse fiber as reinforcement.

The whole dissertation has been divided in to eight chapters to put the analysis independent of each other as far as practicable. Major works on moisture absorption characteristics, dry sliding wear behaviour, anisotropic wear behaviour, erosive wear characteristics and validation of results through RSM technique are given in chapter 3, 4, 5, 6 and 7 respectively.

TABLE OF CONTENTS

Chapter-8 Conclusions and Future Work

Miscellaneous

LIST OF TABLES

LIST OF FIGURES

LIST OF SYMBOLS

ANOVA	Analysis of variance
APO	Anti-parallel orientation
E_r	Erosion rate
FFD	Full factorial design
FTIR	Fourier Transform Infrared
GS	Abrasive grit size
L	Applied Normal Load
BF	Bagasse Fiber
n	Anisotropy coefficient
NO	Normal orientation
P_{break}	Maximum load at failure
PO	Parallel orientation
R^2	Coefficient of determination
R^2_{adj}	Adjusted coefficient of determination
R_e	Volume fraction of reinforcement
RSM	Response Surface Methodology
S_d	Sliding Distance
SEM	Scanning electron microscope
t	Time
Vv	Voids content
W	Wear rate
Δw	Wear loss/ Weight loss
$\hat{w}$	Cumulative weight loss

α	Impingement / Impact angle
η	Erosion efficiency
μ	Coefficient of friction
ρ	Density

Chapter 1

INTRODUCTION

Chapter-1

1.1 BACKGROUND

In the continuing quest for improved performance, which may be specified by various criteria including less weight, more strength and lower cost, currently used materials frequently reach the limit of their usefulness. Thus material scientists, engineers and scientists are always striving to produce either improved traditional materials or completely new materials. Composites are an example of the latter category. Within last fourty to fifty years, there has been a rapid increase in the production of synthetic composites, those incorporating fine fibers in various plastics (polymers) dominating the market. With the increasing global energy crisis and ecological risks, scientists all over the world are shifting their attention towards alternative solution to synthetic fiber. Since 1990s, natural fiber composites are emerging as realistic alternative to glass-reinforced composites in many applications. Natural fiber composites are claimed to offer environmental advantages such as reduced dependence on non-renewable energy/material sources, lower pollutant emissions, lower green house gas emissions, enhanced energy recovery and end of life biodegradability of components. Such superior environmental performances are important driver of increased future use of natural fiber composite.

India endowed with an abundant availability of natural fiber such as Jute, Coir, Sisal, Pineapple, Ramie, Bamboo, Banana etc. has focused on the development of natural fiber composites primarily to explore value-added application avenues. Such natural fiber composites are well suited as wood substitutes in the housing and construction sector. The development of natural fiber composites in India is based on two pronged strategy of preventing depletion of forest resources as well as ensuring good economic returns for the cultivation of natural fibers.

The developments in composite material after meeting the challenges of aerospace sector have cascaded down for catering to domestic and industrial applications. Composites, the wonder material with light-weight; high strength-to-weight ratio and stiffness properties

have come a long way in replacing the conventional materials like metals, wood etc. The material scientists all over the world focused their attention on natural composites reinforced with Jute, Sisal, Coir, Pineapple etc. primarily to cut down the cost of raw materials.

1.2 WHY A COMPOSITE?

Over the last thirty years composite materials, plastics and ceramics have been the dominant emerging materials. The volume and number of applications of composite materials have grown steadily, penetrating and conquering new markets relentlessly. Modern composite materials constitute a significant proportion of the engineered materials market ranging from everyday products to sophisticated niche applications.

While composites have already proven their worth as weight-saving materials, the current challenge is to make them cost effective. The efforts to produce economically attractive composite components have resulted in several innovative manufacturing techniques currently being used in the composites industry. It is obvious, especially for composites, that the improvement in manufacturing technology alone is not enough to overcome the cost hurdle. It is essential that there be an integrated effort in design, material, process, tooling, quality assurance, manufacturing, and even program management for composites to become competitive with metals.

The composites industry has begun to recognize that the commercial applications of composites promise to offer much larger business opportunities than the aerospace sector due to the sheer size of transportation industry. Thus the shift of composite applications from aircraft to other commercial uses has become prominent in recent years.

Increasingly enabled by the introduction of newer polymer resin matrix materials and high performance reinforcement fibres of glass, carbon and aramid, the penetration of these advanced materials has witnessed a steady expansion in uses and volume. The increased volume has resulted in an expected reduction in costs. High performance FRP can now be found in such diverse applications as composite armoring designed to resist explosive impacts, fuel cylinders for natural gas vehicles, windmill blades, industrial drive

shafts, support beams of highway bridges and even paper making rollers. For certain applications, the use of composites rather than metals has in fact resulted in savings of both cost and weight. Some examples are cascades for engines, curved fairing and fillets, replacements for welded metallic parts, cylinders, tubes, ducts, blade containment bands etc.

Further, the need of composite for lighter construction materials and more seismic resistant structures has placed high emphasis on the use of new and advanced materials that not only decreases dead weight but also absorbs the shock & vibration through tailored microstructures. Composites are now extensively being used for rehabilitation/ strengthening of pre-existing structures that have to be retrofitted to make them seismic resistant, or to repair damage caused by seismic activity.

Unlike conventional materials (e.g., steel), the properties of the composite material can be designed considering the structural aspects. The design of a structural component using composites involves both material and structural design. Composite properties (e.g. stiffness, thermal expansion etc.) can be varied continuously over a broad range of values under the control of the designer. Careful selection of reinforcement type enables finished product characteristics to be tailored to almost any specific engineering requirement.

Whilst the use of composites will be a clear choice in many instances, material selection in others will depend on factors such as working lifetime requirements, number of items to be produced (run length), complexity of product shape, possible savings in assembly costs and on the experience & skills the designer in tapping the optimum potential of composites. In some instances, best results may be achieved through the use of composites in conjunction with traditional materials.

1.3 DEFINITION OF COMPOSITE

The most widely used meaning is the following one, which has been stated by Jartiz [1] “Composites are multifunctional material systems that provide characteristics not obtainable from any discrete material. They are cohesive structures made by physically

combining two or more compatible materials, different in composition and characteristics and sometimes in form".

The weakness of this definition resided in the fact that it allows one to classify among the composites any mixture of materials without indicating either its specificity or the laws which should given it which distinguishes it from other very banal, meaningless mixtures.

Kelly [2] very clearly stresses that the composites should not be regarded simple as a combination of two materials. In the broader significance; the combination has its own distinctive properties. In terms of strength to resistance to heat or some other desirable quality, it is better than either of the components alone or radically different from either of them.

Beghezan [3] defines "The composites are compound materials which differ from alloys by the fact that the individual components retain their characteristics but are so incorporated into the composite as to take advantage only of their attributes and not of their short comings", in order to obtain improved materials.

Van Suchetclan [4] explains composite materials as heterogeneous materials consisting of two or more solid phases, which are in intimate contact with each other on a microscopic scale. They can be also considered as homogeneous materials on a microscopic scale in the sense that any portion of it will have the same physical property.

1.4 CHARACTERISTICS OF THE COMPOSITES

Composites consist of one or more discontinuous phases embedded in a continuous phase. The discontinuous phase is usually harder and stronger than the continuous phase and is called the 'reinforcement' or 'reinforcing material', whereas the continuous phase is termed as the ' matrix'.

Properties of composites are strongly dependent on the properties of their constituent materials, their distribution and the interaction among them. The composite properties may be the volume fraction sum of the properties of the constituents or the constituents may interact in a synergistic way resulting in improved or better properties. Apart from the nature of the constituent materials, the geometry of the reinforcement (shape, size and size distribution) influences the properties of the composite to a great extent. The concentration distribution and orientation of the reinforcement also affect the properties.

The shape of the discontinuous phase (which may by spherical, cylindrical, or rectangular cross-sanctioned prisms or platelets), the size and size distribution (which controls the texture of the material) and volume fraction determine the interfacial area, which plays an important role in determining the extent of the interaction between the reinforcement and the matrix.

Concentration, usually measured as volume or weight fraction, determines the contribution of a single constituent to the overall properties of the composites. It is not only the single most important parameter influencing the properties of the composites, but also an easily controllable manufacturing variable used to alter its properties.

1.5 CLASSIFICATION

Composite materials can be classified in different ways [5]. Classification based on the geometry of a representative unit of reinforcement is convenient since it is the geometry of the reinforcement which is responsible for the mechanical properties and high performance of the composites. A typical classification is presented in Table1.1. The two broad classes of composites are

(1) Particulate composites

(2) Fibrous composites.

1.5.1 Particulate Composites

As the name itself indicates, the reinforcement is of particle nature (platelets are also included in this class). It may be spherical, cubic, tetragonal, a platelet, or of other regular or irregular shape, but it is approximately equiaxed. In general, particles are not very effective in improving fracture resistance but they enhance the stiffness of the composite to a limited extent. Particle fillers are widely used to improve the properties of matrix materials such as to modify the thermal and electrical conductivities, improve performance at elevated temperatures, reduce friction, increase wear and abrasion resistance, improve machinability, increase surface hardness and reduce shrinkage.

1.5.2 Fibrous composites

A fiber is characterized by its length being much greater compared to its cross-sectional dimensions. The dimensions of the reinforcement determine its capability of contributing its properties to the composite. Fibers are very effective in improving the fracture resistance of the matrix since a reinforcement having a long dimension discourages the growth of incipient cracks normal to the reinforcement that might other wise lead to failure, particularly with brittle matrices.

Man-made filaments or fibers of non polymeric materials exhibit much higher strength along their length since large flaws, which may be present in the bulk material, are minimized because of the small cross-sectional dimensions of the fibre. In the case of polymeric materials, orientation of the molecular structure is responsible for high strength and stiffness.

Fibers, because of their small cross- sectional dimensions, are not directly usable in engineering applications. They are, therefore, embedded in matrix materials to form fibrous composites. The matrix serves to bind the fibers together, transfer loads to the fibers, and protect them against environmental attack and damage due to handling. In discontinuous fibre reinforced composites, the load transfer function of the matrix is more critical than in continuous fibre composites.

Table- 1.1 Classification of composite

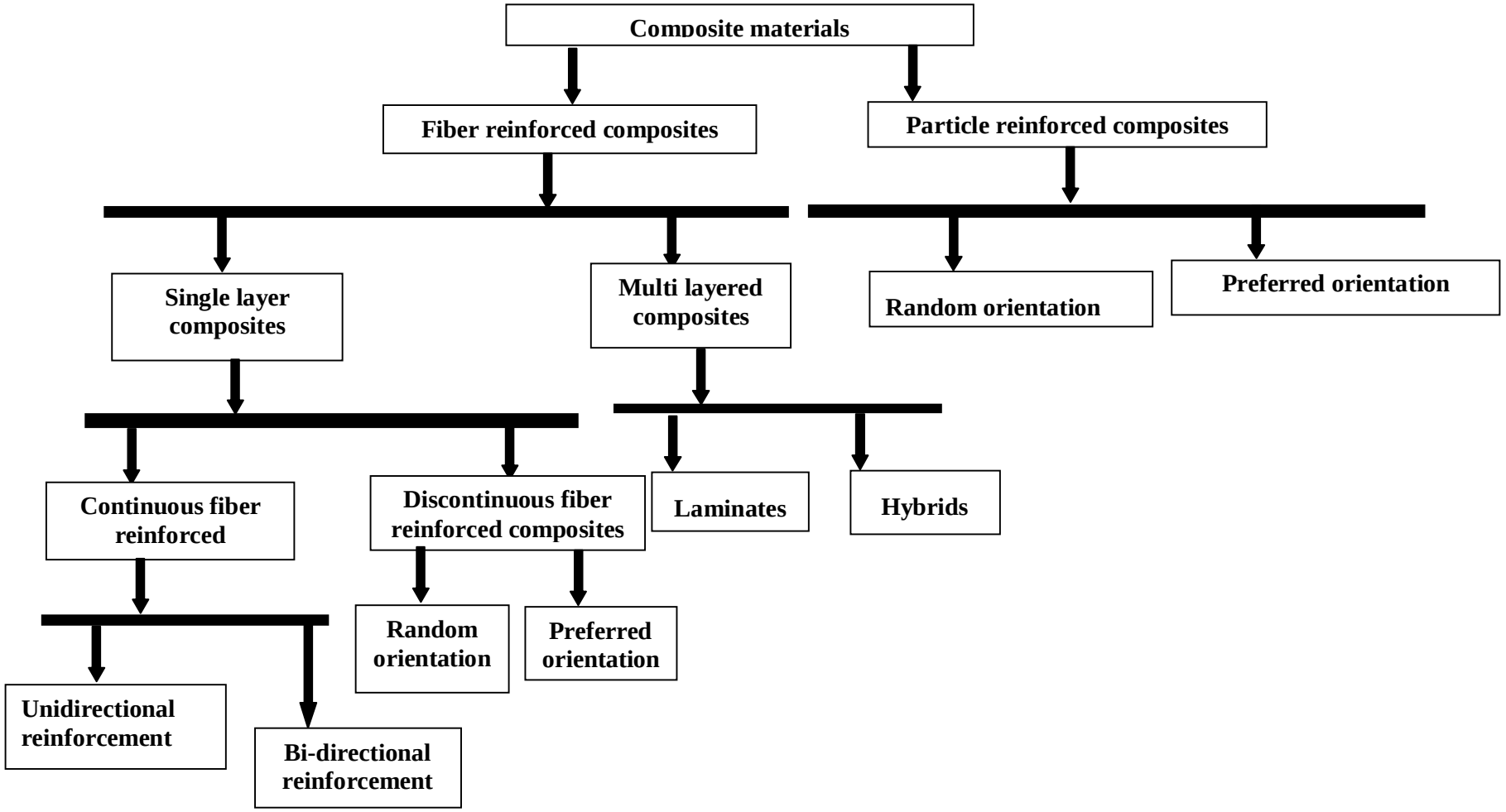

1.6 COMPONENTS OF A COMPOSITE MATERIAL

In its most basic form a composite material is one, which is composed of at least two elements working together to produce material properties that are different to the properties of those elements on their own. In practice, most composites consist of a bulk material (the 'matrix'), and a reinforcement of some kind, added primarily to increase the strength and stiffness of the matrix.

1.6.1 Role of matrix in a composite

Many materials when they are in a fibrous form exhibit very good strength property but to achieve these properties the fibres should be bonded by a suitable matrix. The matrix isolates the fibres from one another in order to prevent abrasion and formation of new surface flaws and acts as a bridge to hold the fibres in place. A good matrix should possess ability to deform easily under applied load, transfer the load onto the fibres and evenly distributive stress concentration.

1.6.2 Materials used as matrices in composites

In its most basic form a composite material is one, which is composed of at least two elements working together to produce material properties that are different to the properties of those elements on their own. In practice, most composites consist of a bulk material (the matrix) and a reinforcement of some kind, added primarily to increase the strength and stiffness of the matrix.

1.6.2.1 BULK PHASES

(1) Metal Matrices

Metal matrix composites possess some attractive properties, when compared with organic matrices. These include (i) strength retention at higher temperatures, (ii) higher transverse strength, (iii) better electrical conductivity, (iv) superior thermal conductivity, (v)

higher erosion resistance etc. However, the major disadvantage of metal matrix composites is their higher densities and consequently lower specific mechanical properties compared to polymer matrix composites. Another notable difficulty is the high-energy requirement for fabrication of such composites.

(2) Polymer Matrices

A very large number of polymeric materials, both thermosetting and thermoplastic, are used as matrix materials for the composites. Some of the major advantages and limitations of resin matrices are shown in Table 1.2.

Table 1.2 Advantages and limitations of polymeric matrix materials

Advantages	Limitations
Low densities	Low transverse strength
Good corrosion resistance	Low operational temperature limits
Low thermal conductivities	
Low electrical conductivities	
Translucence	
Aesthetic Colour effects	

Generally speaking, the resinous binders (polymer matrices) are selected on the basis of adhesive strength, fatigue resistance, heat resistance, chemical and moisture resistance etc. The resin must have mechanical strength commensurate with that of the reinforcement. It must be easy to use in the fabrication process selected and also stand up to the service conditions. Apart from these properties, the resin matrix must be capable of wetting and penetrating into the bundles of fibres which provide the reinforcement, replacing the dead air spaces therein and offering those physical characteristics capable of enhancing the performance of fibres.

(3) Ceramic Matrices

Ceramic fibres, such as alumina and SiC (Silicon Carbide) are advantageous in very high temperature applications, and also where environment attack is an issue. Since ceramics have poor properties in tension and shear, most applications as reinforcement are in the particulate form (e.g. zinc and calcium phosphate). Ceramic Matrix Composites (CMCs) used in very high temperature environments, these materials use a ceramic as the matrix and reinforce it with short fibres, or whiskers such as those made from silicon carbide and boron nitride.

1.6.2.2 REINFORCEMENT

The role of the reinforcement in a composite material is fundamentally one of increasing mechanical properties of the neat resin system. All of the different fibres used in composites have different properties and so affect the properties of the composite in different ways. For most of the applications, the fibres need to be arranged into some form of sheet, known as a fabric, to make handling possible. Different ways for assembling fibres into sheets and the variety of fibre orientations possible to achieve different characteristics.

1.6.2.3 INTERFACE

It has characteristics that are not depicted by any of the component in isolation. The interface is a bounding surface or zone where a discontinuity occurs, whether physical, mechanical, chemical etc. The matrix material must “wet” the fibre. Coupling agents are frequently used to improve wettability. Well “wetted” fibres increase the interface surfaces area. To obtain desirable properties in a composite, the applied load should be effectively transferred from the matrix to the fibres via the interface. This means that the interface must be large and exhibit strong adhesion between fibres and matrix. Failure at the interface (called debonding) may or may not be desirable.

1.7 TYPES OF COMPOSITE MATERIALS:

The composite materials are broadly classified into the following categories as shown in figure 1.1 (a-e);

1.7.1 Fiber-Reinforced Composites:

Reinforced-composites are popularly being used in many industrial applications because of their inherent high specific strength and stiffness. Due to their excellent structural performance, the composites are gaining potential also in tribological applications. In this type composite the second phase is in the form of fibers dispersed in the matrix which could be either plastic or metal. The volume fraction (*Vf*) varies from a few percentage to as high as 70%. Usually the fiber reinforcement is done to obtain high strength and high modulus. Hence it is necessary for the fibers to posses higher modulus than the matrix material, so that the load is transferred to the fiber from the matrix more effectively.

1.7.2 Dispersion Hardened Material:

In this type of material, fine particles of sizes ranging from 0.01μm to 0.14μm are dispersed in matrix. Their concentration varies from 1% to 15% by volume. These fine particles impede dislocation movement in the material and therefore result in very high strength. Also these materials posses improved high temperature strength and creep resistance.

1.7.3 Particulate composite:

In this type of composites, 1μm to 200μm size particles are dispersed in the matrix and volume fraction is generally between 0.01 *Vf* to 0.85 *Vf*.

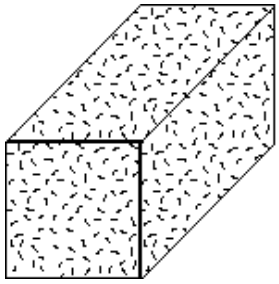

(a) Random fiber (short fiber) reinforced composites

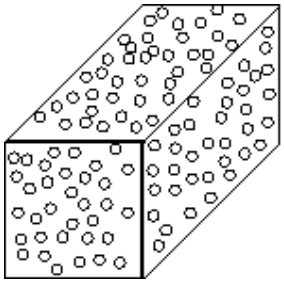

(b) Particles as the reinforcement (Particulate composites)

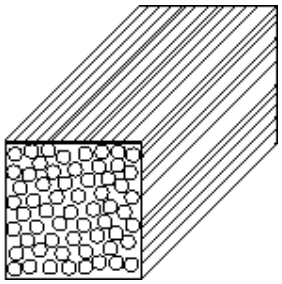

(c) Continuous fiber (long fiber) reinforced Composites

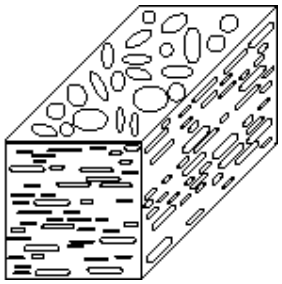

(d) Flat flakes as the reinforcement (Flake composites)

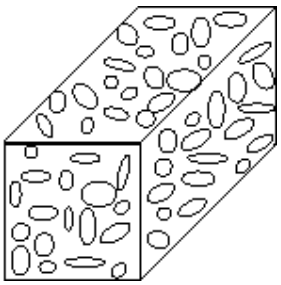

(e) Fillers as the reinforcement (Filler composites)

Figure-1.1 Classification of composite materials

1.8 NATURAL FIBER COMPOSITES: Initiative in Product Development

Now-a-days, research and engineering interest have been shifting from traditional synthetic fiber composite to lignocellulosic natural fiber composite due to their advantages like high strength to weight ratio, non-carcinogenic and bio-degradability [6-9]. Besides the availability of natural fibers and easy of manufacturing have tempted researchers to try locally available inexpensive fiber and to study their feasibility of reinforcement purpose and to what extent they satisfy the required specifications of good reinforced polymer composite for different applications. With low cost and high specific mechanical properties, natural fiber represents a good renewable and biodegradable alternative to the most common synthetic reinforcement, i.e. glass fiber.

The term “natural fiber” covers a broad range of vegetable, animal and mineral fibers. However in the composite industry, it is usually refers to wood fiber and agro based bast, leaf, seed, and stem fibers. These fibers often contribute greatly to the structural performance of plant and, when used in plastic composites, can provide significant reinforcement.

Despite the interest and environmental appeal of natural fibers, their use is limited to non-bearing applications due to their lower strength compared with synthetic fiber reinforced polymer composite. The stiffness and strength shortcomings of bio composites can be overcome by structural configurations and better arrangement in a sense of placing the fibers in specific locations for highest strength performance. Accordingly extensive studies on preparation and properties of polymer matrix composite (PMC) replacing the synthetic fiber with natural fiber like Jute, Sisal, Pineapple, Bamboo and Kenaf were carried out [10-14]. These plant fibers have many advantages over glass fiber or carbon fiber like renewable, environmental friendly, low cost, lightweight, high specific mechanical performance.

Increased technical innovation, identification of new applications, continuing political and environmental pressure and government investments in new methods for fiber harvesting and processing are leading to projections of continued growth in the use of natural fibers in composites, with expectation of reaching 100,000 tons per annum by 2010 [15]. The easy availability of natural fibers and manufacturing have motivated researchers worldwide recently to try locally available inexpensive fibers and to study their feasibility of reinforcement purposes and to what extent they satisfy the required specifications of good reinforced polymer composite for tribological applications [16].

There are many natural resources which India has in abundance. Most of it comes from the forest and agriculture. However in most cases residues from traditional crops such as rice husk or sugarcane bagasse or from the usual processing operations of timber industries do not meet the requisites of being long fibers. This biomass left over are abundant, and their use as a particulate reinforcement in resin matrix composite is strongly considered as a future possibility.

Large varieties of sugar cane grow abundantly in many parts of India and mostly used for production of sugar in sugar industries. Cane is crushed in a series of mills (Figure 1.2), each consisting of at least three heavy rollers. Due to the crushing, the cane stalk will break in small pieces, and subsequent milling will squeeze the juice out. The juice is collected and processed for production of sugar. The resulting crushed and squeezed cane stalk, named bagasse, is considered to be a by-product of the milling process [17]. Bagasse is essentially a waste product that causes mills to incur additional disposal costs.

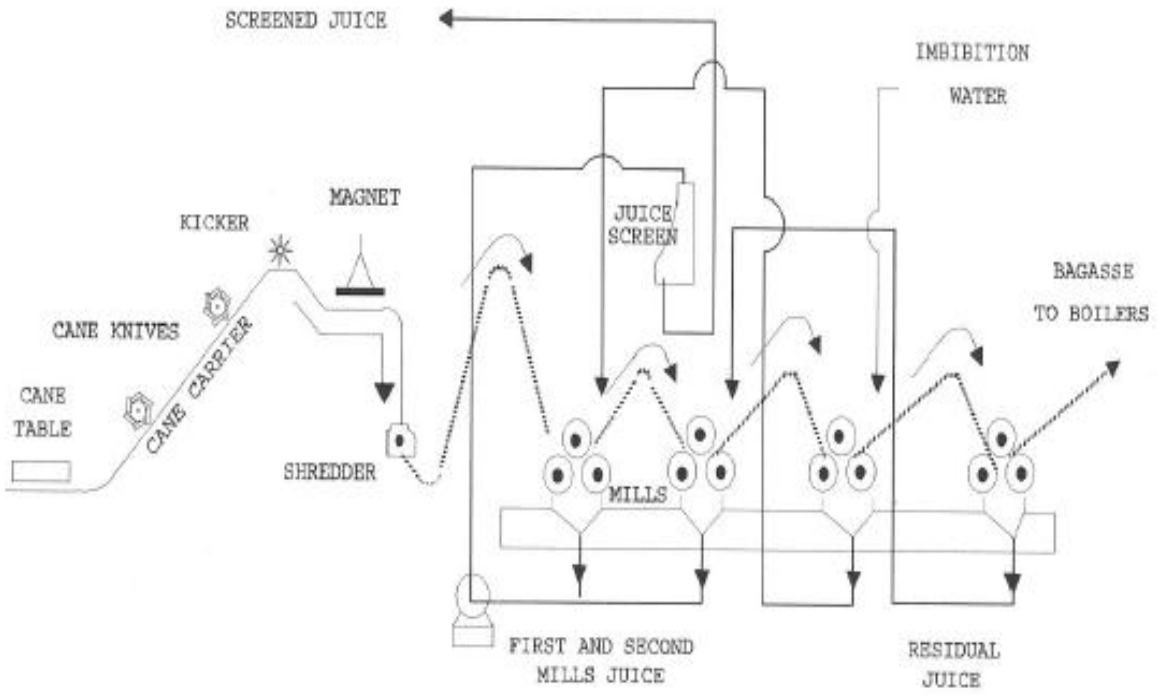

Figure-1.2 Current technological process for extraction of sugar juice from cane in a sugar cane mill

Figure-1.3 Bagasses

This is also considered as a fibrous residue (Figure 1.3) that remains after extraction of juice from the sugar cane stalks. It consists of water, fibers, and small amounts of soluble solids. Percent contribution of each of these components varies according to the variety, maturity, method of harvesting, and the efficiency of the crushing plant. Table 1.3 shows a typical bagasse composition.

Table 1.3 Average Bagasse Composition [17]

ITEM	%
Cellulose	46
Hemicelluloses	24.5
Lignin	19.95
Fats and waxes	3.5
Ash	2.4
Silica	2
Other elements	1.7

Bagasse is mainly used as a burning raw material in the sugar cane mill furnaces. The low caloric power of bagasse makes this a low efficiency process. Also, the sugar cane mill management encounters problems regarding regulations of “clean air” from the environmental protection agency, due to the quality of the smoke released in the atmosphere. Presently 85% of bagasse production is burnt. Even so, there is an excess of bagasse. Usually this excess is deposited on empty fields altering the landscape. Approximately 9% of bagasse is used in alcohol (ethanol) production. Ethanol is not just a good replacement for the fossil fuels, but it is also an environmentally friendly fuel. Apart from this, ethanol is a very versatile chemical raw material from which a variety of chemicals can be produced [18]. But again, due to the low level of sucrose left in bagasse, the efficiency of the ethanol production is quite low.

With increasing emphasis on fuel efficiency, natural fibers such as bagasse based composites enjoy wider applications in automobiles and railway coaches & buses for public transport system. There exist an excellent opportunity in fabricating bagasse based composites towards a wide array of applications in building and construction such as boards and blocks, reconstituted wood, flooring tiles etc. Value added novel applications of natural

fibers and bagasse based composites would not only go in a long way in improving the quality of life of people engaged in bagasse cultivation, but would also ensure international market for cheaper substitution.

Out of the available manufacturing processes, we have adopted hand-lay-up technique to prepare the composite. Different volume fraction by weight of bagasse fiber has been mixed with matrix material and specimens were prepared for structural and tribological studies. In the process fiber properties like strength and density, critical fiber length and optimum volume fraction of fiber reinforcement have also been found out. For increasing bonding strength between fiber and matrix, fiber surface modification has also been carried out. Different tribological test have been conducted under simulated laboratory condition for specific application of developed composite. The surface of fracture and worn out samples have been studied using Scanning Electron Microscope (SEM) to have an idea about the fracture behaviour of the composite.

In the second chapter detailed discussion on reinforcement material, overview of fabrication processes and work related to present investigation available in literature are presented.

In the third chapter effect of environment on mechanical properties of both untreated and treated fiber reinforced composite has been presented.

In the fourth chapter abrasive wear behaviour of the composite has been studied.

Fifth chapter discusses the anisotropic wear behaviour of the composite.

In the sixth chapter solid particle erosion wear behaviour of the composite is presented.

Seventh chapter discusses the Response surface methodology (RSM) to predict the abrasive and erosive wear behaviour of the composite.

Eighth chapter discusses the conclusions drawn from the above studies mentioning the scope for future work.

Chapter 2

LITERATURE SURVEY

Chapter-2

2.1 NATURAL FIBERS: Source and Classification

The use of lignocellulosic fibers as reinforcements for polymeric materials has been growing during the last decade or so to replace synthetic fibers, especially glass fibers in composites, for different industrial sectors, such as packaging, automobiles [19, 20] and even in the building sector [21]. This is mainly due to their unique characteristics, such as availability, biodegradability, low density, non-toxic nature, less abrasiveness to plastic processing equipment, useful mechanical properties and low cost (The price of glass fiber is around Rs 300/- per kg and has a density of 2.5 g/cc. On the other hand, natural fiber costs Rs. 15 to 25/- per kg and has a density of 1.2-1.5 g/cc.) [22]. The leading driver for substituting natural fiber for synthetic fiber i.e. glass can be well recognized from the fact that the tensile strength of natural fiber is substantially lower than that of glass fibers though the modulus is of the same order of magnitude. However, when the specific modulus of natural fibers (modulus per unit specific gravity) is considered, the natural fibers show values that are comparable to or even better than glass fibers. Table 2.1 clearly demonstrates this. Natural organic fibers can be derived from either animal or plant sources. The majority of useful natural textile fibers are plant derived, with the exceptions of wool and silk. All plant fibers are composed of cellulose, whereas fibers of animal origin consist of proteins. Natural fibers in general can be classified based on their origin, and the plant-based fibers can be further categorized based on part of the plant they are recovered from. An overview of natural fibers is presented in figure 2.1 [23].

Generally, plant or vegetable fibers are used to reinforce polymer matrices and a classification of vegetable fibers is given in figure 2.2 [24]. Plant fibers are a renewable resource and have the ability to be recycled. The plant fibers leave little residue if they are burned for disposal, returning less carbon dioxide (CO_2) to the atmosphere than is removed during the plant's growth.

Typically, manufacturing industries have focused on direct, per-pound raw-materials costs when selecting plastics reinforcements, but this ignores the big cost picture. In this simplified approach, natural fibers seldom will come out to be the low-cost alternative. But

when considering the benefits derived from one-step processing, the end cost of the finished component becomes highly competitive through a reduction in both capital and the growing cost of internal labor. Use of natural fibers reduces weight by 10 percent and lowers the energy needed for production by 80 percent, at the same time reduces the cost of the component five percent lower than the comparable fiber glass-reinforced component [25]. Material cost savings, due to the use of natural fibers and high fiber filling levels, coupled with the advantage of being non-abrasive to the mixing and molding equipment make natural fibers an exciting prospect. These benefits mean natural fibers could be used in many applications, including building, automotive, household appliances, and other applications.

Table 2.1: Properties of glass and natural fibers [26]

Properties	**Fiber**						
	E-glass	**Hemp**	**Flax**	**Jute**	**Sisal**	**Coir**	**Ramie**
Density (gm/cc)	2.5	1.48	1.4-1.5	1.3- 1.46	1.33-1.5	1.2	1.5
Tensile strength (MPa)	2000-3500	550-900	345-1500	393-800	400-700	175-220	220-938
Young's Modulus (GPa)	70	70	27.6-80	10-30	9-38	4-6	44-128
Elongation (%)	2.5-3	1.6	1.2-3.2	1.5-1.8	2-14	15-30	2-3.8
Moisture absorption (%)	-	8	7	12	11	10	12-17

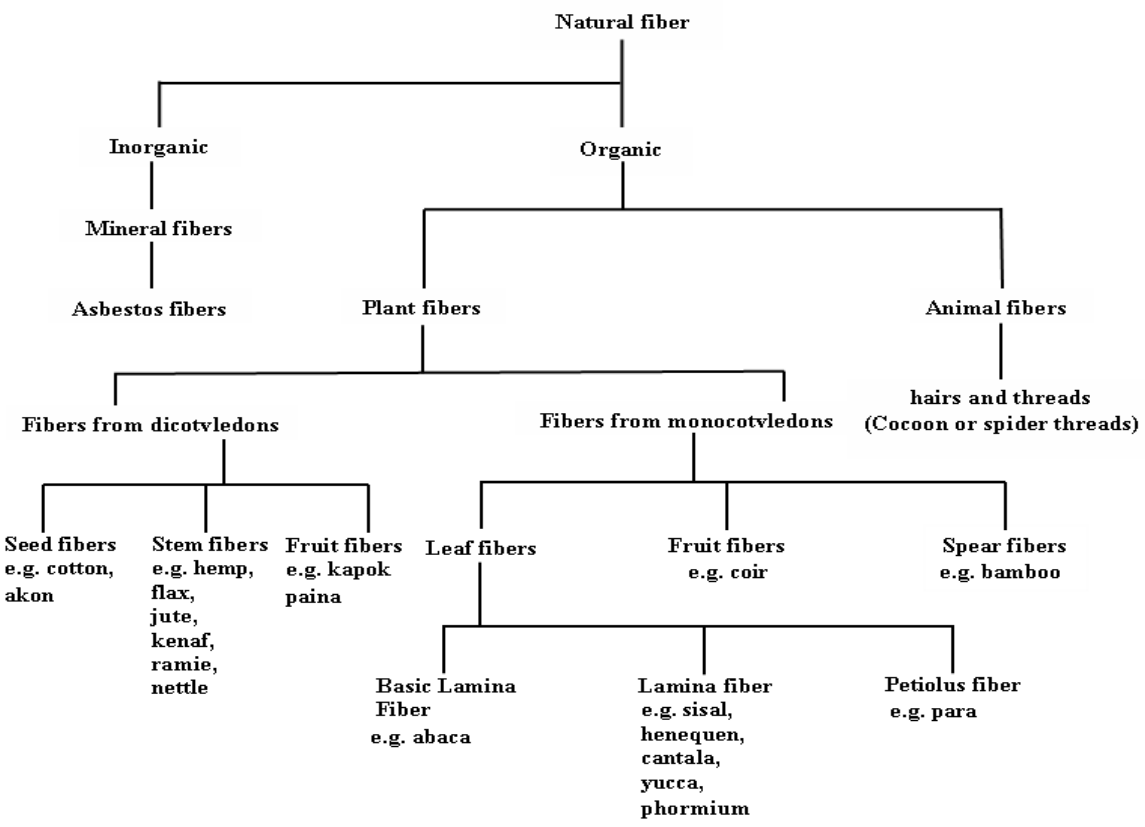

Figure-2.1 Overview of natural fiber

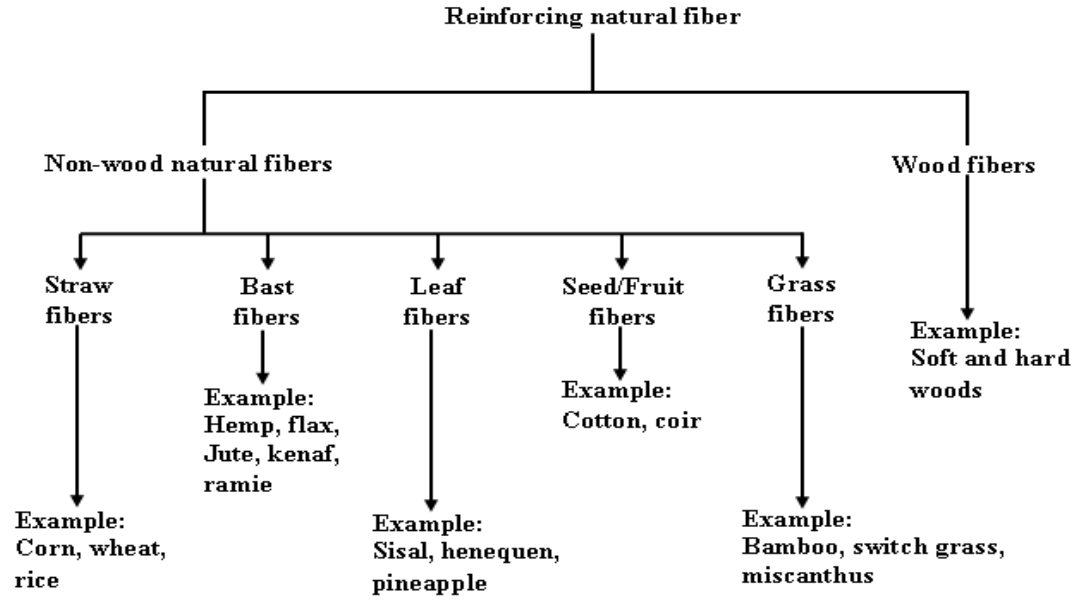

Figure-2.2 Classification of natural fiber that can be used as reinforcements in polymers

2.2 STRUCTURE OF PLANT FIBER

Natural plant fibers are constituents of cellulose fibers, consisting of helically wound cellulose micro fibrils, bound together by an amorphous lignin matrix. Lignin keeps the water in fibers; acts as a protection against biological attack and as a stiffener to give stem its resistance against gravity forces and wind. Hemicellulose found in the natural fibers is believed to be a compatibilizer between cellulose and lignin. The cell wall in a fiber (Figure 2.3) is not a homogenous membrane [27]. Each fiber has a complex, layered structure consisting of a thin primary wall which is the first layer deposited during cell growth encircling a secondary wall. The secondary wall is made up of three layers and the thick middle layer determines the mechanical properties of the fiber. The middle layer consists of a series of helically wound cellular micro-fibrils formed from long chain cellulose molecules. The angle between the fiber axis and the micro-fibrils is called the microfibrillar angle. The characteristic value of microfibrillar angle varies from one fiber to another. These micro-fibrils have typically a diameter of about 10-30 nm and are made up of 30-100 cellulose molecules in extended chain conformation and provide mechanical strength to the fiber.

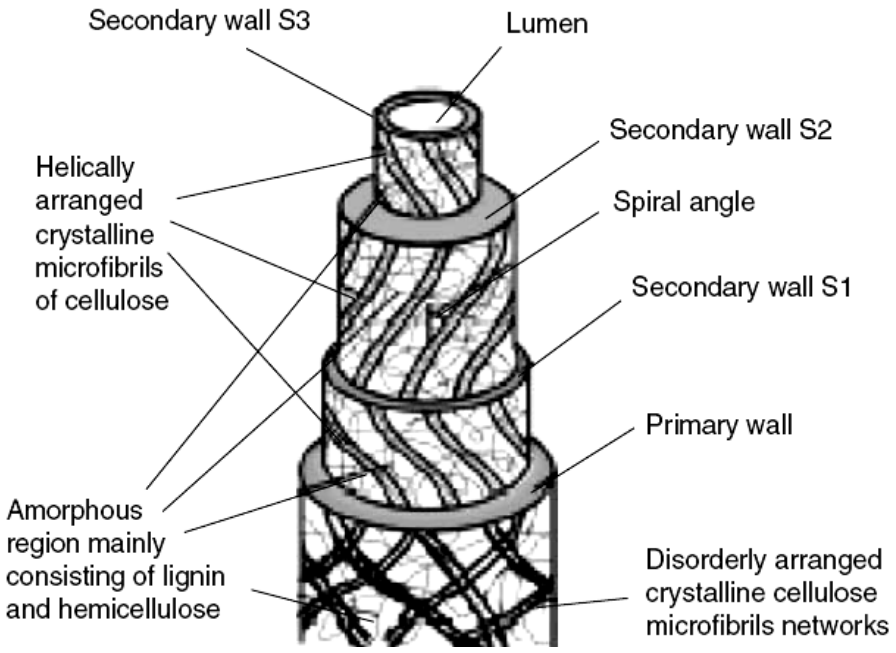

Figure-2.3 Structure of an elementary plant fiber (cell)

2.3 CHEMICAL COMPOSITION OF NATURAL FIBERS

The proportions of chemical components of any natural fiber vary with source of the fiber, area of production, variety, maturation of plant and extraction condition. The major constituents of a fully developed natural fiber are cellulose, hemicellulose, lignin and pectin. These hydroxyl-containing polymers are distributed throughout the fiber wall. [28].

2.3.1 Cellulose

The long thin crystalline micro-fibrils in the secondary cell wall are made of cellulose. It is the reinforcing material and is responsible for the high mechanical strength of fibers. It consists of a linear polymer of D-anhydroglucose units where two adjacent glucose units are linked together by β-1, 4-glycosidic linkages with elimination of one water molecule between their -OH groups at carbon atoms 1 and 4. Chemically, cellulose is defined as a highly crystalline segment alternating with regions of non-crystalline or amorphous cellulose [29, 30].

The glucose monomers in cellulose form hydrogen bonds both within its own chain (intramolecular) forming fibrils and with neighboring chains (intermolecular), forming micro-fibrils. These hydrogen bonds lead to formation of a linear crystalline structure with high rigidity and strength. The amorphous cellulose regions have a lower frequency of intermolecular hydrogen bonding, thus exposing reactive intermolecular -OH groups to be bonded with water molecules. Amorphous cellulose can therefore be considered as hydrophilic in nature due to their tendency to bond with water.

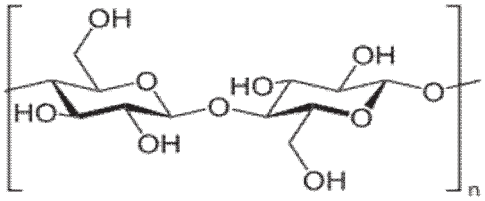

Figure-2.4 Structure of cellulose

On the other hand, very few accessible intermolecular –OH are available in crystalline cellulose and it is far less hydrophilic than amorphous cellulose. Crystalline

micro-fibrils have tightly packed cellulose chains within the fibrils, with accessible –OH groups present on the surface of the structure. Only very strong acids and alkalis can penetrate and modify the crystalline lattice of cellulose.

2.4.2 Hemicelluloses

Hemicelluloses differ from cellulose in three different ways. Firstly, unlike cellulose (containing only 1,4-β-D-glucopyranose units) they contain several different sugar units. Secondly, they exhibit a considerable degree of chain branching, whereas cellulose is a linear polymer. Thirdly, the degree of polymerization of native cellulose is ten to hundred times higher than that of hemicelluloses. Unlike cellulose, the constituents of hemicelluloses differ from plant to plant. Hemicelluloses contain substituent like acetyl (-COCH3) groups and glucoronic acid. By attaching ferulic acid and p-coumaric residues, hemicelluloses can form covalent bonds to lignin [31]. Due to this linking ability of hemicelluloses, degradation of it leads to disintegration of the fibers into cellulose micro-fibrils resulting in lower fiber bundle strength [32].

Mainly the acid residues attached to hemicelluloses make it highly hydrophilic and increase the fiber water uptake, which increases the risk of microbiological fiber degradation. It has been found that hemicelluloses thermally degrade more at lower temperatures (150-180°C) than cellulose (200-230°C) [33].

2.4.3 Lignin

Together with cellulose, lignin is the most abundant and important polymeric organic substance in the plant world. Lignin increases the compression strength of plant fibers by gluing the fibers together to form a stiff structure, making it possible for trees of 100 meters to remain upright. Lignin is essentially a disordered, polyaromatic, and cross-linked polymer arising from the free radical polymerizations of two or three monomers structurally related to phenyl-propane [34]. Free radical coupling of the lignin monomers gives rise to a very condensed, reticulated, and cross-linked structure. The lignin matrix is therefore analogous to a thermoset polymer in conventional polymer terminology. The dissolution of lignin using chemicals aids fiber separation. When exposed to ultraviolet light, lignin undergoes photochemical degradation [35]. The lignin seems to act like a

matrix material within the fibers, making stress transfer on a micro-fibril scale and single fiber scale possible.

2.4.4 Pectin

In plant cells, pectin consists of a complex set of polysachharides that are present in most primary cell walls and contains 1,4-linked α–D-galactosyluronic acid residues. It is a long chain of pectic acid and pectinic acid. Pectin helps to regulate the flow of water in between cells and keeps them rigid. It is the most hydrophilic compound in plant fibers due to the carboxylic acid groups and is easily degraded by defibration with fungi [29].

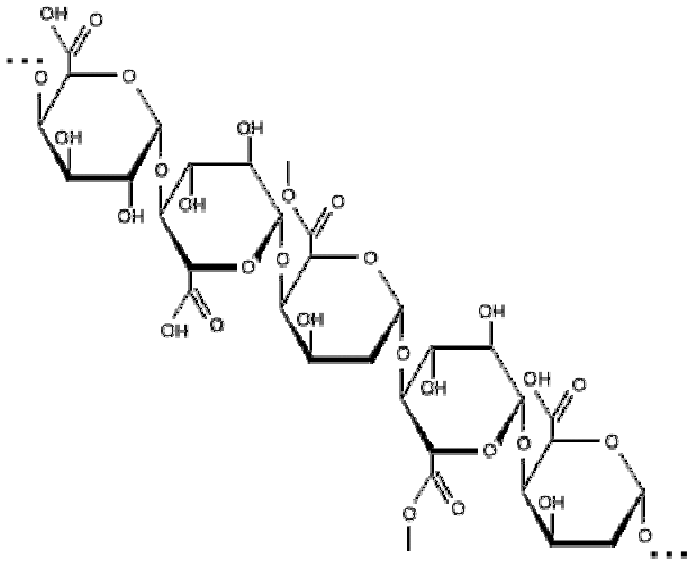

Figure-2.5 Structure of pectin

2.5 MATRIX MATERIAL

Many materials when they are in fibrous form exhibit very good strength properties but to achieve these properties the fiber should be bonded by a suitable matrix. The matrix isolates the fibers from one another in order to prevent abrasion and formation of new surface flaws and acts as a bridge to hold the fibers in place. A good matrix should possess

ability to deform easily under applied load, transfer the load on to the fibers and evenly distribute stress concentration.

A study of the nature of bonding forces in laminates [36] indicates that upon initial loading there is a tendency for the adhesive bond between them account for the high strength properties of the of the laminates.

The polymer matrix binds the fibers together so as to transfer the load to and between them and protect them from environments and handling. Polymer or resin system used to manufacture advanced polymer matrix composites (PMCs) are of two basic types, thermosets and thermoplastics (including bio-derived ones).

2.4.1 Thermosets

Much of the early work used thermosetting resins as matrix material for composite production. Products like tufnol which is made from cotton fibres and epoxy resin, have been available for some time, having good stiffness and strength [37]. In the last few years there has been renewed interest in these products for use in automotive applications [38]. To achieve reinforcing effects in composites it is necessary to have good adhesion between the fibres and resins. Epoxy and phenolic thermosetting resins are known to be able to form covalent cross-links with plant cell walls via -OH groups [39]. Composite manufacture can be achieved using low viscosity epoxy and phenolic resins that cure at room temperature. In addition epoxy resin does not produce volatile products during curing which is most desirable in production of void free composites. Therefore, although epoxy resins are relatively more expensive than polyester, they have potential for the development of high added value plant fiber composites, where long fibres at a high content are required.

The functional group in epoxy resins is called the oxirane, a three-membered strained ring containing oxygen. Epoxy resins, depending on their backbone structure, may be low or high viscosity liquids or solids. In low viscosity resin, it is possible to achieve a good wetting of fibres by the resin without using high temperature or pressure. The impregnation of fibres with high viscosity resins is done by using high temperature and pressure.

A wide range of starting materials can be used for the preparation of epoxy resins thereby providing a variety of resins with controllable high performance characteristics. These resins generally are prepared by reacting to a poly functional amine or phenol with epichlorohydrin in the presence of a strong base. The commercially available diglycidyl ether of bisphenol-A (DGEBA), figure 2.4, is characterized by epoxy equivalent weight, which can be determined either by titration or quantitative infrared spectroscopy. The presence of glycidyl units in these resins enhances the processability but reduces thermal resistance.

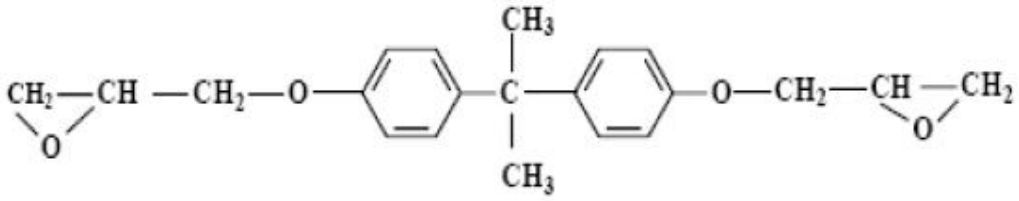

Figure-2.6 Chemical structure of DGEBA

The most widely used curing agents for epoxy resins are primary and secondary amines. The overall reaction rate of an amine with an epoxide is influenced by the steric hindrance and the electron withdrawing or electron donating groups present in the amine [40].

During curing, epoxy resins can undergo three basic reactions.

1. Epoxy groups are rearranged and form direct linkages between themselves.
2. Aromatic and aliphatic -OHs link up to the epoxy groups.
3. Cross-linking takes place with the curing agent through various radical groups.

The advantages of epoxy resins are low polymerization shrinkages unlike polyesters during cure, good mechanical strength, excellent resistance to chemicals and solvents and excellent adhesion to fibres. The epoxy molecule also contains two ring groups at its centre, which are able to absorb both mechanical and thermal stresses better than linear groups, giving epoxy resin very good stiffness, toughness and heat resistance.

The primary disadvantages of the epoxy resins are that they require long curing times and in general, their mould release characteristics are poor. The epoxy resins are characterized by their high adhesive strengths. This property is attributed to the polarity of aliphatic -OH groups and ether groups that exist in both the initial resin and cured system. The polarity associated with these groups promotes electromagnetic bonding forces between epoxy molecules and the polar fibres.

2.4.2 Bio-derived Thermoplastic Matrices

Cellulose fibres (e.g. hemp, flax, jute) are widely used with conventional thermoplastic polymers (e.g. PP, PE) as reinforcement in composite production to improve mechanical properties. In fact, the history of composites from renewable resources is far longer than conventional polymers. The study and utilization of natural polymers is an ancient science. Typical examples, such as paper, silk, skin and bone arts can easily be found in museum around the world. In the biblical Book of Exodus, Moses's mother built the ark from rushes, pitch and slime - a kind of fibre reinforced composite, according to the current classification of material. During the opium war more than 1000 years ago, the Chinese built their castles to defend against invaders using a kind of mineral particle reinforced composite made from gluten rice, sugar, calcium carbonate and sand [41].

However, the availability of petroleum at a lower cost and the bio-chemical inertness of petroleum based products have proven disastrous for the market of natural polymers. It is only about last two decades when the significance of eco-friendly materials has been realized. Now polymers from renewable resources have started drawing an increasing amount of attention. The two main reasons for that are environmental concerns [42], and the realization that the petroleum resources are limited.

Generally, polymers from renewable resources can be classified into three groups: (1) natural polymers such as starch, protein, and cellulose (2) synthetic polymers from natural monomers, such as PLA and (3) polymers from microbial fermentation, such as polyhydroxy butyrate (PHB). Like numerous other petroleum based polymers, many properties of polymers from renewable resources can be improved through composite production [41].

The development of synthetic polymers like PLA using monomers from natural resources has been a driving force for the development of biodegradable polymers from renewable resources. Therefore, in today's world PLA is the most promising among bio-derivable polymers [41]. PLA can be processed (e.g. compression moulding, pultrusion, extrusion and injection moulding) like petroleum based polyolefins and its mechanical property is better than the widely used polymer PP [43]. On degradation PL does not emit any carbon dioxide to the environment like other biodegradable materials from renewable resources. The degradation occurs by hydrolysis to lactic acid, which is metabolized by micro-organisms to water and carbon dioxide. If PLA is comprised together with other biomass, the biodegradation occurs within a couple of weeks and the material can fully disappear within a month [44]. Chemically, it is linear aliphatic polyester of lactic acid which can be obtained by fermentation of renewable agricultural materials like corn, sugarcane and sugar beets. Lactic acid is converted to a cyclic lactide dimer which is then polymerized to PLA through a ring opening reaction.

The major applications of PLA products are in household wastes as plastic bags, barriers for sanitary products and diapers, planting, and disposable cups and plates. However, a number of authors reported the possibilities of developing fully bio-degradable composite products by using biodegradable polymers as matrix and natural fibres as reinforcements [45, 46]. Keller *et al* [47] reported that PLA should produce fiber reinforced composites with high mechanical properties for light weight construction materials. Oksman *et al* [43] observed that PLA had good potential as a polymer matrix in flax fibre reinforcement for composites production. They reported that the composite strength produced with PLA/flax was about 50% better than that of PP/flax composites. Due to the increasing commercial interest for natural fiber reinforced polymer composites for use in automotive applications and building constructions as well as demands for environmentally friendly materials, the development of fully biodegradable composites for many applications could be an interesting area of research.

2.5 NATURAL FIBER REINFORCED POLYMER COMPOSITES

Polymer materials by themselves have found extensive use in noncritical products. Such products are used in advanced engineering applications when reinforced with stronger

materials. Therefore fiber reinforced composites comprised of thermoplastics and natural fibers are a well research area at present for their high specific strength and modulus. The advantages of natural lignocellulosic fibers over traditional reinforcing materials such as carbon, glass fibers, talc and mica are low cost, acceptable specific strength properties, low density, non abrasivity, good thermal properties, enhanced energy recovery and biodegradability [22, 48-49]. The use of natural fibers in plastic matrix includes many benefits such as low volumetric cost, increase of heat deflection temperature, increase of stiffness of thermoplastics and improvement of wood surface appearance. So natural fibers have achieved applications in making several complex structures such as tubes, interior paneling, sandwich plates, decking, furniture parts, sports usages etc.

One of the largest areas of recent growth in natural fiber plastic composites in world-wide is the automotive industry, where natural fibers are advantageously used as a result of their low density and increasing environmental pressures. They are also used in electrical and electronic application for their nonconductive and excellent insulation against heat and noise. Natural fibers composites found application where load bearing capacity and dimensional stability under moist and high thermal conditions are of second order importance. For example, flax fiber reinforced polyolefins are extensively used today in the automotive industry, but the fiber acts mainly as filler material in non-structural interior panels [50]. Natural fiber composites used for structural purposes do exist, but then usually with synthetic thermo-set matrices which of course limit the environmental benefits [51, 52].

Natural fibers like sisal, jute, coir, oil palm, bamboo, wheat and flax straw, waste silk and banana [53, 54, 55-63] have proved to be good and effective reinforcement in thermoset and thermoplastic matrices due to their high aspect ratio and high specific strength- and stiffness [22, 64-66]. Apart from good specific mechanical properties and positive environmental impact, other benefits from using natural fibers worth mentioning are low cost, friendly processing, low tool wear, no skin irritation and good thermal and acoustic insulating properties [66].

A complete biodegradable system may be obtained if the matrix material also comes from a renewable resource. Examples of such materials are lignophenolics, starch and

polylactic acid (PLA). Some of these systems show encouraging results. For example Oksman *et al* [43] have reported that flax fiber composites with PLA matrix can compete with and even outperform flax/polypropylene composites in terms of mechanical properties. In a recent study [67] it was found that composites of poly-L-lactide acid (PLLA) reinforced by flax fibers can show specific tensile modulus equivalent to that of glass/polyester short fiber composites. The specific strength of flax/PLLA composites was lower than that of glass/polyester, but higher than that of flax/polyester.

The limited use of natural fiber composites is also connected with some other major disadvantages still associated with these materials. The fibers generally show low ability to adhere to common non-polar matrix materials for efficient stress transfer. Furthermore, the fibers inherent hydrophilic nature makes them susceptible to water uptake in moist conditions. Natural fiber composites tend to swell considerably with water uptake and as a consequence mechanical properties, such as stiffness and strength, are negatively influenced. However, the natural fiber is not inert. The fiber-matrix adhesion may be improved and the fiber swelling reduced by means of chemical, enzymatic or mechanical modifications [22].

There are many application of natural fiber composite in everyday life. For example, jute is a common reinforcement for composites in India. Jute fiber with polyester resins is used in buildings, elevators, pipes, and panels [68]. Natural fiber composites can also be very cost effective material for application in building and construction areas (e.g. walls, ceiling, partition, window and door frames), storage devices (e.g. bio-gas container, post boxes, etc.), furniture (e.g. chair, table, tools, etc.), electronic devices (outer casting of mobile phones), automobile and railway coach interior parts (inner fenders and bumpers), toys and other miscellaneous applications (helmets, suitcases).

During the last few years, a series of works have been done to replace the conventional synthetic fiber with natural fiber composites [22, 53, 69-74]. For instant, hemp, sisal, jute, cotton, flax and broom are the most commonly used fibers to reinforce polymers like polyolefins [74, 55], polystyrene [56], and epoxy resins. In addition, fibers like sisal, jute, coir, oil palm, bamboo, wheat and flax straw, waste silk and banana [22, 69, 55–63, 75] have proved to be good and effective reinforcement in the thermoset and thermoplastic matrices. Nevertheless, certain aspects of natural fiber reinforced composite

behaviour still poorly understood such as their visco elastic, visco plastic or time-dependent behavior due to creep and fatigue loadings [76], interfacial adhesion [77, 78], and tribological properties. Little information concerning the tribological performance of natural fiber reinforced composite material [59–61, 79] has been reported. In this context, long plant fibres, like hemp, flax [77, 78], and bamboo [60, 61] have considerable potential in the manufacture of composite materials. Likewise, bagasse fibers may also have considerable potential as reinforcement for polymer and may provide advantages when used as a substitute for conventional synthetic glass fiber.

After reviewing the exiting literature available on the natural fiber composite efforts are put to understand the basic needs of the growing composite industry. The conclusions drawn from this is that, the success of combining vegetable natural fibers with polymer matrices results in the improvement of mechanical properties of the composite compared with the matrix material. These fillers are cheap and non toxic can be obtain from renewable source and are easily recyclable. Moreover despite of their low strength, they can lead to composites with high specific strength because of their low density.

Thus the priority of this work is to prepare polymer matrix composites (PMCs) using bagasse fiber as reinforcement material. To improve the interfacial strength between the fiber and the matrix, the surface modification of the fiber has to be done by chemical treatment. The composite will then be subjected to different weathering condition like steam, saline and subzero condition. The potential of bagasse fiber for tribological application has to be investigated through performing different tribological tests like abrasive wear test, two body abrasion test and solid particle erosion test as per ASTM standard. The fiber characterization will be done by Fourier Transfer Infrared (FTIR) spectroscopy before and after the chemical treatment. The flexural strength of the composite will be evaluated along with other mechanical tests.

Chapter 3

MECHANICAL CHARACTERIZATION OF BAGASSE FIBER EPOXY COMPOSITE

CHAPTER – 3

3.1 INTRODUCTION

Researches all over the world today are focusing on ways of utilizing either industrial or agricultural wastes as a source of raw materials for the industry. These wastes utilization would not only be economical, but may also result to foreign exchange earnings and environmental pollution control. Among such resources are the lignocellulosic materials, of which about 2.5 billion tons are available and which have been used since 6000BC [80]. In general natural fibers are hygroscopic in nature and they absorb or release moisture depending on environmental condition. As discussed earlier the components of natural fiber include cellulose, hemicelluloses, lignin, pectin, waxes and water soluble substances. The composition of different fibers may differ with the growing condition and test methods even for the same kind of fiber. Amorphous cellulose and hemicellulose that are present in the natural fiber are mostly responsible for the high moisture absorption, since they contain numerous easily accessible hydroxyl groups which give a high level of hydrophilic character to fiber. The high moisture absorption of the fiber occurs due to hydrogen bonding of water molecules to the hydroxyl groups within the fiber cell wall. This leads to a moisture build-up in the fiber cell wall (fiber swelling) and also in the fiber-matrix interface. This in turn becomes responsible for changes in the dimensions of cellulose-based composites, particularly in the thickness and the linear expansion due to reversible and irreversible swelling of the composites [81]. Another problem associated with fiber swelling is a reduction in the adhesion between the fiber and the matrix, leading to deterioration in the mechanical properties of the composite [82]. A good fiber-matrix bonding can decrease the rate and amount of moisture absorbed by the composite as well as improving the mechanical properties [83]. However in order to overcome this problem chemical modifications are considered to optimize the interface of fiber. Chemicals may activate hydroxyl groups or introduce new moieties that can effectively interlock with the matrix. Different chemical treatments such as mercerization or alkali treatment, isocyanate treatment, acrylation, benzoylation, permanganate treatment, acetone treatment, acetylation, silane treatment etc. are reported by several researchers [74, 84-86] aiming at improving the adhesion with polymer matrix.

For potential application of natural fiber polymer composites a comprehensive study of moisture absorption characteristics and its effect on mechanical properties are required. In this chapter effect of moisture absorption on mechanical properties of both untreated and chemically treated bagasse fiber epoxy composite under different environments (steam, saline water, subzero temperature) are investigated.

3.2 CHEMICAL MODIFICATION OF FIBER

Materials with low environmental impact are of great interest in technological applications: composites based on natural fibers are an interesting alternative when moderate mechanical properties are required. Since the interfacial bonding between the reinforcing fibers and the resin matrix is an important element in realizing the mechanical properties, several authors [26, 87-90] have focused the studies on the treatment of fibers to improve the bonding with resin matrix. The mechanical properties of the composites are controlled by the properties and quantities of the component materials and by the character of the interfacial region between matrix and reinforcement. Lack of good interfacial adhesion makes the use of cellular fiber composites less attractive. Natural-fibre composites combine good mechanical properties with low specific mass. But their high level of moisture absorption, poor wettability and insufficient adhesion between untreated fibre and the polymer matrix leads to debonding with age. To improve the properties of the composites, it is necessary to improve the adhesion between the hydrophilic fiber and the hydrophobic matrix by modifying the fiber surface. The natural reinforcing fibres can be modified by physical and chemical methods. Physical modification changes the structural and surface properties of the fiber there by influencing the mechanical bonding with the matrix. But the chemical modification of the fibers alters the surface properties so that better wetting of the fibers with the matrix is possible. This removes the organic residues from the surface of the fibers which enhances the adhesion because natural fibers are coarse in structure, and thus, enable an interlocking mechanism with the matrix. According to the principles of interface coupling, the hydrophilic carboxyl group of organic acid as the modifier is expected to react with the hydroxyl groups of natural fibre in the surface, and the hydrophobic group should react or have relatively high compatibility with the polymer matrix. The combined effects of these interactions will effectively improve the fibre dispersion and resultant adhesive coupling. There are various chemical treatments available

for the fiber surface modification. Chemical treatment including alkali, silane, acetylation, benzoylation, acrylation, isocynates, maleated coupling agents, permanganate treatment are discussed in details in [26].

Among all the natural reinforcing materials, the fiber of sugarcane bagasse appears to be a promising fiber when the aim is the biodegradation and low cost. Only a few chemical modification methods of the bagasse have been described in literature, including mercerization and acrylic acid treatments [91], mercerization and acetylation [92, 93], succinylation [94], treatment with benzyl chloride [95] and silane [96]. Out of the available treatments, for the present case to have a good bonding between the fiber and the resin matrix bagasse fiber have been treated with acetone and alkali. The subsequent section will elaborate separately the treatment of the fiber surface by these methods, study of mechanical properties of both untreated and treated fiber reinforced polymer composite, the results of fiber modification through FTIR & SEM and environmental effects on mechanical performance of the composite.

3.2.1 Methods of Chemical Modifications

3.2.1.1 Acetone Treatment

When the fiber is treated with acetone the lignin, cellulolignin and other such material get dissolved after treatment of the fiber in acetone. As acetone is a non-polar organic solvent it usually dissolves the non-polar organic component.

The bagasse fibers were washed in soxhlet extractor (figure 3.1) with acetone for approximately 1-1.5hrs. The acetone was evaporated (boiled at 63^0C) and condensed back into the volume with the fibers. This process was repeated four times for each batch. The used acetone was discarded before the new batch was cleaned in the same manner. The acetone changed from transparent to light yellow after treatment due to the presence of waxes and organic materials after the extraction. All the fibers were washed with pressurized water at a temperature of 90^0C for 70 minutes before acetone treatment. The fibers were then dried at room temperature for 24 hrs.

3.2.1.2 Alkaline Treatment

Alkaline treatment or mercerization is one of the most used chemical treatments of natural fibers when used to reinforce thermoplastics and thermosets. The important modification done by alkaline treatment is the disruption of hydrogen bonding in the network structure, thereby increasing surface roughness. This treatment removes a certain amount of lignin, wax and oils covering the external surface of the fiber cell wall, depolymerizes cellulose and exposes the short length crystallites [97]. Addition of aqueous sodium hydroxide (NaOH) to natural fiber promotes the ionization of the hydroxyl group to the alkoxide [98].

$$\textbf{Fiber} - \textbf{OH} + \textbf{NaOH} \rightarrow \textbf{Fiber} - \textbf{O} - \textbf{Na} + \textbf{H}_2\textbf{O}$$

Thus, alkaline processing directly influences the cellulosic fibrill, the degree of polymerization and the extraction of lignin and hemicellulosic compounds [99]. It is reported that alkaline treatment has two effects on the fiber:

1) It increases surface roughness resulting in better mechanical interlocking, and
2) It increases the amount of cellulose exposed on the fiber surface, thus increasing the number of possible reaction sites [74].

Consequently, alkaline treatment has a lasting effect on the mechanical behaviour of flax fiber, especially on fiber strength and stiffness.

The effect of alkali treatments (0%, 1%, 3%, 5%) of bagasse fibers on the flexural strengths were examined using treated fiber composites. As seen from figure 3.2, the maximum improvement in the flexural strength of the composite was observed for 5% NaOH treated fiber composites. It was believed that better interfacial adhesion along with better fibrillation of these fibers contributed effectively to the enhancement in the flexural properties.

For treatment in alkali the bagasse fibers were soaked in a 5% NaOH solution at room temperature maintaining a liquor ratio of 15:1. The fibers were kept immersed in the alkali solution for 2, 4 and 6hrs. The fibers were then washed several times with fresh water to remove any NaOH sticking to the fiber surface, neutralize with dilute acetic acid and finally washed again with distilled water. A final pH of 7 was maintained. The fibers were

then dried at room temperature for 48 hrs followed by oven drying at 100°C for 6hrs. The alkali reaction between bagasse fiber and NaOH is as follows:

$$Bagasse - OH + NaOH \Leftrightarrow Bagasse - O^{-}Na^{+} + H_2O$$

The NaOH reacts with hydroxyl groups of the cementing material hemicellulose, and it brings on the destruction of the cellular structure and thereby the fibers split into filaments. Figure 3.3 shows the flexural strength of the composite for treated fibers with alkali for 2, 4 and 6 hours. The flexural strength properties of the composites at 20 volume % of fiber loading after 4 hrs alkali treatment was 21.95 MPa in contrast to 10.15 Mpa for composites with untreated fibers. This is an improvement of 53%. This improvement however, were 31 and 29 % for composites prepared with 2 and 6 hrs treated fibers respectively. Hence for rest of the investigations composites were prepared with 5% and 4 hours alkali treated fibers for analysis.

3.2.2 SEM Micrographs of Treated Fibers

The morphology of the untreated and treated fiber surfaces has been studied using scanning electron microscope (SEM) JEOL JSM-6480LV. The sample surfaces were gold coated to make them conductive prior to SEM observation. SEM micrographs of the untreated and treated bagasse fibers are shown in figures 3.4 (a-c). It is well established that the cellulose chains of natural fiber are strongly bound by chemical constituents, lignin, and hemicellulose, resulting in the formation of multi-cellular fiber [100]. The surface of untreated fiber appeared rough due to the presence of lignin, wax, oil, and surface impurities [Figure-3.4(a)], which are partially removed with acetone [Figure-3.4(b)] and further removed with alkali treatment [Figure-3.4(c)] These clean surfaces are expected to provide direct bonding between the fiber cellulose and a matrix such as epoxy resin. By comparing treated fibers with the untreated fibers, it can be seen that the alkali treatment resulted in separation of the micro fibrillar structure (fibrillation) and reduction in thickness of fiber because of the removal of cemented materials (i.e. lignin and hemicellulose) [101, 102]. The fibrillation increases effective surface area available for contact with the matrix [67] and hence the interfacial adhesion was improved.

Moreover these two treatments increase the effective surface area by fibrillation which promotes the mechanical interlocking between the fiber and the matrix where as the acetone treatment does not affects the fiber surface very much.

3.2.3 FTIR Spectroscopy

The effect of chemical modifications on the fiber surface was observed by using FTIR spectroscopy. FTIR measurement was performed using an IR-Prestige-21 spectrometer. A total of 100 scans were taken from 400-4000 cm^{-1} with a resolution of 2 cm^{-1} for each sample. The comparison of the representative FTIR spectra of untreated bagasse before and after chemical treatment (acetone and alkali treatment) is shown in figure-3.5(a-c). In comparison to the unmodified bagasse fiber, the acetone treated and alkali treated bagasse showed a reduction in O-H stretching intensity and shifting of the peak from 3409.76 cm^{-1} to 3421.61 and 3418.88 cm^{-1} respectively, indicating participation of some free hydroxyl groups in these chemical reactions. The point of reaction was probably at the lignin –OH and C_2-OH of the glucopyranose unit in the cellulose component. The band of medium intensity at 828.32 cm^{-1} due to b-glycosidic linkage in the unmodified bagasse fiber underwent shifting to a lower wave number, except acetone treated fiber accompanied by an increase in the intensity. This relates to the rotation of glucose residue around the glycosidic bond [103] and indicates a slow transition from unmodified to chemically modified bagasse.

3.3 SINGLE FIBER PULL-OUT TEST

Since we are going to use short, non-continuous fibers in composite it is essential to determine the critical fiber length. For this standard single fiber pull out test was carried out. Figure 3.6 shows the schematic diagram of the sample to be used for test. Single fibers were taken and partially embedded in the mixture of epoxy resin and hardener (ratio 10:1) inside a per-pex sheet mould to prepare the samples. The embedded lengths and diameter of the fiber were measured by electron microscope. The embedded lengths were found to be 3.45 to 12.32 mm with fiber free length of 30 mm. The cast samples were shown in figure 3.7. After curing, the specimens were taken out from the mould. Pull-out test was then conducted on an Instron-4204 tensile testing machine at crosshead speed of 1 mm/min and using 5KN-load cell. Five specimens were prepared for each embedded length and average value was taken.

The experiment was conducted as per Tanaka *et al* [104] and Valadez *et al* [74]. Table 3.1 shows the pull-out load for different embedded fiber length achieved through

single fiber pull-out test. The average maximum load at failure (P_{break}) in fiber tensile testing was found to be 8.803 kg. A regression analysis has been done between fiber embedded length and fiber pullout load to find out the effective fiber embedded length for rupture. This was found to be approximately 9.18 mm. Thus for composite preparation we have to consider higher value than 9.18 mm. In the present work fiber length of 10mm has been taken for preparation of composite.

3.4 COMPOSITE FABRICATION

For preparation of composite the following materials have been used;

1. Bagasse fiber
2. Epoxy
3. Hardener

3.4.1 Preparation of Bagasse Fiber

The sugarcane stalk is composed of an outer rind and inner pith. The upper layers of bagasse consist of a hard fibrous substance called rind while inside is soft material called pith. The pith contains small fibers and the majority of the sucrose, while the rind contains longer and finer fiber, arranged randomly throughout the stem and bound together by lignin and hemicelluloses. It is reported that fibers are often located adjacent to the inner wall of the rind particle. For the present investigation, fresh bagasse fibers were collected from Sakti Sugar Industries located at Dhenkanal, Orissa, India. These fibers were then spread on a water proof sheet and stored in an enclosed shed to reduce the moisture content. After approximately two weeks, the long bagasse fibers (rind portion only) were shortened into a length of 10mm (optimum fiber length found from single fiber pull out test) and width of 1mm with a pair of scissor. Due to the low moisture content of the bagasse samples, no fungi grew during the storage. The bagasse samples were then cleaned via pressurized water for about one hour. This procedure removes fine bagasse particles, sugar residues and organic materials from the samples. Then the fibers were dried with compressed air at a pressure of approximately 145 kPa at 108^0C. The required drying time was determined by

weighing a trial sample every ten minutes until the measured mass becomes constant. A drying time of 40 min was established to provide sufficient drying of the fiber.

3.4.2 Epoxy Resin and Hardener

Epoxy resins are relatively low molecular weight pre-polymers capable of being processed under a variety of conditions. Two important advantages of these over unsaturated polyester resins are: first, they can be partially cured and stored in that state, and second they exhibit low shrinkage during cure. However, the viscosity of conventional epoxy resins is higher and they are more expensive compared to polyester resins. The cured resins have high chemical, corrosion resistance, good mechanical and thermal properties, outstanding adhesion to a variety of substrates, and good and electrical properties. Approximately 45% of the total amount of epoxy resins produced is used in protective coatings while the remaining is used in structural applications such as laminates and composites, tooling, moulding, casting, construction, adhesives, etc.

The type of epoxy resin used in the present investigation is Araldite LY-556 which chemically belongs to epoxide family. Epoxy resins are characterized by the presence of a three-membered ring containing two carbons and an oxygen (epoxy group or epoxide or oxirane ring). Epoxy is the first liquid reaction product of bisphenol-A with excess of epichlorohidrin and this resin is known as Diglycidyl-Ether of Bisphenol-A (DGEBA). DGEBA is used extensively in industry due to its high fluidity, processing ease, and good physical properties of the cured of resin. The hardener with IUPAC name NNO-bis (2amino ethyl ethane-1,2diamin) has been used with the epoxy designated as HY 951. Both the epoxy and hardener were supplied by Ciba-Geigy of India Ltd.

3.4.3 Preparation of composite laminates

A wooden mold of dimension (120x100x6) mm was used for casting the composite sheet. The first group of samples was manufactured with 10, 15, 20 and 30 % volume fraction of fibers**.** Usual hand lay-up technique was used for preparation of the samples. For different volume fraction of fibers, a calculated amount of epoxy resin and hardener (ratio of 10:1 by weight) was thoroughly mixed in a glass jar and placed in a vacuum chamber to remove air bubbles that got introduced. This procedure was performed for 10 minutes

initially. The mixture was re-stirred and the vacuum procedure was performed again for 10 minutes for further removal of bubbles. Figure 3.8 illustrates the mold used to construct the composite. For quick and easy removal of composite sheets, mold release sheet was put over the glass plate and a mold release spray was applied at the inner surface of the mold. After keeping the mold on a glass sheet a thin layer (≈ 2 mm thickness) of the mixture was poured. Then the required amount of fibers was distributed on the mixture. The remainder of the mixture was then poured into the mold. Care was taken to avoid formation of air bubbles. Pressure was then applied from the top and the mold was allowed to cure at room temperature for 72 hrs. During application of pressure some amount of mixture of epoxy and hardener squeezes out. Care has been taken to consider this loss during manufacturing of composite sheets. After 72 hrs the samples were taken out of the mold. Figure 3.9 shows the photograph of the composite and some of the specimen cut for further experimentation. After cutting they were kept in airtight container.

3.5 TESTING OF MECHANICAL PROPERTIES OF COMPOSITE

The study of mechanical properties such as tensile strength, flexural strength, impact strength and hardness of untreated bagasse fiber reinforced (randomly distributed in the epoxy matrix) composite have been conducted as per ASTM standard. The results are tabulated in table 3.2.

3.5.1 Tensile strength:-

The most commonly used specimen geometries such as the dog-bone specimen and straight-sided specimen with end tabs were prepared from the flat samples. A uni-axial load is applied through the ends. The standard test method as per ASTM D 3039-76 has been used; length of the test specimen used is 154 mm. The tensile test is performed in universal testing machine INSTRON H10KS. A cross head speed of 10 mm/min has been used for the test. Each composite of five samples were tested and average value was taken for analysis.

3.5.2 Flexural strength:-

Three point bend test was carried out in an UTM 201 machine in accordance with ASTM D2344-84 to measure the flexural strength of the composites. The loading

arrangement for the specimen and the photograph of the machine used are shown in figure 3.10 & figure 3.11. All the specimens (composites) were of rectangular shape having length varied from 100-125 mm, breadth of 100-110 mm and thickness of 4-6 mm. A span of 100 mm was employed maintaining a cross head speed of 10mm/min.

The flexural strength of composites was found out using the following equation

$$\tau = 3fl/2bt^2 \quad (3.1)$$

Where τ is the flexural strength, f is the load, l is the gauge length, b is the width and t is the thickness of the specimen under test.

3.5.3 Impact strength

The impact strength of the composites was done by using a charpy impact testing machine. The specimens were of rectangular shape having dimensions 50X50X5 mm. The test has been done at a impact speed of 4m/s and an incident energy of 15J. A span of 20 mm was employed maintaining a hammer weight of 0.6kg.

3.5.4 Micro-Hardness

Micro-hardness measurement is done using a Lecco Vickers Hardness (LV 700) tester .A diamond indenter, in the form of a right pyramid with a square base and an angle 136^0 between opposite faces, is forced into the material under a load F. The two diagonals D_1 and D_2 of the indentation left on the surface of the material after removal of the load are measured and their arithmetic mean L is calculated. In the present study, the load considered F = 0.3KgF and Vickers hardness number is calculated using the following equation:

$$Hv = 0.1889F / D^2 \text{ and } L = (D_1+D_2) / 2 \quad (3.2)$$

Where F is the applied load (KgF), L is the diagonal of square impression (mm), D_1 is the horizontal length (mm) and D_2 is the vertical length (mm).

3.5.5 Results of mechanical tests

Figure 3.12 and 3.13 shows the effect of bagasse fiber content on the tensile and flexural strengths of the composites. Fiber content (volume %) varied from 10 to 30 % to investigate its effect on the mechanical properties. From the results it is observed that with increase in fiber content from 10 to 20 % both tensile and flexural strength increases and thereafter with further increase of fiber content both properties tend towards lower values. The optimum fiber content varies with the nature of both fiber and matrix, fiber aspect ratio, fiber-matrix adhesion, etc. the lower mechanical property values at high fiber content might due to the presence of so many fiber ends in the composites, which could cause crack initiation and hence potential composite failure [10]. Basing upon the observations, in subsequent observations 20% volume fraction of fiber content has been maintained.

It is observed from figure 3.14 that the un-notched charpy impact strength of the bagasse fiber epoxy composite showed an increasing trend with increase in fiber content. Similar type of work [53, 105, 106] showed an increase in impact strength with an increase in fiber content, indicating positive contribution of the fiber. Higher impact strength indicates the capability of the composite to absorb energy. This is because of strong interfacial bonding between the fiber and matrix [107]. It also depends on the nature of the fiber, polymer and fiber–matrix interfacial bonding [108].

Figure 3.15 shows the micro hardness values for different volume fraction of bagasse fiber composite. It is seen that with the increase in fiber content in the composite, its hardness value improves although the increment is marginal.

From the above investigation, it can be concluded that the composite containing 20 % volume fraction of fiber provided the best combination of strength. Therefore for further experimentation, 20% fiber volume fraction has been taken into consideration.

3.6 STUDY OF ENVIRONMENTAL EFFECT

To study the effect of environment on mechanical properties of bagasse fiber reinforced epoxy composite, samples with both untreated and treated fibers were subjected to various environments like:

(a) Steam treatment

(b) Saline treatment

(c) Subzero condition

In each conditions a set of composites (washed, washed + acetone treated and washed + alkali treated fibers) were tested for various time lengths. The specimens prior to testing were dried in an oven at 80°C and then were allowed to cool to room temperature and kept in a desiccator. The weight of each samples were taken before subjecting them to steam, saline and subzero environments. After exposing them for 8 hrs the specimens were taken out from the moist environment and all surface moisture was removed with clean dry cloth or tissue paper. The specimens were reweighted to the nearest 0.001 mg within 1 min of removing them from the environmental chamber. The specimens were weighted regularly from 8 to 56 hrs with a gap of 8 hrs of exposure. Steam treatment was conducted at 100^0C with 95 % relative humidity. Subzero treatment was conducted at -23^0C and saline treatment was done with 5% concentration. At the end of the treatment in each condition, the dimensions and weight change were measured.

3.7 RESULTS AND DISCUSSION

3.7.1 Characterization

The dimension and weight change of composite samples for different chemical treatment of fibers at different weathering conditions were measured and presented in table 3.3 to 3.8.

The results of steam swelling and steam absorption are shown in figure 3.16 and 3.17 respectively. It is observed from the results that the swelling increases with an increase in time up to 56 hrs for washed, washed + acetone treated and washed + alkali treated samples however it stabilizes after 40 hrs for washed + acetone treated samples. It is also observed that washed and alkali treated bagasse samples exhibited the least swelling. This behavior is attributed to the hygroscopic nature of the fibers. When the fibers were treated, this property gets decreased and hence less swelling of the fibers when subjected to steam. Absorption of steam (figure 3.17) for all samples increases up to 56 hrs, but the rate of

steam absorption is higher in washed samples than washed and treated samples. However the rate of absorption of moisture is faster at initial period up to about 30-40 hrs then rate of absorption slows down.

During saline treatment (figure 3.18 and figure 3.19) not only moisture absorption takes place but also transport of sodium and chlorine ions do occur leading to some what a chemical reaction with the matrix as well as with the fiber. Due to such effect there is not much deviation of swelling and water absorption amount irrespective of treated and only washed fibers.

Figure 3.20 shows the trend in water swelling from 8 hrs to 56 hrs while figure 3.21 represents the water absorption for sub zero treatment. The rate of absorption of water is linear in all the cases after 40 hrs while for washed treated samples it shows linearity after 32 hrs. The trend in water absorption is washed + alkali treated < washed + acetone treated < washed.

The water swellings of the composites are shown in figure 3.20. It is seen from the plot that washed fiber has the highest swelling while the washed treated samples lies near to each other. There is dramatic shift for washed treated samples which can be visualized from the plot. This type of behavior of the composite for subzero treatment may be due to less intermolecular hydrogen bonding. There is little difference in water absorption for washed treated samples with respect to only washed samples. This is due to the spongy nature of the pith of the bagasse which can absorb more water; but the swelling for washed treated samples is much lower because of removal of lignin content in the surface of fibers and fibrils with the acetone and alkali.

3.7.2 Study of Mechanical Properties

The study of mechanical properties such as tensile strength, flexural strength, impact strength for treated bagasse fiber random distributed in the matrix have been conducted as per ASTM standard. The effect of different chemical modifications of fibers on mechanical properties of the composite have been studied by taking 20 volume % of fiber as an optimum reinforcement as discussed earlier. It is clearly seen from table 3.9 that, the mechanical properties of the composite enhanced significantly due to chemical modification

of fiber surface. Higher increase in properties was observed in the case of alkali treated fiber composite, however acetone treated fiber composite showed a slight improvement in properties (figure 3.22). This improvement in properties occurs due to rough fiber surface produce by removal of natural and artificial impurities, fibrillation of fiber which facilate the mechanical anchoring between fiber and matrix as explained in art 3.2.2. Similar observations were reported by Sreenivasan *et al* [109], Manikandan *et al* [56] while they worked with benzoylated sisal fiber and alkali treated coir fiber.

3.7.3 Study of Failure Modes

SEM micrographs of the fractured samples after subjected to different treatments for chemically modified fibers (acetone figure 3.23) and (alkali figure 3.24) are shown below.

Fig. 3.23 (a) shows the fiber breakage instead of pull out of fibers from the matrix. It also indicates that cellulose structure has been compressed but not so much as to prevent fracture of some fibers. The breakage of fibers indicates better interfacial strength. Fig 3.23 (b) shows the morphology of the samples subjected to subzero condition. There is no trace of fiber breakage in the composite, which indicates good bonding between fiber and the matrix. Swelling of fiber is less hence higher strength. When the composite is subjected to saline environment it indicates flexural strength comparable to subzero environment. Probably, Fig 3.23 (c) the fiber matrix bonding has been improved due to formation of monolayer which controls the propagation of moisture through fibril interfaces.

Fig 3.24 (a) shows that most of the fibers have come out without breaking during fracture for the composite subjected to steam treatment. This might have occurred due to dissolution of cellulose constituent in alkali which creates voids in the fiber structure, increases swelling and makes the fiber weaker. Destruction of mess network and splitting of fibers in to filaments that might have occurred during treatment. Fig 3.24 (b) also shows breaking down of fiber bundles into smaller one. This increases the effective surface area available for wetting by the resin and when subjected to subzero conditions, the absorption of water as explained earlier is less hence indicates higher flexural strength. Fig 3.24(c) shows the micrograph for saline exposed sample. Same type of features are seen as for

subzero condition. The breaking of fibers due to fibrillation is clearly visible hence higher strength.

3.8 CONCLUSIONS

The following conclusions are drawn from the present work.

- The sugar cane residue bagasse, an underutilized renewable agricultural material can successfully be utilized to produce composite by suitably bonding with resin for value added product.

- The effective fiber length for fabrication of bagasse epoxy composite as found out from the single fiber pull-out test is approximately 10 mm or longer.

- On increasing the fiber content, the strength, modulus and work of fracture increases and the best combination is found with 20% volume fraction of fiber.

- The fiber surface modification by chemical treatments significantly improves the fiber matrix adhesion, which in turn improves the mechanical properties of composite. Alkali treatment shows the highest improvement in comparison to acetone treatment. These results are confirmed through SEM and FTIR analysis.

- By comparing the water swelling and absorption behavior of the composites with varying fiber treatment at different environmental conditions, the best mechanical property results are obtained with bagasse fiber that are both washed and treated with alkali.

- From the morphology of the fractured surface for the alkali treated fiber it was found that fiber breakage were the predominant mode of failure.

- For acetone treatment, fibers pullout were the predominant mode of failure. Therefore the strength in acetone treated fiber is somewhat low in comparison to alkali treated fiber. However it is established that fiber matrix bonding has improved a lot by chemical modification in comparision with the untreated fiber.

Table- 3.1 Pullout Testing Results

Embedded Fiber Length (mm)	Pullout Load (Kg)
3.45	1.54
3.69	2.05
4.02	3.28
4.34	3.69
4.47	4.56
4.51	3.58
4.79	4.26
5.8	4.97
6.45	6.92
7.28	7.74
8.75	8.55
9.22	8.68
9.58	8.83*
10.03	8.32*
10.42	8.98*
11.25	8.37*
12.05	9.08*
12.32	9.24*
*Note: " * " did not pullout / ruptured*	

Table-3.2 Mechanical properties of untreated bagasse fiber epoxy composite

Fiber vol %	Flexural Strength (MPa)	Tensile Strength (MPa)	Impact Strength (KJ/m^2)	Hardness (Hv)
0	17.56	13.50	08.67	153.15
10	31.06	50.85	11.00	171.43
15	48.63	59.21	37.00	176.54
20	59.75	64.54	26.50	195.17
30	52.76	48.53	30.15	198.36

Table-3.3 Cumulative volume change in treated fiber composites for steam treatment

Types of composite	Washed			Washed and Acetone treated			Washed and Alkali treated		
Treatment (hrs)	Initial Vol. (mm^3)	Final Vol. (mm^3)	Difference (mm^3)	Initial Vol. (mm^3)	Final Vol. (mm^3)	Difference (mm^3)	Initial Vol. (mm^3)	Final Vol. (mm^3)	Difference (mm^3)
8	8.370	8.475	0.105	8.626	8.713	0.087	10.640	10.711	0.071
16	8.370	8.547	0.177	8.626	8.791	0.165	10.640	10.788	0.148
24	8.370	8.600	0.230	8.626	8.827	0.201	10.640	10.816	0.176
32	8.370	8.626	0.256	8.626	8.841	0.215	10.640	10.835	0.195
40	8.370	8.650	0.280	8.626	8.855	0.229	10.640	10.846	0.206
48	8.370	8.672	0.302	8.626	8.858	0.232	10.640	10.858	0.218
56	8.370	8.672	0.302	8.626	8.861	0.235	10.640	10.863	0.223

Table-3.4 Cumulative volume change in treated fiber composites for saline treatment

Types of composite	Washed			Washed and Acetone treated			Washed and Alkali treated		
Treatment (hrs)	Initial Vol. (mm^3)	Final Vol. (mm^3)	Difference (mm^3)	Initial Vol. (mm^3)	Final Vol. (mm^3)	Difference (mm^3)	Initial Vol. (mm^3)	Final Vol. (mm^3)	Difference (mm^3)
8	8.076	8.129	0.053	11.549	11.593	0.044	13.520	13.550	0.030
16	8.076	8.174	0.098	11.549	11.634	0.085	13.520	13.597	0.077
24	8.076	8.208	0.132	11.549	11.664	0.115	13.520	13.628	0.108
32	8.076	8.240	0.164	11.549	11.705	0.156	13.520	13.647	0.127
40	8.076	8.261	0.185	11.549	11.719	0.170	13.520	13.663	0.143
48	8.076	8.270	0.194	11.549	11.719	0.170	13.520	13.670	0.150
56	8.076	8.278	0.202	11.549	11.719	0.170	13.520	13.675	0.155

Table-3.5 Cumulative volume change in treated fiber composites for subzero treatment

Types of composite	Washed			Washed and Acetone treated			Washed and Alkali treated		
Treatment (hrs)	Initial Vol. (mm^3)	Final Vol. (mm^3)	Difference (mm^3)	Initial Vol. (mm^3)	Final Vol. (mm^3)	Difference (mm^3)	Initial Vol. (mm^3)	Final Vol. (mm^3)	Difference (mm^3)
8	8.090	8.138	0.048	11.130	11.159	0.029	12.670	12.691	0.021
16	8.090	8.180	0.090	11.130	11.184	0.054	12.670	12.699	0.029
24	8.090	8.219	0.129	11.130	11.204	0.074	12.670	12.705	0.035
32	8.090	8.235	0.145	11.130	11.213	0.083	12.670	12.721	0.051
40	8.090	8.254	0.164	11.130	11.221	0.091	12.670	12.737	0.067
48	8.090	8.261	0.171	11.130	11.227	0.097	12.670	12.741	0.071
56	8.090	8.263	0.173	11.130	11.232	0.102	12.670	12.749	0.079

Table-3.6 Cumulative weight change in treated fiber composites for steam treatment

Types of composite	Washed			Washed and Acetone treated			Washed and Alkali treated		
Treatment (hrs)	Initial Vol. (mm^3)	Final Vol. (mm^3)	Difference (mm^3)	Initial Vol. (mm^3)	Final Vol. (mm^3)	Difference (mm^3)	Initial Vol. (mm^3)	Final Vol. (mm^3)	Difference (mm^3)
8	8.460	8.920	0.460	14.630	15.050	0.420	15.530	16.000	0.470
16	8.460	9.050	0.590	14.630	15.200	0.570	15.530	16.170	0.640
24	8.460	9.220	0.760	14.630	15.340	0.710	15.530	16.300	0.770
32	8.460	9.370	0.910	14.630	15.470	0.840	15.530	16.300	0.770
40	8.460	9.490	1.030	14.630	15.600	0.970	15.530	16.390	0.860
48	8.460	9.540	1.080	14.630	15.660	1.030	15.530	16.400	0.870
56	8.460	9.550	1.090	14.630	15.690	1.060	15.530	16.420	0.890

Table-3.7 Cumulative weight change in treated fiber composites for saline treatment

Types of composite	Washed			Washed and Acetone treated			Washed and Alkali treated		
Treatment (hrs)	Initial Vol. (mm^3)	Final Vol. (mm^3)	Difference (mm^3)	Initial Vol. (mm^3)	Final Vol. (mm^3)	Difference (mm^3)	Initial Vol. (mm^3)	Final Vol. (mm^3)	Difference (mm^3)
8	9.670	9.960	0.290	14.360	14.590	0.230	14.510	14.690	0.180
16	9.670	10.140	0.470	14.360	14.810	0.450	14.510	14.760	0.250
24	9.670	10.270	0.600	14.360	14.930	0.570	14.510	14.810	0.300
32	9.670	10.420	0.750	14.360	15.040	0.680	14.510	14.980	0.470
40	9.670	10.530	0.860	14.360	15.150	0.790	14.510	15.100	0.590
48	9.670	10.660	0.990	14.360	15.190	0.830	14.510	15.190	0.680
56	9.670	10.670	1.000	14.360	15.190	0.830	14.510	15.190	0.680

Table-3.8 Cumulative weight change in treated fiber composites for subzero treatment

Types of composite	Washed			Washed and Acetone treated			Washed and Alkali treated		
Treatment (hrs)	Initial Vol. (mm^3)	Final Vol. (mm^3)	Difference (mm^3)	Initial Vol. (mm^3)	Final Vol. (mm^3)	Difference (mm^3)	Initial Vol. (mm^3)	Final Vol. (mm^3)	Difference (mm^3)
8	12.560	12.730	0.170	9.990	10.140	0.150	13.610	13.720	0.110
16	12.560	12.740	0.180	9.990	10.160	0.170	13.610	13.730	0.120
24	12.560	12.760	0.200	9.990	10.170	0.180	13.610	13.750	0.140
32	12.560	12.770	0.210	9.990	10.170	0.180	13.610	13.770	0.160
40	12.560	12.780	0.220	9.990	10.170	0.180	13.610	13.770	0.160
48	12.560	12.780	0.220	9.990	10.170	0.180	13.610	13.770	0.160
56	12.560	12.780	0.220	9.990	10.170	0.180	13.610	13.770	0.160

Table-3.9 Mechanical properties of treated bagasse fiber epoxy composite

Fiber content (%)	Type of fiber	Flexural Strength (MPa)	Tensile Strength (MPa)	Impact Strength (KJ/m^2)
20	Untreated	59.75	64.54	26.5
20	Acetone treated	61.79	86.64	28.69
20	Alkali treated	72.85	93.57	35.21

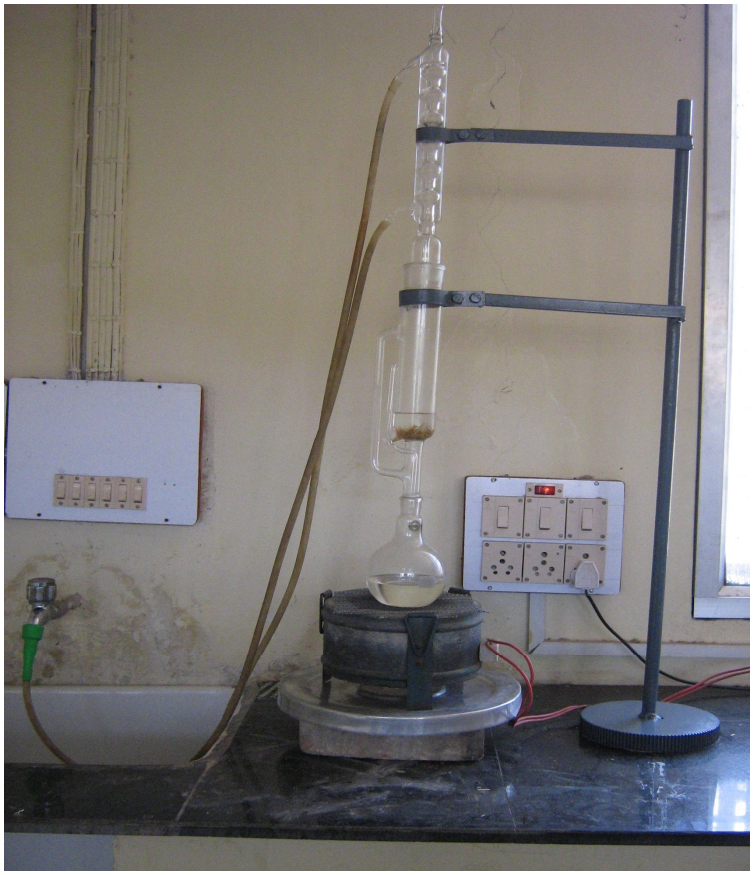

Figure-3.1 Soxhlet Extractor

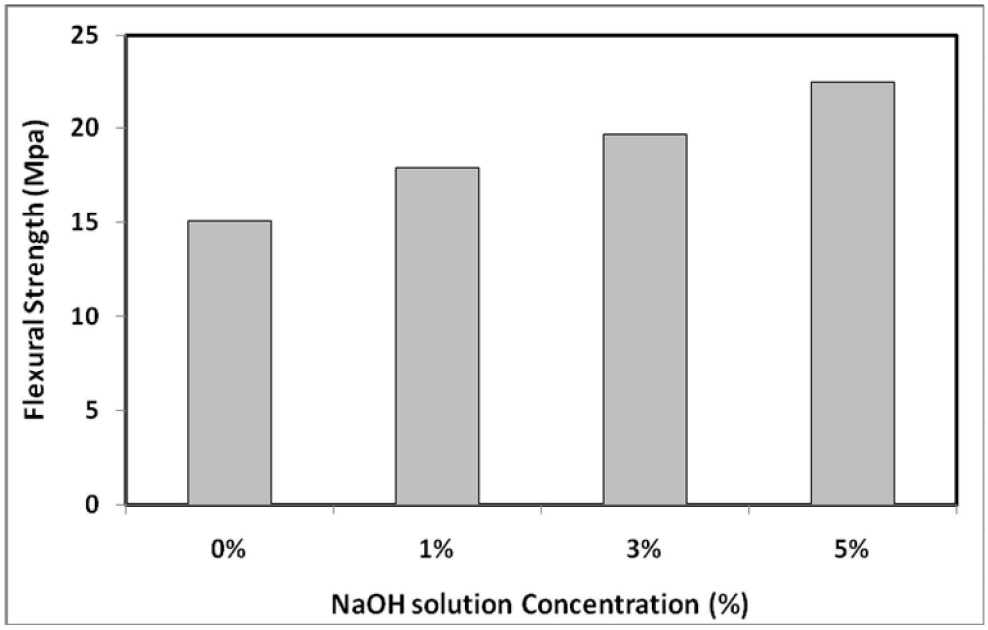

Figure-3.2 Effect of alkali concentration on mechanical properties of composites

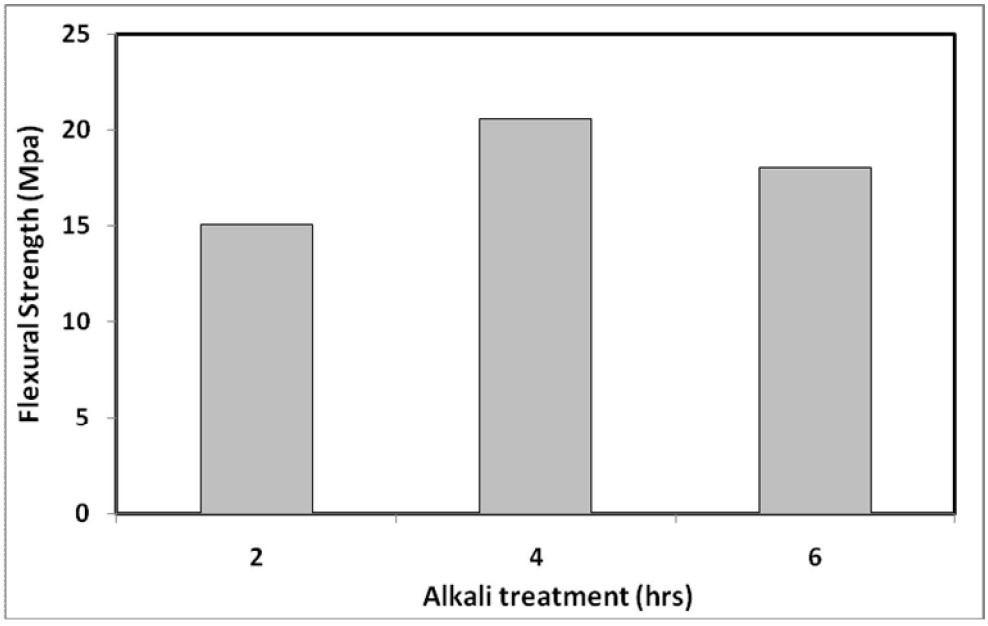

Figure-3.3 Effect of alkali treatment on mechanical properties of composites

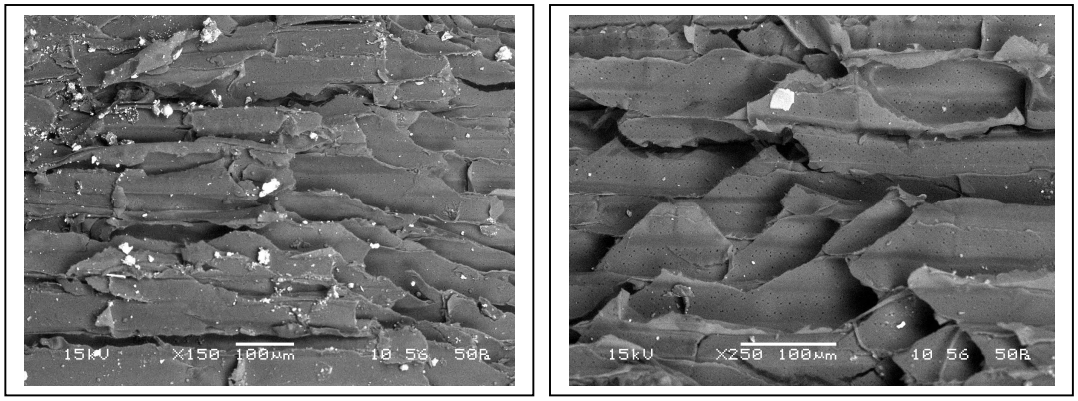

(a) (b)

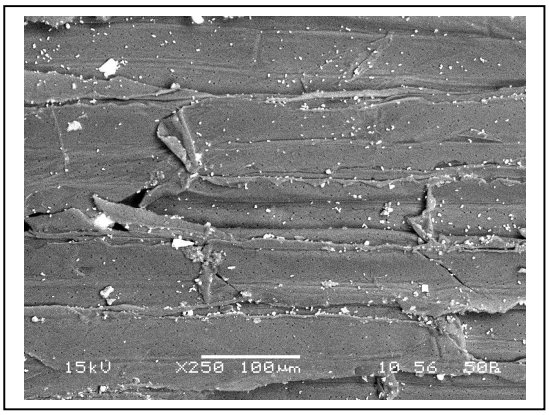

(c)

Figure-3.4 SEM of bagasse fibers (a) before treatment, (b) after acetone and (c) alkali treatment

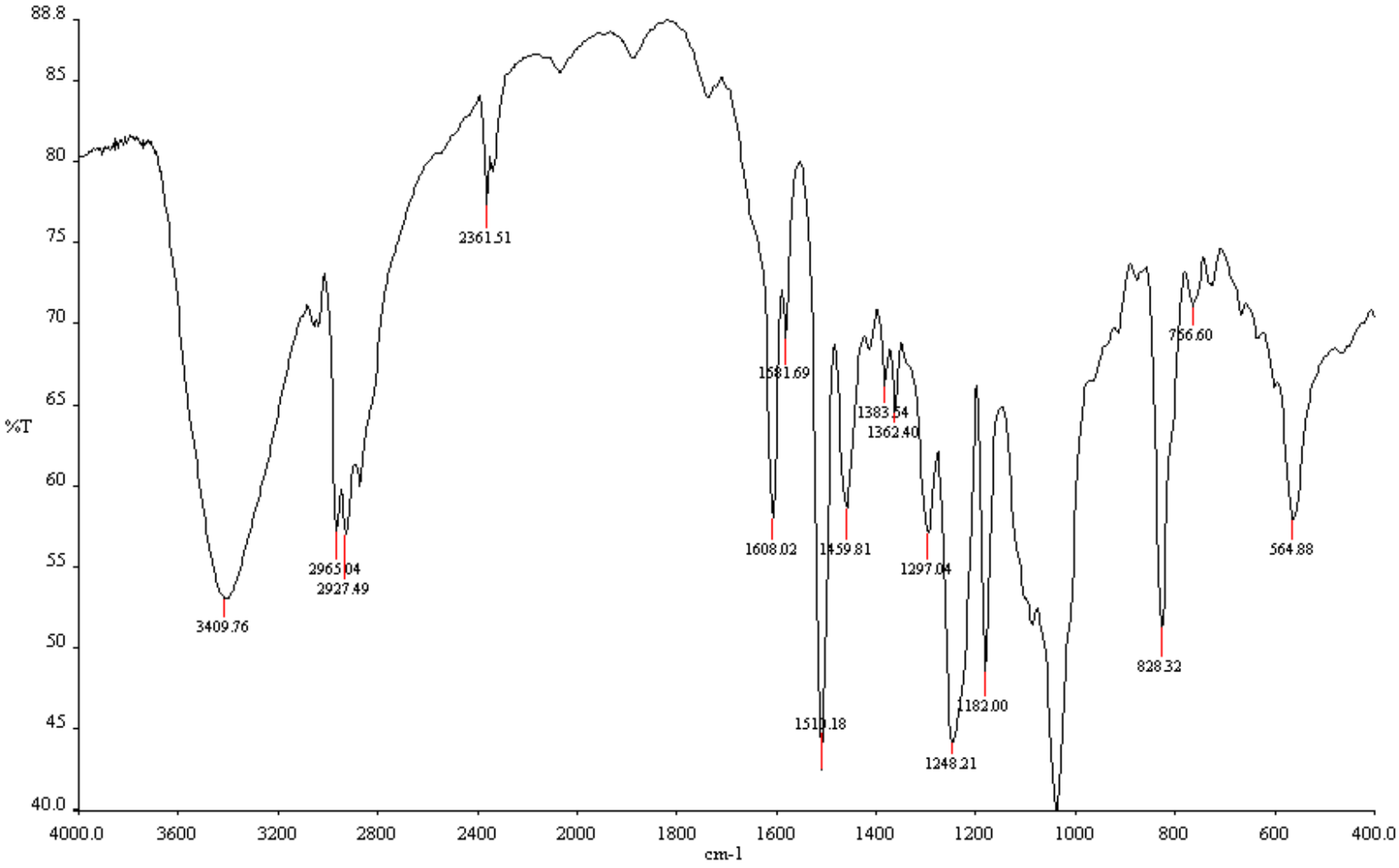

Figure-3.5(a) FTIR spectra of bagasse fiber before chemical modification

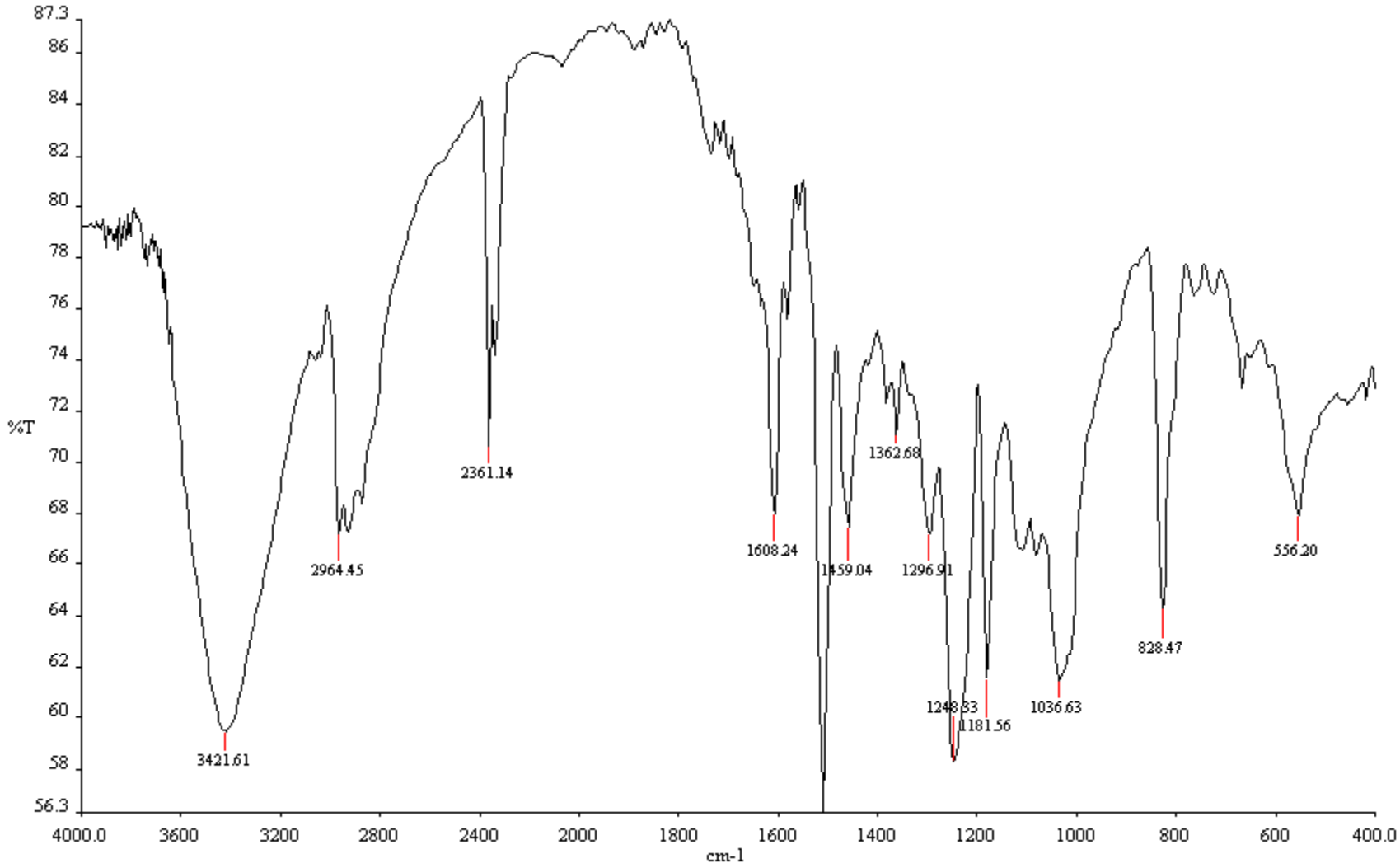

Figure-3.5(b) FTIR spectra of bagasse fiber after acetone treatment

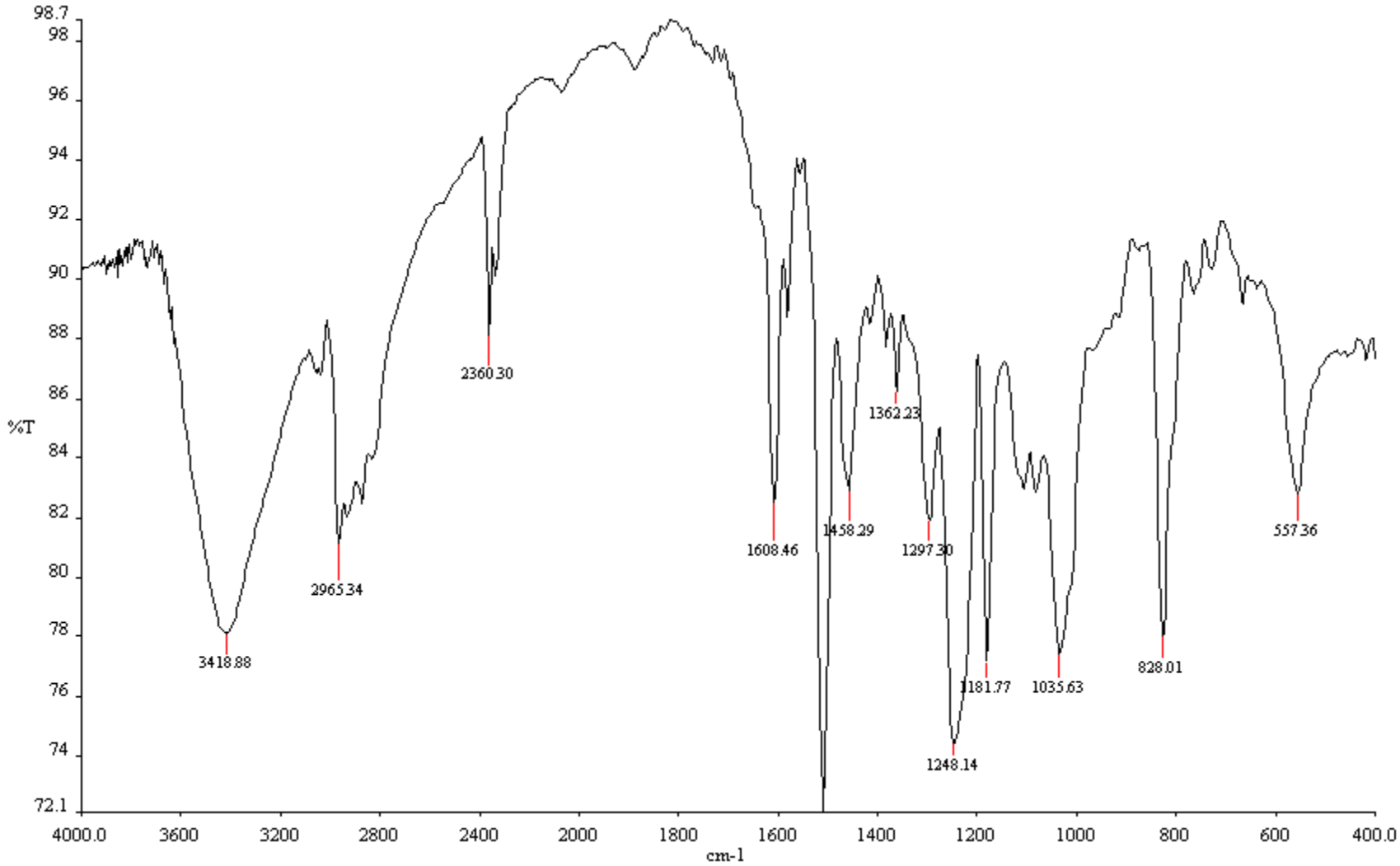

Figure-3.5(c) FTIR spectra of bagasse fiber after alkali treatment

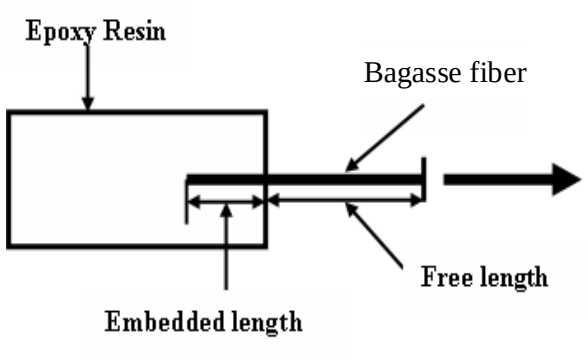

Figure-3.6 Schematic representation of pull out test

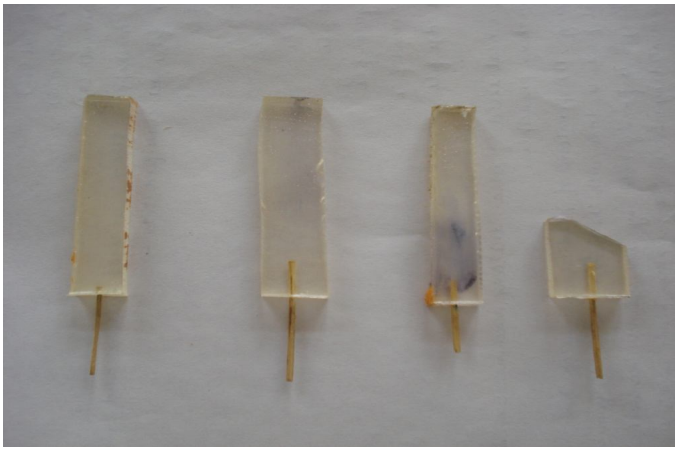

Figure-3.7 Specimen for pullout test

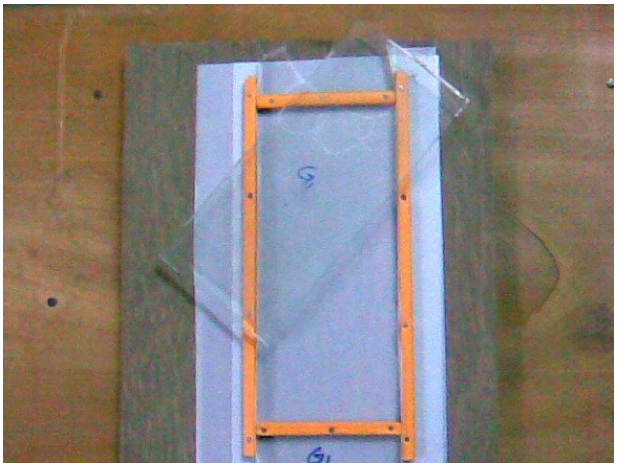

Figure-3.8 Mold used for composite preparation

(a)

(b) **(c)**

Figure-3.9 (a) Photograph of composite slab and (b) Specimen for Tensile test and (c) Flexural Test

Figure-3.10 Universal Testing Machine

Figure-3.11 Universal Testing machine with the specimen in loading position

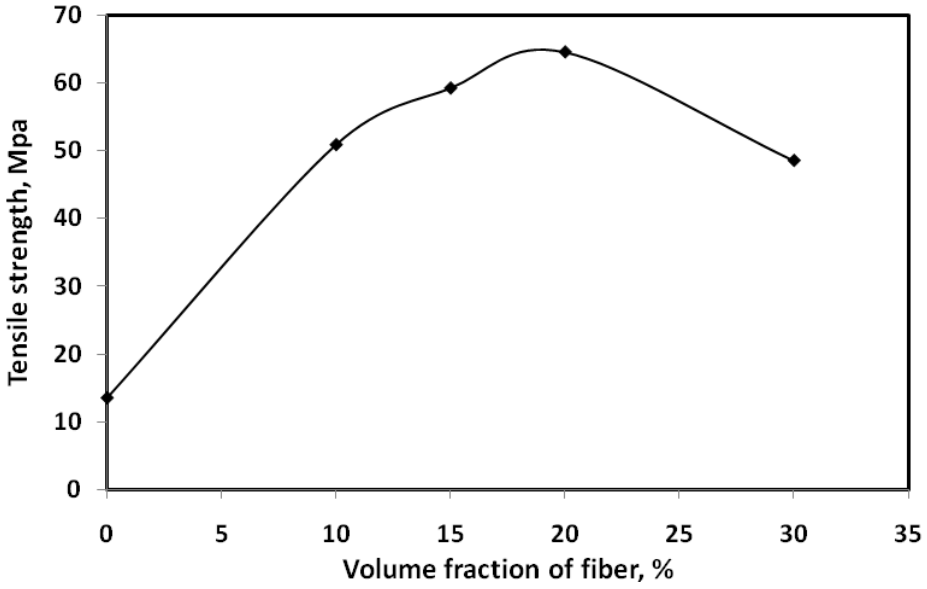

Figure-3.12 Variation of tensile strength with different volume fraction of fiber composites

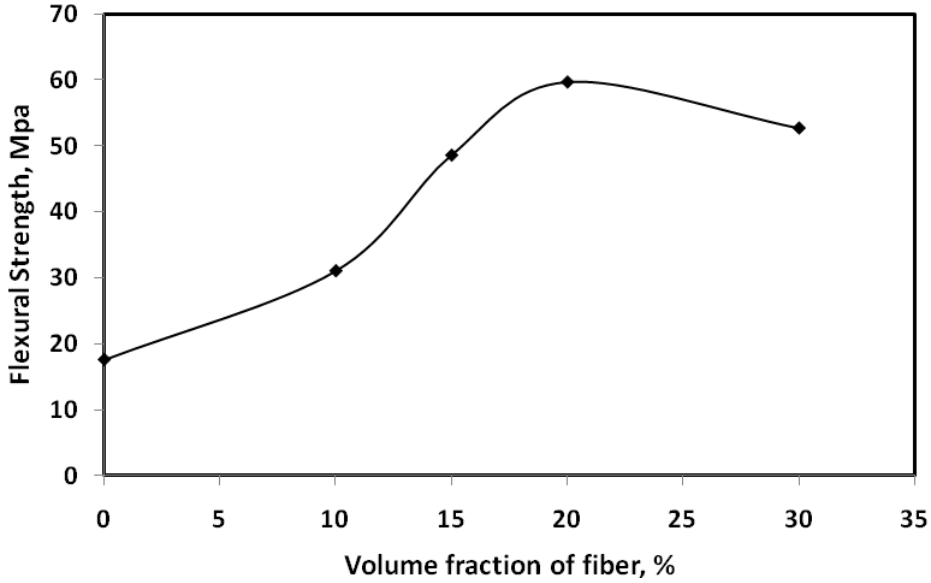

Figure-3.13 Variation of flexural strength with different volume fraction of fiber composites

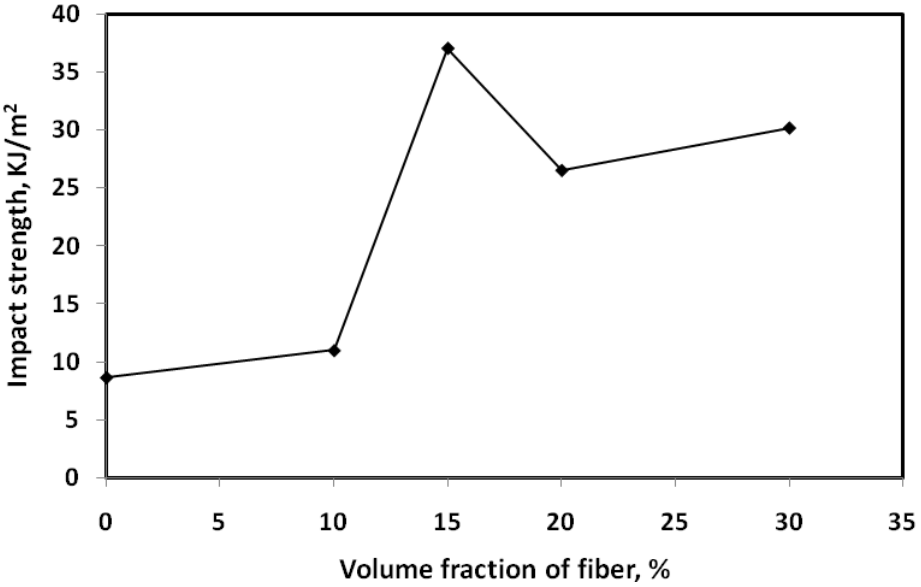

Figure-3.14 Variation of impact strength with different volume fraction of fiber composites

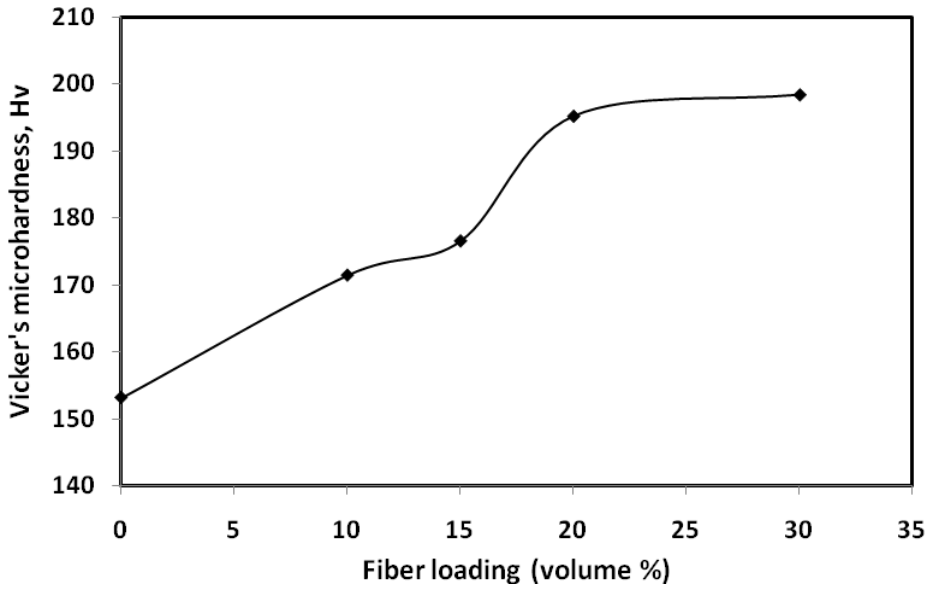

Figure-3.15 Variation of vicker's micro hardness values with different fiber loading conditions

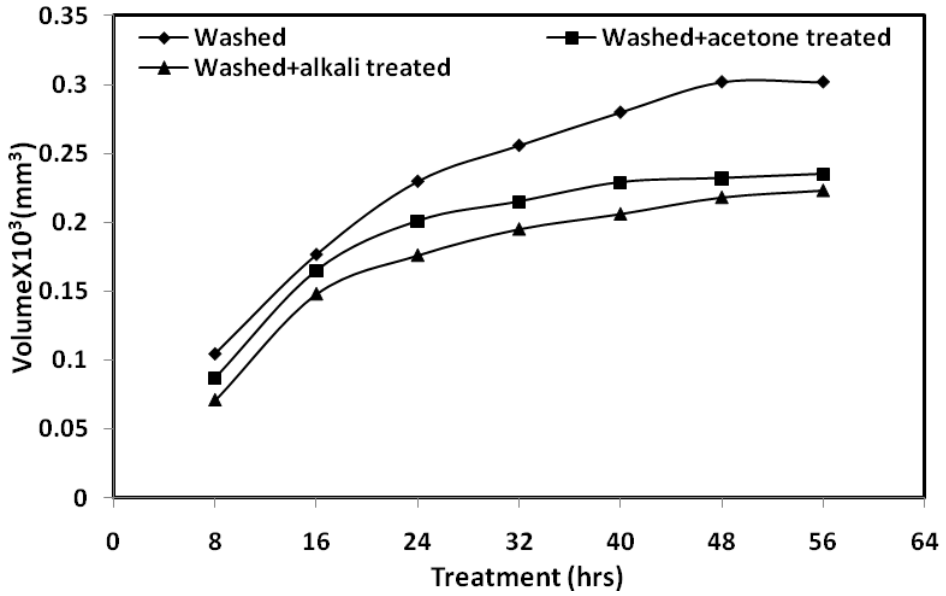

Figure-3.16 Cumulative Volume Change in Different treated fiber Composites for different time of exposure under steam treatment

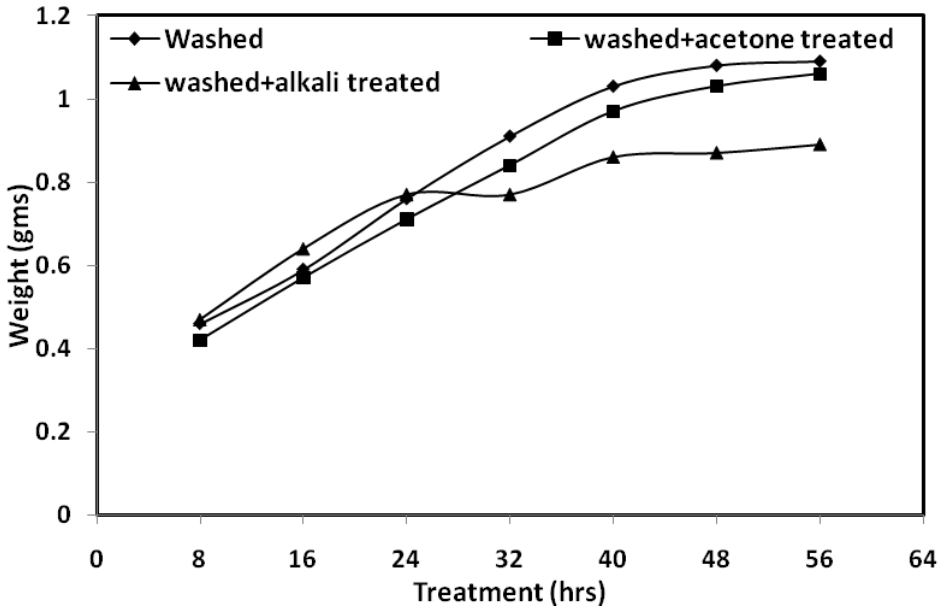

Figure-3.17 Time dependent cumulative weight change (due to % of moisture absorption) for different treated fiber composites exposed to steam condition

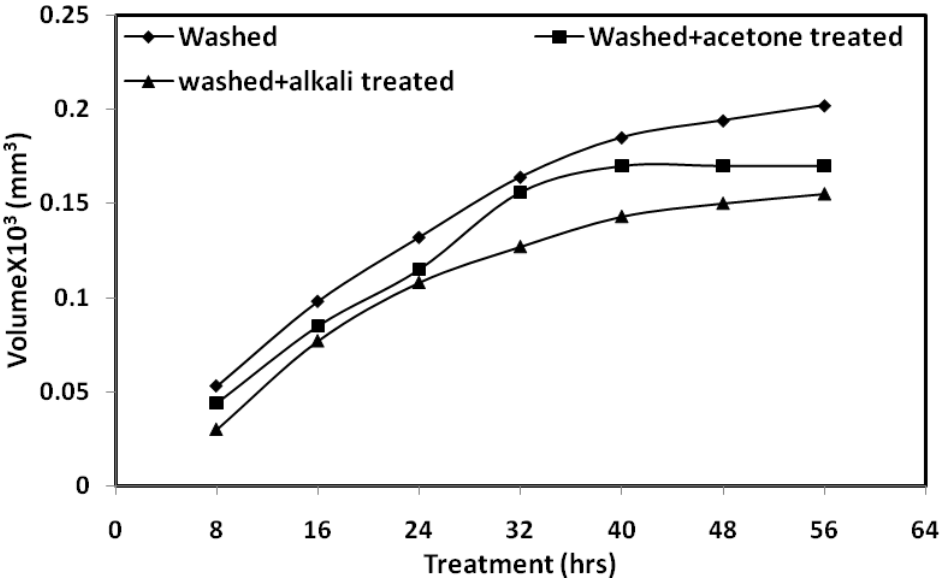

Figure-3.18 Cumulative Volume Change in Different treated fiber Composites for different time of exposure under saline treatment

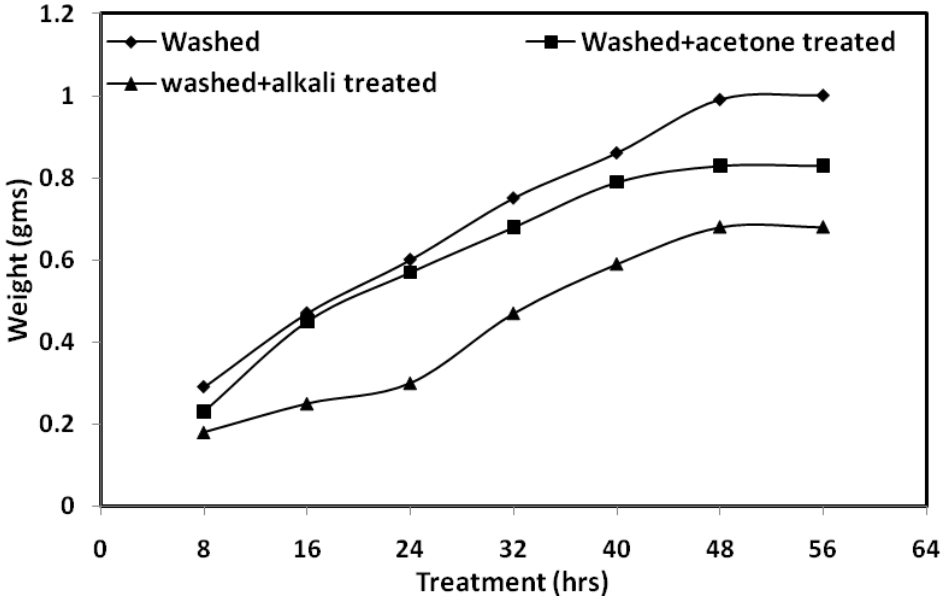

Figure-3.19 Time dependent cumulative weight change (due to % of moisture absorption) for different treated fiber composites exposed to saline condition

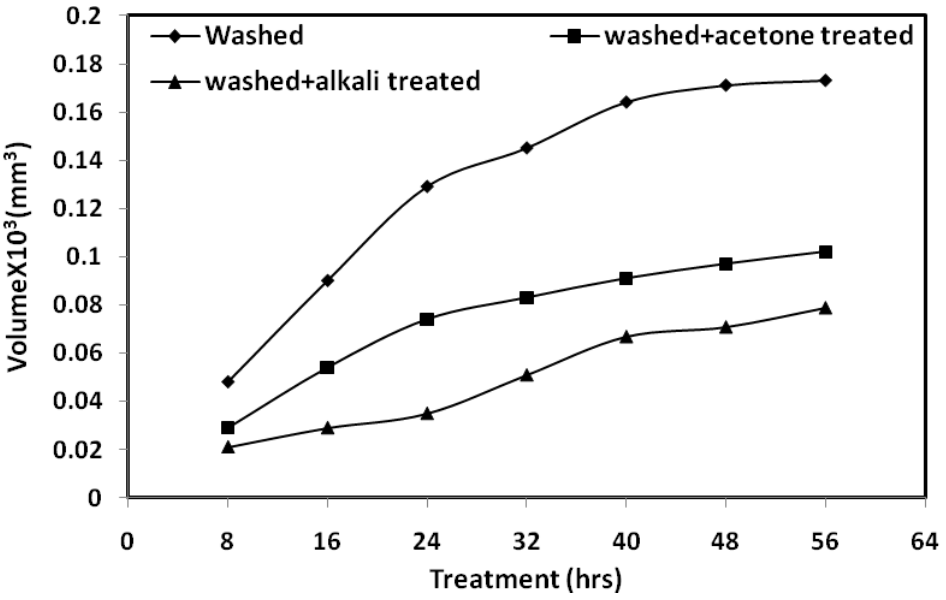

Figure-3.20 Cumulative Volume Change in Different treated fiber Composites for different time of exposure under subzero treatment

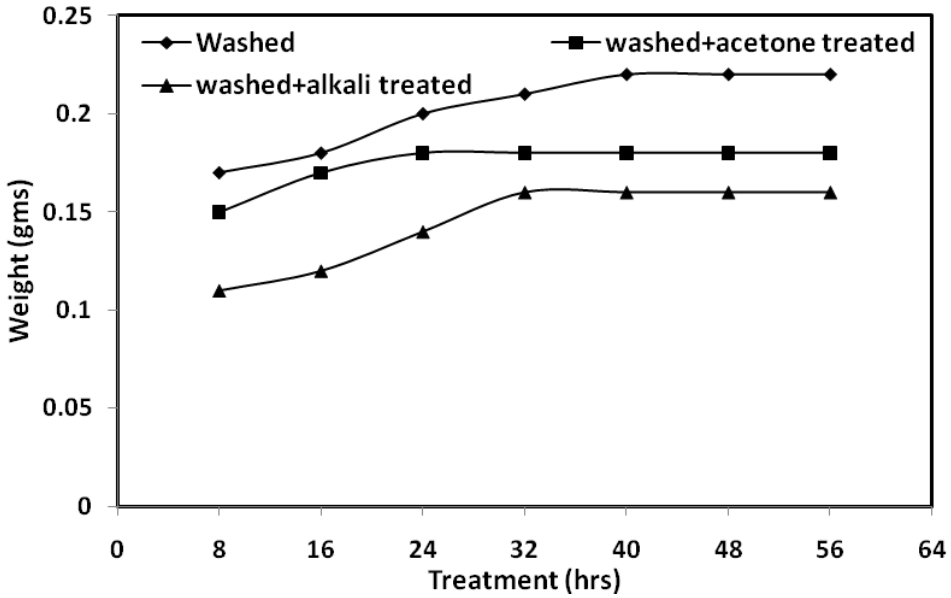

Figure-3.21 **Time dependent cumulative weight change (due to % of moisture absorption) for different treated fiber composites exposed to subzero condition**

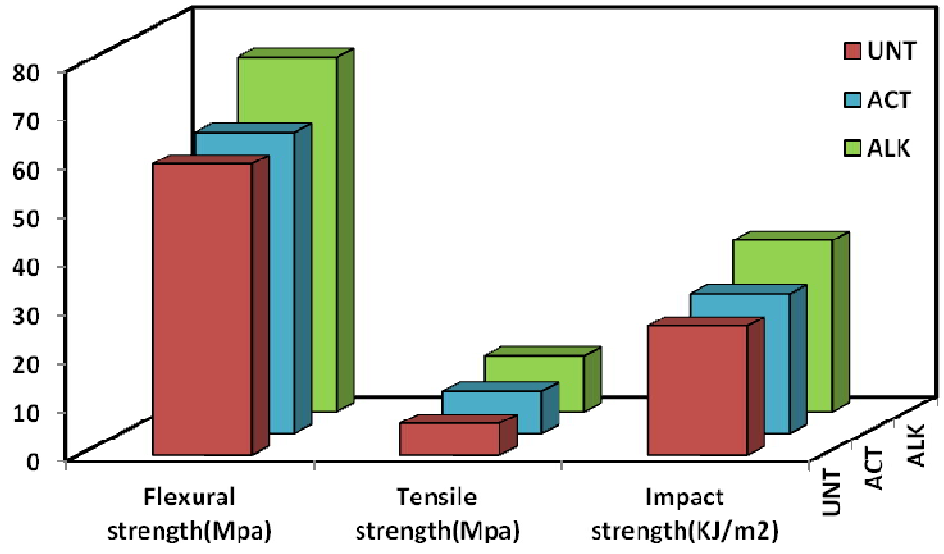

Figure-3.22 **Comparative graphs of the mechanical properties of 20 % volume fraction of composites after chemical treatment of fibers**

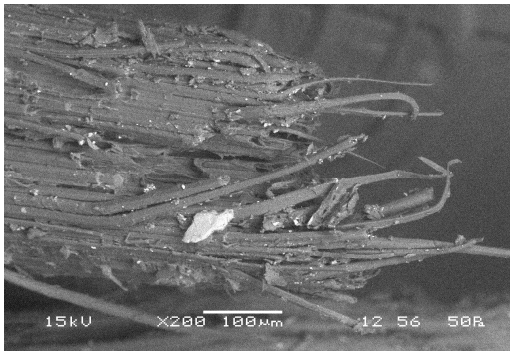

(a)

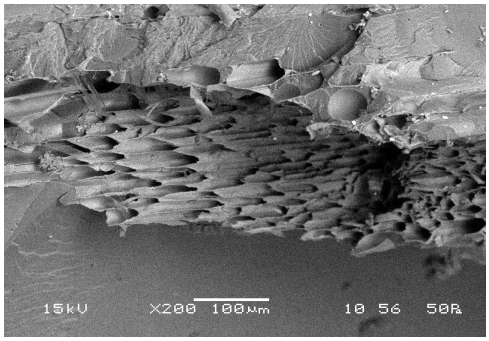

(b)

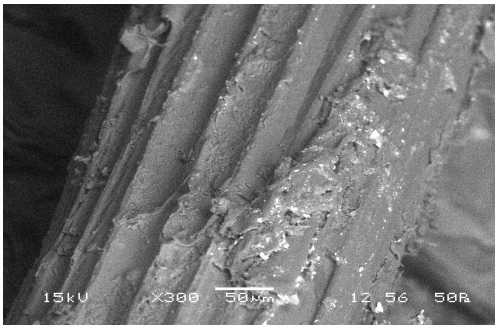

(c)

Figure-3.23 The fracture surface of the samples treated with acetone subjected to (a) Steam (b) Subzero (c) Saline treatment

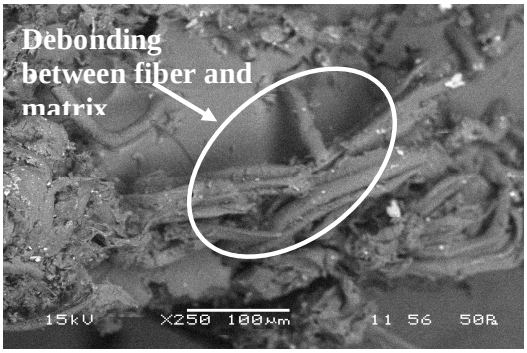

(a)

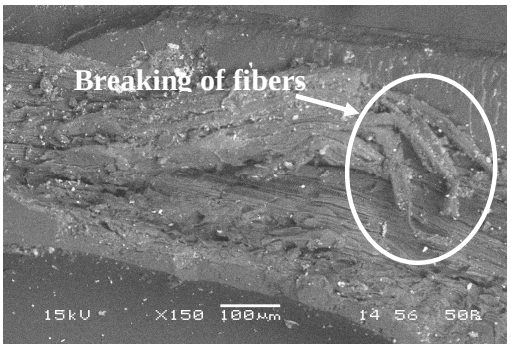

(b)

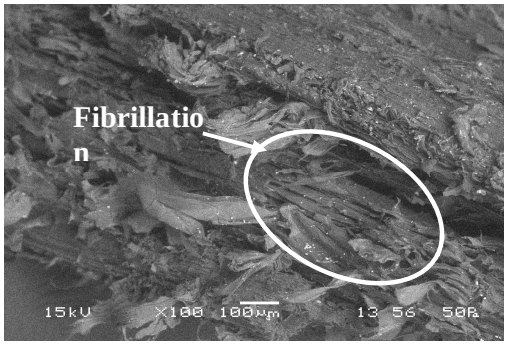

(c)

Figure-3.24 The fracture surface of the samples treated with alkali subjected to (a) Steam (b) Subzero(c) Saline treatment

Chapter 4

ABRASIVE WEAR BEHAVIOUR OF BAGASSE FIBER EPOXY COMPOSITES

Chapter-4

4.1 INTRODUCTION

Wear is probably the most important yet the least understood aspect of tribology. It is certainly the youngest of the tri of topics, friction, lubrication and wear, to attract scientific attention, although its practical significance has been recognizes throughout the ages. The findings of Guillaume Amontons in 1699 [110] establishing scientific studies of friction are almost of 300 years age, while Petrov [111], Tower [112] and Reynolds [113] brought enlightenment to the subject of lubrication a century ago in the hectic 1880s. Substantial Studies of wear can be associated only with the five decades that have elapsed since R. Holm [114] explored the fundamental aspects of surface interactions encountered in electrical contacts.

One third of our global energy consumption has been devoured wastefully in friction. In addition to the primary saving of energy, very significant additional economics can be made by the reduction of the cost involved in the manufacture and replacement of prematurely worn out components. The dissipation of energy by wear impairs strongly to the national economy and the life style of most of the peoples. So, the effective decrease and control of wear of metals are always desired [115].

Wear causes an enormous annual expenditure by industry and consumers. Most of this is replacing or repairing equipment that has worn to the extent that it no longer performs a useful function. For many machine components, this occurs after a very small percentage of the total volume has been worn away. For some industries, such as agriculture, as many as 40% of the components replaced on equipment have failed by abrasive wear. Other major sources of expenditure are losses production consequential upon lower efficiency and plant shutdown, the need to invest more frequently in capital equipment and increased energy consumption as equipment wears. Estimates of direct cost of abrasive wear to industrial nations vary from 1 to 4 % of gross national product and Rigney [116] has estimated that about 10% of all energy generated by man is dissipated in various friction processes.

Wear is not an intrinsic material property but characteristics of the engineering system which depend on load, speed, temperature, hardness, presence of foreign material and the environmental condition [117]. Widely varied wearing conditions cause wear of materials. It may be due to surface damage or removal of material from one or both of two solid surfaces in a sliding, rolling or impact motion relative to one another. In most cases wear occurs through surface interactions at asperities. During relative motion, material on contacting surface may be removed from a surface, may result in the transfer to the mating surface, or may break loose as a wear particle. The wear resistance of materials is related to its microstructure may take place during the wear process and hence, it seems that in wear research emphasis is placed on microstructure [118]. Wear of material depends on many variables, so wear research program must be planned systematically. Therefore researchers have normalized some of the data to make them more useful. The wear map proposed by Lim [119] is very much useful in this regard to understand the wear mechanism in different sliding conditions as well as the anticipated rates of wear.

4.2 RECENT TRENDS IN WEAR RESEARCH

Numerous wear researches have been carried out in the 1940's and 1950's by mechanical engineers and metallurgists to generate data for the construction of motor drive, trains, brakes, bearings, bushings and other types of moving mechanical assemblies [120].

It became apparent during the survey that wear of materials was a prominent topic in a large number of the responses regarding some future priorities for research in tribology. Some 22 experienced technologists in this field, who attended the 1983 'Wear of Materials Conference' in Reston, prepared a ranking list [121]. Their proposals with top priority were further investigations of the mechanism of wear and this no doubt reflects the judgments that particular effects of wear should be studied against a background of the basic physical and chemical processes involved in surface interactions. The list proposed is shown in Table - 4.1.

Peterson [122] reviewed the development and use of tribo-materials and concluded that metals and their alloys are the most common engineering materials used in wear applications. Grey cast iron for example has been used as early as 1388. Much of the wear

research conducted over the past 50 years is in ceramics, polymers, composite materials and coatings [123].

Table-4.1 Priority in wears research [121]

Ranking	Topics
1.	Mechanism of Wear
2.	Surface Coatings and treatments
3.	Abrasive Wear
4.	Materials
5.	Ceramic Wear
6.	Metallic Wear
7.	Polymer Wear
8.	Wear with Lubrication
9.	Piston ring-cylinder liner Wear
10.	Corrosive Wear
11.	Wear in other Internal Combustion Machine component

Wear of materials encountered in industrial situations can be grouped into different categories as shown in Table - 4.2. Though there are situations where one type changes to another or where two or more mechanism plays together.

Table-4.2 Type of wear in industry [120]

Type of wear in Industry	Approximate percentage involved
Abrasive	50
Adhesive	15
Erosion	8
Fretting	8
Chemical	5

4.3 THEORY OF WEAR

Wear occurs as a natural consequence when two surfaces with a relative motion interact with each other. Wear may be defined as the progressive loss of material from contacting surfaces in relative motion. Scientists have developed various wear theories in which the Physico-Mechanical characteristics of the materials and the physical conditions (e.g. the resistance of the rubbing body and the stress state at the contact area) are taken in to consideration. In 1940 Holm [114] starting from the atomic mechanism of wear, calculated the volume of substance worn over unit sliding path.

Barwell and Strang [124] in 1952: Archard [125] in 1953 and Archard and Hirst [126] in 1956 developed the adhesion theory of wear and proposed a theoretical equation identical in structure with Holm's equation. In 1957, Kragelski [127] developed the fatigue theory of wear. This theory of wear has been widely accepted by scientists in different countries. Because of the Asperities in real bodies, their interactions in sliding is discrete, and contact occurs at individual locations, which, taken together, form the real contact area. Under normal force the asperities penetrate into each other or are flattened out and in the region of real contact points corresponding stress and strain rise. In sliding, a fixed volume of material is subjected to the many times repeated action, which weakens the material and leads finally to rupture. In 1973, Fleischer [128] formulated his energy theory of wear. The main concept of this theory is that the separation of wear particles requires that a certain volume of material accumulates a specific critical store of internal energy. It is known that a large part of the work done in sliding is dissipated as heat, and that a small proportion of it accumulates in the material as internal potential energy. When the energy attains a critical value, plastic flow of the material occurs in this volume or a crack is formed. Further theories of wear are found in [127]. Though all the theories are based on different mechanisms of wear, the basic consideration is the frictional work.

In past few decades, numerous research works have been carried out on abrasive wear performance of polymer and polymer based composite in view of their extensive application in the field of industry and agricultural sectors where abrasive wear is a

predominant mode of failure. Conveyor aids, vanes, gears, bushes, seals, bearings, chute liners etc. are some examples of their applications [129-133]. Since abrasive wear is the most severe form of wear accounting for 50% of total wear, several researches have been devoted to exploring abrasive wear of polymer composites. Evans *et al* [134] studied the abrasion wear behavior for 18 polymers and they noticed that low density polyethylene (LDPE) showed the lowest wear rate in abrasion against rough mild steel, but a higher wear rate in abrasion with coarse corundum paper. Unal *et al* [135] studied abrasive wear behaviour of polymeric materials. They concluded that the specific wear rate decreases with the decrease in abrasive surface roughness. They also concluded that, the abrasive wear include micro-cracking, micro-cutting, and micro-ploughing mechanisms. Whereas in another investigation [136] they concluded that the sliding speed has a stronger effect on the specific wear rate. Shipway and Ngao [137] investigated the abrasive behaviour of polymeric materials in micro-scale level. They concluded that the wear behaviour and wear rates of polymers depended critically on the polymer type. Harsha and Tewari [138] investigated the abrasive wear behaviour of poly aryl ether ketone (PAEK) and its composites against SiC abrasive paper. They concluded that the sliding distance, load, abrasive grit size have a significant influence on abrasive wear performance. Further there are many references that illustrate the influence of fillers and fiber reinforcement on the abrasive wear resistance of polymeric composites. Cirino *et al* [139, 140] investigated the sliding and abrasive wear behavior of poly ether-ether-ketone (PEEK) with different continuous fiber types and reported that the wear rate decreases with increase in the fiber content. Chand *et al* [141] studied low stress abrasive wear behavior of short E-glass fiber reinforced polymer composites with and without fillers by using rubber wheel abrasion test apparatus. They reported that higher weight fraction of glass fibers (45%) in the composites improves the wear resistance as compared to the composite containing less glass fibers (40%). Bijwe *et al* [142] tested polyamide 6, poly-tetra-fluoro-ethylene (PTFE) and their various composites in abrasive wear under dry and multi-pass conditions against silicon carbide (SiC) paper on pin-on-disc arrangement. They concluded that the polymers without fillers had better abrasive wear resistance than their composites. Liu *et al* [143] investigated the abrasive wear behaviour of ultrahigh molecular weight polyethylene (UHMWPE) polymer. They concluded that the applied load is the main parameter and the wear resistance improvement of filler reinforced UHMWPE was attributed to the combination of hard particles which prevent the formation of deep, wide and continuous furrows.

With regards to the usage of natural fiber as reinforcement for tribological application in polymeric composite, few works have been attempted. However, in recent years, some work has been done on natural fiber like jute [7], cotton [144, 145], oil palm [146], coir [147], kenaf [148], betel-nut [149], betel palm [150], wood flour [151] and bamboo powder [152] as reinforcement. In these works, the wear resistance of polymeric composites has been improved when natural fiber introduced as reinforcement.

4.4 TYPES OF WEAR

In most basic wear studies where the problems of wear have been a primary concern, the so-called dry friction has been investigated to avoid the influences of fluid lubricants.

Dry friction is defined as friction under not intentionally lubricated conditions but it is well known that it is friction under lubrication by atmospheric gases, especially by oxygen [153].

A fundamental scheme to classify wear was first outlined by Burwell and Strang [154]. Later Burwell [155] modified the classification to include five distinct types of wear, namely (1) Abrasive (2) Adhesive (3) Erosive (4) Surface fatigue (5) Corrosive.

4.4.1 Abrasive wear

Abrasive wear can be defined as the wear that occurs when a hard surface slides against and cuts groove from a softer surface. It can be account for most failures in practice. Hard particles or asperities that cut or groove one of the rubbing surfaces produce abrasive wear. This hard material may be originated from one of the two rubbing surfaces. In sliding mechanisms, abrasion can arise from the existing asperities on one surface (if it is harder than the other), from the generation of wear fragments which are repeatedly deformed and hence get work hardened for oxidized until they became harder than either or both of the sliding surfaces, or from the adventitious entry of hard particles, such as dirt from outside the system. Two body abrasive wear occurs when one surface (usually harder than the second) cuts material away from the second (figure 4.1), although this mechanism very often changes to three body abrasion as the wear debris then acts as an abrasive between the

two surfaces. Abrasives can act as in grinding where the abrasive is fixed relative to one surface or as in lapping where the abrasive tumbles producing a series of indentations as opposed to a scratch. According to the recent tribological survey, abrasive wear is responsible for the largest amount of material loss in industrial practice [156].

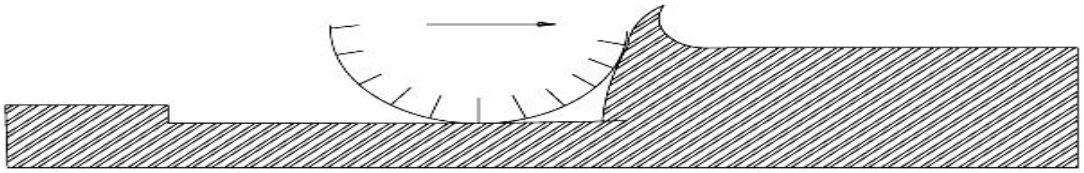

Figure-4.1 Schematic representations of the abrasion wear mechanism

4.4.2 Adhesive wear

Adhesive wear can be defined as the wear due to localized bonding between contacting solid surfaces leading to material transfer between the two surfaces or the loss from either surface (figure 4.2). For adhesive wear to occur it is necessary for the surfaces to be in intimate contact with each other. Surfaces, which are held apart by lubricating films, oxide films etc. reduce the tendency for adhesion to occur.

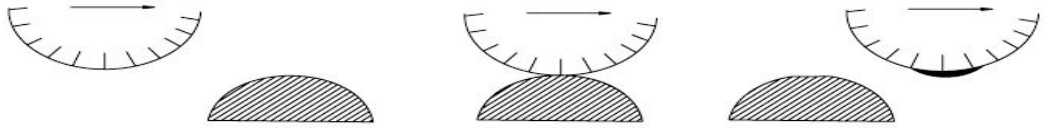

Figure-4.2 Schematic representations of the adhesive wear mechanism

4.4.3 Erosive wear

Erosive wear can be defined as the process of metal removal due to impingement of solid particles on a surface. Erosion is caused by a gas or a liquid, which may or may not carry, entrained solid particles, impinging on a surface (figure 4.3). When the angle of impingement is small, the wear produced is closely analogous to abrasion. When the angle of impingement is normal to the surface, material is displaced by plastic flow or is dislodged by brittle failure.

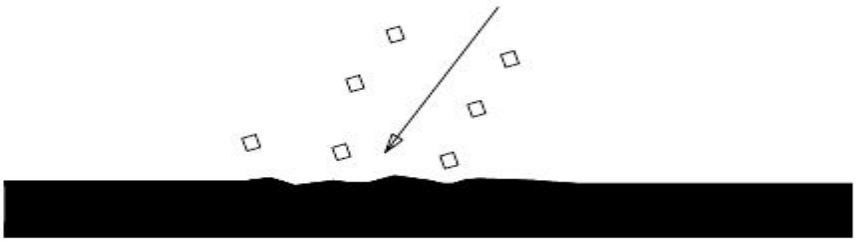

Figure-4.3 Schematic representations of the erosive wear mechanism

4.4.4 Surface fatigue wear

Wear of a solid surface is caused by fracture arising from material fatigue. The term 'fatigue' is broadly applied to the failure phenomenon where a solid is subjected to cyclic loading involving tension and compression above a certain critical stress. Repeated loading causes the generation of micro cracks, usually below the surface, at the site of a pre-existing point of weakness. On subsequent loading and unloading, the micro crack propagates. Once the crack reaches the critical size, it changes its direction to emerge at the surface, and thus flat sheet like particles is detached during wearing (figure 4.4). The number of stress cycles required to cause such failure decreases as the corresponding magnitude of stress increases. Vibration is a common cause of fatigue wear.

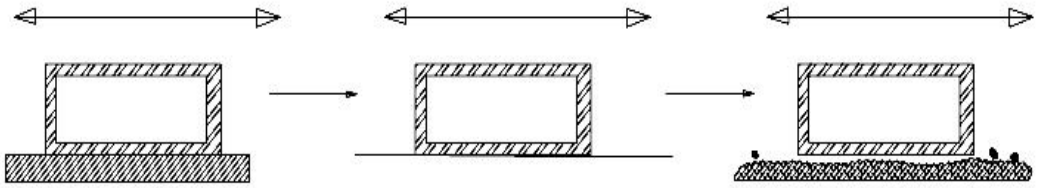

Figure-4.4 Schematic representations of the surface fatigue wear mechanism

4.4.5 Corrosive wear

Most metals are thermodynamically unstable in air and react with oxygen to form an oxide, which usually develop layer or scales on the surface of metal or alloys when their interfacial bonds are poor. Corrosion wear is the gradual eating away or deterioration of unprotected metal surfaces by the effects of the atmosphere, acids, gases, alkalis, etc. This type of wear creates pits and perforations and may eventually dissolve metal parts.

4.5 SYMPTOMS OF WEAR

A summary of the appearance and symptoms of different wear mechanism is indicated in Table - 4.3 and the same is a systematic approach to diagnose the wear mechanisms.

Table-4.3 Symptoms and appearance of different types of wear [157]

Types of wear	Symptoms	Appearance of the worn-out surface
Abrasive	Presence of clean furrows cut out by abrasive particles.	Grooves
Adhesive	Metal transfer is the prime symptoms.	Seizure, catering rough and torn-out surfaces.
Erosion	Presence of abrasives in the fast moving fluid and short abrasion furrows.	Waves and troughs.
Corrosion	Presence of metal corrosion products.	Rough pits or depressions.
Fatigue	Presence of surface or subsurface cracks accompanied by pits and spalls.	Sharp and angular edges around pits.
Impacts	Surface fatigue, small sub-micron particles or formation of spalls.	Fragmentation, peeling and pitting.
Delamination	Presence of subsurface cracks parallel to the surface with semi-dislodged or loose flakes.	Loose, long and thin sheet like particles
Fretting	Production of voluminous amount of loose debris.	Roughening, seizure and development of oxide ridges
Electric attack	Presence of micro craters or a track with evidence of smooth molten metal.	Smooth holes

Literature available on the rate of controlling abrasive wear mechanism demonstrates that it may change abruptly from one another at certain sliding velocities and contact loads, resulting in abrupt increases in wear rates. The conflicting results in the abrasive wear literature arise partly because of the differences in testing conditions, but they also make clear that a deeper understanding of the abrasive wear mechanism is required if an improvement in the wear resistances of the polymer matrix composites is to be achieved. This in turn requires a systematic study of the wear under different loads and velocities. It is generally recognized that abrasive wear is a characteristic of a system and is influenced by many parameters. Laboratory scale investigation if designed properly allows careful control of the tribo system whereby the effects of different variables on wear behaviour of PMCs can be isolated and determined. The data generated through such investigation under controlled conditions may help in correct interpretation of the results.

As new developments are still under way to explore innovative fields for tribo-application of natural fiber base materials, in this chapter an attempt has been made to study the potential of using bagasse fiber for tribological applications. In the current study the effect of fiber loading, sliding velocity, sliding distance and normal load on abrasive wear behaviour of chopped bagasse fiber filled epoxy composite has been evaluated and possible wear mechanism has been discussed with SEM observation.

4.6 EXPERIMENT

4.6.1 Preparation for the test specimens

Different volume fraction (10, 15 and 20 vol %) of chopped bagasse fibers (10mm length) were added to resin with required quantity of hardener. The procedure of mixing the resin is same and as per the procedure explained in chapter-3, Art-3.4.3. A steel mould has been designed specifically for the purpose, fabricated in the work-shop and used for preparation of cylindrical (pin) type specimen of length 35mm & diameter of 10 mm. The mixture of bagasse fiber and resin has been poured into the cylindrical cavity present in the mould and then the two halves of the mould are fixed properly. During fixing some of the resin mix may squeezed out. Adequate care has been taken for squeezing out of resin-mix

during preparation of composites. After closing of the mould the specimens were allowed to solidify in the mould at the room temperature for 24 hrs. For the purpose of comparison the matrix material was also cast under similar condition. After curing the samples were taken out from the mould, finished ground to required shape, sizes for wear testing. Figure 4.5 shows the details of the mold used and the fabricated samples.

4.6.2 Measurement of Density and Voids content

The density and the void content of composite sample have been determined as per ASTM-C 639 and ASTM D-2734-70 standard procedure respectively. The volume fraction of voids (V_v) in the composites was calculated by using equation:

$$V_v = \frac{\rho_t - \rho_a}{\rho_t} \tag{4.1}$$

where ρ_t and ρ_a are the theoretical and actual density of composite respectively.

The values of densities of composites both measured and theoretical are given in table 4.4. The percentage of void content presented in table indicates that void content of composites increase marginally with increase of the fiber content. According to the survey [158], the percentage of void content should be less than 3%. In case of bagasse fiber epoxy composite, for 20% reinforcement, the void content is shown to be 3.123 which seems to be within the acceptable limit.

4.6.3 Dry sliding wear test

Dry sliding wear test has been carried out under multi-pass condition on a pin-on-disc type wear testing machine (As per ASTM G-99 standard) supplied by Magnum Engineers, Bangalore. Figure-4.6 shows the experimental set up. Abrasive paper of 400 grade (grit-23 μm) has been pasted on a rotating disc (EN 32 Steel disc) of 120mm diameter using double-sided adhesive tape. The specimens under tests were fixed to the sample holder. The holder along with the specimen (Pin) was positioned at a particular track diameter. A track radius of 50 mm was selected for this experiment and was kept constant

for the entire investigation. For each test new abrasive paper was used and the sample was abraded for a total sliding distance of 452.4m. During experiment the specimen remains fixed and disc rotates. Load is applied through a dead weight loading system to press the pin against the disc. The speed of the disc or motor rpm can be varied through the controller and interval of time can be set by the help of timer provided at the control panel. The mass loss in the specimen after each test was estimated by measuring the weight of the specimen before and after each test using an electronic balance with an accuracy of ± 0.001 mg. Care has been taken that the specimen under test are continuously cleaned with woolen cloth to avoid entrapment of wear debris and to achieve uniformity in the experimental procedure. Test pieces are cleaned with acetone prior to and after each test. The machine is also fixed with a data acquisition system 'MAGVIEW-2007' software from which the frictional force that arises at the interface of the test sample and the abrasive paper could be read out/recorded directly. The condition under which the experiment has been carried out is given in Table-4.5. For a particular type of composite 25 sets of test pieces were tested.

4.6.4 Calculation for Wear

Wear rate was estimated by measuring the weight loss of the specimen after each test. The weight loss was calculated by taking the weight difference of the sample before and after each test.

The weight loss:

$$(\Delta w) = (w_a - w_b) \text{ gm} \tag{4.2}$$

where Δw is the weight loss in gm and w_a and w_b are the weight of the sample after and before the abrasion test in gm. The abrasive wear rate (W_r) which relates to the mass loss to sliding distance (L) can be calculated by using the following formula:

$$W_r = \Delta w/L \tag{4.3}$$

The friction force was recorded for each pass and then averaged over the total number of passes for each wear test. The average value of co-efficient of friction, μ of composite was calculated from the expression,

$$\mu = F_f / F_n \tag{4.4}$$

Where F_f is the average friction force and F_n is the applied load.

For characterization of the abrasive wear behavior of the composite, the specific wear rate is employed. This is defined as the volume loss of the composite per unit sliding distance and per unit applied normal load. Often the inverse of specific wear rate expresses in terms of the volumetric wear rate as

$$W_s = W_v / V_s F_n \tag{4.5}$$

where V_s is the sliding velocity. The values of weight loss, wear rate, volumetric wear rate and specific wear rate for each batch is listed in Table-4.6 to 4.54.

4.7 RESULTS AND DISCUSSION

Based on the experiment and tabulated results, various graphs are plotted and presented in figures 4.7 to 4.24 for different percentage of reinforcement under different test conditions.

Figures 4.7 to 4.10 show the variation of wear rate with sliding distance for different loads (5, 7.5, 10 and 15N) at a sliding velocity of 0.837m/s (200 RPM). It is seen from the plot that with addition of bagasse fiber the wear rate of epoxy decreases. It has also been observed that the wear rate decreases with increasing sliding distance for all the tested samples. Further it has been observed that, in all cases the range of wear rate is high at the initial stage of sliding distance and achieved a steady state at a distance of about 300 m. In other words, there is less removal of material at longer sliding distances and this could be due to the less penetration of abrasive particle in to the composite sample. Because at initial stage the abrasive paper is fresh and then become smooth due to filling of the space between abrasives by wear debris, which consequently reduce the depth of penetration. It is also observed that the 20 vol% bagasse fiber reinforced composite shows a minimum wear rate under all testing conditions. Since the trend for 300 and 400 RPM remains same, it has not been presented here.

The variation of specific wear rate of neat epoxy and different volume fraction of fiber (10, 15 and 20%) composites with sliding velocity at varying applied loads (5N, 7.5N, 10N and 15N) are presented in figures 4.11 to 4.14. It is seen that for lower loading conditions (5N and 7.5N) the increase in specific wear rate is linear with sliding velocity. But at higher loading conditions (10N and 15N) when the velocity increases from 1.256 m/s to 1.675 m/s, there is a decrease in specific wear rate. It is also noted that the wear rate is very high for neat epoxy than other composite samples. During sliding the normal and tangential loads are transmitted through the contact points by adhesive and plowing actions, whereas the hard asperities on the counter face or the hard particles between the sliding surfaces plow and micro cut the soft surfaces. Thus, during sliding both adhesive and abrasive wear mechanisms are operative, resulting in powdery wear debris at different sliding velocities. The frictional heat increases with increase in sliding velocity, which reduced the brittleness of both matrix and reinforcing fibers. This behavior may be attributed to brittleness of the bagasse fibers.

Figures 4.15 to 4.18 show the variation of specific wear rate of the composite for different fiber volume fractions. It is clear from the plot that, irrespective of sliding velocity the specific wear rate decreases with increase in fiber volume fraction. For sliding velocity of 0.837m/s and 1.675m/s, the decrease of specific wear rate is at a faster rate in comparison to velocity of 1.256m/s. This is more pronounced at higher load i.e. at 7.5N and 10N. However the decrease is marginal for velocity of 1.256m/s from 15 to 20% of fiber volume fraction. Thus it can be concluded here that 20% fiber volume fraction can be taken as optimum with a velocity of 1.256m/s for the composite under study.

Figures 4.19 to 4.21 show the variation of volumetric wear rate with normal loads for different volume fraction of fiber composites at different velocities. It is observed from the plots that volumetric wear rate increases with the increase of normal loads. Wear rate was relatively low at normal load (5N) because of lower penetration and less number of abrasive particles in action with the rubbing surfaces. Abrasion wear was greatly increased at higher load because most of the abrasive particles come into action and creates more grooves. The grooving action results more material removal and can be termed as ploughing. This can also be attributed to the fact that at higher loads the frictional thrust

increases, which result in increased debonding and fracture. A similar effect of normal load on volumetric wear rate has been observed by Cirino *et al* [139] in the case of carbon epoxy composite and Verma *et al* [159] for GRP composite. Thus it can be said that bagasse fiber addition is very effective in improving the tribological properties of epoxy specially its wear resistance.

Figures 4.22 to 4.24 show the effect of load on co-efficient of friction. The friction co-efficient results showed decreasing trends with load for all volume fraction of fiber at different velocities. Reduction in friction co-efficient is noticed with addition of bagasse fiber in the matrix. This reduction in co-efficient of friction occurs likely as a result of fibers standing above the surface making contacting surface area of the specimen smaller. As the volume fraction of fiber increases from 10-20% more number of fibers are in contact; hence less co-efficient of friction. Therefore 20 % volume fraction of fiber shows the best friction performance and neat epoxy is the worst. A similar trend was reported by Chand *et al* [145] while studying the tribological properties graphite modified cotton fiber reinforced polyester composites.

4.8 WORN SURFACE MORPHOLOGY

The worn surface morphologies of neat epoxy and its composites have been examined by scanning electron microscopy (SEM). The worn surfaces of neat epoxy samples are shown in figure 4.25 (a) and (b). The removal of debris of brittle fragmented matrix forms the wear tracks has been observed in figure 4.25(a). In addition to this plastic deformation and adherence are also noticed at higher load of 10N on the worn surface of neat epoxy [Figure 4.25 (b)]. This might have happened due to thermal softening effect caused because of generation of high frictional heat at sliding surface under higher normal load. The filling of space between the abrasives by the wear debris formed during abrasion with consecutive runs can be seen in Figure 4.25 (c).

The composite surface detoriation under 10 N load of 10 volume % reinforcement is clearly illustrated in figure 4.25 (d). The brittle surface fracture events that produced large size wear debris are clearly visible. This might have happened due to high thermo

mechanical loading which leads to the removal of material from the resinous region and weakened the interfacial area between fiber and matrix.

Figure 4.25 (e) shows the worn surface of the composite sample with 15% fiber under 10N load. The possible wear mechanism is that during the test, the abrasive particles were interacted with fiber or matrix on the same phase all the time during the sliding test and no fiber-matrix interface came in the path during the test. This might be the reason for micro cutting and ploughing of the matrix and shearing or tearing of fiber along the fiber zone.

The wear mechanism of 20% bagasse fiber filled polymer composite at a load of 10N is shown in figure 4.25 (f). The micrograph shown suggests that the wear mechanism is dominated by removal due to excessive deterioration of fibre surface. Some of the fibre tissues were sheared and became loose. In spite of that, the fibre ends seems to carry maximum of the load during the sliding. Though the extent of damage and fiber stripping is more pronounced also, at some places micro cracks appeared on the surface which is mainly due to the side force, still the composite shows higher wear resistance because the applied load was mainly borne by fiber itself.

4.9 CONCLUSIONS

Based on the experimental results of abrasive wear of bagasse fiber reinforce epoxy composite, tested under different normal loads, sliding velocity and sliding distances, the following conclusions have been drawn.

- Bagasse fiber reinforced epoxy composite have been successfully fabricated with fairly uniform distribution of fibers.

- Dispersion of fibers in the matrix improves the hardness of matrix material and also the wear behaviour of composite. The effect is increases in interfacial area between the matrix and the fiber leading to increase in strength.

- The abrasive wear rate is found more sensitive to normal load in comparison to sliding velocity and it also increase marginally with increase in sliding velocity.

- The specific wear rate of composite decreases with the increases of sliding distance because the space between the abrasive filled by the debris, which reduced the depth of penetration of abrasive particle in to the composite sample.

- Co-efficient of friction decreases as load increases for different volume fraction of fiber composites.

- Fragmentation, adherence and plastic deformation are primary wear mechanisms for the neat epoxy. However the addition of bagasse fiber reduces this adherence and plastic deformation to a great extent. The worn surface of bagasse fiber epoxy composite is characterized by furrows.

- The worn surfaces of the composite shows that micro cutting, micro ploughing of fiber is mainly responsible for debonding of fiber from the matrix. However, it is also clear that applied load was mainly borne by fiber itself.

Table-4.4 Density and voids content of neat epoxy and Bagasse fiber reinforced composite samples

Fiber content (%)	Measured Density (gm/cm^3)	Theoretical Density (gm/cm^3)	Volume fraction of voids (%)
0	1.082	1.100	1.636
10	1.089	1.110	1.892
15	1.092	1.122	2.674
20	1.095	1.131	3.123

Table-4.5 Test parameter for Dry Sliding wear test

Test Parameters	Units	Values
Volume fraction of fiber	%	0, 10, 15 and 20
Load (L)	N	5, 7.5, 10 and 15
Sliding Velocity (v)	m/s	0.837, 1.256 and 1.675
Track radius (r)	mm	50
Temperature	^0C	20

Table-4.6

Neat Epoxy Load-5N RPM-200

Vs=0.83776m/s

m_1 (gm)	m_2 (gm)	Δm (gm)	T (sec)	F_f (kgf)	μ	$R.DX10^3$ (m)	$WX10^{-6}$ (N/m)	W_VX10^{-11} (m^3/sec)	W_SX10^{-11} (m^3/N.m)
2.54	2.43	0.11	900	0.485	0.97	0.754	1.430	11.111	2.653
2.54	2.40	0.14	1800	0.490	0.98	1.508	0.910	7.071	1.688
2.54	2.36	0.18	2700	0.480	0.96	2.262	0.780	6.061	1.447
2.54	2.34	0.20	3600	0.475	0.95	3.016	0.650	5.051	1.206
2.54	2.33	0.21	4500	0.485	0.97	3.770	0.546	4.242	1.013
2.54	2.31	0.23	5400	0.480	0.96	4.524	0.498	3.872	0.924

Table-4.7

Neat Epoxy Load-5N RPM-300

Vs=1.25664m/s

m_1 (gm)	m_2 (gm)	Δm (gm)	T (sec)	F_f (kgf)	μ	$R.DX10^3$ (m)	$WX10^{-6}$ (N/m)	W_VX10^{-11} (m^3/sec)	W_SX10^{-11} (m^3/N.m)
2.67	2.46	0.21	900	0.495	0.99	1.131	1.820	21.212	3.376
2.67	2.43	0.24	1800	0.490	0.98	2.262	1.040	12.121	1.929
2.67	2.41	0.26	2700	0.485	0.97	3.393	0.751	8.754	1.393
2.67	2.39	0.28	3600	0.480	0.96	4.524	0.607	7.071	1.125
2.67	2.38	0.29	4500	0.490	0.98	5.655	0.503	5.859	0.932
2.67	2.36	0.31	5400	0.485	0.97	6.786	0.448	5.219	0.831

Table-4.8

Neat Epoxy Load-5N RPM-400

Vs=1.67552m/s

m_1 (gm)	m_2 (gm)	Δm (gm)	T (sec)	F_f (kgf)	μ	$R.DX10^3$ (m)	$WX10^{-6}$ (N/m)	W_VX10^{-11} (m^3/sec)	W_SX10^{-11} (m^3/N.m)
3.01	2.59	0.42	900	0.500	1.00	1.508	2.730	42.424	5.064
3.01	2.53	0.48	1800	0.490	0.98	3.016	1.560	24.242	2.894
3.01	2.49	0.52	2700	0.495	0.99	4.524	1.126	17.508	2.090
3.01	2.46	0.55	3600	0.490	0.98	6.032	0.894	13.889	1.658
3.01	2.44	0.57	4500	0.495	0.99	7.540	0.741	11.515	1.375
3.01	2.42	0.59	5400	0.495	0.99	9.048	0.639	9.933	1.186

Table-4.9

Neat Epoxy Load-7.5N RPM-200

Vs=0.83776m/s

m_1 (gm)	m_2 (gm)	Δm (gm)	T (sec)	F_f (kgf)	μ	$R.DX10^3$ (m)	$WX10^{-6}$ (N/m)	W_VX10^{-11} (m^3/sec)	W_SX10^{-11} (m^3/N.m)
2.85	2.71	0.14	900	0.720	0.96	0.754	1.820	14.141	2.251
2.85	2.68	0.17	1800	0.705	0.94	1.508	1.105	8.586	1.366
2.85	2.65	0.20	2700	0.713	0.95	2.262	0.867	6.734	1.072
2.85	2.62	0.23	3600	0.713	0.95	3.016	0.747	5.808	0.924
2.85	2.60	0.25	4500	0.720	0.96	3.770	0.650	5.051	0.804
2.85	2.58	0.27	5400	0.720	0.96	4.524	0.585	4.545	0.723

Table-4.10

Neat Epoxy Load-7.5N RPM-300

Vs=1.25664m/s

m_1 (gm)	m_2 (gm)	Δm (gm)	T (sec)	F_f (kgf)	μ	$R.DX10^3$ (m)	$WX10^{-6}$ (N/m)	W_VX10^{-11} (m^3/sec)	W_SX10^{-11} (m^3/N.m)
2.33	2.07	0.26	900	0.720	0.96	1.131	2.253	26.263	2.787
2.33	1.95	0.38	1800	0.698	0.93	2.262	1.646	19.192	2.036
2.33	1.90	0.43	2700	0.713	0.95	3.393	1.242	14.478	1.536
2.33	1.87	0.46	3600	0.720	0.96	4.524	0.996	11.616	1.233
2.33	1.85	0.48	4500	0.713	0.95	5.655	0.832	9.697	1.029
2.33	1.83	0.50	5400	0.720	0.96	6.786	0.722	8.418	0.893

Table-4.11

Neat Epoxy Load-7.5N RPM-400

Vs=1.67552m/s

m_1 (gm)	m_2 (gm)	Δm (gm)	T (sec)	F_f (kgf)	μ	$R.DX10^3$ (m)	$WX10^{-6}$ (N/m)	W_VX10^{-11} (m^3/sec)	W_SX10^{-11} (m^3/N.m)
2.47	1.98	0.49	900	0.735	0.98	1.508	3.184	49.495	3.939
2.47	1.93	0.54	1800	0.735	0.98	3.016	1.755	27.273	2.170
2.47	1.90	0.57	2700	0.728	0.97	4.524	1.235	19.192	1.527
2.47	1.87	0.60	3600	0.720	0.96	6.032	0.975	15.152	1.206
2.47	1.85	0.62	4500	0.735	0.98	7.540	0.806	12.525	0.997
2.47	1.84	0.63	5400	0.728	0.97	9.048	0.682	10.606	0.844

Table-4.12

Neat Epoxy Load-10N RPM-200

Vs=0.83776m/s

m_1 (gm)	m_2 (gm)	Δm (gm)	T (sec)	F_f (kgf)	μ	$R.DX10^3$ (m)	$WX10^{-6}$ (N/m)	W_VX10^{-11} (m^3/sec)	W_SX10^{-11} (m^3/N.m)
2.98	2.77	0.21	900	0.91	0.91	0.754	2.730	21.212	2.532
2.98	2.73	0.25	1800	0.90	0.90	1.508	1.625	12.626	1.507
2.98	2.69	0.29	2700	0.88	0.88	2.262	1.256	9.764	1.166
2.98	2.65	0.33	3600	0.89	0.89	3.016	1.072	8.333	0.995
2.98	2.63	0.35	4500	0.89	0.89	3.770	0.910	7.071	0.844
2.98	2.62	0.36	5400	0.91	0.91	4.524	0.780	6.061	0.723

Table-4.13

Neat Epoxy Load-10N RPM-300

Vs=1.25664m/s

m_1 (gm)	m_2 (gm)	Δm (gm)	T (sec)	F_f (kgf)	μ	$R.DX10^3$ (m)	$WX10^{-6}$ (N/m)	W_VX10^{-11} (m^3/sec)	W_SX10^{-11} (m^3/N.m)
2.50	2.10	0.40	900	0.95	0.95	1.131	3.466	40.404	3.215
2.50	2.03	0.47	1800	0.90	0.90	2.262	2.036	23.737	1.889
2.50	1.96	0.54	2700	0.96	0.96	3.393	1.560	18.182	1.447
2.50	1.92	0.58	3600	0.89	0.89	4.524	1.256	14.646	1.166
2.50	1.87	0.63	4500	0.85	0.85	5.655	1.092	12.727	1.013
2.50	1.83	0.67	5400	0.88	0.88	6.786	0.968	11.279	0.898

Table-4.14

Neat Epoxy Load-10N RPM-400

Vs=1.67552m/s

m_1 (gm)	m_2 (gm)	Δm (gm)	T (sec)	F_f (kgf)	μ	$R.DX10^3$ (m)	$WX10^{-6}$ (N/m)	W_VX10^{-11} (m^3/sec)	W_SX10^{-11} (m^3/N.m)
3.00	2.44	0.56	900	0.97	0.97	1.508	3.639	56.566	3.376
3.00	2.37	0.63	1800	0.95	0.95	3.016	2.047	31.818	1.899
3.00	2.32	0.68	2700	0.96	0.96	4.524	1.473	22.896	1.366
3.00	2.27	0.73	3600	0.96	0.96	6.032	1.186	18.434	1.100
3.00	2.24	0.76	4500	0.96	0.96	7.540	0.988	15.354	0.916
3.00	2.21	0.79	5400	0.98	0.98	9.048	0.856	13.300	0.794

Table-4.15

Neat Epoxy Load-15N RPM-200

Vs=0.83776m/s

m_1 (gm)	m_2 (gm)	Δm (gm)	T (sec)	F_f (kgf)	μ	$R.DX10^3$ (m)	$WX10^{-6}$ (N/m)	W_VX10^{-11} (m^3/sec)	W_SX10^{-11} (m^3/N.m)
2.34	2.10	0.24	900	1.350	0.90	0.754	3.119	24.242	1.929
2.34	2.06	0.28	1800	1.260	0.84	1.508	1.820	14.141	1.125
2.34	2.02	0.32	2700	1.215	0.81	2.262	1.386	10.774	0.857
2.34	1.97	0.37	3600	1.275	0.85	3.016	1.202	9.343	0.744
2.34	1.95	0.39	4500	1.245	0.83	3.770	1.014	7.879	0.627
2.34	1.94	0.40	5400	1.245	0.83	4.524	0.867	6.734	0.536

Table-4.16

Neat Epoxy Load-15N RPM-300

Vs=1.25664m/s

m_1 (gm)	m_2 (gm)	Δm (gm)	T (sec)	F_f (kgf)	μ	$R.DX10^3$ (m)	$WX10^{-6}$ (N/m)	W_VX10^{-11} (m^3/sec)	W_SX10^{-11} (m^3/N.m)
2.84	2.23	0.61	900	1.365	0.91	1.131	5.286	61.616	3.269
2.84	2.19	0.65	1800	1.230	0.82	2.262	2.816	32.828	1.742
2.84	2.16	0.68	2700	1.260	0.84	3.393	1.964	22.896	1.215
2.84	2.11	0.73	3600	1.245	0.83	4.524	1.581	18.434	0.978
2.84	2.09	0.75	4500	1.230	0.82	5.655	1.300	15.152	0.804
2.84	2.08	0.76	5400	1.260	0.84	6.786	1.098	12.795	0.679

Table-4.17

Neat Epoxy Load-15N RPM-400

Vs=1.67552m/s

m_1 (gm)	m_2 (gm)	Δm (gm)	T (sec)	F_f (kgf)	μ	$R.DX10^3$ (m)	$WX10^{-6}$ (N/m)	W_VX10^{-11} (m^3/sec)	W_SX10^{-11} (m^3/N.m)
2.79	2.18	0.61	900	1.425	0.95	1.508	3.964	61.616	2.452
2.79	2.14	0.65	1800	1.425	0.95	3.016	2.112	32.828	1.306
2.79	2.10	0.69	2700	1.410	0.94	4.524	1.495	23.232	0.924
2.79	1.97	0.82	3600	1.380	0.92	6.032	1.332	20.707	0.824
2.79	1.95	0.84	4500	1.410	0.94	7.540	1.092	16.970	0.675
2.79	1.93	0.86	5400	1.425	0.95	9.048	0.931	14.478	0.576

Table-4.18

Volume Fraction of fiber-10% Load-5N RPM-200

Vs=0.83776m/s

m_1 (gm)	m_2 (gm)	Δm (gm)	T (sec)	F_f (kgf)	μ	$R.DX10^3$ (m)	$WX10^{-6}$ (N/m)	W_VX10^{-11} (m^3/sec)	W_SX10^{-11} (m^3/N.m)
2.19	2.08	0.11	900	0.475	0.95	0.754	1.430	11.752	2.806
2.19	2.07	0.12	1800	0.475	0.95	1.508	0.780	6.410	1.530
2.19	2.04	0.15	2700	0.470	0.94	2.262	0.650	5.342	1.275
2.19	2.03	0.16	3600	0.470	0.94	3.016	0.520	4.274	1.020
2.19	2.03	0.16	4500	0.470	0.94	3.770	0.416	3.419	0.816
2.19	2.02	0.17	5400	0.475	0.95	4.524	0.368	3.027	0.723

Table-4.19

Volume Fraction of fiber -10% Load-5N RPM-300

Vs=1.25664m/s

m_1 (gm)	m_2 (gm)	Δm (gm)	T (sec)	F_f (kgf)	μ	$R.DX10^3$ (m)	$WX10^{-6}$ (N/m)	W_VX10^{-11} (m^3/sec)	W_SX10^{-11} (m^3/N.m)
2.80	2.65	0.15	900	0.490	0.98	1.131	1.300	16.026	2.551
2.80	2.64	0.16	1800	0.475	0.95	2.262	0.693	8.547	1.360
2.80	2.61	0.19	2700	0.470	0.94	3.393	0.549	6.766	1.077
2.80	2.59	0.21	3600	0.475	0.95	4.524	0.455	5.609	0.893
2.80	2.58	0.22	4500	0.470	0.94	5.655	0.381	4.701	0.748
2.80	2.57	0.23	5400	0.480	0.96	6.786	0.332	4.095	0.652

Table-4.20

Volume Fraction of fiber -10% Load-5N RPM-400

Vs=1.67552m/s

m_1 (gm)	m_2 (gm)	Δm (gm)	T (sec)	F_f (kgf)	μ	$R.DX10^3$ (m)	$WX10^{-6}$ (N/m)	W_VX10^{-11} (m^3/sec)	W_SX10^{-11} (m^3/N.m)
3.01	2.67	0.34	900	0.495	0.99	1.508	2.210	36.325	4.336
3.01	2.59	0.42	1800	0.490	0.98	3.016	1.365	22.436	2.678
3.01	2.53	0.48	2700	0.485	0.97	4.524	1.040	17.094	2.040
3.01	2.50	0.51	3600	0.485	0.97	6.032	0.829	13.622	1.626
3.01	2.46	0.55	4500	0.495	0.99	7.540	0.715	11.752	1.403
3.01	2.44	0.57	5400	0.495	0.99	9.048	0.617	10.150	1.212

Table-4.21

Volume Fraction of fiber -10% Load-7.5N RPM-200

Vs=0.83776m/s

m_1 (gm)	m_2 (gm)	Δm (gm)	T (sec)	F_f (kgf)	μ	$R.DX10^3$ (m)	$WX10^{-6}$ (N/m)	W_VX10^{-11} (m^3/sec)	W_SX10^{-11} (m^3/N.m)
2.94	2.77	0.17	900	0.728	0.97	0.754	2.210	18.162	2.891
2.94	2.76	0.18	1800	0.698	0.93	1.508	1.170	9.615	1.530
2.94	2.74	0.20	2700	0.713	0.95	2.262	0.867	7.123	1.134
2.94	2.73	0.21	3600	0.705	0.94	3.016	0.682	5.609	0.893
2.94	2.72	0.22	4500	0.698	0.93	3.770	0.572	4.701	0.748
2.94	2.71	0.23	5400	0.683	0.91	4.524	0.498	4.095	0.652

Table-4.22

Volume Fraction of fiber -10% Load-7.5N RPM-300

Vs=1.25664m/s

m_1 (gm)	m_2 (gm)	Δm (gm)	T (sec)	F_f (kgf)	μ	$R.DX10^3$ (m)	$WX10^{-6}$ (N/m)	W_VX10^{-11} (m^3/sec)	W_SX10^{-11} (m^3/N.m)
3.11	2.90	0.21	900	0.728	0.97	1.131	1.820	22.436	2.381
3.11	2.77	0.34	1800	0.713	0.95	2.262	1.473	18.162	1.927
3.11	2.72	0.39	2700	0.668	0.89	3.393	1.126	13.889	1.474
3.11	2.66	0.45	3600	0.690	0.92	4.524	0.975	12.019	1.275
3.11	2.63	0.48	4500	0.690	0.92	5.655	0.832	10.256	1.088
3.11	2.61	0.50	5400	0.698	0.93	6.786	0.722	8.903	0.945

Table-4.23

Volume Fraction of fiber -10% Load-7.5N RPM-400

Vs=1.67552m/s

m_1 (gm)	m_2 (gm)	Δm (gm)	T (sec)	F_f (kgf)	μ	$R.DX10^3$ (m)	$WX10^{-6}$ (N/m)	W_VX10^{-11} (m^3/sec)	W_SX10^{-11} (m^3/N.m)
2.96	2.75	0.21	900	0.728	0.97	1.508	1.365	22.436	1.785
2.96	2.57	0.39	1800	0.720	0.96	3.016	1.267	20.833	1.658
2.96	2.45	0.51	2700	0.735	0.98	4.524	1.105	18.162	1.445
2.96	2.37	0.59	3600	0.713	0.95	6.032	0.959	15.759	1.254
2.96	2.30	0.66	4500	0.720	0.96	7.540	0.858	14.103	1.122
2.96	2.23	0.73	5400	0.728	0.97	9.048	0.791	12.999	1.034

Table-4.24

Volume Fraction of fiber -10% Load-10N RPM-200

Vs=0.83776m/s

m_1 (gm)	m_2 (gm)	Δm (gm)	T (sec)	F_f (kgf)	μ	$R.DX10^3$ (m)	$WX10^{-6}$ (N/m)	W_VX10^{-11} (m^3/sec)	W_SX10^{-11} (m^3/N.m)
2.77	2.58	0.19	900	0.89	0.89	0.754	2.470	20.299	2.423
2.77	2.51	0.26	1800	0.85	0.85	1.508	1.690	13.889	1.658
2.77	2.48	0.29	2700	0.84	0.84	2.262	1.256	10.328	1.233
2.77	2.45	0.32	3600	0.91	0.91	3.016	1.040	8.547	1.020
2.77	2.44	0.33	4500	0.86	0.86	3.770	0.858	7.051	0.842
2.77	2.43	0.34	5400	0.86	0.86	4.524	0.737	6.054	0.723

Table-4.25

Volume Fraction of fiber -10% Load-10N RPM-300

Vs=1.25664m/s

m_1 (gm)	m_2 (gm)	Δm (gm)	T (sec)	F_f (kgf)	μ	$R.DX10^3$ (m)	$WX10^{-6}$ (N/m)	W_VX10^{-11} (m^3/sec)	W_SX10^{-11} (m^3/N.m)
2.88	2.47	0.41	900	0.91	0.91	1.131	3.553	43.803	3.486
2.88	2.41	0.47	1800	0.86	0.86	2.262	2.036	25.107	1.998
2.88	2.37	0.51	2700	0.89	0.89	3.393	1.473	18.162	1.445
2.88	2.34	0.54	3600	0.85	0.85	4.524	1.170	14.423	1.148
2.88	2.3	0.56	4500	0.83	0.83	5.655	0.970	11.966	0.952
2.88	2.29	0.59	5400	0.93	0.93	6.786	0.852	10.506	0.836

Table-4.26

Volume Fraction of fiber -10% Load-10N RPM-400

Vs=1.67552m/s

m_1 (gm)	m_2 (gm)	Δm (gm)	T (sec)	F_f (kgf)	μ	$R.DX10^3$ (m)	$WX10^{-6}$ (N/m)	W_VX10^{-11} (m^3/sec)	W_SX10^{-11} (m^3/N.m)
2.97	2.38	0.590	900	0.97	0.97	1.508	3.834	63.034	3.762
2.97	2.33	0.640	1800	0.95	0.95	3.016	2.080	34.188	2.040
2.97	2.30	0.670	2700	0.94	0.94	4.524	1.451	23.860	1.424
2.97	2.28	0.690	3600	0.96	0.96	6.032	1.121	18.429	1.100
2.97	2.26	0.710	4500	0.94	0.94	7.540	0.923	15.171	0.905
2.97	2.24	0.730	5400	0.95	0.95	9.048	0.791	12.999	0.776

Table-4.27

Volume Fraction of fiber -10% Load-15N RPM-200

Vs=0.83776m/s

m_1 (gm)	m_2 (gm)	Δm (gm)	T (sec)	F_f (kgf)	μ	$R.DX10^3$ (m)	$WX10^{-6}$ (N/m)	W_VX10^{-11} (m^3/sec)	W_SX10^{-11} (m^3/N.m)
2.89	2.66	0.23	900	1.410	0.94	0.754	2.989	24.573	1.955
2.89	2.60	0.29	1800	1.275	0.85	1.508	1.885	15.491	1.233
2.89	2.58	0.31	2700	1.230	0.82	2.262	1.343	11.040	0.879
2.89	2.56	0.33	3600	1.065	0.71	3.016	1.072	8.814	0.701
2.89	2.5	0.34	4500	1.200	0.80	3.770	0.884	7.265	0.578
2.89	2.54	0.35	5400	1.170	0.78	4.524	0.758	6.232	0.496

Table-4.28

Volume Fraction of fiber -10% Load-15N RPM-300

Vs=1.25664m/s

m_1 (gm)	m_2 (gm)	Δm (gm)	T (sec)	F_f (kgf)	μ	$R.DX10^3$ (m)	$WX10^{-6}$ (N/m)	W_VX10^{-11} (m^3/sec)	W_SX10^{-11} (m^3/N.m)
3.01	2.45	0.56	900	1.335	0.89	1.131	4.852	59.829	3.174
3.01	2.41	0.60	1800	1.230	0.82	2.262	2.600	32.051	1.700
3.01	2.35	0.66	2700	1.200	0.80	3.393	1.906	23.504	1.247
3.01	2.32	0.69	3600	1.230	0.82	4.524	1.495	18.429	0.978
3.01	2.28	0.73	4500	1.215	0.81	5.655	1.265	15.598	0.828
3.01	2.25	0.76	5400	1.155	0.77	6.786	1.098	13.533	0.718

Table-4.29

Volume Fraction of fiber -10% Load-15N RPM-400

Vs=1.67552m/s

m_1 (gm)	m_2 (gm)	Δm (gm)	T (sec)	F_f (kgf)	μ	$R.DX10^3$ (m)	$WX10^{-6}$ (N/m)	W_VX10^{-11} (m^3/sec)	W_SX10^{-11} (m^3/N.m)
2.47	1.86	0.61	900	1.455	0.97	1.508	3.964	65.171	2.593
2.47	1.80	0.67	1800	1.395	0.93	3.016	2.177	35.791	1.424
2.47	1.76	0.71	2700	1.380	0.92	4.524	1.538	25.285	1.006
2.47	1.73	0.74	3600	1.365	0.91	6.032	1.202	19.765	0.786
2.47	1.69	0.78	4500	1.410	0.94	7.540	1.014	16.667	0.663
2.47	1.6	0.83	5400	1.425	0.95	9.048	0.899	14.779	0.588

Table-4.30

Volume Fraction of fiber -15% Load-5N RPM-200

Vs=0.83776m/s

m_1 (gm)	m_2 (gm)	Δm (gm)	T (sec)	F_f (kgf)	μ	R.DX10^3 (m)	WX10^{-6} (N/m)	W_VX10^{-11} (m^3/sec)	W_SX10^{-11} (m^3/N.m)
2.44	2.36	0.08	900	0.470	0.94	0.754	1.040	8.801	2.101
2.44	2.34	0.10	1800	0.470	0.94	1.508	0.650	5.501	1.313
2.44	2.32	0.12	2700	0.480	0.96	2.262	0.520	4.400	1.051
2.44	2.31	0.13	3600	0.475	0.95	3.016	0.422	3.575	0.854
2.44	2.30	0.14	4500	0.460	0.92	3.770	0.364	3.080	0.735
2.44	2.29	0.15	5400	0.450	0.90	4.524	0.325	2.750	0.657

Table-4.31

Volume Fraction of fiber -15% Load-5N RPM-300

Vs=1.25664m/s

m_1 (gm)	m_2 (gm)	Δm (gm)	T (sec)	F_f (kgf)	μ	R.DX10^3 (m)	WX10^{-6} (N/m)	W_VX10^{-11} (m^3/sec)	W_SX10^{-11} (m^3/N.m)
2.86	2.74	0.12	900	0.490	0.98	1.131	1.040	13.201	2.101
2.86	2.72	0.14	1800	0.460	0.92	2.262	0.607	7.701	1.226
2.86	2.70	0.16	2700	0.470	0.94	3.393	0.462	5.867	0.934
2.86	2.70	0.16	3600	0.465	0.93	4.524	0.347	4.400	0.700
2.86	2.69	0.17	4500	0.470	0.94	5.655	0.295	3.740	0.595
2.86	2.68	0.18	5400	0.455	0.91	6.786	0.260	3.300	0.525

Table-4.32

Volume Fraction of fiber -15% Load-5N RPM-400

Vs=1.67552m/s

m_1 (gm)	m_2 (gm)	Δm (gm)	T (sec)	F_f (kgf)	μ	$R.DX10^3$ (m)	$WX10^{-6}$ (N/m)	W_VX10^{-11} (m^3/sec)	W_SX10^{-11} (m^3/N.m)
2.71	2.40	0.31	900	0.485	0.97	1.508	2.015	34.103	4.071
2.71	2.36	0.35	1800	0.475	0.95	3.016	1.137	19.252	2.298
2.71	2.34	0.37	2700	0.480	0.96	4.524	0.802	13.568	1.620
2.71	2.30	0.41	3600	0.475	0.95	6.032	0.666	11.276	1.346
2.71	2.28	0.43	4500	0.480	0.96	7.540	0.559	9.461	1.129
2.71	2.25	0.46	5400	0.475	0.95	9.048	0.498	8.434	1.007

Table-4.33

Volume Fraction of fiber -15% Load-7.5N RPM-200

Vs=0.83776m/s

m_1 (gm)	m_2 (gm)	Δm (gm)	T (sec)	F_f (kgf)	μ	$R.DX10^3$ (m)	$WX10^{-6}$ (N/m)	W_VX10^{-11} (m^3/sec)	W_SX10^{-11} (m^3/N.m)
2.71	2.57	0.14	900	0.713	0.95	0.754	1.820	15.402	2.451
2.71	2.55	0.16	1800	0.675	0.90	1.508	1.040	8.801	1.401
2.71	2.54	0.17	2700	0.720	0.96	2.262	0.737	6.234	0.992
2.71	2.52	0.19	3600	0.668	0.89	3.016	0.617	5.226	0.832
2.71	2.52	0.19	4500	0.623	0.83	3.770	0.494	4.180	0.665
2.71	2.51	0.20	5400	0.660	0.88	4.524	0.433	3.667	0.584

Table-4.34

Volume Fraction of fiber -15% Load-7.5N RPM-300

Vs=1.25664m/s

m_1 (gm)	m_2 (gm)	Δm (gm)	T (sec)	F_f (kgf)	μ	R.DX10^3 (m)	WX10^{-6} (N/m)	W_VX10^{-11} (m^3/sec)	W_SX10^{-11} (m^3/N.m)
2.45	2.30	0.15	900	0.720	0.96	1.131	1.300	16.502	1.751
2.45	2.27	0.18	1800	0.630	0.84	2.262	0.780	9.901	1.051
2.45	2.24	0.21	2700	0.728	0.97	3.393	0.607	7.701	0.817
2.45	2.22	0.23	3600	0.698	0.93	4.524	0.498	6.326	0.671
2.45	2.21	0.24	4500	0.690	0.92	5.655	0.416	5.281	0.560
2.45	2.20	0.25	5400	0.668	0.89	6.786	0.361	4.584	0.486

Table-4.35

Volume Fraction of fiber -15% Load-7.5N RPM-400

Vs=1.67552m/s

m_1 (gm)	m_2 (gm)	Δm (gm)	T (sec)	F_f (kgf)	μ	R.DX10^3 (m)	WX10^{-6} (N/m)	W_VX10^{-11} (m^3/sec)	W_SX10^{-11} (m^3/N.m)
2.61	2.28	0.33	900	0.713	0.95	1.508	2.145	36.304	2.889
2.61	2.24	0.37	1800	0.698	0.93	3.016	1.202	20.352	1.620
2.61	2.22	0.39	2700	0.705	0.94	4.524	0.845	14.301	1.138
2.61	2.20	0.41	3600	0.683	0.91	6.032	0.666	11.276	0.897
2.61	2.19	0.42	4500	0.705	0.94	7.540	0.546	9.241	0.735
2.61	2.18	0.43	5400	0.713	0.95	9.048	0.466	7.884	0.627

Table-4.36

Volume Fraction of fiber -15% Load-10N RPM-200

Vs=0.83776m/s

m_1 (gm)	m_2 (gm)	Δm (gm)	T (sec)	F_f (kgf)	μ	$R.DX10^3$ (m)	$WX10^{-6}$ (N/m)	W_VX10^{-11} (m^3/sec)	W_SX10^{-11} (m^3/N.m)
2.92	2.82	0.10	900	0.92	0.92	0.754	1.300	11.001	1.313
2.92	2.77	0.15	1800	0.83	0.83	1.508	0.975	8.251	0.985
2.92	2.75	0.17	2700	0.81	0.81	2.262	0.737	6.234	0.744
2.92	2.72	0.20	3600	0.83	0.83	3.016	0.650	5.501	0.657
2.92	2.71	0.21	4500	0.83	0.83	3.770	0.546	4.620	0.552
2.92	2.69	0.23	5400	0.83	0.83	4.524	0.498	4.217	0.503

Table-4.37

Volume Fraction of fiber -15% Load-10N RPM-300

Vs=1.25662m/s

m_1 (gm)	m_2 (gm)	Δm (gm)	T (sec)	F_f (kgf)	μ	$R.DX10^3$ (m)	$WX10^{-6}$ (N/m)	W_VX10^{-11} (m^3/sec)	W_SX10^{-11} (m^3/N.m)
2.77	2.53	0.24	900	0.91	0.91	1.131	2.080	26.403	2.101
2.77	2.42	0.35	1800	0.82	0.82	2.262	1.516	19.252	1.532
2.77	2.41	0.36	2700	0.80	0.80	3.393	1.040	13.201	1.051
2.77	2.38	0.39	3600	0.830	0.83	4.524	0.845	10.726	0.854
2.77	2.36	0.41	4500	0.81	0.81	5.655	0.711	9.021	0.718
2.77	2.34	0.43	5400	0.84	0.84	6.786	0.621	7.884	0.627

Table-4.38

Volume Fraction of fiber -15% Load-10N RPM-400

Vs=1.67552m/s

m_1 (gm)	m_2 (gm)	Δm (gm)	T (sec)	F_f (kgf)	μ	$R.DX10^3$ (m)	$WX10^{-6}$ (N/m)	W_VX10^{-11} (m^3/sec)	W_SX10^{-11} (m^3/N.m)
3.04	2.66	0.38	900	0.99	0.99	1.508	2.470	41.804	2.495
3.04	2.61	0.43	1800	0.86	0.86	3.016	1.397	23.652	1.412
3.04	2.59	0.45	2700	0.84	0.84	4.524	0.975	16.502	0.985
3.04	2.57	0.47	3600	0.88	0.88	6.032	0.764	12.926	0.771
3.04	2.55	0.49	4500	0.84	0.84	7.540	0.637	10.781	0.643
3.04	2.53	0.51	5400	0.82	0.82	9.048	0.552	9.351	0.558

Table-4.39

Volume Fraction of fiber -15% Load-15N RPM-200

Vs=0.83776m/s

m_1 (gm)	m_2 (gm)	Δm (gm)	T (sec)	F_f (kgf)	μ	$R.DX10^3$ (m)	$WX10^{-6}$ (N/m)	W_VX10^{-11} (m^3/sec)	W_SX10^{-11} (m^3/N.m)
2.98	2.85	0.13	900	1.200	0.80	0.754	1.690	14.301	1.138
2.98	2.81	0.17	1800	1.185	0.79	1.508	1.105	9.351	0.744
2.98	2.79	0.19	2700	1.140	0.76	2.262	0.823	6.967	0.554
2.98	2.77	0.21	3600	1.215	0.81	3.016	0.682	5.776	0.460
2.98	2.76	0.22	4500	1.230	0.82	3.770	0.572	4.840	0.385
2.98	2.74	0.24	5400	1.170	0.78	4.524	0.520	4.400	0.350

Table-4.40

Volume Fraction of fiber -15% Load-15N RPM-300

Vs=1.25662m/s

m_1 (gm)	m_2 (gm)	Δm (gm)	T (sec)	F_f (kgf)	μ	$R.DX10^3$ (m)	$WX10^{-6}$ (N/m)	W_VX10^{-11} (m^3/sec)	W_SX10^{-11} (m^3/N.m)
2.59	2.35	0.24	900	1.200	0.80	1.131	2.080	26.403	1.401
2.59	2.24	0.35	1800	1.230	0.82	2.262	1.516	19.252	1.021
2.59	2.20	0.39	2700	1.200	0.80	3.393	1.126	14.301	0.759
2.59	2.17	0.42	3600	1.125	0.75	4.524	0.910	11.551	0.613
2.59	2.15	0.44	4500	1.095	0.73	5.655	0.763	9.681	0.514
2.59	2.13	0.46	5400	1.215	0.81	6.786	0.664	8.434	0.447

Table-4.41

Volume Fraction of fiber -15% Load-15N RPM-400

Vs=1.67552m/s

m_1 (gm)	m_2 (gm)	Δm (gm)	T (sec)	F_f (kgf)	μ	$R.DX10^3$ (m)	$WX10^{-6}$ (N/m)	W_VX10^{-11} (m^3/sec)	W_SX10^{-11} (m^3/N.m)
2.94	2.55	0.39	900	1.350	0.90	1.508	2.535	42.904	1.707
2.94	2.47	0.47	1800	1.290	0.86	3.016	1.527	25.853	1.029
2.94	2.43	0.51	2700	1.260	0.84	4.524	1.105	18.702	0.744
2.94	2.39	0.55	3600	1.320	0.88	6.032	0.894	15.127	0.602
2.94	2.37	0.57	4500	1.260	0.84	7.540	0.741	12.541	0.499
2.94	2.36	0.58	5400	1.245	0.83	9.048	0.628	10.634	0.423

Table-4.42

Volume Fraction of fiber -20% Load-5N RPM-200

Vs=0.83776m/s

m_1 (gm)	m_2 (gm)	Δm (gm)	T (sec)	F_f (kgf)	μ	$R.DX10^3$ (m)	$WX10^{-6}$ (N/m)	W_VX10^{-11} (m^3/sec)	W_SX10^{-11} (m^3/N.m)
2.84	2.79	0.05	900	0.475	0.95	0.754	0.650	5.617	1.341
2.84	2.77	0.07	1800	0.450	0.90	1.508	0.455	3.932	0.939
2.84	2.77	0.07	2700	0.465	0.93	2.262	0.303	2.621	0.626
2.84	2.76	0.08	3600	0.460	0.92	3.016	0.260	2.247	0.536
2.84	2.75	0.09	4500	0.445	0.89	3.770	0.234	2.022	0.483
2.84	2.75	0.09	5400	0.450	0.90	4.524	0.195	1.685	0.402

Table-4.43

Volume Fraction of fiber -20% Load-5N RPM-300

Vs=1.25662m/s

m_1 (gm)	m_2 (gm)	Δm (gm)	T (sec)	F_f (kgf)	μ	$R.DX10^3$ (m)	$WX10^{-6}$ (N/m)	W_VX10^{-11} (m^3/sec)	W_SX10^{-11} (m^3/N.m)
3.04	2.95	0.09	900	0.390	0.78	1.131	0.780	10.111	1.609
3.04	2.93	0.11	1800	0.475	0.95	2.262	0.477	6.179	0.983
3.04	2.92	0.12	2700	0.470	0.94	3.393	0.347	4.494	0.715
3.04	2.90	0.14	3600	0.475	0.95	4.524	0.303	3.932	0.626
3.04	2.89	0.15	4500	0.455	0.91	5.655	0.260	3.370	0.536
3.04	2.88	0.16	5400	0.465	0.93	6.786	0.231	2.996	0.477

Table-4.44

Volume Fraction of fiber -20% Load-5N RPM-400

Vs=1.67552m/s

m_1 (gm)	m_2 (gm)	Δm (gm)	T (sec)	F_f (kgf)	μ	$R.DX10^3$ (m)	$WX10^{-6}$ (N/m)	W_VX10^{-11} (m^3/sec)	W_SX10^{-11} (m^3/N.m)
2.74	2.50	0.24	900	0.465	0.93	1.508	1.560	26.963	3.218
2.74	2.48	0.26	1800	0.455	0.91	3.016	0.845	14.605	1.743
2.74	2.47	0.27	2700	0.445	0.89	4.524	0.585	10.111	1.207
2.74	2.46	0.28	3600	0.450	0.90	6.032	0.455	7.864	0.939
2.74	2.45	0.29	4500	0.465	0.93	7.540	0.377	6.516	0.778
2.74	2.44	0.30	5400	0.470	0.94	9.048	0.325	5.617	0.671

Table-4.45

Volume Fraction of fiber -20% Load-7.5N RPM-200

Vs=0.83776m/s

m_1 (gm)	m_2 (gm)	Δm (gm)	T (sec)	F_f (kgf)	μ	$R.DX10^3$ (m)	$WX10^{-6}$ (N/m)	W_VX10^{-11} (m^3/sec)	W_SX10^{-11} (m^3/N.m)
2.86	2.79	0.07	900	0.683	0.91	0.754	0.910	7.864	1.252
2.86	2.78	0.08	1800	0.675	0.90	1.508	0.520	4.494	0.715
2.86	2.77	0.09	2700	0.653	0.87	2.262	0.390	3.370	0.536
2.86	2.76	0.10	3600	0.668	0.89	3.016	0.325	2.809	0.447
2.86	2.75	0.11	4500	0.668	0.89	3.770	0.286	2.472	0.393
2.86	2.74	0.12	5400	0.675	0.90	4.524	0.260	2.247	0.358

Table-4.46

Volume Fraction of fiber -20% Load-7.5N RPM-300

Vs=1.25662m/s

m_1 (gm)	m_2 (gm)	Δm (gm)	T (sec)	F_f (kgf)	μ	$R.DX10^3$ (m)	$WX10^{-6}$ (N/m)	W_VX10^{-11} (m^3/sec)	W_SX10^{-11} (m^3/N.m)
2.88	2.77	0.11	900	0.690	0.92	1.131	0.953	12.358	1.311
2.88	2.73	0.15	1800	0.615	0.82	2.262	0.650	8.426	0.894
2.88	2.72	0.16	2700	0.600	0.80	3.393	0.462	5.992	0.636
2.88	2.71	0.17	3600	0.608	0.81	4.524	0.368	4.775	0.507
2.88	2.69	0.19	4500	0.600	0.80	5.655	0.329	4.269	0.453
2.88	2.68	0.20	5400	0.623	0.83	6.786	0.289	3.745	0.397

Table-4.47

Volume Fraction of fiber -20% Load-7.5N RPM-400

Vs=1.67552m/s

m_1 (gm)	m_2 (gm)	Δm (gm)	T (sec)	F_f (kgf)	μ	$R.DX10^3$ (m)	$WX10^{-6}$ (N/m)	W_VX10^{-11} (m^3/sec)	W_SX10^{-11} (m^3/N.m)
2.65	2.41	0.24	900	0.713	0.95	1.508	1.560	26.963	2.146
2.65	2.37	0.28	1800	0.675	0.90	3.016	0.910	15.729	1.252
2.65	2.36	0.29	2700	0.720	0.96	4.524	0.628	10.860	0.864
2.65	2.35	0.30	3600	0.668	0.89	6.032	0.487	8.426	0.671
2.65	2.34	0.31	4500	0.623	0.83	7.540	0.403	6.966	0.554
2.65	2.33	0.32	5400	0.660	0.88	9.048	0.347	5.992	0.477

Table-4.48

Volume Fraction of fiber -20% Load-10N RPM-200

Vs=0.83776m/s

m_1 (gm)	m_2 (gm)	Δm (gm)	T (sec)	F_f (kgf)	μ	$R.DX10^3$ (m)	$WX10^{-6}$ (N/m)	W_VX10^{-11} (m^3/sec)	W_SX10^{-11} (m^3/N.m)
2.51	2.41	0.10	900	0.90	0.90	0.754	1.300	11.235	1.341
2.51	2.39	0.12	1800	0.77	0.77	1.508	0.780	6.741	0.805
2.51	2.38	0.13	2700	0.84	0.84	2.262	0.563	4.868	0.581
2.51	2.37	0.14	3600	0.86	0.86	3.016	0.455	3.932	0.469
2.51	2.36	0.15	4500	0.84	0.84	3.770	0.390	3.370	0.402
2.51	2.35	0.16	5400	0.81	0.81	4.524	0.347	2.996	0.358

Table-4.49

Volume Fraction of fiber -20% Load-10N RPM-300

Vs=1.25662m/s

m_1 (gm)	m_2 (gm)	Δm (gm)	T (sec)	F_f (kgf)	μ	$R.DX10^3$ (m)	$WX10^{-6}$ (N/m)	W_VX10^{-11} (m^3/sec)	W_SX10^{-11} (m^3/N.m)
2.75	2.5	0.23	900	0.97	0.97	1.131	1.993	25.840	2.056
2.75	2.47	0.28	1800	0.85	0.85	2.262	1.213	15.729	1.252
2.75	2.45	0.30	2700	0.80	0.80	3.393	0.867	11.235	0.894
2.75	2.44	0.31	3600	0.71	0.71	4.524	0.672	8.707	0.693
2.75	2.43	0.32	4500	0.80	0.80	5.655	0.555	7.190	0.572
2.75	2.42	0.33	5400	0.78	0.78	6.786	0.477	6.179	0.492

Table-4.50

Volume Fraction of fiber -20% Load-10N RPM-400

Vs=1.67552m/s

m_1 (gm)	m_2 (gm)	Δm (gm)	T (sec)	F_f (kgf)	μ	$R.DX10^3$ (m)	$WX10^{-6}$ (N/m)	W_VX10^{-11} (m^3/sec)	W_SX10^{-11} (m^3/N.m)
3.13	2.93	0.20	900	0.90	0.90	1.508	1.300	22.469	1.341
3.13	2.87	0.26	1800	0.89	0.89	3.016	0.845	14.605	0.872
3.13	2.82	0.31	2700	0.83	0.83	4.524	0.672	11.609	0.693
3.13	2.80	0.33	3600	0.76	0.76	6.032	0.536	9.269	0.553
3.13	2.78	0.35	4500	0.79	0.79	7.540	0.455	7.864	0.469
3.13	2.76	0.37	5400	0.78	0.78	9.048	0.401	6.928	0.413

Table-4.51

Volume Fraction of fiber -20% Load-15N RPM-200

Vs=0.83776m/s

m_1 (gm)	m_2 (gm)	Δm (gm)	T (sec)	F_f (kgf)	μ	$R.DX10^3$ (m)	$WX10^{-6}$ (N/m)	W_VX10^{-11} (m^3/sec)	W_SX10^{-11} (m^3/N.m)
3.34	3.21	0.13	900	1.200	0.80	0.754	1.690	14.605	1.162
3.34	3.19	0.15	1800	1.065	0.71	1.508	0.975	8.426	0.671
3.34	3.18	0.16	2700	1.095	0.73	2.262	0.693	5.992	0.477
3.34	3.17	0.17	3600	1.035	0.69	3.016	0.552	4.775	0.380
3.34	3.16	0.18	4500	1.080	0.72	3.770	0.468	4.044	0.322
3.34	3.15	0.19	5400	1.125	0.75	4.524	0.412	3.558	0.283

Table-4.52

Volume Fraction of fiber -20% Load-15N RPM-300

Vs=1.25662m/s

m_1 (gm)	m_2 (gm)	Δm (gm)	T (sec)	F_f (kgf)	μ	$R.DX10^3$ (m)	$WX10^{-6}$ (N/m)	W_VX10^{-11} (m^3/sec)	W_SX10^{-11} (m^3/N.m)
2.76	2.50	0.26	900	1.200	0.80	1.131	2.253	29.210	1.550
2.76	2.47	0.29	1800	1.125	0.75	2.262	1.256	16.290	0.864
2.76	2.45	0.31	2700	1.050	0.70	3.393	0.895	11.609	0.616
2.76	2.43	0.33	3600	1.095	0.73	4.524	0.715	9.269	0.492
2.76	2.42	0.34	4500	1.095	0.73	5.655	0.589	7.640	0.405
2.76	2.41	0.35	5400	1.035	0.69	6.786	0.505	6.554	0.348

Table-4.53

Volume Fraction of fiber -20% Load-15N RPM-400

Vs=1.67552m/s

m_1 (gm)	m_2 (gm)	Δm (gm)	T (sec)	F_f (kgf)	μ	$R.DX10^3$ (m)	$WX10^{-6}$ (N/m)	W_VX10^{-11} (m^3/sec)	W_SX10^{-11} (m^3/N.m)
2.89	2.62	0.27	900	1.335	0.89	1.508	1.755	30.334	1.207
2.89	2.58	0.31	1800	1.125	0.75	3.016	1.007	17.414	0.693
2.89	2.56	0.33	2700	1.185	0.79	4.524	0.715	12.358	0.492
2.89	2.55	0.34	3600	1.140	0.76	6.032	0.552	9.549	0.380
2.89	2.54	0.35	4500	1.215	0.81	7.540	0.455	7.864	0.313
2.89	2.53	0.36	5400	1.125	0.75	9.048	0.390	6.741	0.268

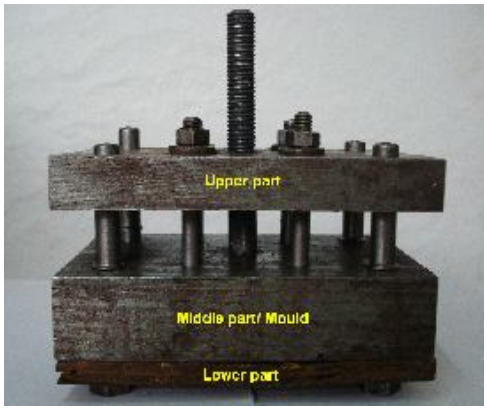

Figure-4.5 (a)

Figure-4.5 (b)

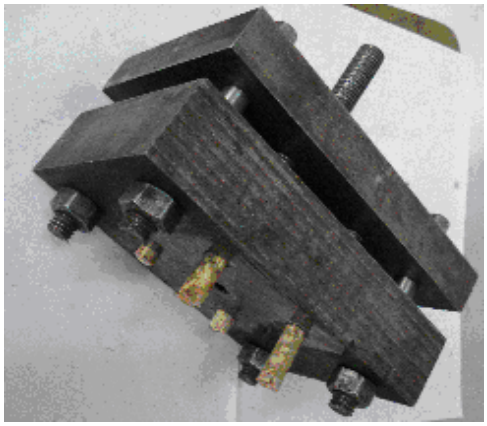

Figure-4.5 (c)

Figure-4.5 (d)

Figure-4.5. Steel Mould and prepared pin type composite samples; (a) Mould used for preparing samples, (b) Two halves of the mould, (c) Mould with Pin types composite samples, (d) Fabricated Composite Pins

Figure-4.6 (a)

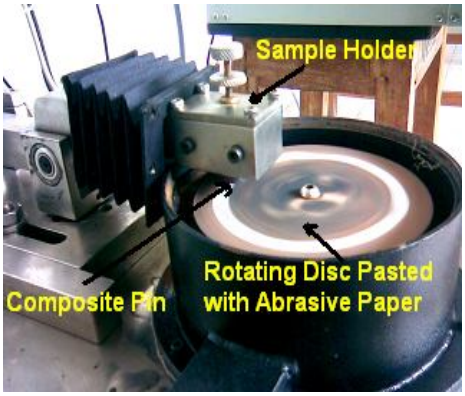

Figure-4.6 (b)

Figure-4.6 Experimental set-up; (a) Pin-on-disc type wear testing machine, (b) Composite sample under abrasive wear test

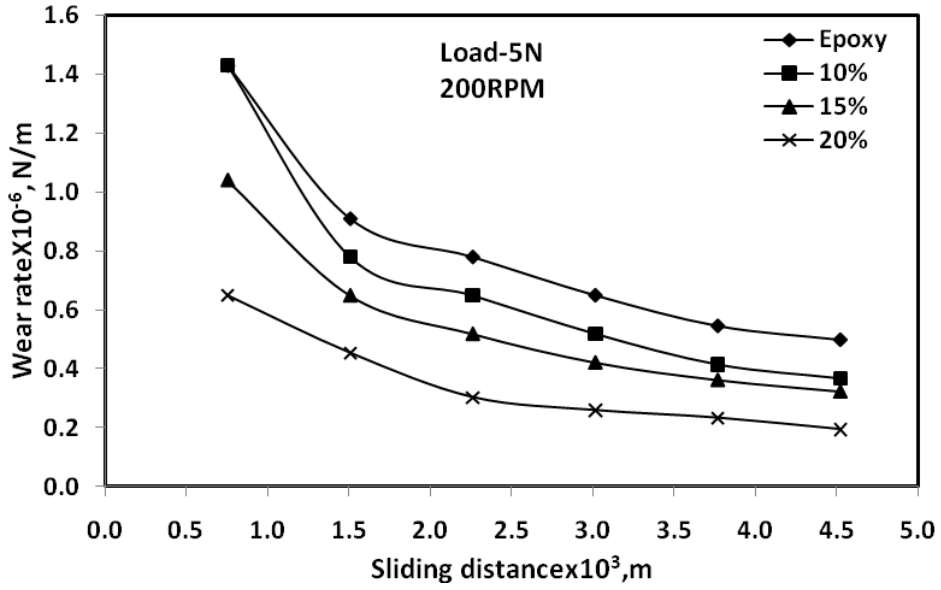

Figure-4.7 Variation of wear rate with sliding distance at 5N load and 200 RPM

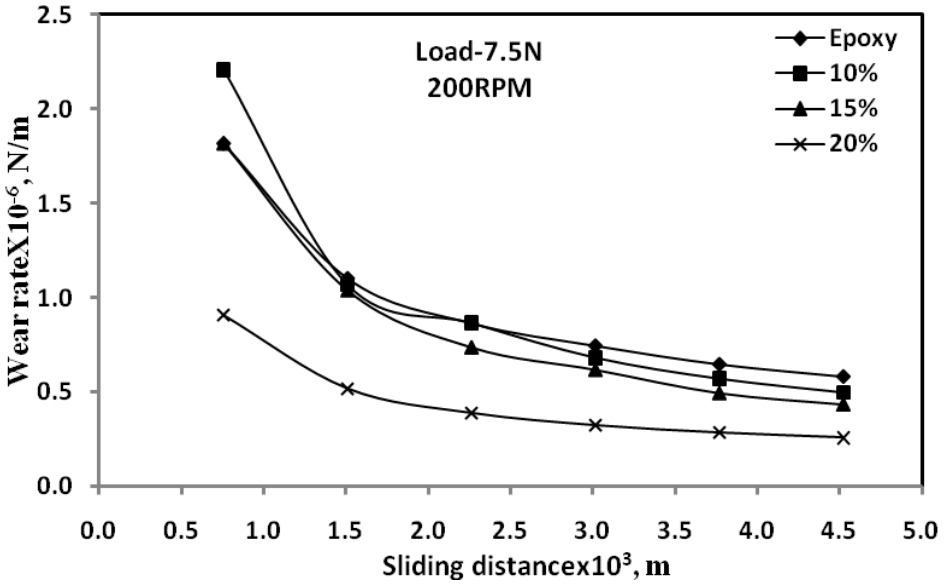

Figure-4.8 Variation of wear rate with sliding distance at 7.5N load and 200 RPM

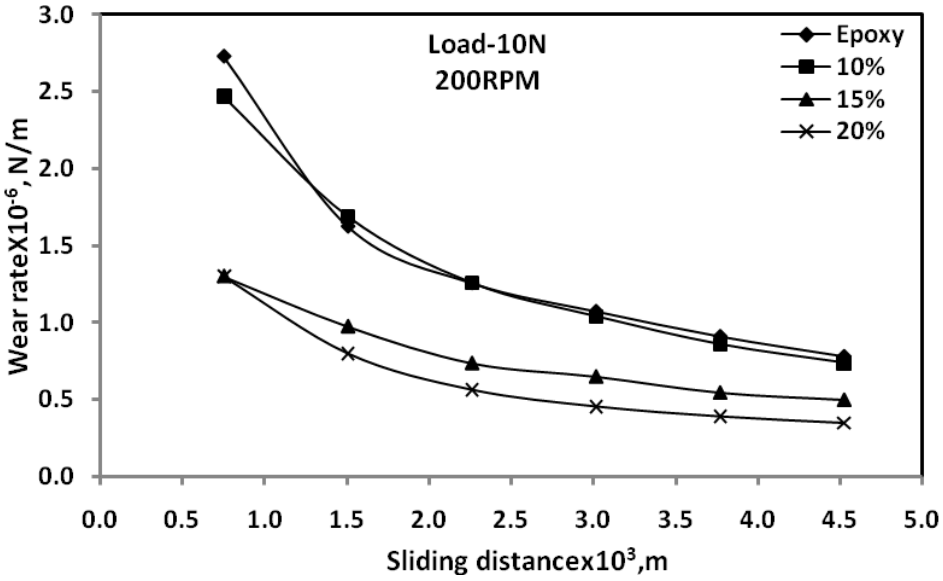

Figure-4.9 Variation of wear rate with sliding distance at 10N load and 200 RPM

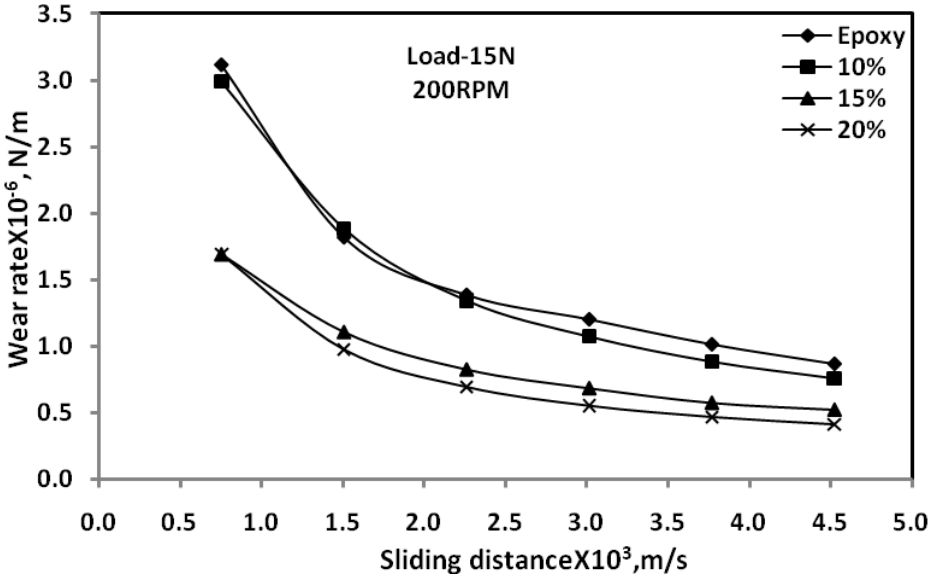

Figure-4.10 Variation of wear rate with sliding distance at 15N load and 200 RPM

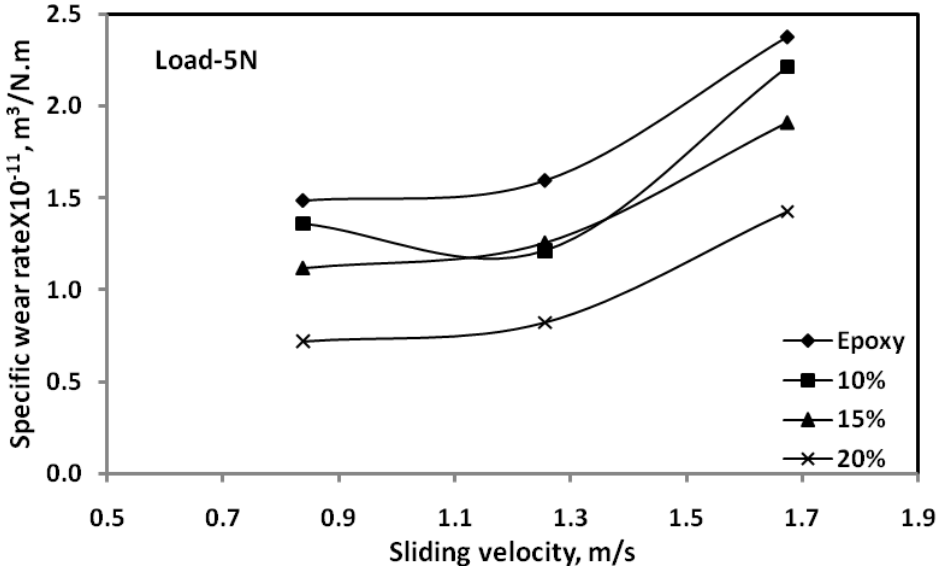

Figure-4.11 Variation of specific wear rate with sliding velocity at 5N load

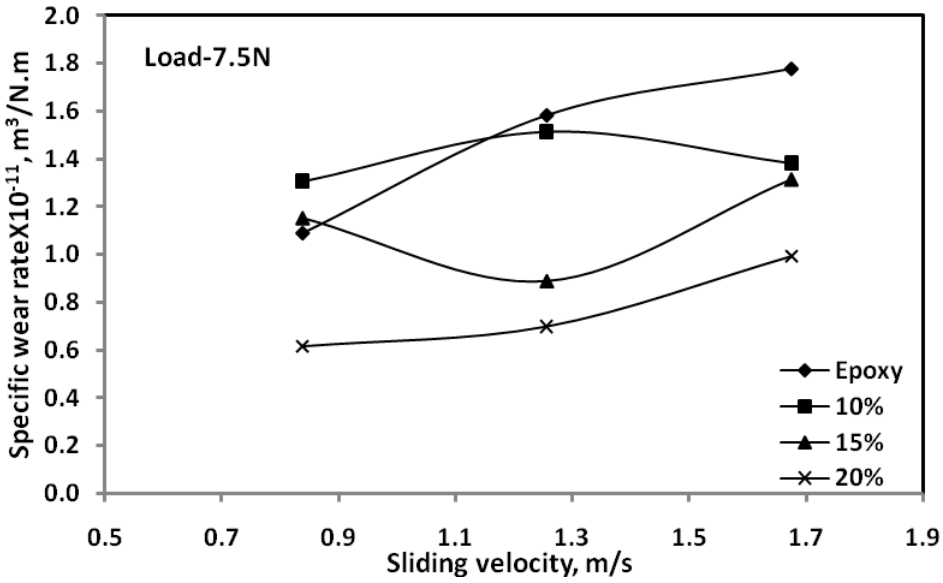

Figure-4.12 Variation of specific wear rate with sliding velocity at 7.5N load

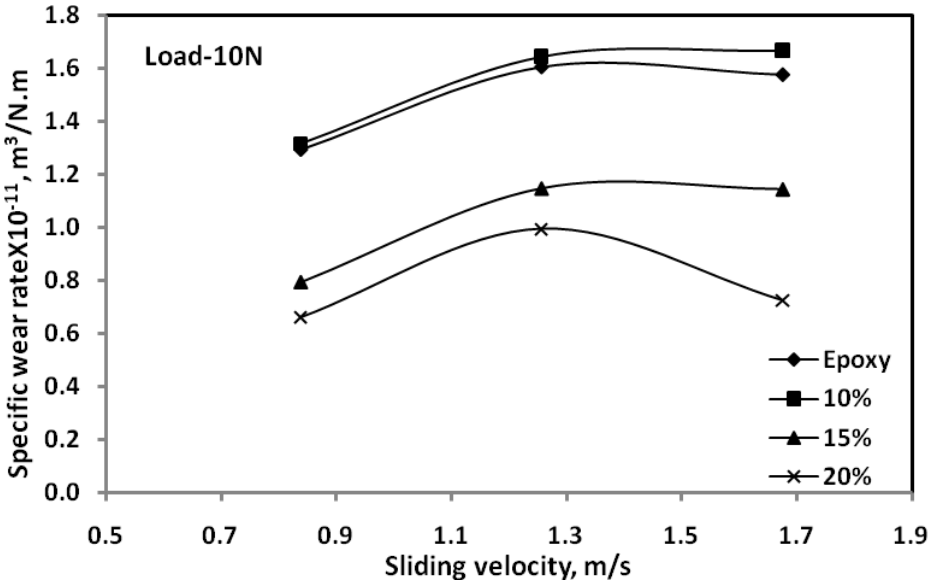

Figure-4.13 Variation of specific wear rate with sliding velocity at 10N load

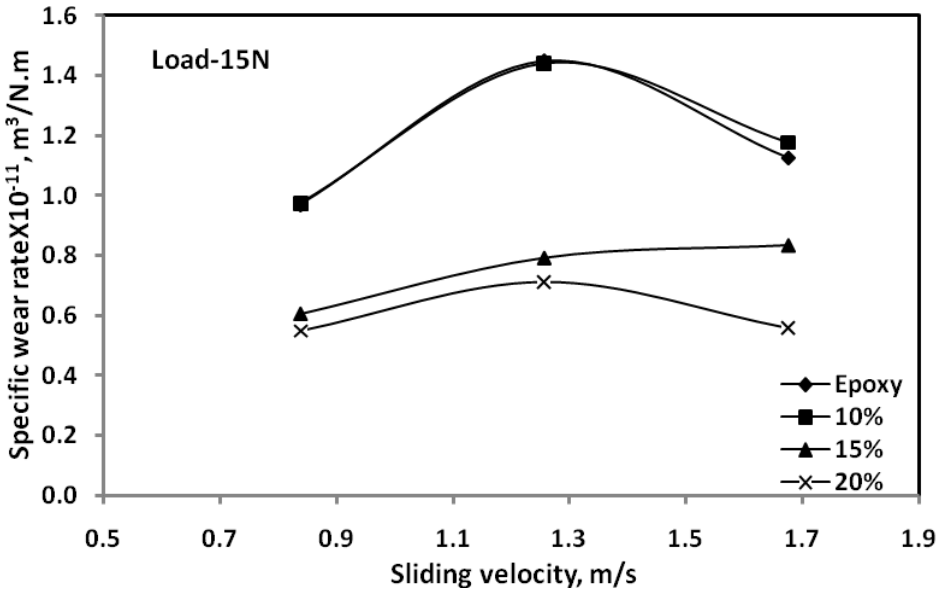

Figure-4.14 Variation of specific wear rate with sliding velocity at 15N load

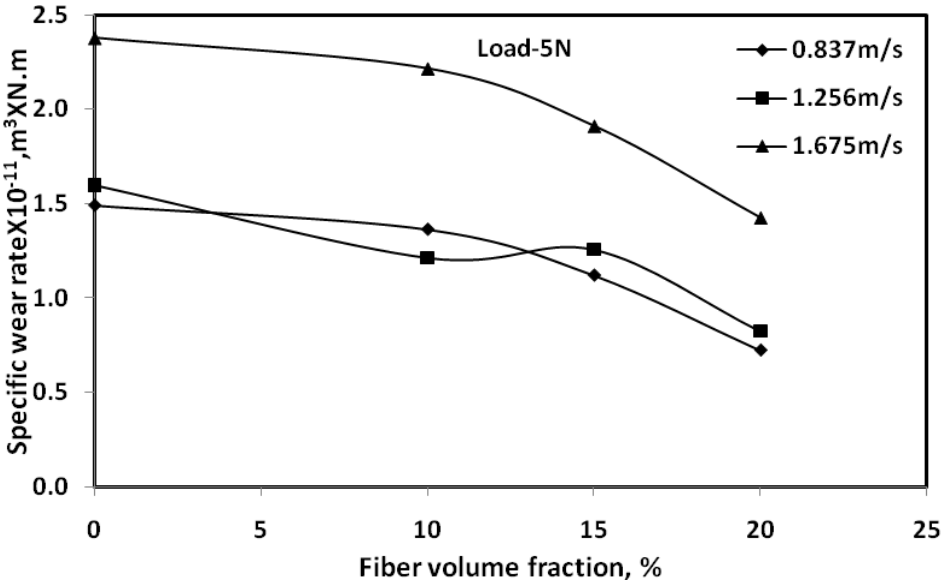

Figure-4.15 Variation of specific wear rate with filler volume fraction of fiber composite at 5N load

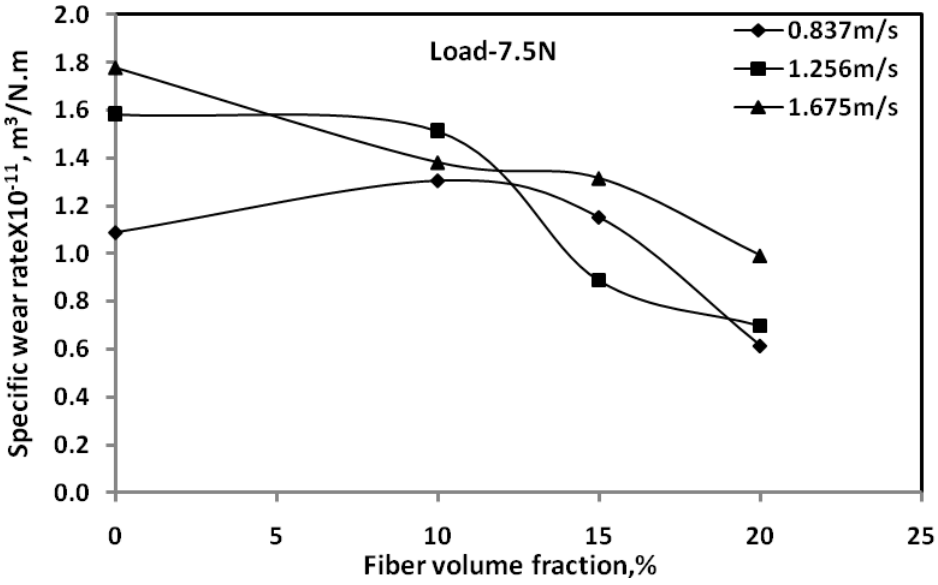

Figure-4.16 Variation of specific wear rate with filler volume fraction of fiber composite at 7.5N load

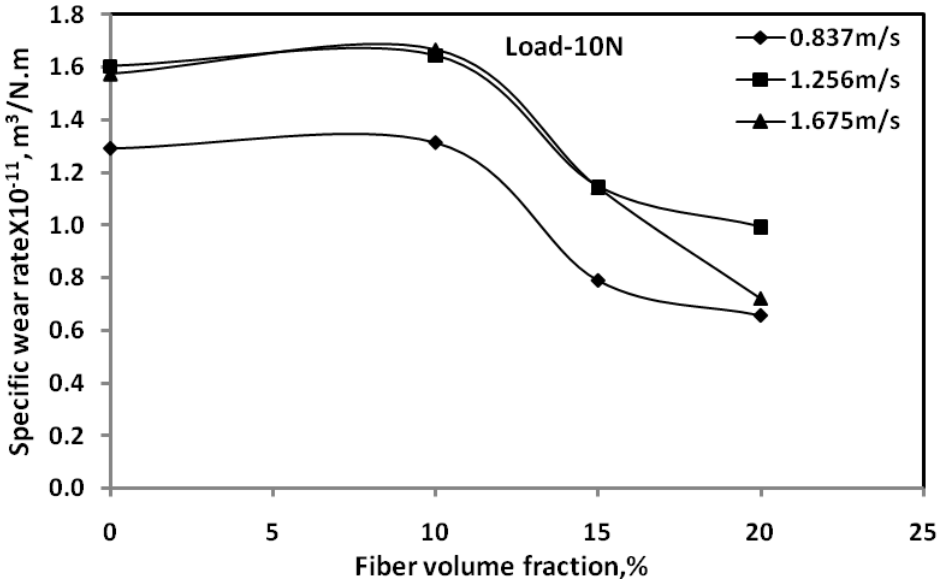

Figure-4.17 Variation of specific wear rate with filler volume fraction of fiber composite at 10N load

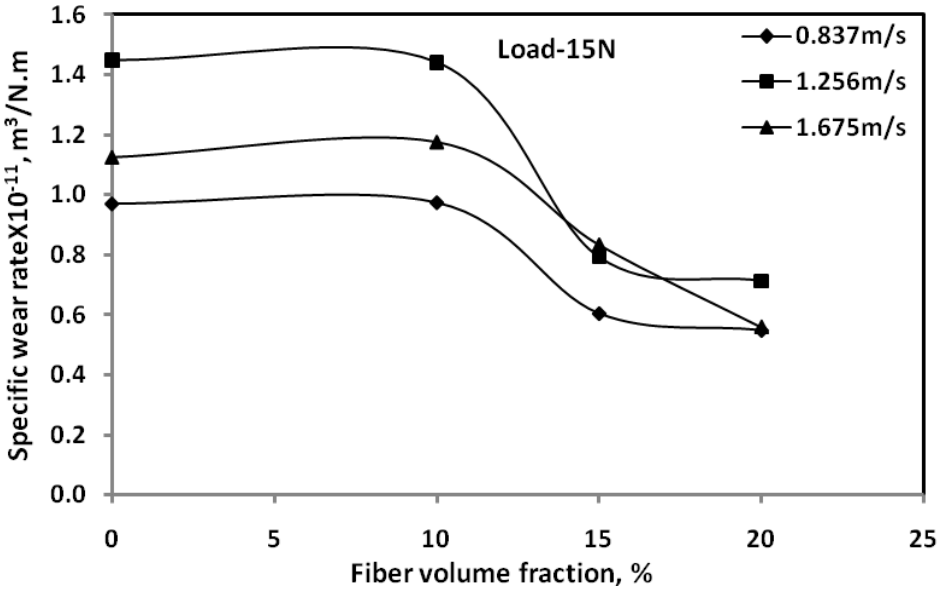

Figure-4.18 Variation of specific wear rate with filler volume fraction of fiber composite at 10N load

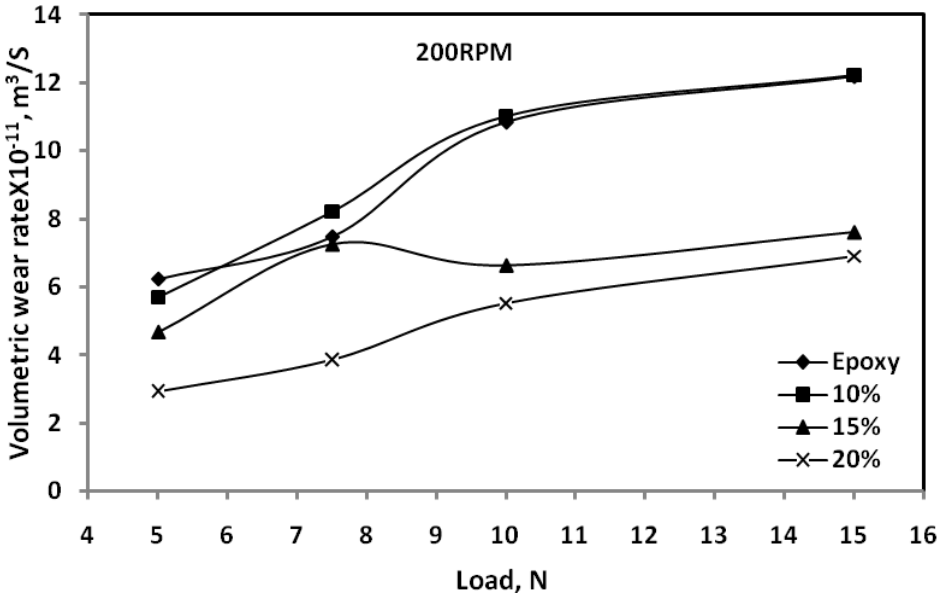

Figure-4.19 Variation of volumetric wear rate with load for all composites at a sliding velocity of 0.837m/s

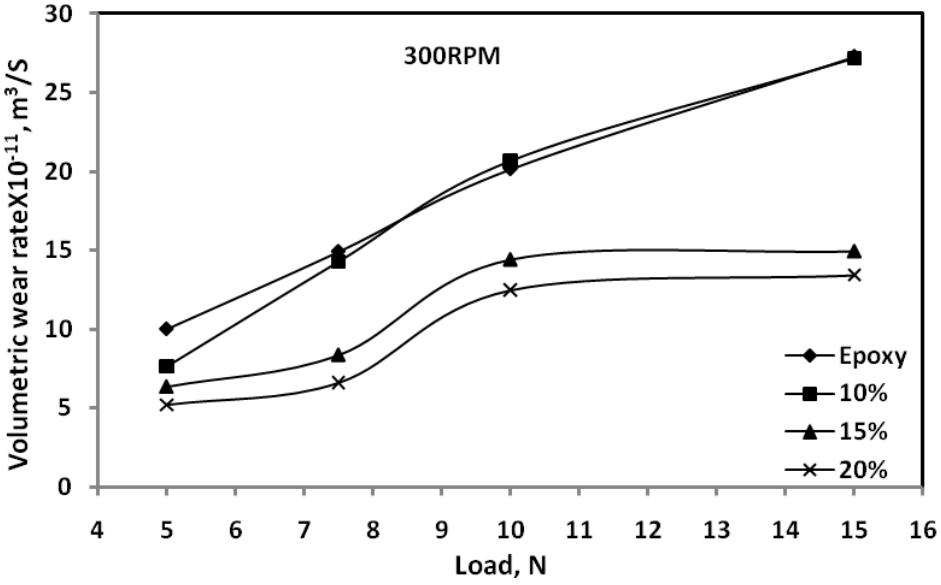

Figure-4.20 Variation of volumetric wear rate with load for all composites at a sliding velocity of 1.256m/s

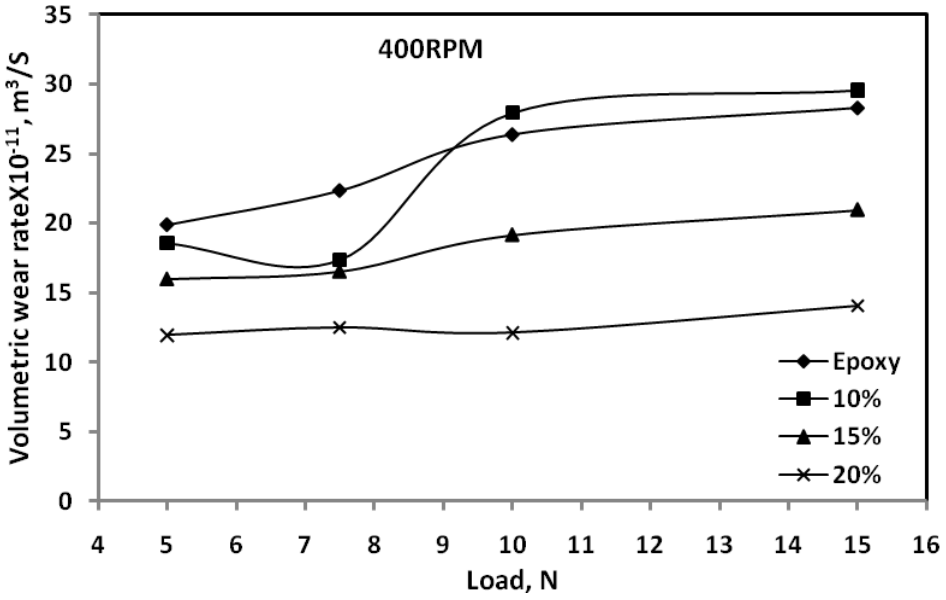

Figure-4.21 Variation of volumetric wear rate with load for all composites at a sliding velocity of 1.675m/s

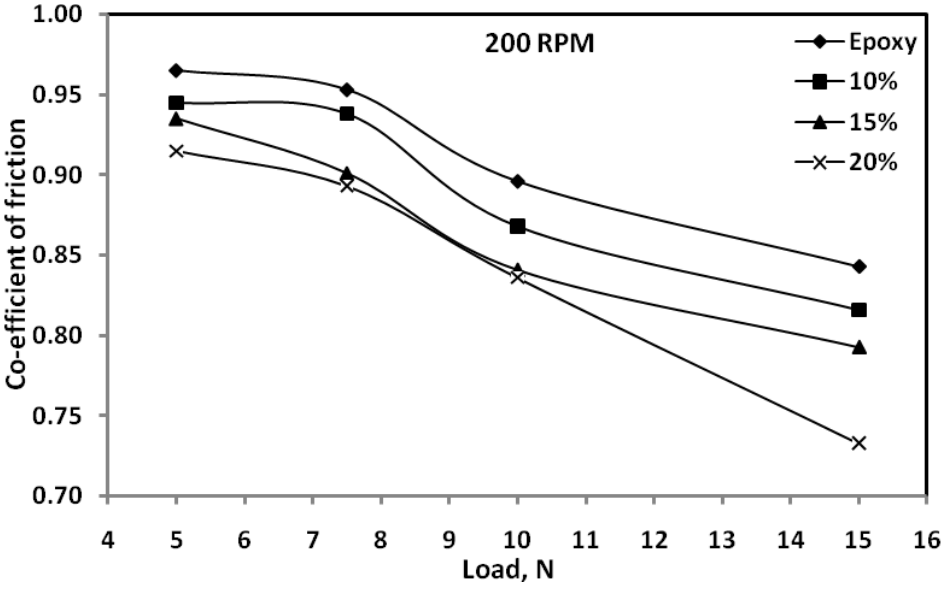

Figure-4.22 Variation of co-efficient of friction with load for all composites at a sliding velocity of 0.837m/s

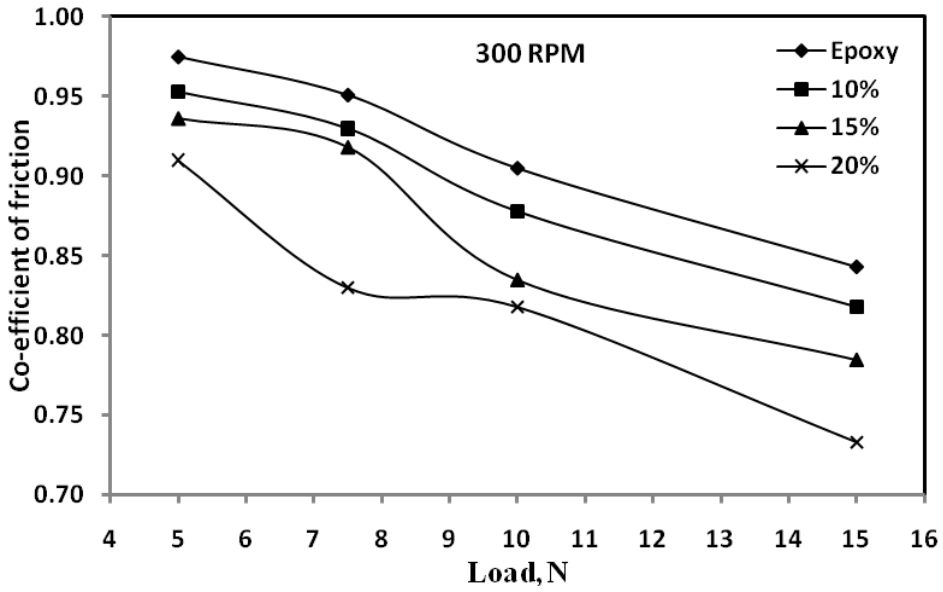

Figure-4.23 Variation of co-efficient of friction with load for all composites at a sliding velocity of 1.256m/s

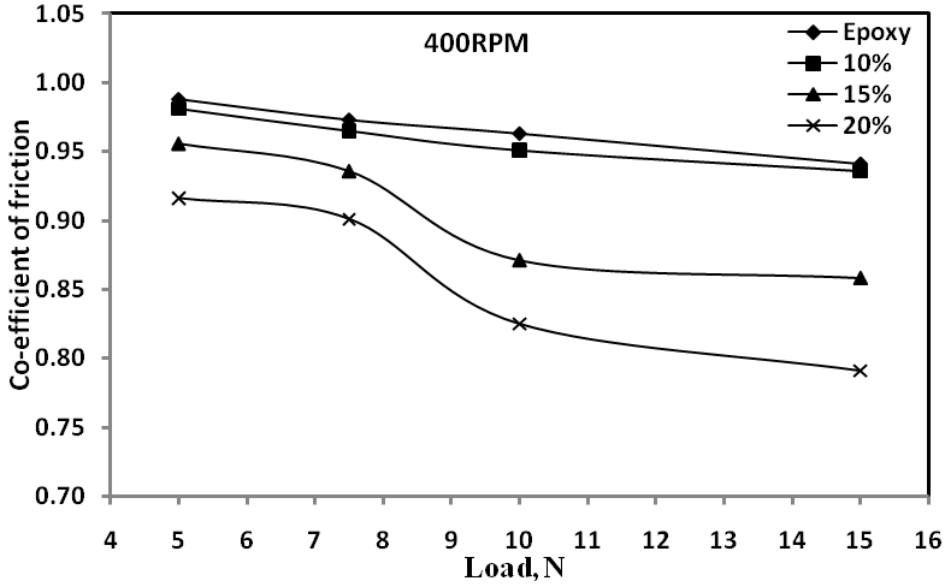

Figure-4.24 Variation of co-efficient of friction with load for all composites at a sliding velocity of 1.675m/s

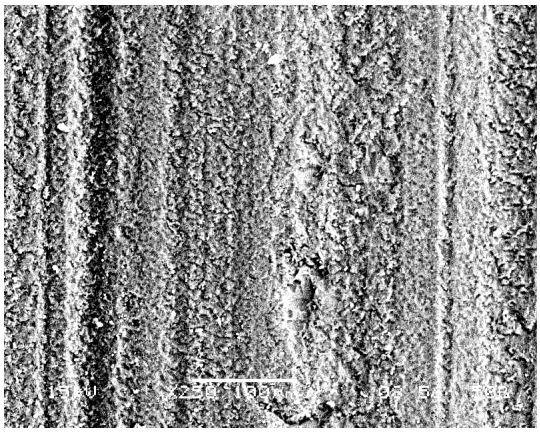

Figure-4.25(a)

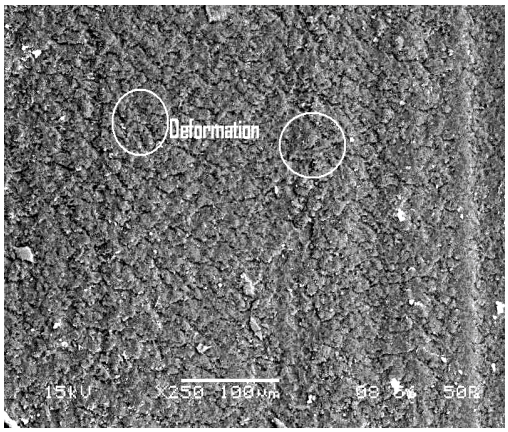

Figure-4.25(b)

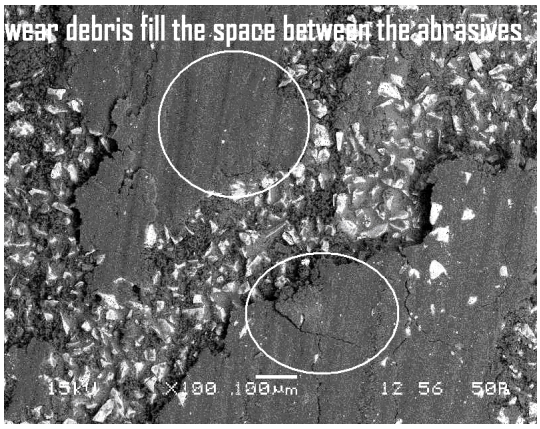

Figure-4.25(c)

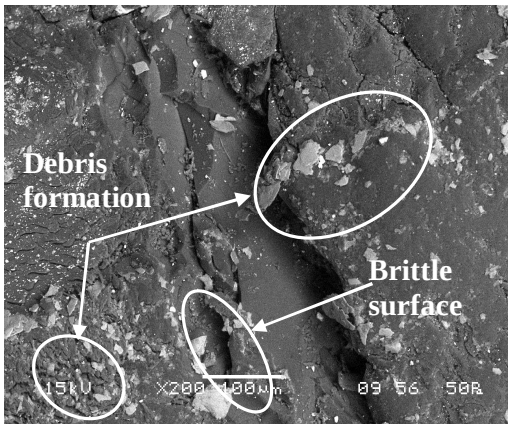

Figure-4.25(d)

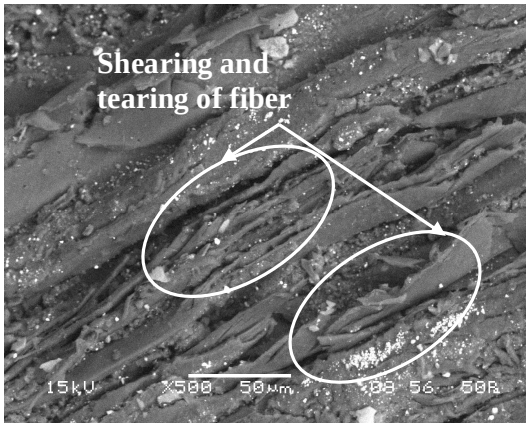

Figure-4.25(e)

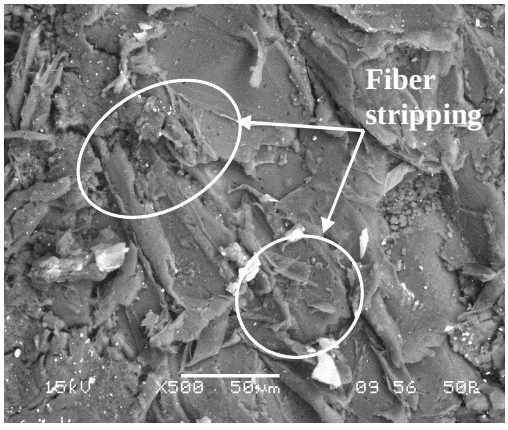

Figure-4.25(f)

Figure-4.25 Scanning electron micrograph of worn surface of (a) Neat epoxy under 10N load, (b) Neat epoxy under 15N load, (c) abrasive surface after test, (d) 10%, (e) 15% and (f) 20% bagasse fiber reinforced composites under 10N load and 0.837 m/s sliding velocity

Chapter 5

WEAR ANISOTROPY OF BAGASSE FIBER REINFORCED EPOXY COMPOSITE

Chapter-5

5.1 INTRODUCTION

Despite the interest and environmental appeal of natural fibers; their use has been limited to non-tribological application due to their lower strength and stiffness compared with synthetic fiber reinforced polymer composite. However, the stiffness and strength shortcomings of bio composites can be overcome by structural configuration and better arrangement in a sense of placing fibers in specific locations for highest strength performance. Unidirectional continuous fiber-reinforced polymer composites exhibit significant tribological anisotropy due to their heterogeneity. As described in the literature [160-164] fiber orientation with respect to sliding direction is one of the most important parameters affecting properties of composites including friction and wear behaviour of FRP composite. It is also said that properties of natural fiber composites are influenced by fiber loading, dispersion, orientation, and fiber to matrix interface [165]. Natural fibers such as sisal and jute are naturally occurring composites containing cellulose fibrils embedded in lignin matrix. These cellulosic fibrils are aligned along the length of the fiber irrespective of its origin. Such an alignment leads to maximum tensile strength and provides rigidity in that direction of the fiber. Experimental investigation has shown that the largest wear resistance in FRP composites occurred when the sliding was normal to the fiber orientation, while the lowest wear resistance occurred when the fiber orientation was in the transverse direction. Experiments have also shown that the coefficient of friction and the wear in FRP composites depend on several factors including the material combination, the fiber orientation, and the surface roughness.

Cirino *et al* [162] studied the dry abrasive wear behaviour of continuous aramid fiber reinforced epoxy composite and found that among three orientations of aramid fiber in epoxy matrix i.e. normal, parallel and anti-parallel directions, normal orientation produces optimum wear resistance. Shim *et al* [164] reported the effect of fiber orientation on friction and wear properties of graphite fiber composites and discovered that the differences in friction and wear behaviour of specimens with different fiber orientation are mainly due to the anisotropic properties caused by the microstructure of fiber orientation in the matrix.

Lhymn [161] investigated the tribological properties of unidirectional polyphenylene sulfide-carbon fiber laminate composites and reports that fibers that are oriented normal to sliding surface exhibits better wear resistance. He also attempted to qualitatively explain the effect of fiber orientation in terms of the difference in the inter-laminar shear strength and the fracture strain of the three principal fiber orientations. Sung *et al* [160] reported the same type of result while they worked for Kevlar-epoxy composites. Whereas results of Friedrich *et al* [166] for with unidirectional carbon fiber-glass matrix composite showed maximum wear resistance in case of anti-parallel orientation.

Though extensive work on wear anisotropy of synthetic fiber has already been done, the wear anisotropic of natural fiber composite is meager. Recently some attempt has been taken to study the wear anisotropy of on natural fibers like cotton [167], bamboo [168-169], sisal [170], jute [171], and kenaf [148]. Amin [167] reported the effect of unidirectional cotton fiber reinforcement on the friction and sliding wear characteristics of polyester with varying sliding speed, fiber volume fraction, and fiber orientation. Chand *et al* [168] while studying the high stress abrasive wear study on bamboo, proposed a generalized equation for anisotropy dependence of bamboo with load and abrasive grit size. In another paper [169] they have studied the wear behavior of bamboo in different orientations such as LL, LT and TT, and observed that in bamboo the wear rate follows the trend $W_{TT} < W_{LT} < W_{LL}$. Tong *et al* [8] reported the three-body abrasive wear (low stress) results of bamboo against a free abrasive consisting of quartz sand and bentonite in the past on a rotary-disk type abrasive wear tester. Chand *et al* [170] while working on influence of fiber orientation on high stress wear behaviour of sisal fiber reinforced epoxy composites, reported that the wear rate for sisal fiber follows the trend; $W_{TT} < W_{LT} < W_{LL}$. Similar results also observed while they worked with jute fiber reinforced polyester composite [171]. Chin *et al* [148] investigated wear and friction performance of kenaf fibers reinforced epoxy composite in three different fiber orientations with respect to the sliding direction and reported that the composite exhibited better wear performance in normal (N-O) compared to parallel (P-O), anti-parallel (AP-O) orientations.

Acceptance of bagasse fiber epoxy composite in various engineering application is possible if tribological properties of these materials are thoroughly investigated. EI-Tayeb [172-173] recently reported the abrasive and adhesive wear behaviour of bagasse fiber reinforced polymer composite but there is no evidence in the literature regarding abrasive

wear performance of bagasse fiber composites in different directions. Wear properties of bagasse fiber reinforced composite in different directions would have an advantage in development and application of this composite. In fibre reinforced composite, structure, dimension and orientation of fibres are important factors affecting their tribological properties. Wear data on natural composite structure of bagasse can provide clues and ideas for design of composites for making anti-friction materials and wear resistant materials. It is expected that the wear behavior of bagasse fiber in different orientations such as NO, PO and APO will be different. Hence, in this chapter the effect of bagasse fiber orientation, sliding distance and applied load on the abrasive wear properties of bagasse fiber reinforced epoxy composite has been determined and discussed.

5.2 EXPERIMENTAL

5.2.1 Sample preparation

The composite samples were prepared by using the thermosetting epoxy resin LY556 and hardener HY 951 obtained from Ciba - Geigy of India Limited. Bagasse fibers were incorporated in the resin matrix in different orientations. Composites were prepared by using epoxy to hardener ratio as 10:1. Usual hand lay-up technique was used to manufacture the composite sheet at room temperature. Samples were cut in to standard size of $20\times20\times20mm^3$ from the composite sheets. The samples were polished and finished to 150 microns prior to testing. Schematic diagram of composites showing different fiber orientations and sliding direction with designations of samples are shown in figure 5.1.

5.2.2 Two body abrasive wear test (Single-pass condition)

Two-body Abrasion wear studies in the single-pass condition have been conducted on a Two-body abrasion wear tester (Figure-5.2), supplied by Magnum Engineers, Bangalore, India. The specimens are abraded against water-proof silicon carbide (SiC) abrasive papers of different grades (150, 180, 320, and 400) suitably fixed on the machine bed. The samples were finished ground to have a uniform contact on the abrasive paper. The specimen was mounted on a sample holder which is fixed on the reciprocating ram and then loaded as per requirement by placing a dead weight on the load pan. The experiment was conducted at a selected constant speed of 1000 mm/min, with different loads (1, 3, 5, 7 and

10 N). The weight loss was measured at a sliding distance of 27 m. After each test the specimen was removed from the holder and cleaned with a brush to remove any wear debris/particle which might have attached to the specimen. The specimen was again cleaned with acetone prior to weighing. The weight loss was measured by precision electronic weighing machine with an accuracy of ± 0.001gm. The wear rate was calculated as discussed in chapter-4, Art-4.6.4, for dry sliding wear rate. For each test five samples were tested and average value was calculated. The results thus achieved from this test are tabulated and shown in Table-5.1 to 5.4.

5.3 RESULTS AND DISCUSSION

Figure 5.3–5.6 shows the variation of wear rate with different applied load for different directionally oriented (PO, APO and NO) samples. It is clear from these figures that wear rate of the composite increases with the increase in normal load for different directionally oriented fibers. However the magnitude of the wear rate is not the same. Minimum wear rate has been observed for NO sample, whereas PO sample exhibits maximum wear rate. The wear rate follows the trend; $W_{NO} < W_{APO} < W_{PO}$ which indicate an-isotropic wear behaviour. In case of NO-type sample the long fibers are well embedded in the matrix and only the cross sections of the vascular bundles come in contact with abrasive particle which oppose the movement of the abrading particles, as a result minimum wear occurred. There is a possibility of maximum real contact area with fibers in the sliding direction in the case of the PO-type sample, which leads to maximum wear in comparison to APO-type and NO-type sample. In this case the abrasion in the composite might have taken place due to the removal of a complete layer of fiber, micro cutting of the cell, delamination of fibers leading to micro-cutting and breaking of resin. This in turn leads to formation of debris. In APO-type sample the exposed area of fiber is less in comparison to PO-type but higher than that in NO-type. The removal of complete fiber is restricted due to phase discontinuity i.e. because of the presence of matrix phase present between the fibers. Chand *et al* [168] reports the same type of results when they studied the abrasive wear behaviour of bamboo.

Figure 5.7 shows the variation of wear rate with different grit sizes at a load of 10N. It is observed that with increase of the abrasive grit size from 400 to 150, wear rate

increases for all the samples. As pointed by Chand *et al* [169], the wear rate is primarily dependent on the depth and width of the groove made by the abrasives. At coarser abrasives, the depth of penetration of the abrasive particle is so high that a large portion of material is removed from the specimen surface leaving behind large cavities in the worn surface. The depth of cut is increased significantly with coarser grit size. If the applied load is fixed, then the effective stress on individual abrasives increases with coarser abrasive particles, as the load is shared by less number of abrasives. When the abrasive particles are finer in size, they make only elastic contact with the test specimen surface, as the effective stress in individual abrasive is less. As a result, these abrasive particles only support the applied load without contributing sufficient material removal. The radius of abrasive tip varies with increase in size, but, the width of groove increases substantially with increase in abrasive size. This may be attributed to the fact, the effective stress on each individual abrasive increase substantially when become coarser in size, and becomes more effective to penetrate deeper into the surface. Similar trend has been observed for 1, 3, 5, 7 and 10N load therefore has not been shown here.

Chand *et al* [168] introduced term anisotropy co-efficient while they worked with bamboo. In the similar way an attempt has been made here to introduce anisotropy co-efficient for bagasse fiber. Anisotropy coefficient is defined as the ratio of the wear loss value in perpendicular to parallel fibre direction in unidirectional fibre reinforced composites. Physical significance of anisotropy coefficient is to show the anisotropy magnitude of material property in the composites. Anisotropy coefficient can be written

Anisotropy coefficient $\boldsymbol{(n) = W_{NO}/W_{PO}}$ (if property *W* is less in NO case than PO case)

or $\boldsymbol{n = W_{PO}/W_{NO}}$ (if property *W* is less in PO case than NO case)

n = 1 for isotropic composites; n = 0, for ideal anisotropic composites (or Infinite anisotropic composites); $0 < n < 1$ for anisotropic composites.

Generally the value of anisotropy coefficient will lie between 0 and 1. In the present case, the wear rate of NO samples is less than that of the PO samples. So $n = W_{NO}/W_{PO}$. The dependency of wear anisotropy coefficient for different loads and different abrasive grit size for bagasse fiber polymer composite has also been determined in this study. Figure 5.8

shows the variation of wear anisotropy coefficient with different applied loads 1, 3, 5, 7 and 10N for 27m sliding distance. It was observed that with increase of load from 1 to 10 N, W_{NO}/W_{PO} increases and minimum anisotropy occurred at 7N load. The relationship for the wear anisotropy for all unidirectional fiber reinforced composite is $n=f(L)$ as proposed by Chand *et al* [168]. A similar relationship has been found following the equation for the present case (i.e)

$$W_{NO}/W_{PO} = -aL^2 + bL - c \quad (5.1)$$

where W_{NO} and W_{PO} are the wear in normal and parallel directions of fibres orientation and L is the applied load. Constants a, b and c for bagasse fiber reinforced epoxy composite are 0.006, 0.102, and 0.236, respectively.

Figure 5.9 shows the dependence of wear anisotropy on different abrasive grit size. With increase of grit size, wear rate increases. But this experimental study exhibited the decreasing trend of wear anisotropy coefficient with increasing abrasive grit size (GS) and the peak in the anisotropy has been occurred at 400 grit size. The relationship between wear anisotropy coefficient and grit size is found to be

$$W_{NO}/W_{PO} = -eS^3 + fS^2 - gS + h \quad (5.2)$$

where S is the abrasive grit size and e, f, g and h are constants. The coefficient of correlation R^2 value is 1. Values of constants e, f, g and h are found to be 3E−08, 2E−05, 0.0032 and 0.9577 respectively at 27m sliding distance.

5.4 WORN SURFACE MORPHOLOGY

Figure 5.10 (a-c) shows the worn surface morphology of PO, APO and NO samples done through Scanning Electron Microscope studies. In case of parallel orientation (PO), the matrix material between fibres was removed due to delamination caused by hard asperities allowing the passage for the subsequent removal of whole fiber during abrasion, which is visible in figure 5.10 (a).

The possibility of the real contact area with fibres in the sliding direction probably is more in PO samples than the APO and NO sample, which led to the highest wear. In APO samples, hard abrasive particles were moving through different interfaces and different layers of matrix and fibre bundle alternatively. So the composite in APO was subjected to micro-cutting action that was hampered due to phase discontinuity, which was alternately coming after every fibre/matrix. Thus in this mode the removal of material was mainly due to micro-cutting in the resin matrix and, bending and tearing of fibre transversely at their ends (figure 5.10 b).

In case of normal fibre direction (NO) samples (figure 5.10 c), it is seen that there is more resistance to the removal of fiber as they are deeply embedded in the matrix. Since the cellulosic fibers are oriented normal to the sliding direction, only cross section of vascular bundles come in contact to the abrasive particles, that is why the removal of material becomes difficult for NO samples. The cross sections of vascular bundle of fibres created more resistance in the path of the abrasion and restricted the movement of abrading particles, which reduced the wear in the NO sample.

5.5 CONCLUSIONS

From the experiment, observation and the SEM studies the following conclusions were made.

- The wear anisotropy of Bagasse fiber reinforced epoxy composite depends on load and abrasive grit size.

- Maximum wear resistance (minimum wear rate) is observed in NO-Type sample and the wear rate under sliding mode follows the trend; $W_{NO} < W_{APO} < W_{PO}$ which indicates an anisotropic wear behaviour.

- An equation between abrasive wear anisotropy and load for unidirectional Bagasse fiber-reinforced epoxy composites is proposed. Another relationship between abrasive wear anisotropy with abrasive grit is also suggested.

- Abrasive grit size and normal load have a significant influence on abrasive wear loss, irrespective of fiber orientations.

- In PO type samples the abrasion takes place due to micro ploughing and delamination of fiber where as in APO type samples, micro cutting is highly responsible for wear process. In NO type samples micro cutting of fiber cross-section leads the wear mechanism process.

Table-5.1 Weight loss of PO samples at different grit sizes and sliding distances

Abrasive Grit size	Sliding distance(m)	Weight loss (gms) under load				
		1N	3N	5N	7N	10N
150	06.75	0.013	0.018	0.032	0.039	0.048
	13.50	0.021	0.029	0.053	0.056	0.062
	20.25	0.025	0.050	0.077	0.102	0.147
	27.00	0.034	0.072	0.100	0.140	0.218
180	06.75	0.022	0.020	0.043	0.058	0.067
	13.50	0.027	0.036	0.068	0.075	0.081
	20.25	0.034	0.061	0.083	0.098	0.156
	27.00	0.047	0.086	0.101	0.140	0.215
320	06.75	0.010	0.039	0.012	0.031	0.153
	13.50	0.016	0.053	0.034	0.059	0.167
	20.25	0.029	0.061	0.064	0.102	0.180
	27.00	0.038	0.075	0.105	0.115	0.191
400	06.75	0.010	0.019	0.041	0.041	0.121
	13.50	0.014	0.034	0.053	0.062	0.149
	20.25	0.022	0.049	0.066	0.081	0.158
	27.00	0.030	0.058	0.078	0.090	0.168

Table-5.2 Weight loss of APO samples at different grit sizes and sliding distances

Abrasive Grit size	Sliding distance(m)	Weight loss (gms) under load				
		1N	3N	5N	7N	10N
150	06.75	0.012	0.017	0.041	0.031	0.052
	13.50	0.014	0.028	0.049	0.068	0.139
	20.25	0.017	0.036	0.062	0.095	0.165
	27.00	0.020	0.040	0.070	0.110	0.198
180	06.75	0.006	0.013	0.018	0.015	0.030
	13.50	0.008	0.022	0.040	0.032	0.062
	20.25	0.014	0.029	0.053	0.061	0.091
	27.00	0.020	0.040	0.070	0.110	0.183
320	06.75	0.008	0.031	0.027	0.021	0.092
	13.50	0.010	0.038	0.040	0.052	0.121
	20.25	0.012	0.045	0.051	0.065	0.138
	27.00	0.021	0.059	0.060	0.090	0.150
400	06.75	0.005	0.012	0.019	0.014	0.081
	13.50	0.008	0.019	0.031	0.029	0.097
	20.25	0.014	0.033	0.045	0.052	0.109
	27.00	0.020	0.040	0.050	0.070	0.127

Table-5.3 Weight loss of NO samples at different grit sizes and sliding distances

Abrasive Grit size	Sliding distance(m)	Weight loss (gms) under load				
		1N	3N	5N	7N	10N
150	06.75	0.003	0.016	0.021	0.038	0.039
	13.50	0.004	0.020	0.035	0.061	0.082
	20.25	0.008	0.027	0.061	0.082	0.121
	27.00	0.010	0.034	0.070	0.100	0.163
180	06.75	0.002	0.009	0.020	0.038	0.031
	13.50	0.003	0.013	0.028	0.052	0.065
	20.25	0.005	0.018	0.036	0.073	0.097
	27.00	0.010	0.023	0.043	0.094	0.160
320	06.75	0.001	0.011	0.012	0.022	0.065
	13.50	0.004	0.016	0.031	0.040	0.084
	20.25	0.008	0.029	0.043	0.057	0.109
	27.00	0.010	0.040	0.050	0.070	0.135
400	06.75	0.004	0.008	0.013	0.004	0.022
	13.50	0.005	0.016	0.018	0.027	0.055
	20.25	0.007	0.024	0.029	0.042	0.078
	27.00	0.010	0.029	0.040	0.060	0.093

Table-5.4 Weight loss and wear rate of PO, APO and NO samples at different loads and grit sizes for a sliding distance of 27 m

Abrasive grit size	Load (N)	PO type samples		APO type samples		NO type samples	
		Wt. loss (gms)	Wear rate $X10^{-5}$ (N/m)	Wt. loss (gms)	Wear rate $X10^{-5}$ (N/m)	Wt. loss (gms)	Wear rate $X10^{-5}$ (N/m)
150	1	0.034	1.234	0.020	0.726	0.010	0.363
	3	0.072	2.613	0.040	1.452	0.034	1.234
	5	0.100	3.630	0.070	2.541	0.070	2.541
	7	0.140	5.081	0.110	3.993	0.100	3.630
	10	0.218	7.913	0.198	7.187	0.163	5.916
180	1	0.047	1.706	0.020	0.726	0.010	0.363
	3	0.086	3.121	0.040	1.452	0.023	0.835
	5	0.101	3.666	0.070	2.541	0.043	1.561
	7	0.140	5.018	0.110	3.993	0.094	3.412
	10	0.215	7.804	0.183	6.642	0.160	5.807
320	1	0.038	1.379	0.021	0.762	0.010	0.363
	3	0.075	2.722	0.059	2.141	0.040	1.452
	5	0.105	3.811	0.060	2.178	0.050	1.815
	7	0.115	4.174	0.090	3.267	0.070	2.541
	10	0.191	6.933	0.150	5.444	0.135	4.900
400	1	0.030	1.089	0.020	0.726	0.010	0.363
	3	0.058	2.105	0.040	1.452	0.029	1.053
	5	0.078	2.831	0.050	1.815	0.040	1.452
	7	0.090	3.267	0.070	2.541	0.060	2.178
	10	0.168	6.098	0.127	4.610	0.093	3.376

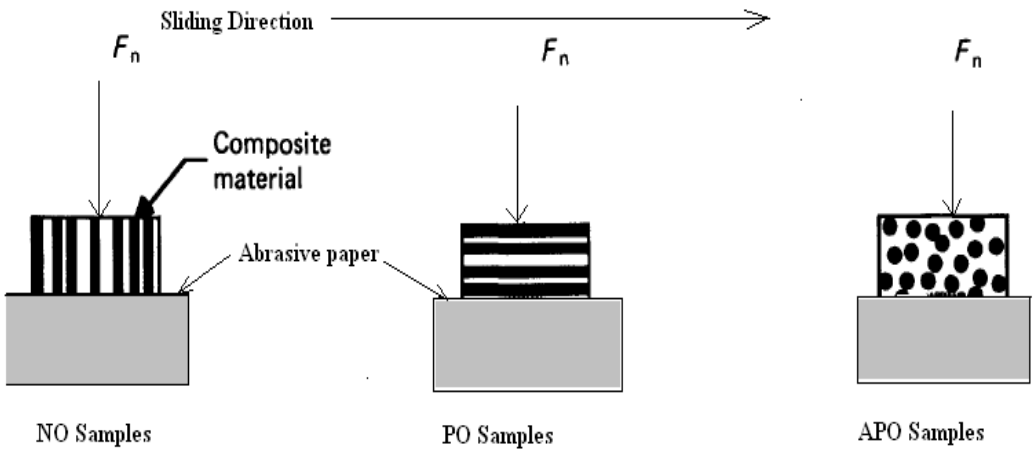

Figure-5.1 Schematic diagram of different fiber oriented composite with respect to sliding direction

Figure-5.2 Two-body Abrasion wear tester

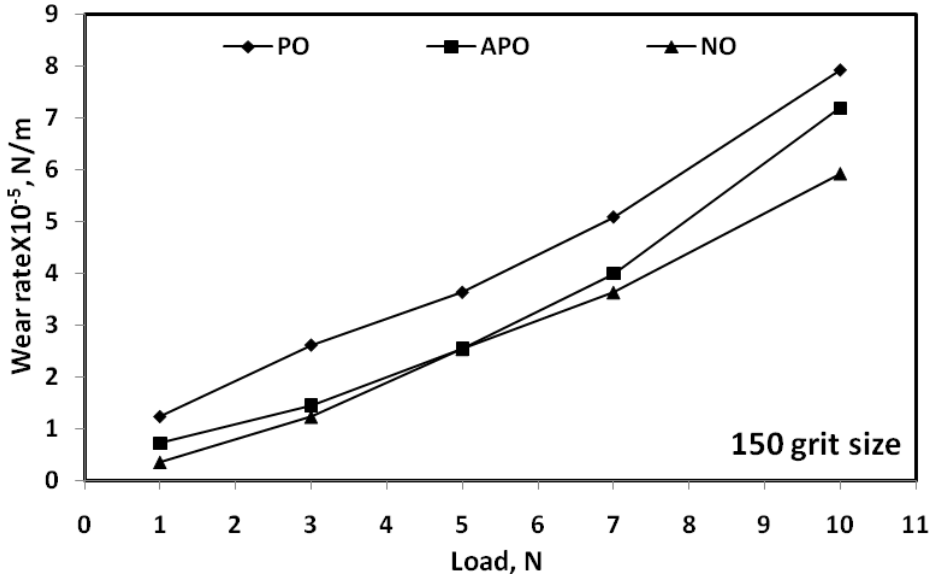

Figure-5.3 Variation of wear rate with load at 150 grit size abrasives for P, AP and N orientation of fiber samples

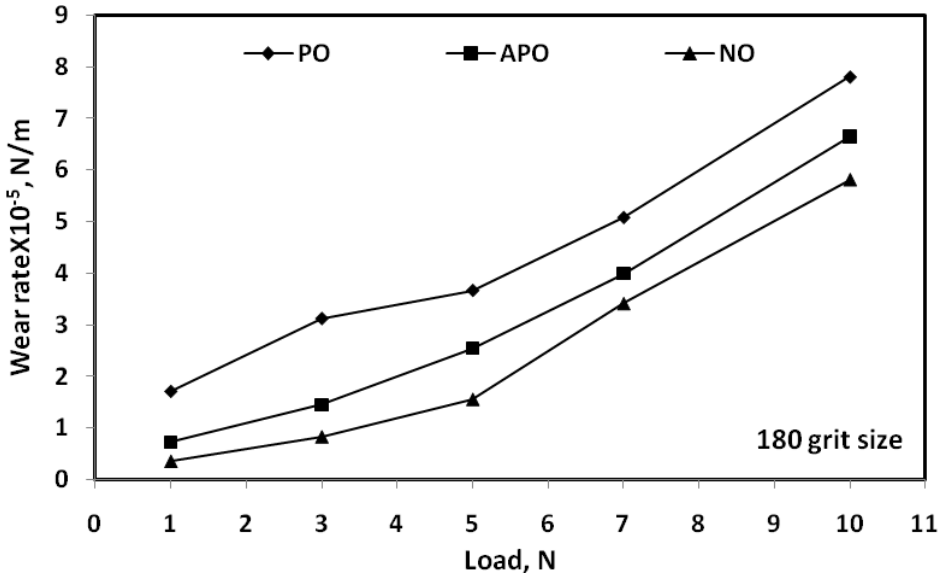

Figure-5.4 Variation of wear rate with load at 180 grit size abrasives for P, AP and N orientation of fiber samples

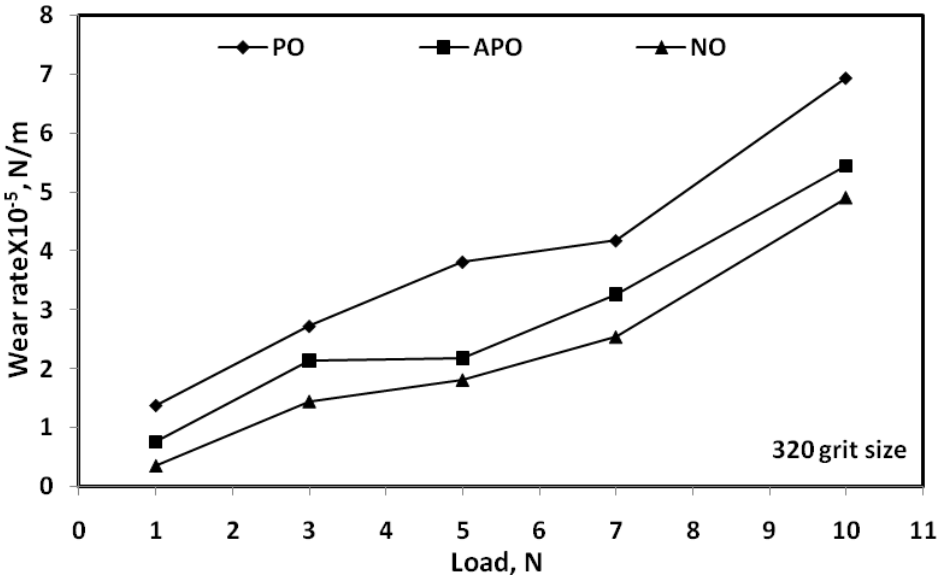

Figure-5.5 Variation of wear rate with load at 320 grit size abrasives for P, AP and N orientation of fiber samples

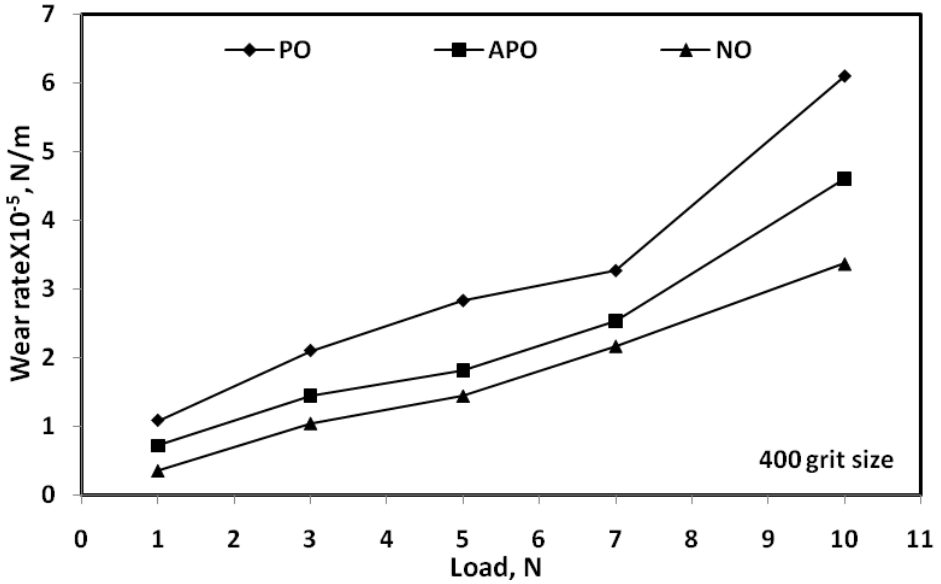

Figure-5.6 Variation of wear rate with load at 400 grit size abrasives for P, AP and N orientation of fiber samples

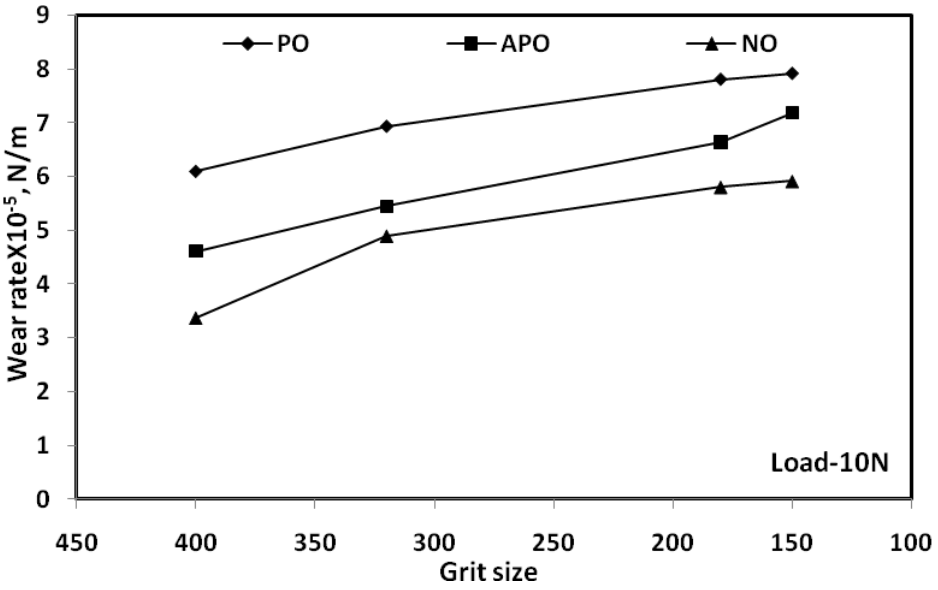

Figure-5.7 Variation of wear rate with grit size at a load of 10N for P, AP and N orientation of fiber samples

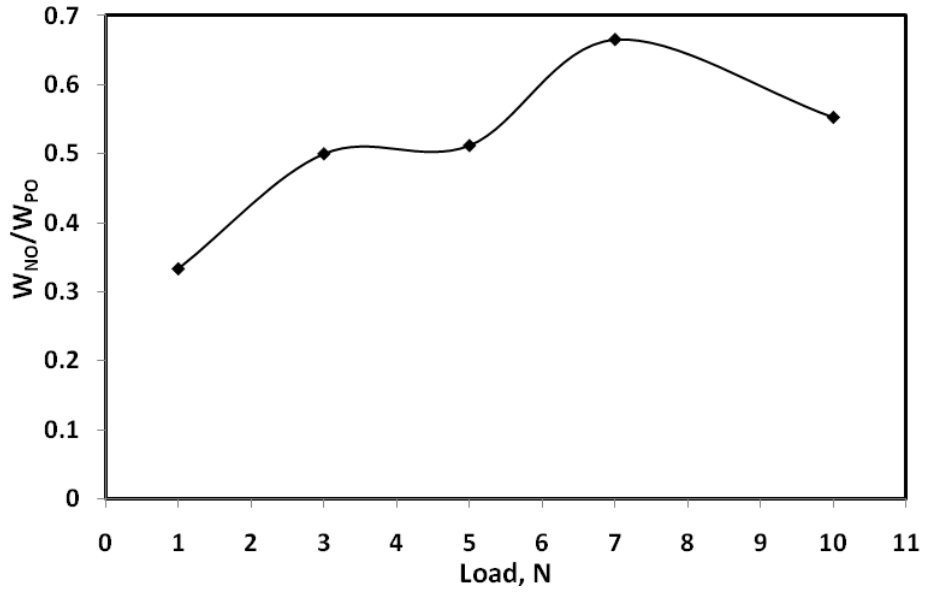

Figure-5.8 Graph between wear anisotropy vs load for Bagasse fiber reinforced polymer composite

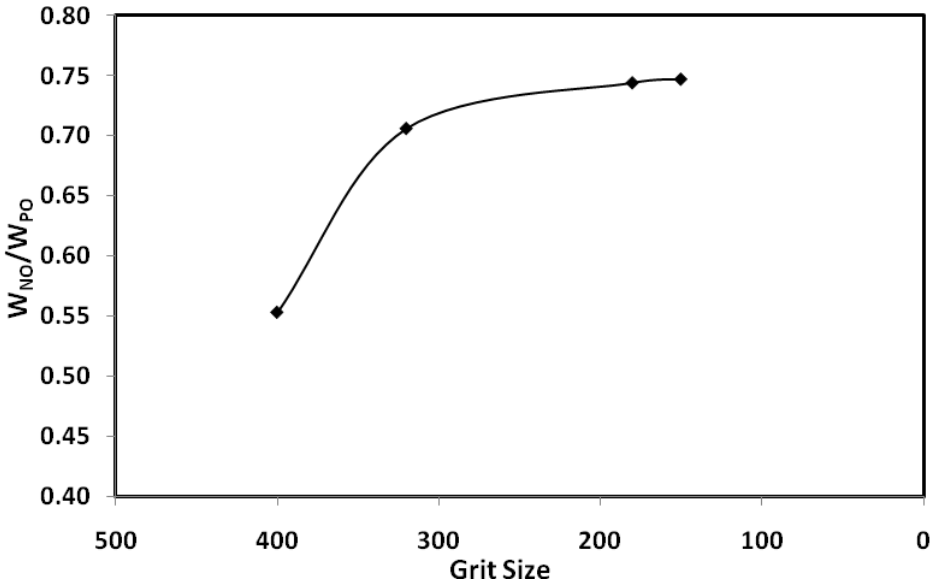

Figure-5.9 Graph between wear anisotropy vs grit size for Bagasse fiber reinforced polymer composite

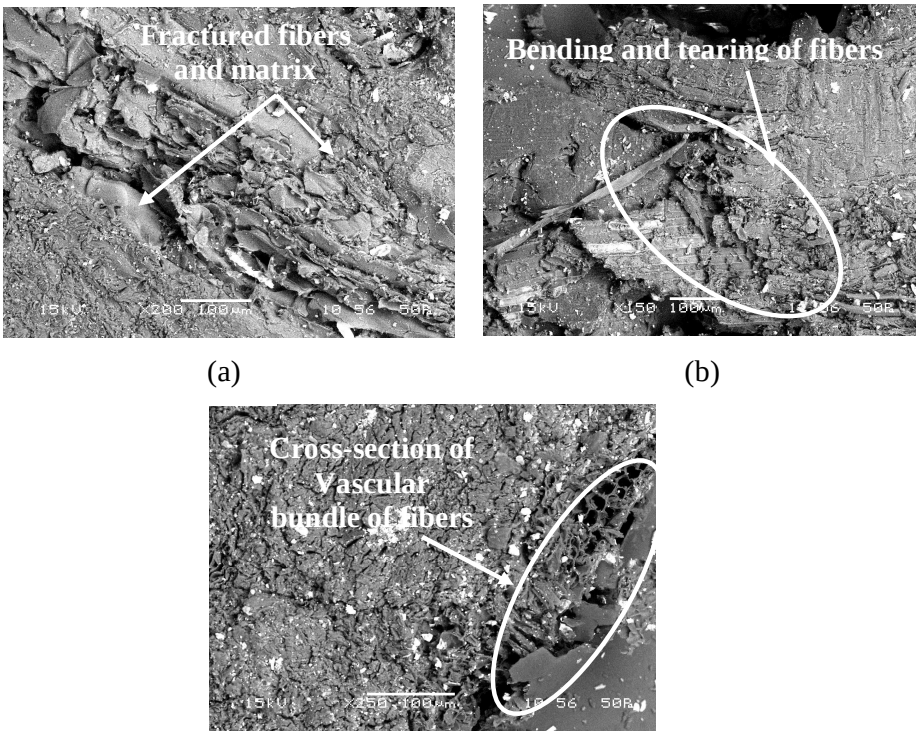

(a) (b)

(c)

Figure-5.10 SEM micrographs of abraded surface of (a) PO and (b) APO and (c) NO samples

Chapter 6

SOLID PARTICLE EROSION STUDIES OF BAGASSE FIBER EPOXY COMPOSITES

Chapter-6

6.1 INTRODUCTION

Solid particle erosion manifests itself thinning of components, surface roughening, surface degradation, macroscopic scooping appearance and reduction in functional life of the structure. Hence, solid particle erosion has been considered as a serious problem as it is responsible for many failures in engineering applications. Hence several attempts to understand the basic mechanisms of the erosion were started in the last half of the 20^{th} century and have been continued to the present. In the year of 1995 an article on the past and the future of erosion was presented by Finnie [174]. In this article, the influencing parameters and dominating mechanisms during solid particle erosion were reviewed on the erosion response of metals and ceramic materials. In the same year another article was published by Meng *et al* [175] to provide information about the existing wear models and prediction equations.

6.2 DEFINITION

According to Bitter [176], erosion is a material damage caused by the attack of particles entrained in a fluid system impacting the surface at high speed. Hutchings [177] defines it as an abrasive wear process in which the repeated impact of small particles entrained in a moving fluid against a surface result in the removal of material from the surface. Erosion due to the impact of solid particles can either be constructive (material removal desirable) or destructive (material removal undesirable), and therefore, it can be desirable to either minimize or maximize erosion, depending on the application. The constructive applications include sand blasting, high-speed water-jet cutting, blast stripping of paint from aircraft and automobiles, blasting to remove the adhesive flash from bonded parts, erosive drilling of hard materials. Whereas the solid particle erosion is destructive in industrial applications such as erosion of machine parts, surface degradation of steam turbine blades, erosion of pipelines carrying slurries and particle erosion in fluidized bed combustion systems. In most erosion processes, target material removal typically occurs as the result of a large number of impacts of irregular angular particles, usually carried in pressurized fluid streams.

6.3 SOLID PARTICLE EROSION OF POLYMER COMPOSITES

Polymers and their composites are increasingly being used in many areas starting from aerospace to process industries. These are extensively used in tribo applications such as bearings, gears etc where liquid lubricants cannot be used because of various constraints. Apart from adhesive wear mode, some polymers and composites have exhibited excellent tribo-potential in other wear situations also such as abrasive, fretting, reciprocating and erosive [178]. Polymers and composites are increasingly being used in applications such as radomes, surfing boats, gas and steam turbine blades, gears for locomotives, conveyor belts, helicopter blades, pump impellers in mineral slurry processing where the components encounter impact of lot of abrasives like dust, sand, splinters of materials, slurry of solid particles and consequently the materials undergo erosive wear [179-181]. Hence it becomes imperative to study erosive wear behavior of polymeric engineering materials in various operating condition.

Many researchers [182-206] have evaluated the resistance of various types of polymers like nylon [187, 188], epoxy [204, 205], polypropylene [194, 197], polyethylene [194], UHMWPE [202], PEEK [195, 200] and various polymer based composites [182, 175, 189-202] to solid particle erosion. Little information concerning the tribological performance of natural fiber reinforced polymer composite material [203-204] has been reported. Therefore the study of erosion characteristics of natural fiber reinforced polymer composites is of vital importance. As pointed out by Roy *et al* [185] the erosive resistance of polymer composite is low in comparison to monolithic materials. It is also established that erosive wear of reinforced polymer composite is usually higher than unreinforced polymer matrix [186].

The most important factors influencing the erosion rate of the composite materials can be summarized under four categories; (i) The properties of the target materials (matrix material properties and morphology, reinforcement type, amount and orientation, interface properties between the matrices and reinforcements, etc.), (ii) Environment and testing conditions (temperature, chemical interaction of erodent with the target), (iii) Operating parameters (angle of impingement, impinging velocity, particle flux–mass per unit time,

etc.) and (iv) The properties of the erodent (size, shape, type, hardness, etc.) [181, 186, 209-210]. Thus it seems that the erosion resistance of the material can be evaluated after investigating the combination of above parameters. In general, erosive behaviour of materials can be grouped into ductile and brittle when erosion rate is evaluated as a function of impact angle. The ductile behaviour is characterized by maximum erosion at low impact angle in the range of 15°–30°. On the other hand, if maximum erosion occurs at 90°, then the behavior can be termed as brittle. Reinforced composites have also been some time found to exhibit an intermediate behaviour known as semi-ductile with maximum erosion occurring at an angle in the range of 45°–60° [211]. However, the above classification is not absolute as the erosion behaviour of a material has a strong dependence on erosion conditions such as impact angle, impact velocity and erodent properties such as shape, hardness, size etc. In the literature, the erosion behaviour of polymers and its composites has also been characterized by the value of the velocity exponent, '*n*' ($E \alpha v^n$) [179].

Visualizing the importance of polymer composites lot of work has been done by various researchers to evaluate the erosion resistance of various types of polymers and their composites to solid particle erosion [209, 212-214]. Most of these workers have carried out wide range of thermosets and thermoplastics PMCs with synthetic fibers like glass, carbon, graphite and Kevlar. However there is no information available on erosive wear behaviour of natural fiber reinforced polymer composites. Hence the purpose of this research is to investigate the erosive wear behavior of natural fiber (bagasse) reinforced epoxy composite. Experiments were carried out to study the effect of fiber volume fraction, impingement angle and particle velocity on the erosive wear behavior of the composite and result of these investigations are presented in the subsequent sections.

6.4 EXPERIEMENT

6.4.1 Preparation for the test specimens

The preparation of the test specimens were carried out as per the procedure discussed in chapter 3, Art-3.4.3. Specimens of dimension 20 x 20 x 4 mm were cut from the composite slabs. Adequate care has been taken to keep the thickness constant (4 mm) for all the samples.

6.4.2 Test apparatus & Experiment

The solid particle erosion experiments were carried out as per ASTM G76 standard on the erosion test rig shown in figure 6.1. The rig consists of an air compressor, a conveyer belt type particle feeder, and an air particle mixing and accelerating chamber. The compressed dry air is mixed with the erodent particles (silica sand 200 ± 50 micron size), which are fed at a constant rate from a conveyor belt-type feeder in to the mixing chamber and then accelerated by passing the mixture through a tungsten carbide converging nozzle of 4 mm diameter to bombard the target. These accelerated particles impact the specimen, and the specimen could be held at various angles with respect to the impacting particles using an adjustable sample holder. The machine is also loaded with a fixture to set the distance between the target material and the nozzle. For the present case stand off distances of 10, 15 and 20 mm were selected. The test apparatus has also been fitted with a rotating double disc to measure the velocity of the erodent particle. The impact velocities of the erodent particles has been evaluated experimentally using this rotating double disc method developed and as explained by Ives and Ruff [215]. The velocities obtained from this method for various pressures are given in table 6.1. The conditions under which the erosion test has been carried out are given in table 6.2. A standard test procedure is employed for each erosion test. Wear was measured by mass loss method. Eroded samples were cleaned with a fine brush to remove any sand particles attached to the surface and then wiped with a cotton plug dipped in acetone to avoid any entrapment of wear debris, prior and after each test. Then they were dried and weighed to an accuracy of 0.001 gm using an electronic balance, The test samples after loading in the test rig were eroded for 10 minute at a given impingement angle and then weighed again to determine weight loss (ΔW). The erosion rate (Er) is then calculated by using the following equation:

$$E_r = \frac{\Delta W}{W_e} \tag{6.1}$$

where ΔW is the mass loss of test sample in gm and We is the mass of eroding particles (i.e., testing time × particle feed rate). This procedure has been repeated until the erosion rate attains a constant steady state value. In the present study the same procedure is repeated for 5 times (i.e. expose time was 10 min).

The erosion efficiency (η) for the process was obtained by using the equation:

$$\eta = \frac{2E_r H}{\rho \times V^2} \tag{6.2}$$

where '*Er*' is erosion rate (gm/gm), '*H*' is hardness of eroding material (Pa) and '*V*' is velocity of impact (m/s), as proposed by Sundararajan *et al* [216]. Experimental results of the erosion test for different volume fraction of bagasse fiber reinforced epoxy composites with different impingement angle and velocities are tabulated and presented in table 6.3 - 6.6.

6.5 RESULTS AND DISCUSSION

Based on the tabulated results various graphs were plotted and presented in figure 6.2 to 6.13 for different percentage of reinforcement under different test conditions.

Figures 6.2 – 6.5 illustrate the erosion wear rate of the both neat epoxy and bagasse fiber reinforced epoxy composite as a function of angle of impingement under different impact velocities (v = 48-109 m/sec). It is evident from the plot that the erosion rate for the composite as well as for pure epoxy increases with the impact angles. It attains a peak value (α_{max}) at 90° and a minimum erosion rate (α_{min}) at 30°. Generally it has been recognized that peak erosion occurs at low impact angle (15°-30°) for ductile materials and at a higher angle (90°) for brittle materials [217]. However if the maximum erosion occurs in the angular range 45^0–60^0, it describes the semi-ductile behaviour of the material [205]. From the experimental results it is clear that bagasse fiber reinforced composites respond to solid particle impact in a purely brittle manner since the maximum erosion occurs at 90° impact angle for all the velocity range. However the erosion rate is found to be different for different velocities. The same type of behavior was also reported by Pool *et al* [199] while studying the UD and woven graphite reinforced epoxy composite. Deo and Acharya [218] while studying the erosive wear behavior of Lantana camara fiber reinforced epoxy composite showed that their composite behaves in a semi ductile in nature. Thus it can be concluded that the behavior of natural fiber composite to solid particle erosion depends on type of fiber. It is further noticed that irrespective of impact velocity and impact angle, the

erosion rate is highest for pure epoxy and lowest for 20 vol % bagasse fiber reinforced epoxy composite.

The variation of steady state erosion rate of all composite samples with filler volume fraction for different impact velocities at different impingement angles are shown in the form of histogram in figure 6.6 to 6.9. It can be observed from this histogram that erosion rate of all composite samples increases with increase in the impact velocity. It is also clear from the plot that best erosion resistance under all impact condition is achieved for the composite made of 20% bagasse fiber. The variation in erosion resistance for 20% bagasse fiber at 90° impact angle for all impact velocity is negligible. Irrespective of impact angle and impact velocity it has also been observed that there is a steady decrease in erosion rate with increase in fiber content. This indicates that the erosion rate of composite is dominated only by the volume fraction of fiber. Similar type of observation was reported by Miyazaki *et al* [198] while they worked with glass and carbon fiber reinforced poly-ether-ether-ketone composites.

In the solid particle erosion experiments, the velocity of the erosive particles has a very strong effect on erosion rate. For any material under investigation, once the steady state conditions have reached, the erosion rate (*Er*) can be expressed as a simple power function of impact velocity (*V*) [179]:

$$Er = kV^n \tag{6.3}$$

Where *k* is the constant of proportionality includes the effect of all the other variables. The value of '*n*' and '*k*' are found by least-square fitting of the data points in plots which for the above power law at different impact angles, are summarized in Table 6.7. According to Pool *et al* [179], for polymeric materials behaving in ductile manner, the velocity exponent '*n*' varies in the range 2–3 while for polymer composites behaving in a brittle fashion the value of '*n*' should be in the range of 3–5. Figure 6.10 to 6.13 illustrates the variation of erosion rate with impact velocity at different impingement angles for neat epoxy and its composites. The least square fits to data point were obtained by using power law and the values of n and k are summarized in table 6.8. The velocity exponents found for 30°, 45°, 60° and 90°

impingement angles are in the range of 0.8519-2.5073, 1.0175-2.2852, 0.8887-1.3712 and 0.1942-0.9304 respectively. The velocity exponent at various impingement angles found for the present cases are in conformity with Tilly and Sage [219], Miyazaki and Hamao [199] and Arjula *et al* [220].

It has been reported by Sundararajan *et al* [185, 216] that a term erosion efficiency (η) can be used to describe the nature and erosion mechanism. This parameter indicates the efficiency with which the volume that is displaced by impacting erodent particle is actually removed. They have also reported that ductile material possess very low erosion efficiency (i.e) $\eta <<<$ 100%, where as the brittle material exhibits an erosion efficiency even greater than 100%. The values of erosion efficiencies of composites under study are calculated using equation 6.2 and are listed in table 6.8 along with their hardness (*H*) and operating conditions. Figure 6.14 and 6.15 shows the variation of erosion efficiency with different impact velocities for lower (30°) and higher (90°) impingement angles. It shows the erosion efficiency of all tested samples decrease with increase in impact velocities. It has also been observed that the erosion efficiency of bagasse fiber reinforced epoxy composite varies from 2.7% to 59.7% for different impact velocities studied. Similar observations are also reported by Srivastava *et al* [221] for glass fiber reinforced fly-ash filled epoxy composite. Basing on their work, they have identified the brittle and ductile response of various materials considering the erosion mechanism. They have the opinion that ideal micro ploughing involving just the displacement of material from the crater without any fracture (and hence no erosion) will have zero erosion efficiency. Alternately, in the case of ideal micro cutting, efficiency will be 100%. And if erosion occurs by the formation of a lip and its subsequent fracture, then erosion efficiency will be in the range 0–100%. In contrast, as happens with brittle material, if the erosion takes place by sapling and removal of large chunks of material by interlinking lateral or radial cracks, then the erosion efficiency is expected to be even greater than 100%. Thus it can be concluded that erosion efficiency is not exclusively a material property; but also depends on other operational variables such as impact velocity and impingement angle. The data shown in table 6.8 also indicates that erosion efficiency of bagasse fiber epoxy composite decreases with increase in fiber content where as the neat epoxy exhibits a higher value under all testing conditions. This lower erosion efficiency of 20% bagasse fiber epoxy composite indicates a better erosion resistance in comparison to neat epoxy.

Figure 6.16 to 6.19 describes the variation of erosion rate of 20 % volume fraction bagasse fiber composite at different stand off distances (SOD) (10, 15 and 20mm) for various impact velocities. It is clear from the plots that the erosion rate decreases from 10mm SOD to 15 mm SOD and further increase of SOD to 20 mm the erosion rate again increases for all impact velocities. Therefore 15 mm SOD can be taken as optimum. Therefore it can be concluded that the stand off distance (SOD) has also a very strong effect on the erosive wear behavior of the composite.

6.6 SURFACE MORPHOLOGY

To characterize the morphology of eroded surfaces and the mode of material removal, the eroded samples are observed under a scanning electron microscope (SEM). Figure 6.20 (a) shows the micrographs of the 20 vol % of bagasse fiber reinforced epoxy composite eroded at 30°. It clearly indicates the fracture of fibers. More number of fibers is seen to be damaged but not extensively removed, though tangential component of the impact force is more effective due to oblique impact.

Figure 6.20(b) shows micrograph of the surfaces of the same composites eroded at an impingement angle of 45°. It appears that the composite encountered intensive debonding and breakage of the fibers, which were not, supported enough by the matrix. The continuous impingement of silica sand on the fiber breaks the fiber because of formation of cracks perpendicular to their length. Also the bending of fibers becomes possible because of softening of the surrounding matrix which in turn lowers the strength of the surrounding fibers. Same type of behaviour has also been reported by Sari *et al* [222] while they worked with carbon fiber reinforced poly ether amide composites under low particle speed.

Figure 6.20 (c) shows the surface of the composite eroded at an impingement angle of 60°. The micrograph of eroded surface clearly indicates the process of fiber damage and pulverization. This probably is the dominant mechanism which leads to high wear rate of composite. The tangential component of the impact force probably is more effective in micro cracking followed by micro cutting of fibers in many places leading to severe pulverization of fibers.

Figure 6.20 (d) shows the eroded surface of the composite for the impingement angle of 90°. Fracture of fibers is clearly visible. Cracks that are generated cannot propagate easily because of fibers present. It is obvious that in the case of normal erosion all available energy is dissipated by impact. During energy dissipation it causes fracture of a fiber, crack propagation in both the direction, forward and backward, towards the eroding surface is very difficult since cracks have to cross the ductile matrix between the fibers. Thus, wear of such composite was mainly due to easy fracture of brittle fiber and subsequent removal of fiber debris.

6.7 CONCLUSIONS

Based on the study of the erosive wear behavior of BFRP composites at various impingement angles, impact velocities for different fiber volume fraction with silica sand as erodent the following conclusions are drawn.

- The composite exhibited a maximum erosion rate at an impingement angle of 90° under present experimental condition indicating brittle behavior.

- Fiber volume fraction and velocity of impact has a significant influence on the erosion rate of the composite.

- In BFRP composites, erosion rate (*Er)* displays power law behaviour with particle velocity (*v*) as $Er \; \alpha \; v^n$. The velocity exponents are in the range of 1.01–2.50 for various materials studied for different impingement angles (30°–90°) and impact velocities (48–109 m/s). And also the value of *n* for composites is higher than that of the matrix.

- The erosion efficiency of bagasse fiber reinforced epoxy composite decreases with increase in fiber content. The 20% volume fraction of bagasse fiber epoxy composite indicates a better erosion resistance in comparison to neat epoxy composite.

- The morphologies of the eroded surfaces observed by SEM suggests that overall erosion damage of the composite is mainly due to micro cracking, matrix material

removal in the resin area and breakage of fiber as well as that of the material from the fiber-resin interface zone.

- Possible use of these composites in components such as pipes carrying coal dust, desert structure, low cost housing, boats/sporting equipments, partition boards, doors and window panels is recommended.

Table-6.1

Particle velocities under different air pressure

Sl. No.	Air Pressure (Bar)	Particle Velocity (m/s)
1	1	48
2	2	70
3	3	82
4	4	109

Table-6.2

Experimental conditions for the erosion test

Test Parameters	
Erodent	Silica sand
Erodent size (μm)	200±50
Erodent shape	Angular
Hardness of silica particle(HV)	1420±50
Impingement angle (α_0)	30°, 45°, 60° and 90°
Impact velocity (m/s)	48, 70, 82 and 109
Erodent feed rate (gm/min)	0.572 ±0.02
Test temperature	27°C
Nozzle to sample distance (mm)	10, 15 and 20

Table-6.3 Weight loss and erosion rate of neat epoxy composite with impingement angle after erosion of 10 mins

Velocity of impact (m/s)	Impact Angle(°)	Weight loss'Δw' (gms)	Erosion rate X 10^{-3} (gm/gm)
48 m/s	30	0.009	1.573
	45	0.012	2.097
	60	0.017	2.971
	90	0.028	4.894
70 m/s	30	0.010	1.747
	45	0.014	2.447
	60	0.019	3.321
	90	0.027	4.719
82 m/s	30	0.016	2.796
	45	0.023	4.020
	60	0.031	5.418
	90	0.052	9.089
109 m/s	30	0.017	2.971
	45	0.026	4.544
	60	0.033	5.768
	90	0.055	9.613

Table-6.4 Weight loss and erosion rate of 10% bagasse fiber epoxy composite with impingement angle after erosion of 10 mins

Velocity of impact (m/s)	Impact Angle(°)	Weight loss'Δw' (gms)	Erosion rate X 10^{-3} (gm/gm)
48 m/s	30	0.004	0.699
	45	0.006	1.048
	60	0.012	2.097
	90	0.025	4.369
70 m/s	30	0.004	0.699
	45	0.009	1.573
	60	0.013	2.272
	90	0.026	4.544
82 m/s	30	0.010	1.747
	45	0.015	2.621
	60	0.019	3.321
	90	0.031	5.418
109 m/s	30	0.011	1.922
	45	0.020	3.495
	60	0.025	4.369
	90	0.035	6.117

Table-6.5 Weight loss and erosion rate of 15% bagasse fiber epoxy composite with impingement angle after erosion of 10 mins

Velocity of impact (m/s)	Impact Angle(°)	Weight loss'Δw' (gms)	Erosion rate X 10^{-3} (gm/gm)
48 m/s	30	0.002	0.349
	45	0.003	0.524
	60	0.008	1.398
	90	0.023	4.02
70 m/s	30	0.003	0.524
	45	0.004	0.699
	60	0.008	1.398
	90	0.024	4.195
82 m/s	30	0.006	1.048
	45	0.012	2.097
	60	0.018	3.146
	90	0.025	4.369
109 m/s	30	0.009	1.573
	45	0.012	2.097
	60	0.019	3.321
	90	0.027	4.719

Table-6.6 Weight loss and erosion rate of 20% bagasse fiber epoxy composite with impingement angle after erosion of 10 mins

Velocity of impact (m/s)	Impact Angle(°)	Weight loss'Δw' (gms)	Erosion rate X 10^{-3} (gm/gm)
48 m/s	30	0.001	0.174
	45	0.002	0.349
	60	0.006	1.048
	90	0.018	3.146
70 m/s	30	0.002	0.349
	45	0.003	0.524
	60	0.007	1.223
	90	0.020	3.495
82 m/s	30	0.003	0.524
	45	0.010	1.747
	60	0.014	2.447
	90	0.022	3.845
109 m/s	30	0.008	1.398
	45	0.011	1.747
	60	0.017	2.971
	90	0.026	4.544

Table-6.7 Parameters characterizing the velocity dependence of erosion rate of neat epoxy and its composites

Filler volume fraction (%)	Impact angle (°)	K X 10^{-5}	n	R^2
0 (Neat Epoxy)	30	6.00	0.8519	0.8131
	45	4.00	1.0175	0.8601
	60	9.00	0.8887	0.8142
	90	10.00	0.9304	0.6830
10	30	0.30	1.3819	0.7181
	45	0.30	1.5301	0.9564
	60	5.00	0.9304	0.8658
	90	80.00	0.4274	0.8690
15	30	0.02	1.9154	0.9374
	45	0.03	1.8869	0.7880
	60	1.00	1.1901	0.7062
	90	19.00	0.1942	0.9472
20	30	0.0009	2.5073	0.9704
	45	0.008	2.2852	0.8314
	60	0.50	1.3712	0.8419
	90	50.00	0.4470	0.9594

Table-6.8 Erosion efficiency of various composite samples

Impact Velocity (m/s)	Impact angle (°)	Erosion Efficiency (η)			
		Neat Epoxy	10% BF	15% BF	20% BF
		H=153.15 (N/mm^2)	H=171.43 (N/mm^2)	H=176.54 (N/mm^2)	H=195.17 (N/mm^2)
48	30	19.327	9.552	4.898	2.692
	45	25.765	14.321	7.354	5.400
	60	36.504	28.655	19.619	16.215
	90	60.131	59.702	56.415	48.675
70	30	10.093	4.491	3.458	2.539
	45	14.137	10.107	4.612	3.812
	60	19.186	14.598	9.225	8.897
	90	27.263	29.197	27.681	25.426
82	30	11.771	8.180	5.039	2.778
	45	16.925	12.272	10.084	9.262
	60	22.810	15.550	15.128	12.973
	90	38.266	25.369	21.009	20.384
109	30	7.079	5.093	4.281	4.195
	45	10.827	9.262	5.707	5.242
	60	13.743	11.578	9.038	8.914
	90	22.905	16.210	12.842	13.634

Table-6.9 Erosion rate of various composite samples at different SODs

Impact Velocity (m/s)	SOD (mm)	Erosion rate (g/g)			
		Neat Epoxy	10 % BF	15 % BF	20 % BF
48	10	4.894	4.369	4.020	3.146
	15	0.699	0.524	0.349	0.194
	20	2.447	1.573	0.699	0.524
70	10	4.719	4.544	4.195	3.495
	15	3.845	0.873	0.349	0.349
	20	7.166	4.020	1.573	1.223
82	10	9.089	5.418	4.369	3.845
	15	5.418	1.223	0.349	0.349
	20	10.837	7.341	5.243	1.922
109	10	9.613	6.117	4.719	4.544
	15	6.467	4.020	3.146	1.747
	20	23.946	18.877	10.138	5.418

Figure-6.1 **Details of erosion test rig. (1) Sand hopper, (2) Conveyor belt system for sand flow, (3) Pressure transducer, (4) Particle-air mixing chamber, (5) Nozzle, (6) X–Y and h axes assembly, (7) Sample holder**.

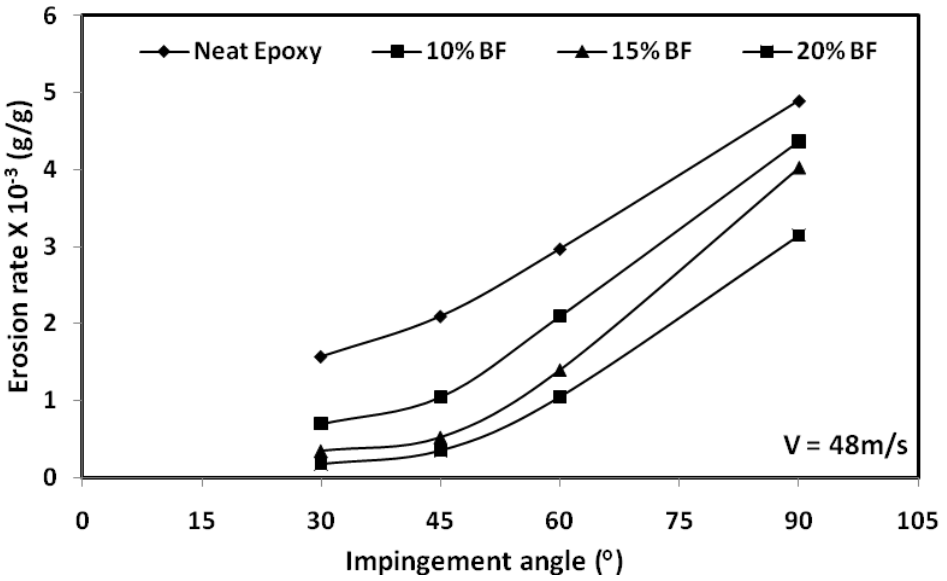

Figure-6.2 Variation of erosion rate with impingement angle for different volume fraction of bagasse fiber composite at an impact velocity of 48 m/s

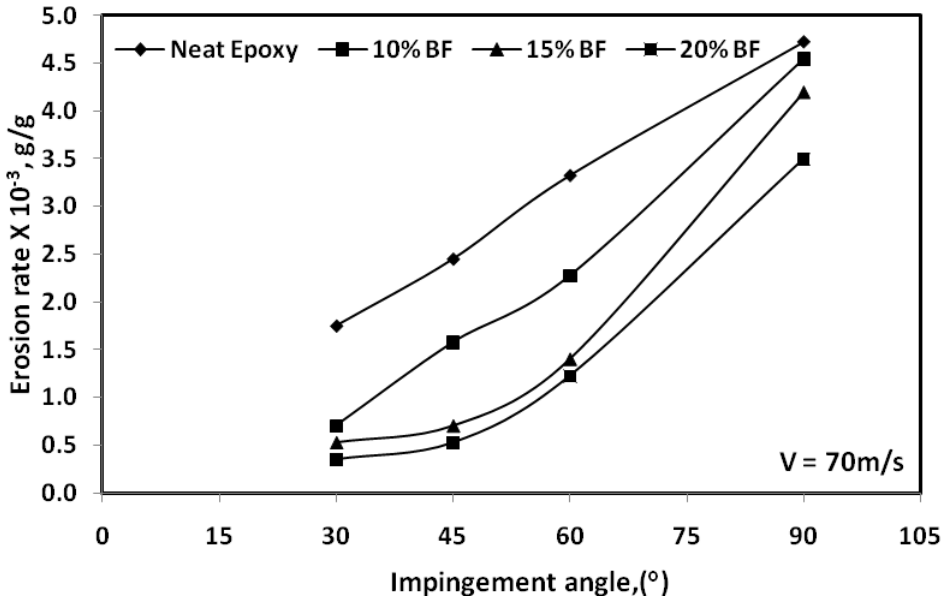

Figure-6.3 Variation of erosion rate with impingement angle for different volume fraction of bagasse fiber composite at an impact velocity of 70 m/s

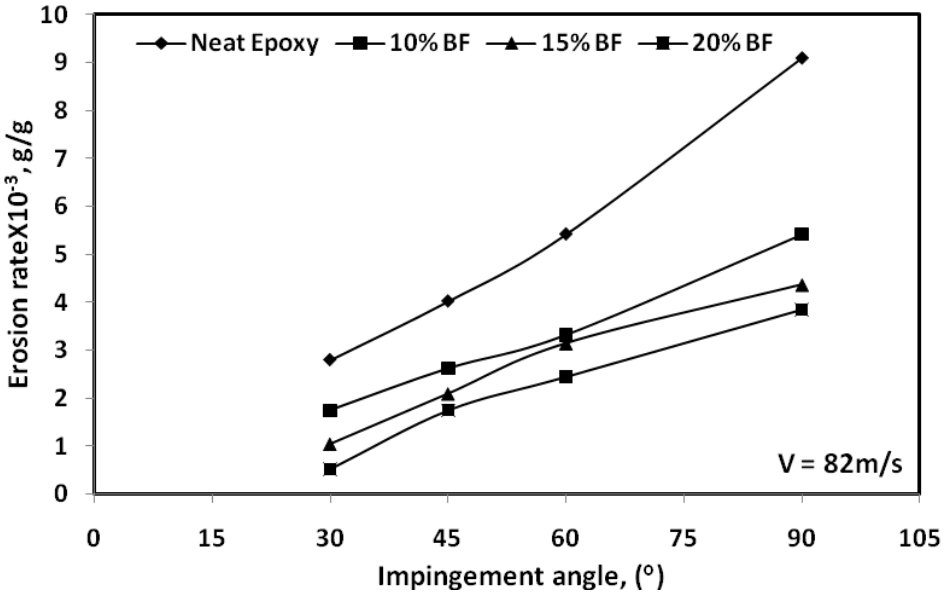

Figure-6.4 Variation of erosion rate with impingement angle for different volume fraction of bagasse fiber composite at an impact velocity of 82 m/s

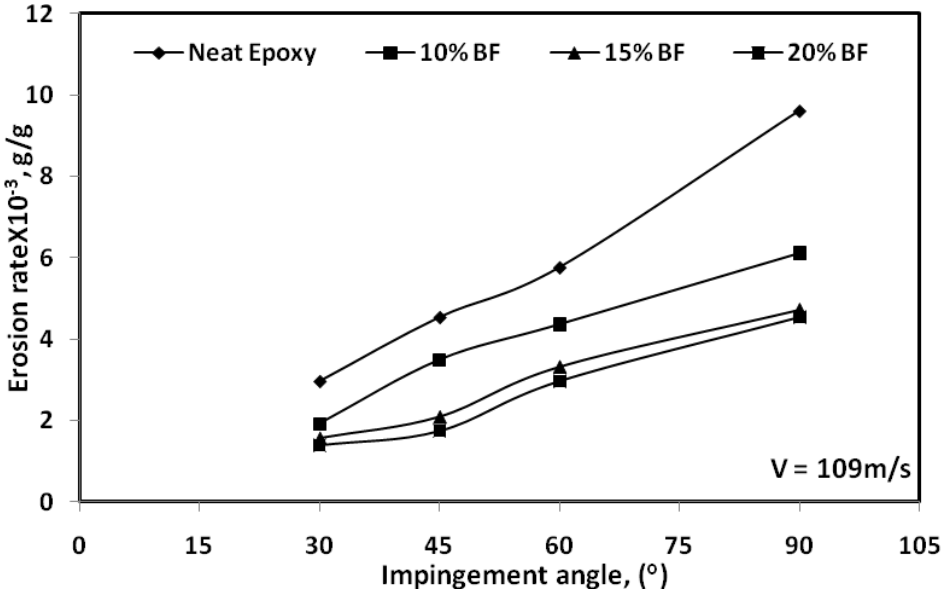

Figure-6.5 Variation of erosion rate with impingement angle for different volume fraction of bagasse fiber composite at an impact velocity of 109 m/s

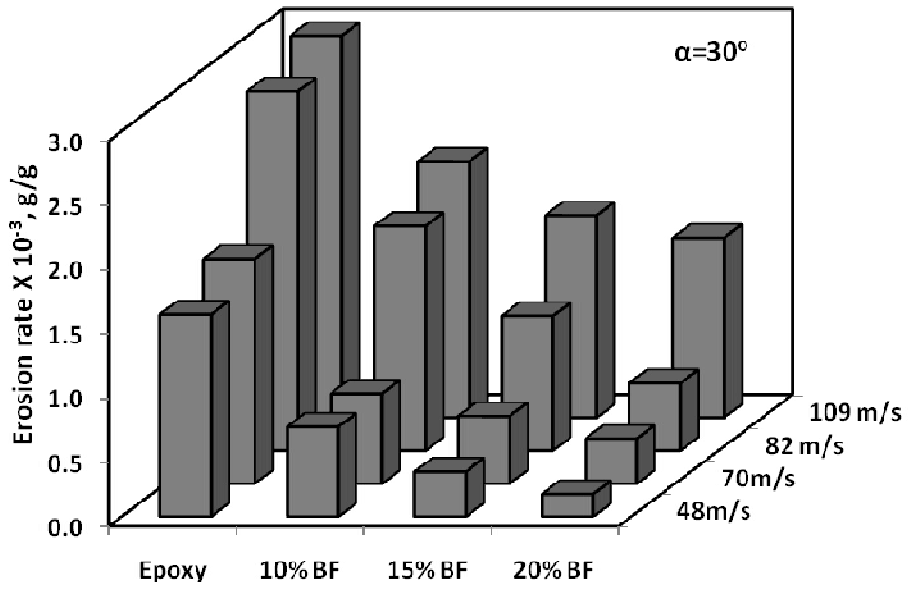

Figure-6.6 Variation of erosion rate as a function of filler volume fraction for different impact velocities at an impact angle of 30°

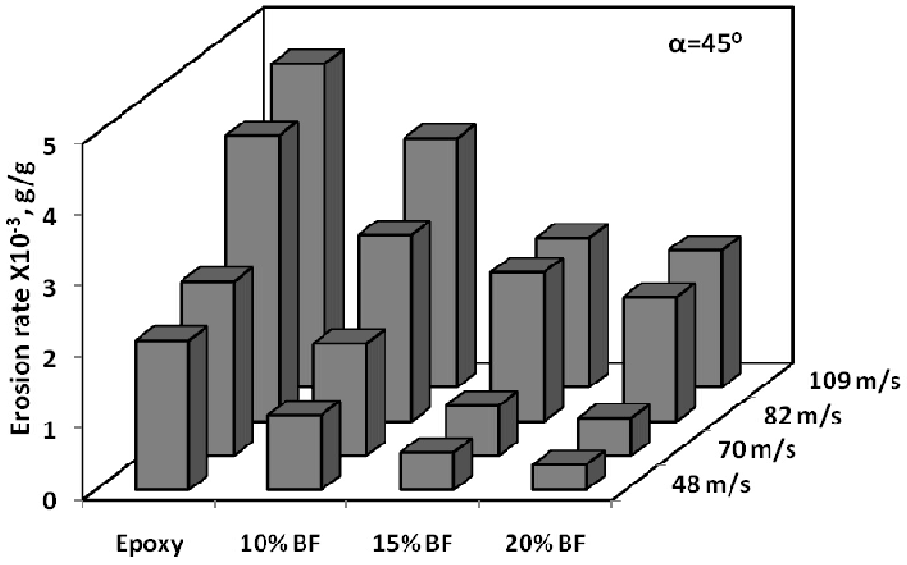

Figure-6.7 Variation of erosion rate as a function of filler volume fraction for different impact velocities at an impact angle of 45°

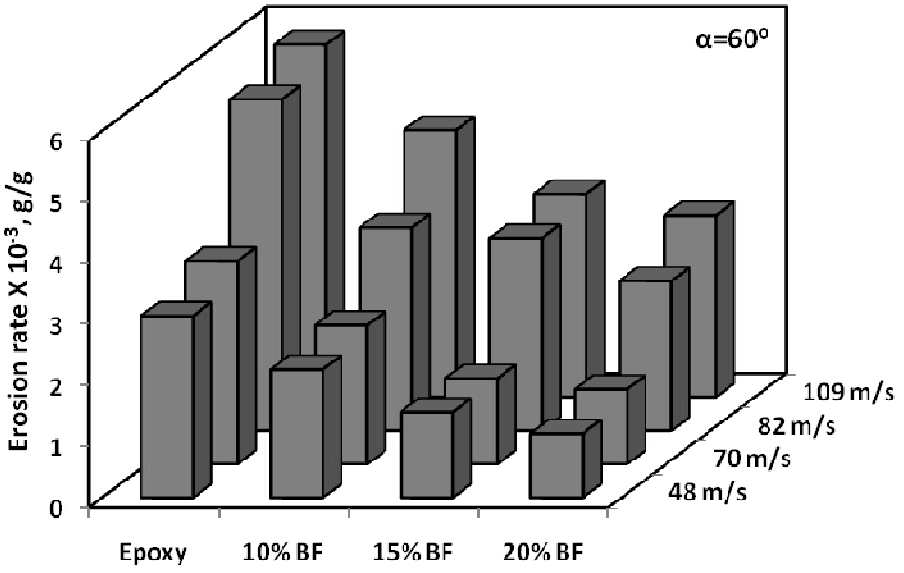

Figure-6.8 Variation of erosion rate as a function of filler volume fraction for different impact velocities at an impact angle of 60°

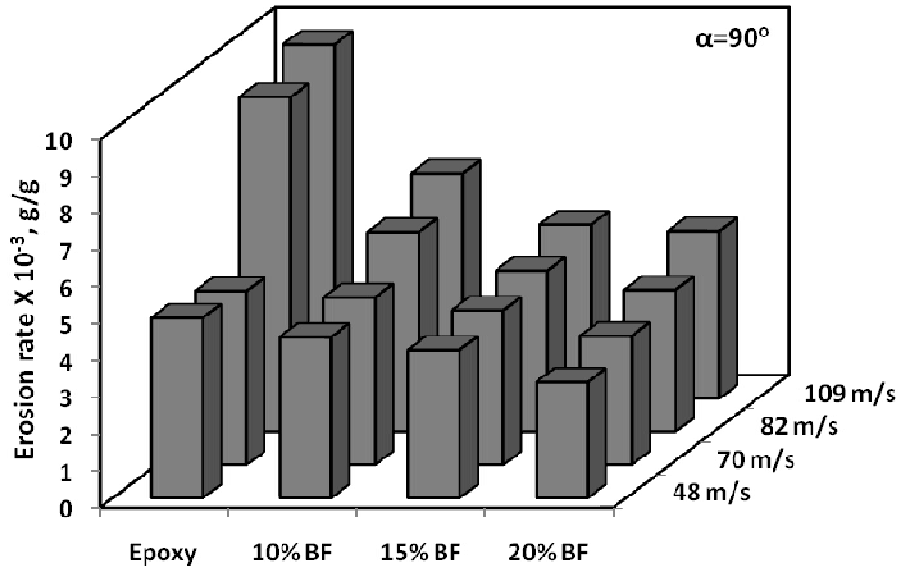

Figure-6.9 Variation of erosion rate as a function of filler volume fraction for different impact velocities at an impact angle of 90°

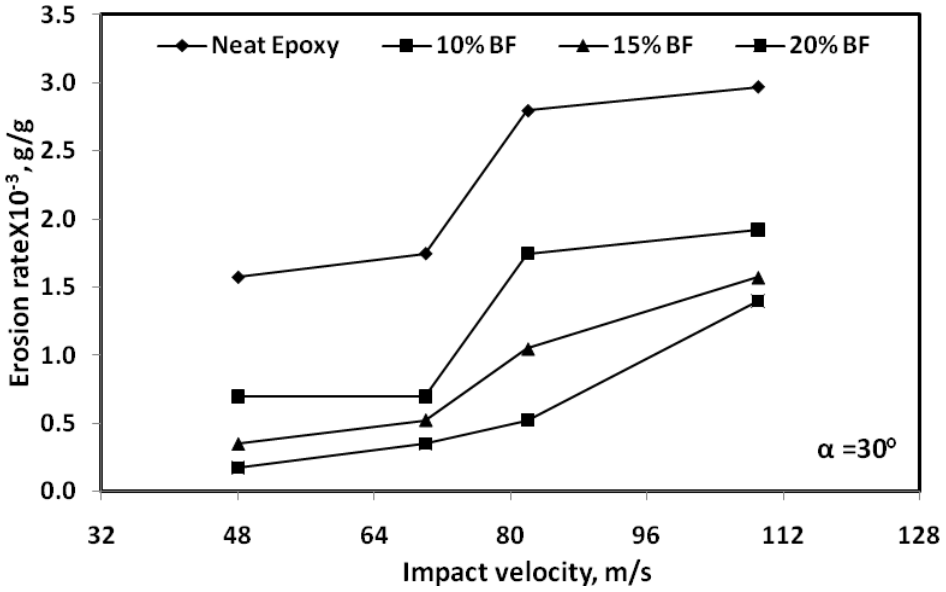

Figure-6.10 Variation of erosion rate as a function of impact velocity for different volume fraction of bagasse fiber composite at an impact angle of 30°

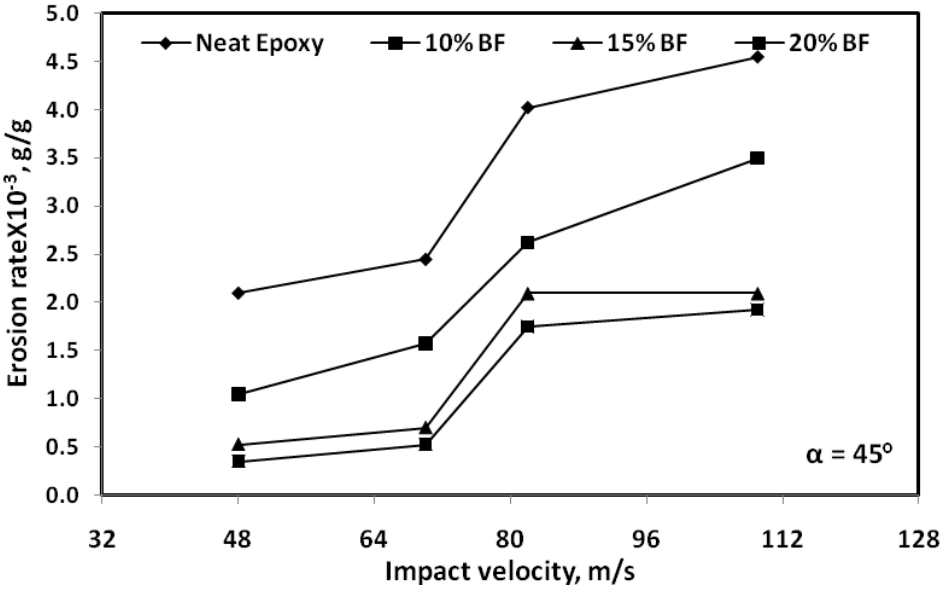

Figure-6.11 Variation of erosion rate as a function of impact velocity for different volume fraction of bagasse fiber composite at an impact angle of 45°

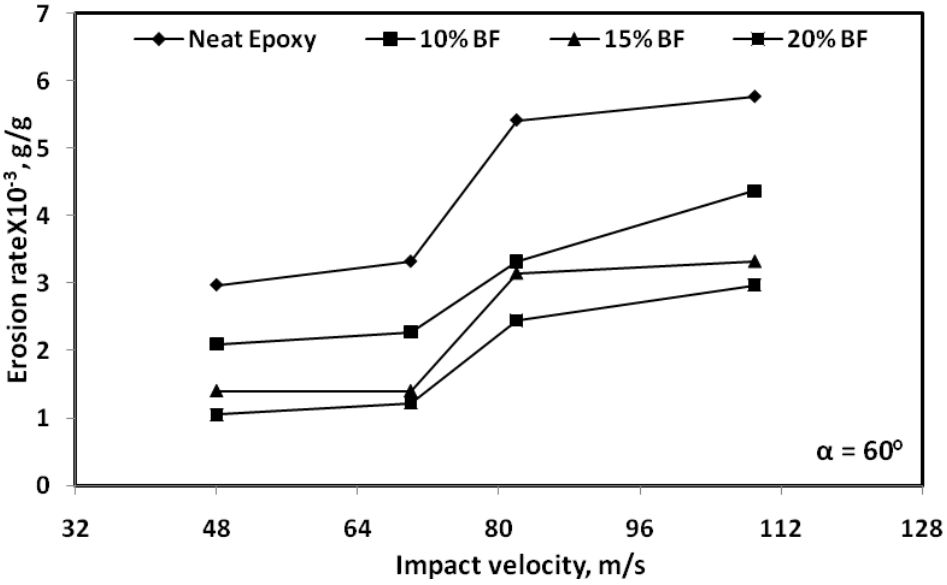

Figure-6.12 Variation of erosion rate as a function of impact velocity for different volume fraction of bagasse fiber composite at an impact angle of 60°

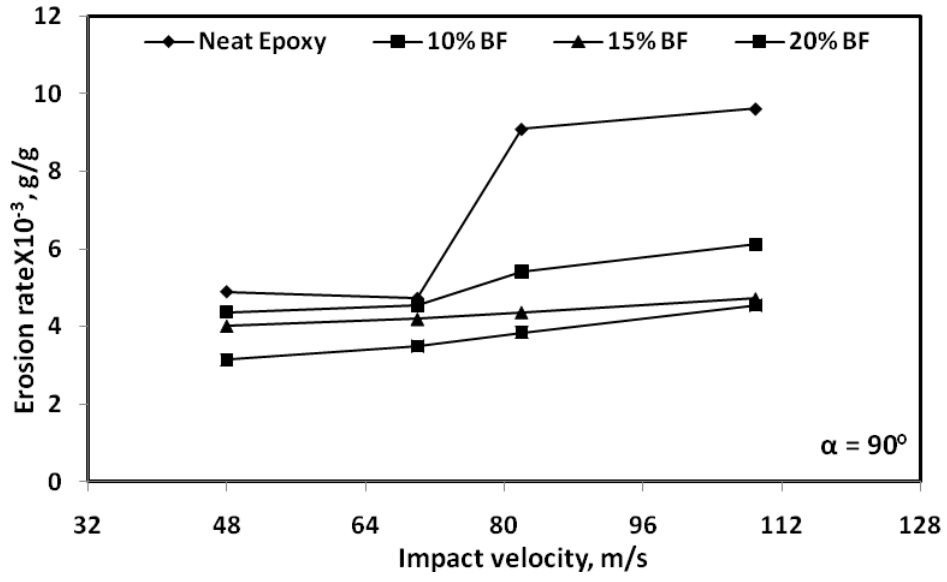

Figure-6.13 Variation of erosion rate as a function of impact velocity for different volume fraction of bagasse fiber composite at an impact angle of 90°

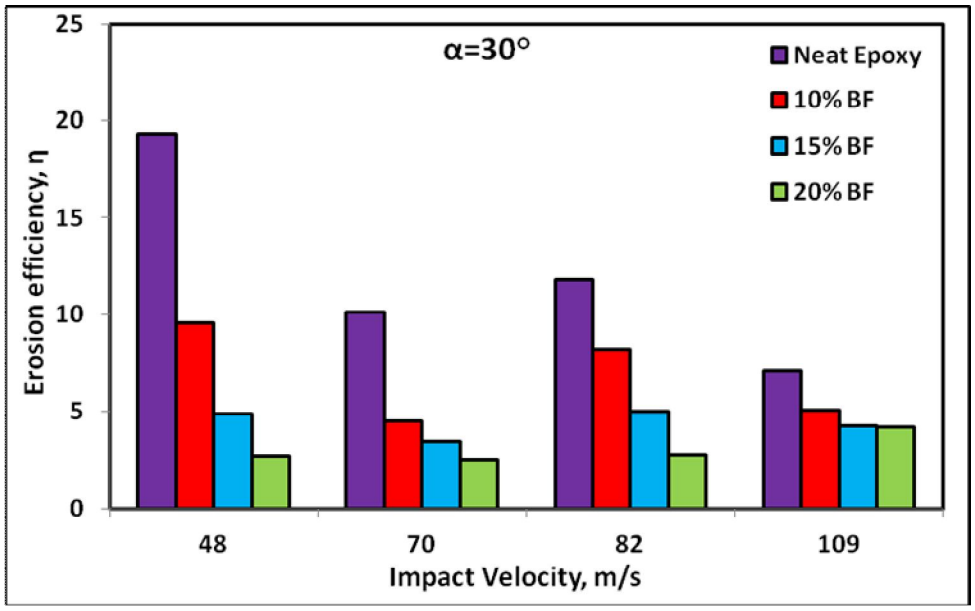

Figure-6.14 **Variation of erosion efficiency with velocity of impact for different volume fraction of bagasse fiber composite at lower impingement angle of 30°**

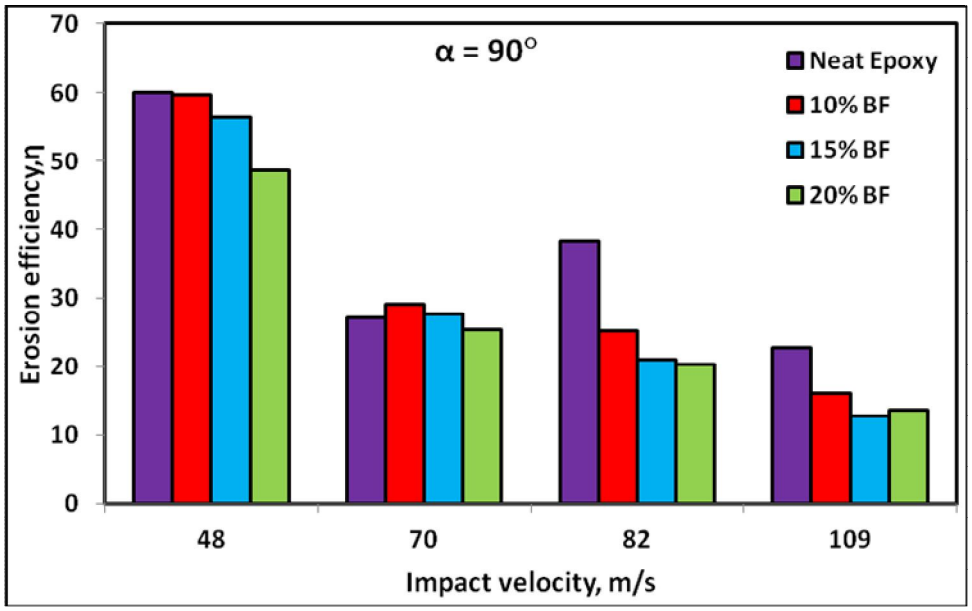

Figure-6.15 **Variation of erosion efficiency with velocity of impact for different volume fraction of bagasse fiber composite at higher impingement angle of 90°**

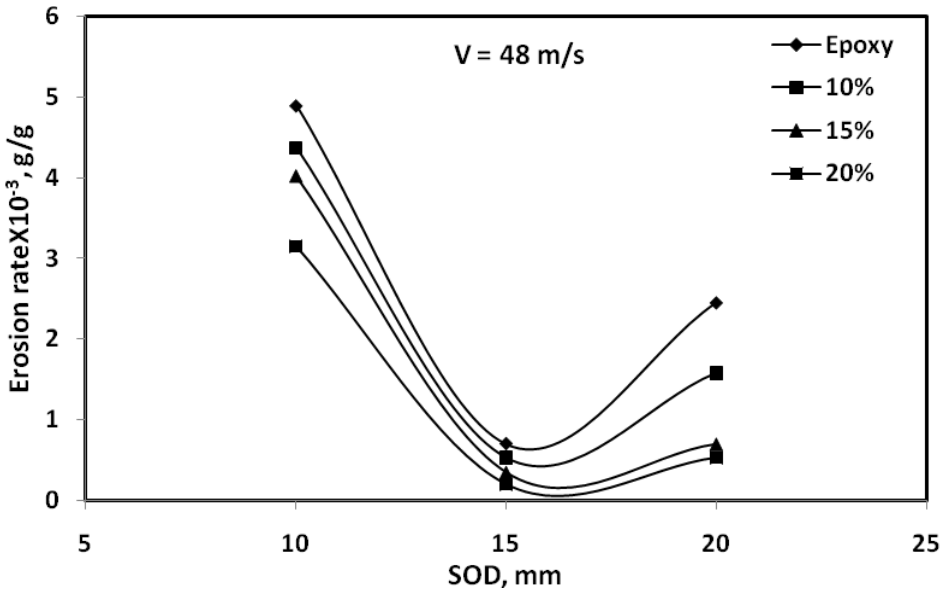

Figure-6.16 Variation of erosion rate as a function of SOD for different volume fraction of bagasse fiber epoxy composite at an impact velocity of 48 m/s

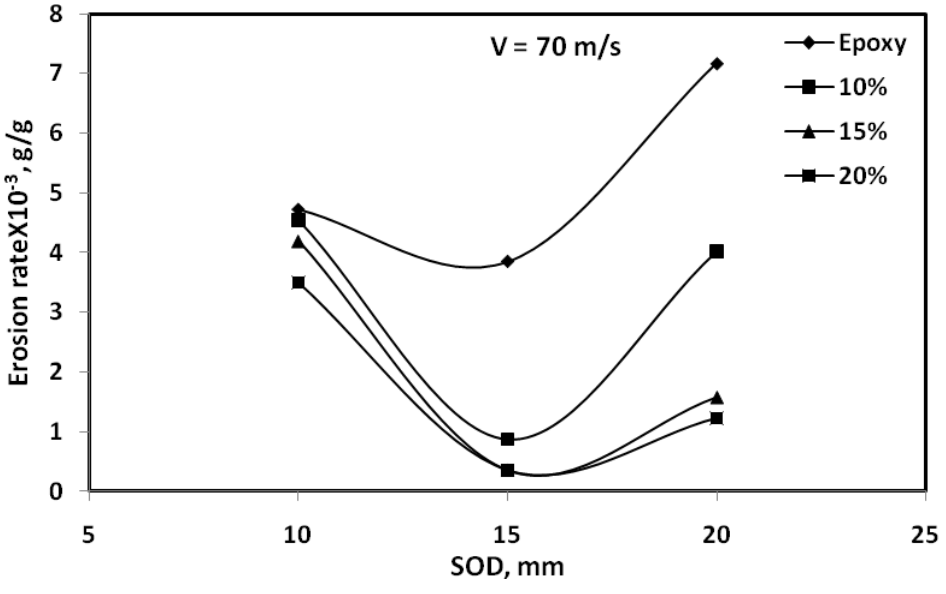

Figure-6.17 Variation of erosion rate as a function of SOD for different volume fraction of bagasse fiber epoxy composite at an impact velocity of 70 m/s

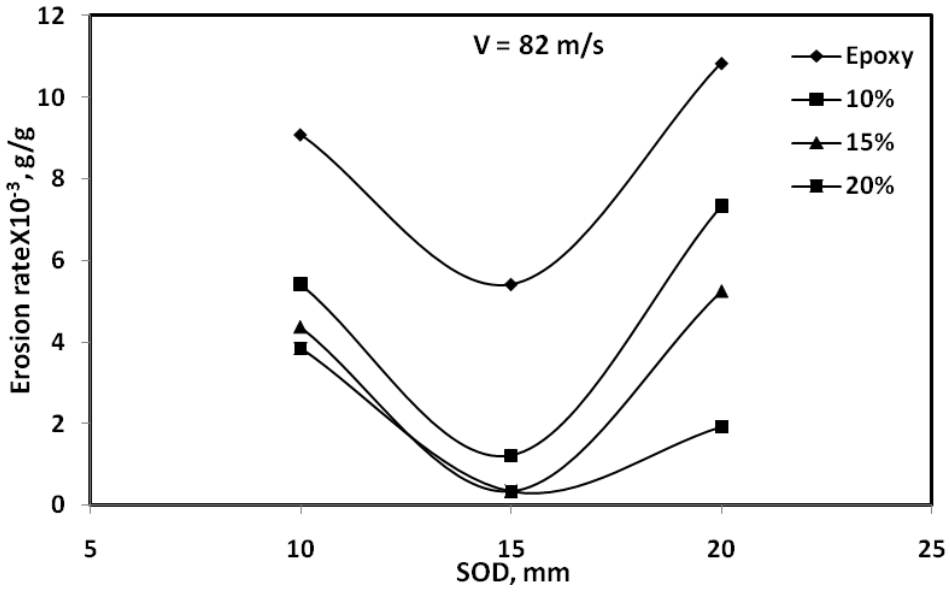

Figure-6.18 Variation of erosion rate as a function of SOD for different volume fraction of bagasse fiber epoxy composite at an impact velocity of 82 m/s

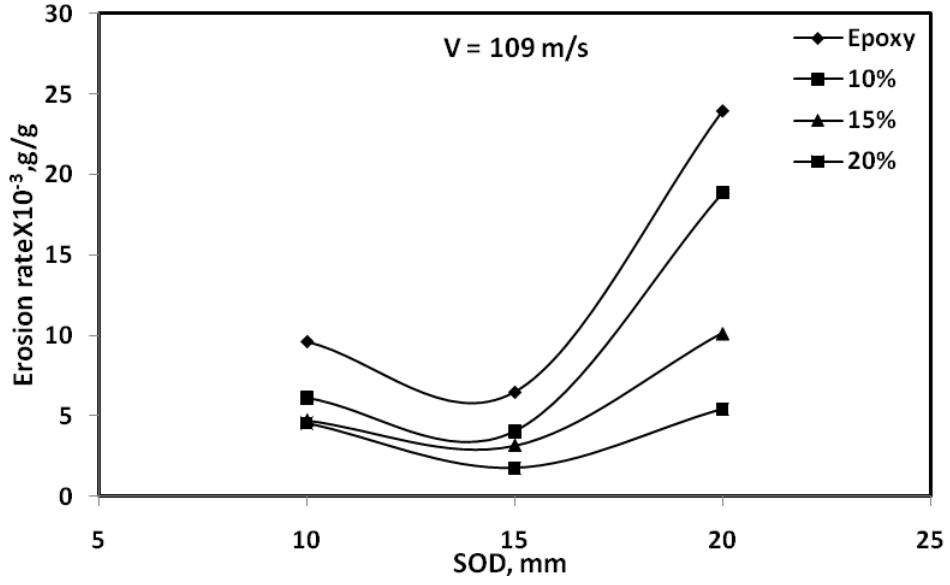

Figure-6.19 Variation of erosion rate as a function of SOD for different volume fraction of bagasse fiber epoxy composite at an impact velocity of 109 m/s

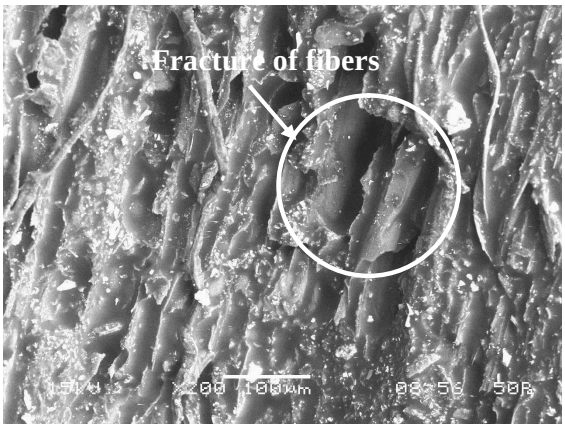

(a)

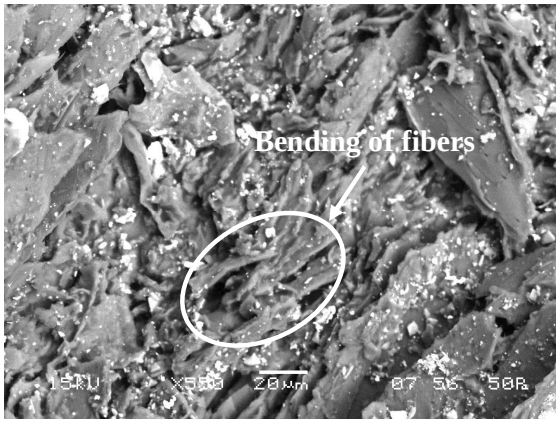

(b)

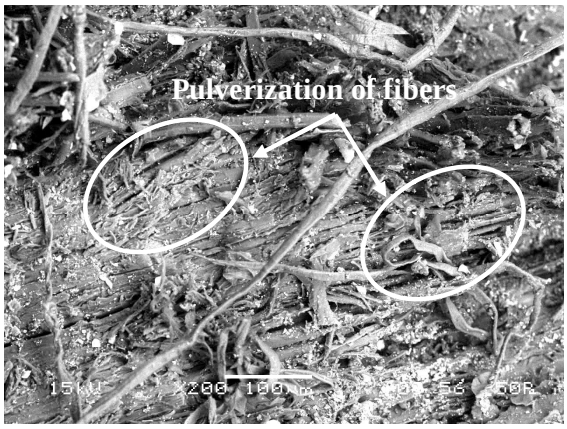

(c)

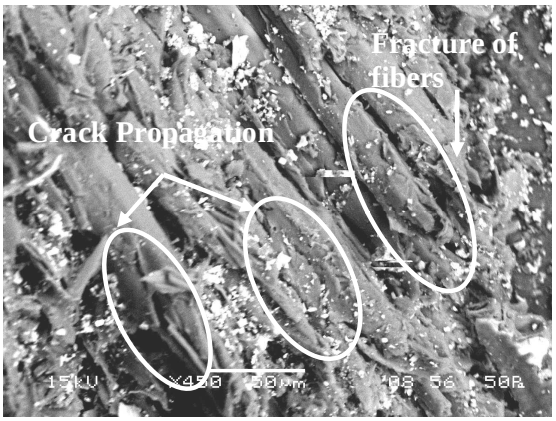

(d)

Figure-6.20 SEM micrograph of surfaces eroded at (a) 30°, (b) 45°, (c) 60° and (d) 90° impact angles

Chapter 7

MODELING OF ABRASIVE AND EROSIVE WEAR BEHAVIOUR OF BAGASSE FIBER EPOXY COMPOSITES BY RESPONSE SURFACE METHODOLOGY

Chapter-7

7.1 INTRODUCTION

Response Surface Methodology (*RSM)* is a practical and useful tool for designing, formulating, developing, and analyzing scientific phenomenon related to any process and product. It is also efficient in the improvement of existing studies on processes and products. The most extensive applications of RSM are found in the industrial world, particularly in situations where several input variables potentially influence some performance measures or quality characteristics of the product or process. The most common applications of *RSM* are in Industrial, Biological and Clinical Sciences, Social Sciences, Food Sciences, and Engineering Sciences. Also, in recent years more emphasis has been imposed by the chemical and processing field for finding regions where there is an improvement in response instead of finding the optimum response [223]. RSM was introduced by G. E. P. Box and K. B. Wilson in 1951 with an idea to use a set of designed experiments to obtain an optimal response [224]. However according to Mead and Pike, the origin of RSM started in 1930 with use of Response Curves [223]. Box and Wilson suggested using a first-degree polynomial model to do this. They acknowledged that this model was only an approximation, but can be used because such a model was easy to estimate and apply, even when little was known about the process.

In the past few decades RSM has been used by several researchers for prediction of tool life, surface roughness, wear resistance, etc. [225-228]. A considerable amount of these works were based on Metal Matrix composites (MMCs). However the modeling and prediction of wear performance of polymeric material and their composite are very limited. Shipway and Ngao [137] investigated the abrasive behaviour of polymeric materials in micro-scale level by using RSM. Similarly, in another study Sagbas *et al* [229] used this method for modeling and predicting the abrasive wear behaviour of polyoxy-methylenes. It has been found that literature is almost nil on studying of erosive wear behaviour of polymeric composite. In view of the above literature, it is felt that enough scope of work exists on the use of RSM technique to predict the wear performance of natural fiber composite. Therefore, in the present work, an attempt has been made to develop predictive

models for abrasive wear and erosive wear behaviour of bagasse fiber reinforced epoxy composite under various testing conditions by using Response Surface Methodology.

7.2 RESPONSE SURFACE METHODOLOGY (RSM)

The Response Surface Methodology is a collection of mathematical and statistical techniques useful for the modeling and the analysis of problems in which a response of interest is influenced by several process variables and the objective is to optimize this response [224]. It consists of a group of techniques used in the empirical study of relationships between one or more measured responses and a number of input factors (process parameters). It comprises (1) designing a set of experiments, (2) determining a mathematical model, (3) testing of adequacy of the model developed (statistical significance) and (4) determining the optimal value of the response, in such a manner that, at least, a better understanding of the overall system behavior is obtained. The empirical relationship is frequently obtained by fitting polynomial models. First-order and second-order experiment designs are set up with the purpose of collecting data for fitting such models [230, 231].

In this chapter, a second-order (quadratic) polynomial response surface mathematical model is employed to analyze the parametric influences on various response criteria. The second-order model helps to understand main effect as well as the quadratic effect of each factors separately and the two-way interaction amongst these factors combined. This second-order mathematical model can be represented as follows:

$$y = \beta_0 + \sum_{i=1}^{k} \beta_i x_i + \sum_{i=1}^{k} \beta_i x_i^2 + \sum_{i=1}^{k} \sum_{j=1}^{k} \beta_{ij} x_i x_j + \varepsilon \qquad \text{for } i<j \qquad (7.1)$$

where β_0, β_i (i = 1, 2, . . . , k) and β_{ij} (i = 1, 2, . . . , k, j = 1, 2, . . . , k) are the unknown as regression coefficients to be estimated by using the method of least squares. In this equations ε are experimentally random errors and x_1, $x_{2.....}$ x_k are the input variables that influence the response y, k is the number of input factors. The least square technique is

being used to fit a model equation containing the said regressors or input variables by minimizing the residual error measured by the sum of square deviations between the actual and the estimated responses. This involves the calculation of estimates for the regression coefficients, i.e. the coefficients of the model variables including the intercept or constant term. The dimensions of the regression coefficients and the constant are evaluated such that, the model equation maintains dimension similarity. However calculated coefficients and model adequacy need to be tested for statistical significance. In this respect, the statistical test named ANOVA (Analysis of Variance) has been performed.

Analysis of variance (ANOVA) is used to check the adequacy of the model for the responses in the experimentation. ANOVA calculates the Fishers F-ratio, which is the ratio between the regression mean square and the mean square error. If the calculated value of F-value is higher than the tabulated F-value, then the model is said to be adequate at desired significance level α. In the current work the α-level is set at 0.05, i.e. the confidence level is set at 95%.

For testing the significance of individual model coefficients, the model is refined by adding or deleting coefficients through backward elimination, forward addition or stepwise elimination or addition algorithms. It involves the determination of P- value or probability of significance that relates the risk of falsely rejecting a given hypothesis. If the P-value is less or equal to the selected α-level, then the effect of presence of the variable term is significant. If the P-value is greater than the selected α-value, then it is considered that the presence of the variable term in the model is not significant. Sometimes the individual variables may not be significant. If the effect of interaction terms is significant, then the effect of each factor is different at different levels of the other factors.

The computation part of ANOVA can be made easily using available statistical soft-wear packages like MINITAB, DESIGN EXPERT, etc. In the present study, MINITAB RELEASE-14 soft-wear has been used.

Additional checks are also needed in order to determine the goodness of fit of the mathematical models by determining the coefficient of determination (R^2) and adjusted coefficient of determination (R^2_{adj}). The R^2 is the proportion of the variation in the

dependent variable explained by the regression model. On the other hand, R^2_{adj} is the coefficient of determination adjusted for the number of independent variables in the regression model. For a good model, values of R^2 and R^2_{adj} should be close to each other and also they should be close to 1.

To have an assessment of pure error and model fitting error, some of the experimental trials are replicated. The adequacy of the models is also investigated by the examination of residuals. The residuals, which are the difference between the respective observed responses and the predicted responses, are examined using the normal probability plots of the residuals and the plots of the residuals versus the predicted response. If the model is adequate, the points on the normal probability plots of the residuals should form a straight line. On the other hand, the plots of the residuals versus the predicted response should be structure-less, i.e., they should contain no obvious pattern.

After analyzing all the statistical significance, the response surface analysis is then done in terms of the fitted surface. If the fitted surface is an adequate approximation of the true response function, then analysis of the fitted surface will be approximately equivalent to analysis of the actual system.

The objective of using RSM is not only to investigate the response over the entire factor space but also to locate the region of interest where the response reaches its optimum or near optimal value. By studying carefully the response surface model, the combination of factors, which gives the best response, can be established. This process can be summarized as shown in Figure-7.1.

7.3 MODELING OF ABRASIVE WEAR OF BAGASSE FIBER REINFORCED EPOXY COMPOSITE

Basically the abrasive wear of polymer matrix composite (PMC) is influenced by several factors like abrasive grain size, type of reinforcement, type of polymer, size of reinforcement, amount of reinforcement or volume fraction of reinforcement, sliding distance, sliding velocity, applied normal load, etc. In this field statistical tools play an

important role to develop mathematical models to predict the wear loss in terms of different factors and analyze the effects of different factors and their interaction on the abrasive wear behaviour. Keeping this in view, an attempt has been made to obtain an empirical model of wear loss as a function of volume fraction of fiber, sliding velocity and normal load by using RSM. In this study, the experimental wear loss data have been taken from chapter-4.

7.3.1 Design of Experiment (DOE)

The design of experiments technique permits us to carry out the modeling and the analysis of the influence of process variables (process input) on the response variables (process output). In the present study volume fraction of fiber (R_e, vol%), sliding velocity (V, m/s) and normal load (L, N) have been selected as design factors while other parameters (abrasive grit size and sliding distance) have been assumed to be constant over the experimental domain. A full factorial design (FFD) has been selected with three design factors of which reinforcement and load with four levels each and velocity of three levels to describe response of the wear loss and to estimate the parameters in the second-order model. Thus overall 48 set of combinations of abrasive wear experimental data are required. In this work the set of combinations of abrasive wear experimental data are taken from chapter-4 (Table-4.5). The important factors and their levels for the abrasive wear test are shown in Table-7.1.

The FFD design of experiment runs with independent control variables and response are shown in Table-7.2. In the wear loss (Δw) values are taken from Table-4.6 to 4.53, chapter-4.

7.3.2 Development of the response surface model for the wear loss (Δ*w*)

The results (data in Table-7.2) have been explored to the Minitab 14 software for further analysis following the steps outlined in Section-7.2. The second order regression equation has been developed for predicting wear loss (Δw) within selected experimental conditions using RSM. This second order equation in terms of the coded values of the independent variables can be expressed as:

$$\Delta w = -0.719211 + 0.027715 \times R_e + 0.068496 \times L + 0.742531 \times V - 0.000926 \times R_e^2 - 0.002067 \times L^2 - 0.101460 \times V^2 - 0.000938 \times R_e \times L - 0.012359 \times R_e \times V + 0.005217 \times L \times V \quad (7.2)$$

ANOVA has been performed at a confidence level of 95% to check the adequacy of the proposed full model of wear loss i.e. equation-7.2, and the significance of the individual model coefficients. The results of ANOVA performed are listed in Table-7.3 & 7.4.

Table-7.3 presents the ANOVA table for the proposed second order model for wear loss given in equation-7.2. It can be appreciated that the P-value is less than 0.05 which means that the model is significant at 95% confidence level. Also the calculated value of the F-ratio is more than the standard value of the F-ratio (obtained from F-table) for wear loss. It means the model is adequate at 95% confidence level to represent the relationship between the wear loss (response) and process variables (inputs factors) of the abrasive wear process. Furthermore, the significance of presence each coefficient in the full model has been examined by the P-values. If the P-value is less than 0.05 then the corresponding coefficient is statistically significant for a confidence level of 95% [226].The ANOVA results of statistical significance of each coefficient are represented in Table-7.4. In this case two terms i.e. L×V and V^2 are found insignificant. The backward elimination procedure has been selected to automatically eliminate the insignificant model terms. By doing so, the reduced improved model for the wear loss can be presented as:

$$\Delta w = -0.632453 + 0.027715 \times R_e + 0.075048 \times L + 0.536567 \times V - 0.000926 \times R_e^2 - 0.002067 \times L^2 - 0.000938 \times R_e \times L - 0.012359 \times L \times V \quad (7.3)$$

Again ANOVA has been performed on the reduced model and the results are presented in Table-7.5. From this table, it has been noticed that, the reduced improved model for wear loss is still significant. The response regression coefficients of the terms in the reduced model of wear loss i.e. equation-7.3, are also shown in Table-7.6. The value of R^2 and R^2_{adj} of the proposed reduced models are found 0.918 and 0.904 respectively. The value of R^2 indicates that the model as fitted explains 91.8% of the variability in wear loss.

Figure-7.2 depicts the main effect plots for the wear loss considered in the present study. It is thus very much clear from the plot the volume fraction of fiber and normal load rate are significant for wear loss while sliding velocity on wear loss is very less which reveals the statement as discussed in chapter-4.

The normal probability plots of the residuals and the plots of the residuals versus the predicted response for wear loss 'Δw' are shown in Figure-7.3 and 7.4. A check on the plot in the Figure-7.4 shows that the residuals generally fall on a straight line implying that the errors are distributed normally. Also Figure-7.4 revealed that it has no obvious pattern and unusual structure. This implies the model proposed is adequate and there is no reason to suspect any violation of the independence or constant variance assumption.

7.4 MODELING OF EROSION WEAR OF BAGASSE FIBER REINFORCED EPOXY COMPOSITE

The influence of volume fraction of fiber, impact velocity and impingement angle on erosive wear behaviour of bagasse fiber epoxy composite has already been studied independently keeping all parameters at fixed levels in chapter-6. But in actual practice the resultant erosion rate is the combined effect of impact of more than one interacting variables. However, the impact of above parameters in an interacting environment becomes difficult. To this end, an attempt has been made to analyze the influence of more than one parameter on solid particle erosion of bagasse fiber epoxy composite by using Response Surface Methodology (RSM).

7.4.1 Design of experiment (DOE)

In the current study volume fraction of fiber (R_e, vol %), impact velocity (V, m/s) and impingement angle (α) has been selected as design factors while other parameters (Abrasive shape and size, and Stand-up-distance) are assumed to be constant over the experimental domain. Full factorial design (FFD) has been used with three design factors of each of four levels to describe response of the erosion rate (E_r). Total $4^3 = 64$ sets of

combination of experimental data have been taken from chapter-6 (Table-6.3 to 6.9). The important factors and their levels for the erosive wear test are shown in Table-7.7 and the design of experiment runs along with test results (response) are illustrated in Table-7.8.

7.4.2 Development of the response surface model for the erosion rate (E_r)

Similar to the procedure as explained in section 7.3.2**,** the full models for erosion rate was developed by taking the data from Table-7.10. The second order regression equation for erosion rate (E_r) can be expressed as:

$$\begin{aligned} E_r &= 0.002967 - 0.001287 \times R_e + 0.001972 \times \alpha + 0.001115 \times V + 0.000195 \times R_e^2 \\ &+ 0.000271 \times \alpha^2 + 0.000030 \times V^2 - 0.000406 \times R_e \times \alpha - 0.000429 \times R_e \times V \\ &+ 0.000217 \times V \times \alpha \end{aligned} \quad (7.4)$$

Similarly ANOVA has been carried out on the full model at a confidence level of 95% and the results in Table-7.9 & 7.10. The proposed second order model for erosion rate is found significant (Table-7.10). The significance of individual coefficient in the full model are also observed through Table-7.10 and it has been noticed that the terms R_e^2, α^2, V^2 and $\alpha \times V$ are insignificant. The reduced model for erosion rate is then obtained after eliminating the insignificant terms through MINITAB's backward elimination procedure. The reduced improved model for erosion rate (E_r) can be represented as:

$$\begin{aligned} E_r &= 0.003248 - 0.001301 \times R_e + 0.001982 \times \alpha + 0.001089 \times V - 0.000406 \times R_e \times \alpha \\ &- 0.000429 \times V \times R_e \end{aligned} \quad (7.5)$$

To check the significance of reduced model and regression coefficients, again ANOVA has been performed and the results are listed in Table-7.11 & 7.12. The reduced improved model and regression coefficients present in reduced model are found significant. Also the R^2 value is found high, close to 1, which is desirable.

The main effect plots for the erosion rate have been illustrated in Figure 7.5. This figure clearly indicates that impingement angle has significant influence on wear rate in comparison to fiber volume fraction and impact velocity.

7.4.3 Adequacy Checking of Erosion Wear Rate Model

For assessment of pure error and model fitting error, 20% of the experiments, i.e. 16 experiments were chosen at random for replication, which are shown in Table-7.15.

The residuals, which are the difference between the respective, observe responses and the predicted responses have been examined by using the normal probability plots of the residuals and the plots of the residuals (Figure-7.6 & 7.7). It has been observed that residuals are falling on a straight line, which indicating normal distribution of error. Whereas the plot of residuals versus the predicted response for erosion wear rate has no obvious pattern.

7.5 CONCLUSIONS

The full factorial design experimentation followed by RSM approach in this study has been intended to model the abrasive and erosive wear response of Bagasse fiber reinforced epoxy composite with respect to different processing parameters. This has been done by performing statistically designed experiments, estimating the coefficients in the mathematical models, predicting the response, checking for adequacy of the model. The mathematical models which are developed to predict the abrasive and erosive wear characteristics are found statistically valid and sound within the range of the factors. The results of the main effect plot (influence of individual process variables on response) are conformity with the findings of the chapet-4 and chapter-6.

Table-7.1 Important factors and their levels for abrasive wear

Sl. No.	Factor	Unit	Levels
1	Fiber volume fraction (Re)	vol %	0 10 15 20
2	Sliding velocity (V)	m/s	0.837 1.256 1.675
3	Applied load (L)	N	5 7.5 10 15

Table-7.2 Experimental results for Abrasive wear of bagasse reinforced epoxy composite

Runs	Factorial value			Response
	Re (vol %)	L (N)	V (m/s)	Wt. loss
1	0	5.0	0.837	0.23
2	0	5.0	1.256	0.31
3	0	5.0	1.675	0.59
4	0	7.5	0.837	0.27
5	0	7.5	1.256	0.50
6	0	7.5	1.675	0.63
7	0	10.0	0.837	0.36
8	0	10.0	1.256	0.67
9	0	10.0	1.675	0.79
10	0	15.0	0.837	0.40
11	0	15.0	1.256	0.76
12	0	15.0	1.675	0.86
13	10	5.0	0.837	0.17
14	10	5.0	1.256	0.23

Table.7.2 Contd.

Runs	Factorial value			Response
	Re (vol %)	L (N)	V (m/s)	Wt. loss
15	10	5.0	1.675	0.57
16	10	7.5	0.837	0.23
17	10	7.5	1.256	0.50
18	10	7.5	1.675	0.73
19	10	10.0	0.837	0.34
20	10	10.0	1.256	0.59
21	10	10.0	1.675	0.73
22	10	15.0	0.837	0.35
23	10	15.0	1.256	0.76
24	10	15.0	1.675	0.83
25	15	5.0	0.837	0.15
26	15	5.0	1.256	0.18
27	15	5.0	1.675	0.46
28	15	7.5	0.837	0.20
29	15	7.5	1.256	0.25
30	15	7.5	1.675	0.43
31	15	10.0	0.837	0.23
32	15	10.0	1.256	0.43
33	15	10.0	1.675	0.51
34	15	15.0	0.837	0.24
35	15	15.0	1.256	0.46
36	15	15.0	1.675	0.58
37	20	5.0	0.837	0.09

Table.7.2 Contd.

Runs	Factorial value			Response
	Re (vol %)	L (N)	V (m/s)	Wt. loss
38	20	5.0	1.256	0.16
39	20	5.0	1.675	0.30
40	20	7.5	0.837	0.12
41	20	7.5	1.256	0.20
42	20	7.5	1.675	0.32
43	20	10.0	0.837	0.16
44	20	10.0	1.256	0.33
45	20	10.0	1.675	0.37
46	20	15.0	0.837	0.19
47	20	15.0	1.256	0.35
48	20	15.0	1.675	0.36

Table-7.3. ANOVA for wear loss 'Δw' (Full model)

Source	DF	Seq.SS	Adj. SS	Adj. MS	$F_{calculated}$	P
Regression	9	1.95611	1.956114	0.217346	48.97	0.000
Linear	3	1.76619	0.118818	0.039606	8.92	0.000
Square	3	0.10936	0.109359	0.036453	8.21	0.000
Interaction	3	0.08057	0.080569	0.026856	6.05	0.002
Residual error	38	0.16867	0.168668	0.004439		
Total	47	2.12478				

Seq. SS = Sequential sums of squares, Adj. SS = Adjusted sums of squares, Adj. MS = Adjusted mean squares.

Table-7.4. Estimated regression coefficients for wear loss '∆w' (Full model)

Term	Coef.	SE Coef.	P	
Constant	-0.719211	0.221997	0.002	
Re	0.027715	0.007271	0.000	
L	0.068496	0.020633	0.002	
V	0.742531	0.304779	0.020	
R_e*R_e	-0.000926	0.000217	0.000	
*L*L*	-0.002067	0.000868	0.022	
*V*V*	-0.101460	0.116193	0.388	(Insignificant)
R_e*L	-0.000938	0.000352	0.011	
R_e*V	-0.012359	0.003801	0.002	
*L*V*	0.005217	0.007602	0.497	(Insignificant)
R^2 = 92.1%		R^2_{adj} = 90.2%		

Coef. =Coefficient, SE Coef. =Standard error for the estimated coefficient, R^2 = Coefficient of determination and $R^2_{adj.}$ = Adjusted R^2.

Table-7.5 ANOVA for wear loss '∆w' (Reduced model)

Source	DF	Seq.SS	Adj. SS	Adj. MS	$F_{calculated}$	P
Regression	7	1.95064	1.950639	0.278663	64.01	0.000
Linear	3	1.76619	0.598114	0.199371	45.80	0.000
Square	2	0.10597	0.105974	0.052987	12.17	0.000
Interaction	2	0.07848	0.078479	0.039239	9.01	0.001
Residual error	40	0.17414	0.174142	0.004354		
Total	47	2.12478				

Table-7.6 Estimated regression coefficients for wear loss 'Δw' (Reduced model)

Term	Coef.	SE Coef.	P
Constant	-0.632453	0.110604	0.000
Re	0.027715	0.007201	0.000
L	0.075048	0.018115	0.000
V	0.536567	0.050679	0.000
R_e*R_e	-0.000926	0.000215	0.000
*L*L*	-0.002067	0.000860	0.021
R_e*L	-0.000938	0.000348	0.010
R_e*V	-0.012359	0.003764	0.002
R^2 = 91.8%	R^2_{adj} = 90.4%		

Table-7.7 Important factors and their levels for erosive wear

Sl. No.	Factor	Unit	Levels			
1	Fiber volume fraction (Re)	vol %	0	10	15	20
2	Impingement angle (α)	Degree	30	45	60	90
3	Impact velocity (V)	m/s	48	70	82	109

Table-7.8. Experimental results along with design matrix for Erosive wear of bagasse fiber reinforced epoxy composite

Runs	Factorial value			Response
	Re (vol %)	α (°)	V (m/s)	Erosion rate 'Er' (g/g)
1	0	30	48	0.001573
2	0	30	70	0.001747
3	0	30	82	0.002796
4	0	30	109	0.002971
5	0	45	48	0.002097
6	0	45	70	0.002447
7	0	45	82	0.004020
8	0	45	109	0.004544
9	0	60	48	0.002971
10	0	60	70	0.003321
11	0	60	82	0.005418
12	0	60	109	0.005768
13	0	90	48	0.004894
14	0	90	70	0.004719
15	0	90	82	0.009089
16	0	90	109	0.009613
17	10	30	48	0.000699
18	10	30	70	0.000699
19	10	30	82	0.001747
20	10	30	109	0.001922
21	10	45	48	0.001048
22	10	45	70	0.001573

Table 7.8 Contd.

Runs	Factorial value			Response
	Re (vol %)	α (°)	V (m/s)	Erosion rate (g/g)
23	10	45	82	0.002621
24	10	45	109	0.003495
25	10	60	48	0.002097
26	10	60	70	0.002272
27	10	60	82	0.003321
28	10	60	109	0.004369
29	10	90	48	0.004369
30	10	90	70	0.004544
31	10	90	82	0.005418
32	10	90	109	0.006117
33	15	30	48	0.000349
34	15	30	70	0.000524
35	15	30	82	0.001048
36	15	30	109	0.001573
37	15	45	48	0.000524
38	15	45	70	0.000699
39	15	45	82	0.002097
40	15	45	109	0.002097
41	15	60	48	0.001398
42	15	60	70	0.001398
43	15	60	82	0.003146
44	15	60	109	0.003321
45	15	90	48	0.00402
46	15	90	70	0.004195

Table 7.8 Contd.

Runs	Factorial value			Response
	Re (vol %)	α (°)	V (m/s)	Erosion rate (g/g)
47	15	90	82	0.004369
48	15	90	109	0.004719
49	20	30	48	0.000174
50	20	30	70	0.000349
51	20	30	82	0.000524
52	20	30	109	0.001398
53	20	45	48	0.000349
54	20	45	70	0.000524
55	20	45	82	0.001747
56	20	45	109	0.001747
57	20	60	48	0.001048
58	20	60	70	0.001223
59	20	60	82	0.002447
60	20	60	109	0.002971
61	20	90	48	0.003146
62	20	90	70	0.003495
63	20	90	82	0.003845
64	20	90	109	0.004544

Table-7.9. ANOVA for Erosion rate '*Er*' (Full model)

Source	DF	Seq.SS	Adj. SS	Adj. MS	$F_{calculated}$	P
Regression	9	0.000228	0.000228	0.000025	83.67	0.000
Linear	3	0.000219	0.000218	0.000073	239.82	0.000
Square	3	0.000001	0.000001	0.000000	1.55	0.211
Interaction	3	0.000007	0.000007	0.000002	8.10	0.000
Residual error	54	0.000016	0.000016	0.000000		
Total	63	0.000245				

Seq. SS = Sequential sums of squares, Adj. SS = Adjusted sums of squares, Adj. MS = Adjusted mean squares.

Table-7.10. Estimated regression coefficients for Erosion rate '*Er*' (Full model)

Term	Coef.	SE Coef.	P	
Constant	0.002967	0.000163	0.000	
Re	-0.001287	0.000095	0.000	
α	0.001972	0.000095	0.000	
V	0.001115	0.000098	0.000	
R_e*R_e	0.000195	0.000155	0.215	(Insignificant)
$\alpha*\alpha$	0.000271	0.000155	0.087	(Insignificant)
*V*V*	0.000030	0.000144	0.835	(Insignificant)
$R_e*\alpha$	-0.000406	0.000126	0.002	
R_e*V	-0.000429	0.000129	0.002	
$\alpha*V$	0.000217	0.000129	0.098	(Insignificant)
R^2 = 93.3%		R^2_{adj} = 92.2%		

Coef. =Coefficient, SE Coef. =Standard error for the estimated coefficient, R^2 = Coefficient of determination and $R^2_{adj.}$ = Adjusted R^2.

Table-7.11 ANOVA for Erosion rate '*Er*' (Reduced model)

Source	DF	Seq.SS	Adj. SS	Adj. MS	$F_{calculated}$	P
Regression	5	0.000226	0.000226	0.000045	140.61	0.000
Linear	3	0.000219	0.000224	0.000075	232.28	0.000
Interaction	2	0.000007	0.000007	0.000003	10.12	0.000
Residual error	58	0.000019	0.000019	0.000000		
Total	63	0.000245				

Table-7.12 Estimated regression coefficients for Erosion rate '*Er*' (Reduced model)

Term	Coef.	SE Coef.	P
Constant	0.003248	0.000073	0.000
Re	-0.001301	0.000097	0.000
α	0.001982	0.000097	0.000
V	0.001089	0.000100	0.000
R_e*α	-0.000406	0.000130	0.003
R_e*V	-0.000429	0.000133	0.002
R^2 = 92.4%	R^2_{adj} = 91.7%		

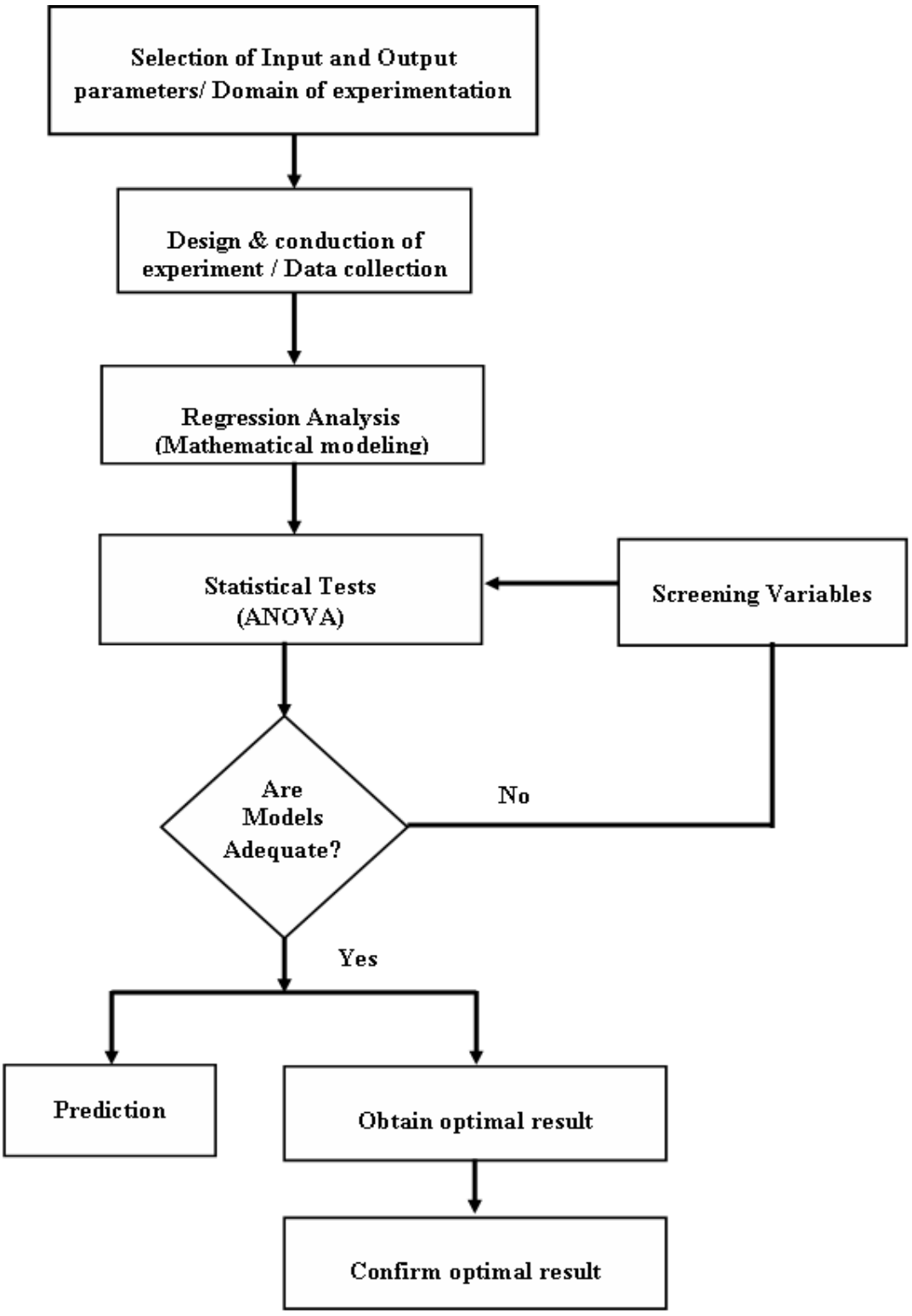

Figure-7.1 Procedure of Response Surface Methodology

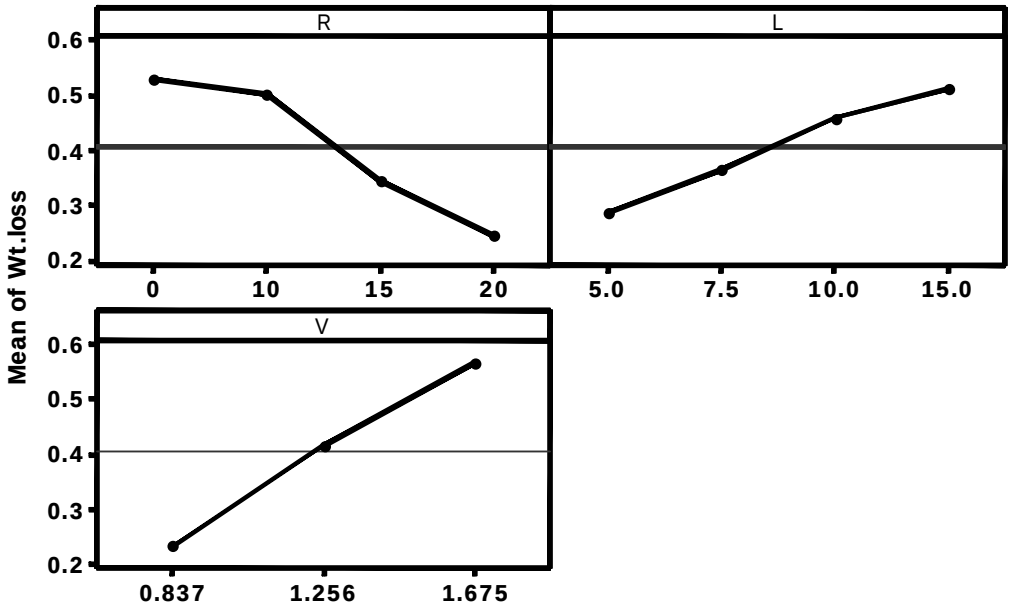

Figure-7.2 Main effect plot of wear loss '∆w'

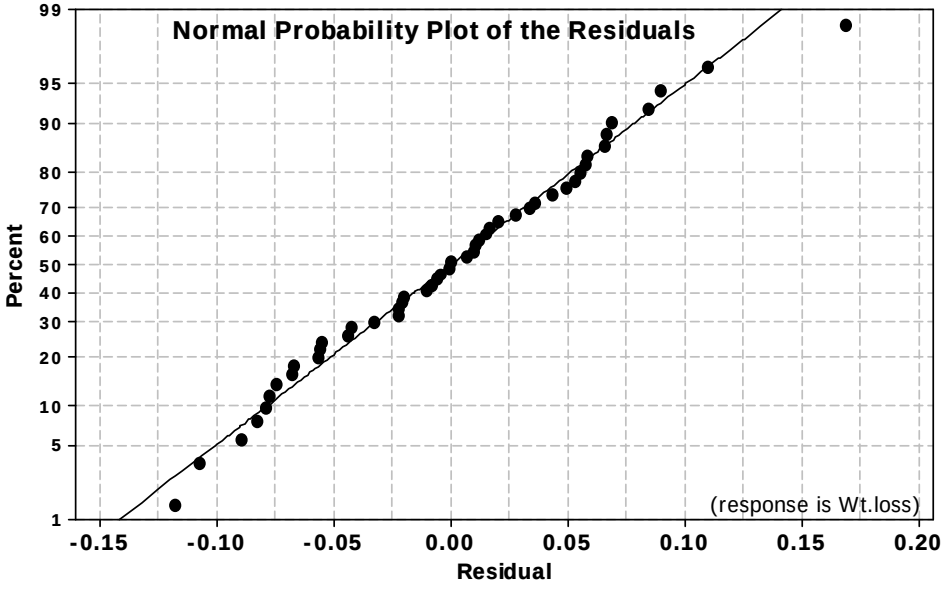

Figure-7.3 Normal probability plot of the residuals (Response is ∆*w*)

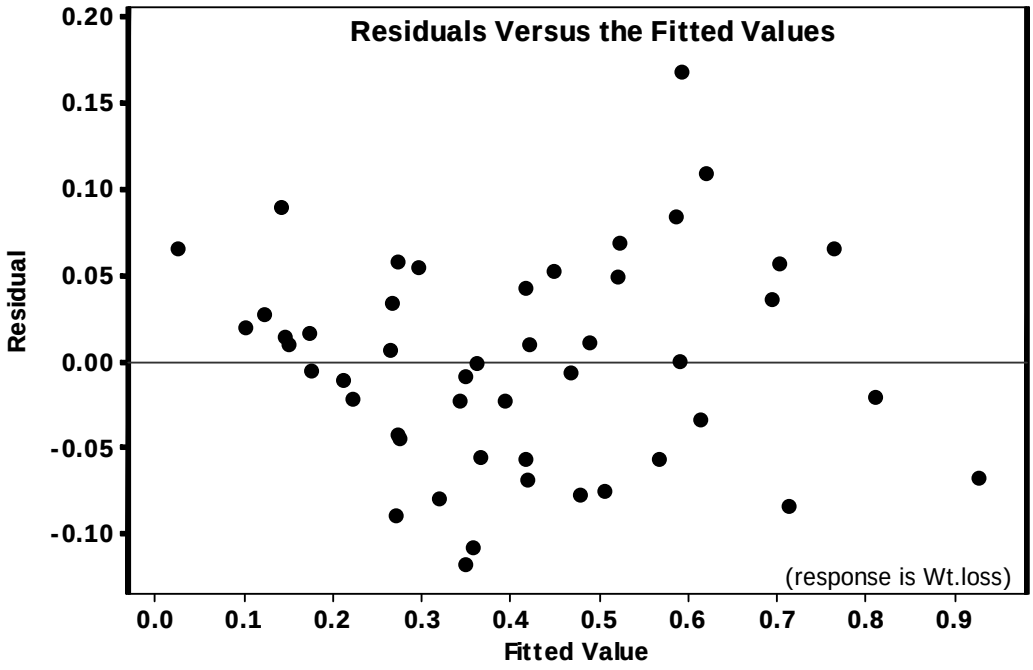

Figure-7.4 Plot of Residuals versus predicted response for wear loss 'Δw'

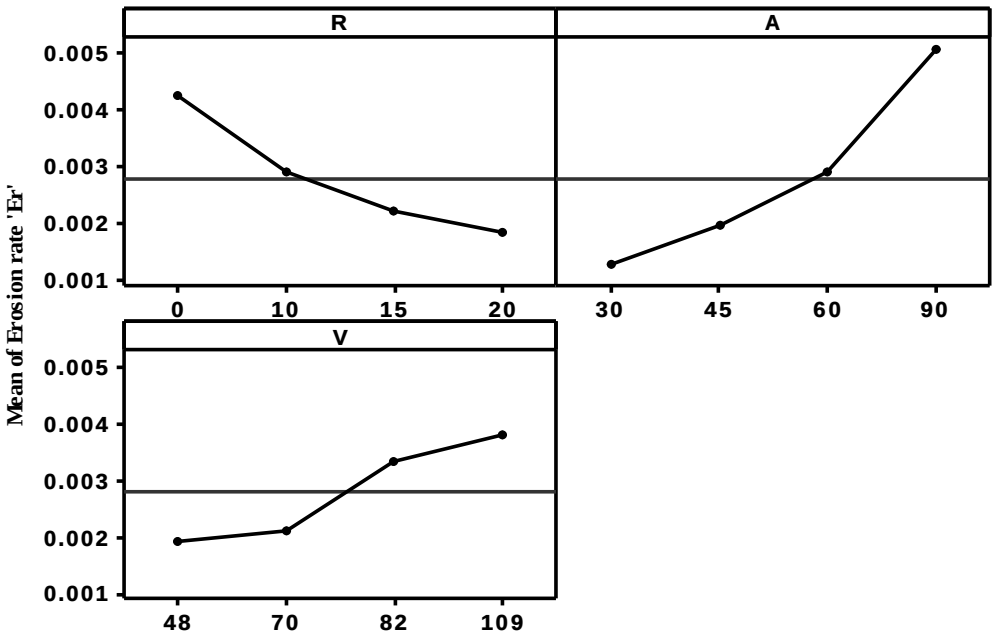

Figure-7.5 Main effect plot of Erosion rate 'E_r'

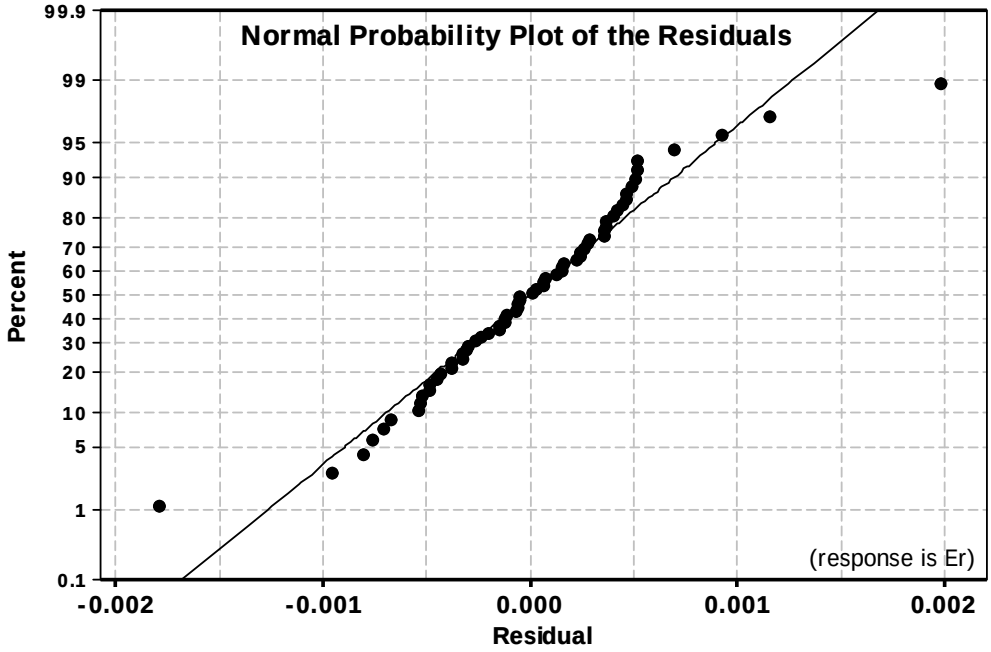

Figure-7.6 Normal probability plot of the residuals (Response is E_r)

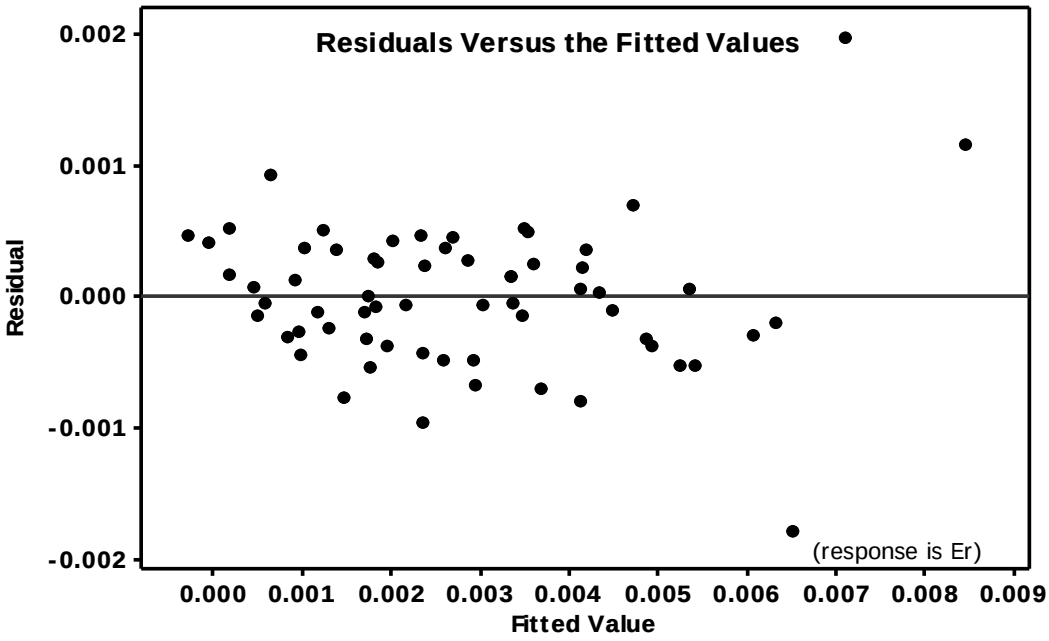

Figure-7.7 Plot of residuals verses predicted response for erosion rate *Er*

Chapter 8

CONCLUSIONS AND FUTURE WORK

Chapter-8

8.1 CONCLUSIONS

The conclusions drawn from the present investigations are as follows:

1. Bagasse can successfully be utilized to produce composite by suitably bonding with resin for the development of value added products.

2. There is a good dispersibility of bagasse fiber in the matrix, which improves the hardness, strength, and work fracture of the composite. Twenty volume percent of reinforcement fiber gives the best combination among the tested composites.

3. The surface modification of fiber significantly improves the fiber matrix adhesion which in turn enhances the mechanical properties of the composite. The alkali treatment provides the highest improvement in strength in-comparison to acetone treatment.

4. The abrasive wear resistance of neat epoxy is appreciably enhanced by incorporation of bagasse fiber. The specific wear rate of the composite also decreases with addition of fiber. In this present study the optimum fiber volume fraction which gives maximum wear resistance to the composite is found to be 20 vol%.

5. The abrasive wear rate of the Bagasse fiber epoxy composite is influenced by several parameters e.g. sliding velocity, sliding distance and normal load. The wear rate of the composite is found to be more sensitive to normal load in comparison to sliding velocity. The co-efficient of friction of the composite decreases with addition of bagasse fiber which confirms that the addition of this fiber is beneficial in reducing the wear of neat epoxy.

6. The trend $W_{NO} < W_{APO} < W_{PO,}$ for Bagasse fiber epoxy composite confirms the an-isotropic wear behaviour.

7. Bagasse fiber epoxy composite shows a brittle behaviour to solid particle erosion. From the experimental results the erosion efficiency (η) is found in the range 2.70% to 59.7%.

8. The predictive models for abrasive and erosive wear behaviour of developed composite under various testing conditions have been performed through Response Surface Methodology. The models developed are found statistically valid and sound within the range of factors.

8.2 RECOMMENDATION FOR FURTHER RESEARCH

1. In the present investigation a hand-lay-up technique was used to fabricate the composite. However there exists other manufacturing process for polymer matrix composite. They could be tried and analyzed, so that a final conclusion can be drawn there from. However the results provided in this thesis can act as a base for the utilization of this fiber.

2. From this work it is found that chemical modification of the fiber with alkali and acetone significantly improves the mechanical performance of the composite. Other chemical modification methods such as silane treatment, acetylation treatment, acrylation treatment isocynates treatment, Permanganate treatment, Maleated coupling agents could be tried and a final conclusion can be drawn there after.

3. In the current study different tribological tests has been carried out on the untreated Bagasse fiber epoxy composite. The same work could be extended to treated fiber composite.

4. In the erosion test sand particle of 200±50 microns only have been used. This work can be further extended to other particle size and types of particle like glass bead etc, to study the effect of particle size and type of particles on wear behaviour of the composite.

REFERENCES

[1] Jartiz, A.E., 1965, “Design,” pp. 18.

[2] Kelly, A., 1967, Sci. American, 217, (B), pp. 161.

[3] Berghezan, A., 1966, “Non-ferrous Materials,” Nucleus, 8: pp. 5–11.

[4] Van Suchtelen**.,** 1972, "Product properties: a new application of composite materials," Philips Res**.** Reports**,** Vol**.** 27**,** pp**.** 28.

[5] Agarwal, B.D. and Broutman, L.J., 1980, “Analysis and performance of fiber composites,” John Wiley & Sons, New York, pp.3-12.

[6] Chand N., Rohatgi P.K., 1994, “Natural fibers and their composites”, Publishers, Periodical Experts, Delhi.

[7] Chand N., Dwivedi U.K., 2006, “Effect of coupling agent on high stress abrasive wear of chopped jute/PP composites”, Journal of Wear, 261: pp. 1057.

[8] Tong J., Ren L., Li J., Chen B., 1995, “Abrasive wear behaviour of bamboo”, Tribology International, 28 (5),: pp. 323-327.

[9] Jain S., Kumar R., Jindal U.C., 1992, “Mechanical behaviour of bamboo and bamboo composites.” Journal of Material Science, 27: p. 4598-4604.

[10] Hinrichsen, G., Khan, M.A. and Mohanty, A.K., 2000, “Composites”: Part A, Elsevier Science Ltd, 31:pp.143–150.

[11] Joseph, P.V., Kuruvilla J, Thomas S., 1999, “Composites Science And Technology”; 59(11): pp.1625-1640.

[12] Mukherjee, P. S. & Satyanarayana, K. G., 1986, “Structure and properties of some vegetable fibers-II. Pineapple leaf fiber,” J. Material Science 21, pp. 51–56.

[13] Hirao, K., Inagaki, H., Nakamae, K., Kotera, M. and Nishino, T. K., 2003, “Kenaf Reinforced Biodegradable Composite,” Composites Science and Technology, 63: pp.1281-1286.

[14] Vazquez, A., Dominguez V. A., Kenny J. M., 1999, “Bagasse Fiber-Polypropylene Based. Composites.” Journal of Thermoplastic Composite Materials.” 12, (6): pp. 477-497.

[15] Clemons, Craig M., Caulfield, Daniel F., 2005, “Natural Fibers, Functional fillers for plastics,” Weinheim: Wiley-VCH: pp.195-206.

[16] Ei-Tayeb N.S.M., 2008, “A study on the potential of sugarcane fibers/polyester composite for tribological applications,” Wear, 265, pp. 223-235.

[17] Elsunni M. M., and Collier J. R., 1996, “Processing of Sugar Cane Rind into Nonwoven Fibers.” Journal of American Society of Sugar Cane Technologists, 16: pp. 94– 110.

[18] Paturau J.M., 1989, “By-Products of Sugar Cane Industry”, 3rd Edition, Elsevier, Amsterdam.

[19] Wambua P, Ivens J, Verpoest I., 2003, Natural fibers: can they replace glass in fiber reinforced plastics, Compos Sci Technol; 63 : 1259–64.

[20] Schuh TG. Renewable materials for automotive applications. http // www . ienica . net / fibersseminar/schuh.pdf (Accessed in February 2006).

[21] Khedari J, Charoemvai S, Hiruanlabh J., 2003, New insulating particle boards from durian peel and coconut coir. Build Environ; 38 : 435–441.

[22] Bledzki J, Gassan J., 1999, Composites reinforced with cellulose based fibres. Prog Polym Sci; 24 : 221–274.

[23] Franck, R.R., 2005, “Bast and Other Plant Fibers,” Cambridge: Woodhead Publishing Limited.

[24] Robson D. and Hague J.A., 1995, “Comparison of wood and plant fibre properties,” in Third International Conference on Wood-fiber-plastic composites, Madison, Wisconsin, USA: Forest Products Society.

[25] Professor Heinrich Flegel, Director of Production technology, Daimler Chrysler Research Centern UIm, Germany.

[26] Li Xue, Tabil G. Lope and Panigrahi Satyanarayan, 2007, “Chemical Treatments of Natural Fiber for Use in Natural Fiber-Reinforced Composites: A Review” J Polym Environ, 15:25–33.

[27] Rong, M.Z., Zhang, M.Q., Liu, Y., Yang, G.C. and Zeng, H.M., 2001, “The effect of fiber treatment on the mechanical properties of unidirectional sisal-reinforced epoxy composites,” Compos. Sci. Technol., 61; pp. 1437–1447.

[28] Haigler, C. H., 1985, ‘The Functions and Biogenesis of Native Cellulose,” Cellulose Chemistry and Its Applications. T. P. Nevell and S. H. Zeronian. West Sussex, Ellis Horwood Limited**:** pp.30-83.

[29] Thygesen, A. et al., 2006, “Comparison of composites made from fungal de-fibrated hemp with composites of traditional hemp yarn”, Industrial Crops and Products.

[30] Rowell, R.M., Young, R.A., and Rowell, J.K., 1997, “Chemical Composition of fibers: Paper and Composites from Agro-based Resources,”Lewis Publishers,CRC

Press, pp.85-91.

[31] Bjerre, A.B. and Schmidt, A.S., 1997, "Development of chemical and biological processes for production of bioethanol: Optimization of the wet oxidation process and characterization of products," Riso-R-967(EN), Riso National Laboratory. pp. 5-9.

[32] Morvan, C., Jauneau, A., Flaman, A., Millet, J. and Demarty, M., 1990, "Degradation of flax polysaccharides with purified endo-polygalacturonase", Carbohydrate Polymers, 13(2): pp.149-163.

[33] Madsen, B., 2004, "Properties of plant fibre yarn polymer composites – An experimental study," 2004, PhD Thesis, Department of civil Engineering, Technical University of Denmark.

[34] Sakakibara, A. and Shiraishi, N., 1991, "Wood and Cellulose Chemistry," New York: Marcel Dekker.

[35] Rowell, R.M., 1995, "A new generation of composite materials from agro-based fibre," in The Third International Conference on Frontiers of Polymers and Advanced Materials, Kuala Lumpur, Malaysia.

[36] Outwater J.O., 1956, "The mechanics of plastics reinforcement in tension," Modern Plastics; 33 (7).

[37] Robson, D. et al., 1996, "Survey of natural materials for use in structural composites as reinforcement and matrices," Woodland Publishing Ltd, Abingdon.

[38] Kohler, R. and Wedler, M., 1994, Techtextil-Symposium, pp. 1.

[39] Joseph, K., Varghese, S., Kalaprasad, G., Thomas, S., Prasannakumari, L., Koshy, P., Pavithran, C., 1996, "Influence of interfacial adhesion on the mechanical properties and fracture behaviour of short sisal fiber reinforced polymer composites," European Polymer Journal, 32: pp. 1243-1250.

[40] Patel, R.D., Patel, R.G. and Patel, V.S., 1988, J. Therm. Anal., 34: pp. 1283.

[41] Yu, L., Dean, K. and Li, L. 2006, "Polymer blends and composites from renewable resources," Prog. Polym. Sci., 31: pp. 576-602.

[42] Bax, B. and Mussig, J., 2008, "Impact and tensile properties of PLA/Cordenka and PLA/flax composites", Composites Science and Technology, 68: pp. 1601-1607.

[43] Oksman, K., M. Skrifvars, and J.F.Selin, 2003, "Natural fibres as reinforcement in polylactic acid (PLA) composites," Composites Science and Technology, 2003. 63: pp. 1317-1324.

[44] Meinander, K., 1997, " Polylactides - degradable polymers for fibers and films",

Macromolecular Symp, 123: pp. 147-154.

[45] Jiang, L. and Hinrichsen, G., 1999, “Flax and cotton fiber reinforced biodegradable polyester amide composites,” 2. Die Angewandte Makromolekulare Chemie, 268: pp. 18-21.

[46] Riedel, U. and Nickel, J., 1999, “Natural fiber-reinforced biopolymers as construction materials - new discoveries,” Die Angewandte Makromolekulare Chemie, 272: pp. 34-40.

[47] Keller, A., et al., 2000, “Degradation kinetics of biodegradable fiber composites,” Journal of Polymers and the Environment, 8(2): pp. 91-96.

[48] Rana A.K., Mandal A., 1998, et al. Short fiber-reinforced polypropylene composites: effect of compatibilizer. J Appl Polym Sci; 69 : pp. 329–38.

[49] Mitra B.C., Basak R.K., Sarkar M., 1998, Studies on jute-reinforced composites: its limitations, and some solutions through chemical modifications of fibers. J Apply Polym Sci; 67 : pp. 1093–100.

[50] Holbery, J., Houston, D., 2006, “Natural-Fiber-Reinforced Polymer Composites in Automotive Applications”, JOM, 58(11): pp.80-6.

[51] Burgueno, R., Quagliata, M.J., Mehta, G.M., Mohanty, A.K., Misra, M. and Drzal, L.T. 2005, “Sustainable Cellular Biocomposites from Natural Fibers and Unsaturated Polyester Resin for Housing Panel Applications”, Journal of Polymers and the Environment, 13(2): pp.139-149.

[52] Rials, T.G., Wolcott, M.P. and Nassar, J.M., 2001, “Interfacial Contributions in Lignocellulosic Fiber-Reinforced Polyurethane Composites”, Journal of Applied Polymer Science, 80(4): pp.546-555.

[53] Joseph S., Sreekalab M.S., Oommena Z., Koshyc P., Thomas S., 2002, A comparison of the mechanical properties of phenol formaldehyde composites reinforced with banana fibres and glass fibres, Compos. Sci. Technol., 62, pp. 1857–1868.

[54] Roe P.J., Ansel M.P., 1985, Jute reinforced polyester composites, J. Mater. Sci., 20, pp. 4015.

[55] Rana A.K., Mitra B.C., Banerjee A.N., 1999, Short jute fibre-reinforced polypropylene composites: dynamic mechanical study, J. Appl. Polym. Sci. 71, pp. 531–539.

[56] Manikandan Nair K.C., Diwan, S.M., Thomas S., 1996, “Tensile properties of short sisal fibre reinforced polystyrene composites”, J. Appl. Polym. Sci., 60, pp.

1483–1497.

[57] Jacoba M., Thomasa S., Varugheseb K.T., 2004, “Mechanical properties of sisal/oil palm hybrid fiber reinforced natural rubber composites”, Compos. Sci. Technol., 64, pp. 955–965.

[58] Pothana L.A., Oommenb Z., Thomas S., 2003, Dynamic mechanical analysis of banana fiber reinforced polyester composites, Compos. Sci. Technol., 63, (2), pp. 283–293.

[59] Yousif B.F., EI-Tayeb N.S.M., 2006, “Mechanical and tribological characteristics of OPRP and CGRP composites,” in: The Proceedings ICOMAST, GKH Press, Melaka, Malaysia, 2006, pp. 384–387, ISBN 983-42051- 1-2.

[60] Tong J., Arnell R.D., Ren L.-Q., 1998, “Dry sliding wear behaviour of bamboo”, Wear, 221, pp. 37–46.

[61] Tong J., Ma Y., Chen D., Sun, J., Ren L., 2005, “Effects of vascular fiber content on abrasive wear of bamboo,” Wear, 259, pp. 37–46.

[62] Hornsby P.R., Hinrichsen E., Tarverdi K., 1997, “Preparation and properties of polypropylene composites reinforced with wheat and flax straw fibres”, Part II. Analysis of composite microstructure and mechanical properties, J. Mater. Sci. 32, pp. 1009–1015.

[63] Pothan L.A., Thomas S., Neelakantan N.R., 1997, “Short banana fibre reinforced polyester composites: mechanical, failure and aging characteristics”, J. Reinf. Plast. Comp., 16, pp. 744.

[64] Mueller, D.H. and Krobjilowski, A., 2003, “New Discovery in the Properties of Composites Reinforced with Natural Fibers”, Journal of Industrial Textiles, 33(2): pp.111-129.

[65] Eichhorn, S.J., Baillie, C.A., Zafeiropoulos, N., Mwaikambo, L.Y., Ansell, M.P., Dufresne, A., Entwistle, K.M., Herrera-Franco, P.J., Escamilla, G.C., Groom, L.H., Hughes, M., Hill, C., Rials, T.G. and Wild, P.M., 2001, “Review: Current international research into cellulosic fibres and composites”, Journal of Materials Science, 36(9): pp.2107-2131.

[66] Brouwer, W.D., 2000, “Natural Fibre Composites in Structural Components: Alternative Applications for Sisal,” FAO, Common Fund for Commodities–Alternative Applications for Sisal and Henequen – Technical Paper No. 14.

[67] Bodros, E., Pillin, I., Montrelay, N., Baley, C., 2007, “Could biopolymers reinforced by randomly scattered flax fiber be used in structural applications”,

Composites Science and Technology, 67(3-4): pp.462-470.

[68] Pal, P.K., 1984, “Plastics Rubber Process Appl,” 4: pp. 215-219.

[69] Mohanty, A.K., Misra, M. and Drzal, L.T., 2002, “Sustainable bio-composites from renewable resources: opportunities and challenges in the green materials world,” J. Polym. Environ. 10: pp. 19–26.

[70] Roe, P.J. and Ansel, M.P., 1985, “Jute reinforced polyester composites”, J. Mater. Sci. 20: pp.4015.

[71] Qiu Zhang, X. M., Zhi Rong, M., Shia, G. and Cheng Yang, G., 2003, “Self reinforced melt processable composites of sisal”, Compos. Sci. Technol. 63 : pp.177–186.

[72] Baiardo, M., Zini, E. and Scandola, M., 2004, ‘Flax fibre–polyester composites’, J.Compos.: Part A 35 : pp.703–710.

[73] George, J., Sreekala, M.S., and Thomas, S., 2002, “A review on interface modification and characterization of natural fibre reinforced plastic composites”, Ploym. Eng. Sci. 41 (9): pp.1471–1485.

[74] Valadez-Gonzales, A., Cetvantes-Uc, J.M., Olayo, R. and Herrera Franco, P.J., 1999, “Effect of fibre surface treatment on the fibre-matrix bond strength of natural fibre reinforced composites”, Composites, Part B 30 (3): pp.309–320.

[75] El-Tayeb, N.S.M., 2009, “Development and characterisation of low-cost polymeric composite materials”, Materials and Design 30: pp.1151–1160.

[76] Gassan J., 2002, “A study of fiber and interface parameters affecting the fatigue behaviour of natural fiber composites”, Composite Part A 33: pp.369–374.

[77] Hepworth, D.G., Hobson, R.N., Bruce, D.M. and Farrent, J.W., 2003, “The use of unretted hemp in composite manufacture”, Composites A 31: pp.1279–1283.

[78] Joseph, P.V., Kuruvilla, J. and Sabu T., 2002, “Short sisal fibre reinforced polypropylene composites: the role of interface modification on ultimate properties”, Comps. Interf. 9 (2): pp.171–205.

[79] El-Sayed, A.A., El-Sherbiny, M.G., Abo-El-Ezz, A.S. and Aggag, G.A., 1995, “ Friction and wear properties of polymeric composite materials for bearing applications”, Wear 184: pp.45–53.

[80] Kozlowski R, Rawluk M, Barriga J. State of the art-production, processing and applications of fibrous plants. In: Sivam RL, Arau´ jo RC, editors. 2nd international conference on textile engineering (SINTEX-2004) Proceedings, September 7–11; 2004, Natal, in CDROM, Paper No.TIP-1-007.

[81] Rowell, R.M., 1997, “Chemical modification of agro-resources for property enhancement”, Paper and Composites from Agro-based Resources, CRC Press. p. 351-375.

[82] Espert, A., Vilaplana, F. and Karlsson, S., 2004, “Comparison of water absorption in natural cellulosic fibres from wood and one-year crops in polypropylene composites and its influence on their mechanical properties”, Compos Part A ; 35: pp.1267–76.

[83] Sanadi, A.R., CaulField, D.F. and Jacobson, R.E., 1997, “Agro-Fibre Thermoplastic Composites”, Paper and composites from agro-based resources, Boca Raton: CRC Press: Lewis Publishers, Chapter 12, pp. 377-401.

[84] Maya Jacob John, Anandjiwala Rajesh D., 2008, “Recent Developments in Chemical Modification and Characterization of Natural Fiber-Reinforced Composites”, Polymer composites, pp.187-207.

[85] Joseph, K., Thomas, S. and Pavithran, C., 1996, “Effect of chemical treatment on the tensile properties of short sisal fibre-reinforced polyethylene composites”, Polymer 37: pp. 5139–49.

[86] Joseph, P.V., Joseph, K. and Thomas, S., 1999, “Effect of processing variables on the mechanical properties of sisal-fiber-reinforced polypropylene composites”, Compos Sci Techol., 59: pp.1625–40.

[87] Mukherjee, R.N., Pal S.K., Sanyal S.K., Phani K.K., 1984, “Role of interface in fiber reinforced polymer composites with special reference to natural fibers.” Journal of Polymer Material, (1),: pp. 69-81.

[88] Gassan J, Bledzki AK, 1999, “Alkali treatment of jute fibers: relationship between structure and mechanical properties.” Journal of Applied Polymer Science, (71): p. 623-629.

[89] Zadorecki P., Flodin P., 1985, “Surface modification of cellulose fibers. I. Spectroscopic characterization of surface-modified cellulose fibers and their copolymerization with styrene.” J Appl Polym Sci, (30): pp. 2419–2429.

[90] Zadorecki, P. and Flodin, P., 1985, “Surface modification of cellulose fibres. II. The effect of cellulose fibre treatment on the performance of cellulose– polyester composites.” J Appl Polym Sci, (3): pp. 3971–3983.

[91] Vilay, V., Mariatti, M., Taib, R. M., & Todo, M., 2008. Effect of fiber surface treatment and fiber loading on the properties of bagasse fiber-reinforced

unsaturated polyester composites. Composites Science and Technology, 68, pp. 631–638.

[92] Filho, G. R., da Cruz, S. F., Pasquini, D., Cerqueira, D. A., de Prado, V. S., & de Assunção, R. M. N., 2000, Water flux through cellulose triacetate films produced from heterogeneous acetylation of sugar cane bagasse. Journal of Membrane Science, 177, pp. 225–231.

[93] Luz, S. M., Tio, J. D., Rocha, G. J. M., Gonçalves, A. R., & Del'Arco, A. P. Jr., 2008, Cellulose and cellulignin from sugarcane bagasse reinforced polypropylene composites: Effect of acetylation on mechanical properties. Composites A, 39, pp. 1362–1369.

[94] Liu, C. F., Sun, R. C., Zhang, A. P., Ren, J. L., Wang, X. A., Qin, M. H., et al. 2007, Homogeneous modification of sugarcane bagasse cellulose with succinic anhydride using a ionic liquid as reaction medium. Carbohydrate Research, 342, pp. 919–926.

[95] Luz, S. M., Gonçalvez, A. R., & Del'Arco, A. P. Jr., 2007, Mechanical behavior and microstructural analysis of sugarcane bagasse fibers reinforced polypropylene composites. Composites A, 38, pp. 1455–1461.

[96] Bilba, K., & Arsene, M.-A., 2008, Silane treatment of bagasse fiber for reinforcement of cementitious composites. Composites A, 39, pp. 1488–1495.

[97] Mohanty, A.K., Misra, M. and Drzal, L.T., 2001, Compos Interfaces 8: pp.313.

[98] Agrawal, R., Saxena, N.S., Sharma, K.B., Thomas, S. and Sreekala, M.S., 2000, Material Science Engg. A 277: pp.77.

[99] Jahn, A., Schroder, M.W., Futing, M. and Schezel, K, Diepenbrock, 2002, Wear , Spectrochim,Acta A: Mol Biomol Spectrosc 58: pp.2271.

[100] Sreekala, M. S.; Kumaran, M. G.; Sabu, M. G., 1998, "Oil Palm Fibers: Morphology, Chemical Composition, Surface Modification, and Mechanical Properties", J Appl Polym Sci, 66(5), pp.821-835.

[101] Ray, D. and Sarkar, B. K., 2001, "Characterization of alkali-treated jute fibers for physical and mechanical properties", J Appl Polym Sci , 80, pp. 1013–1020.

[102] Aziz, S. H., and Ansell, M. P., 2004, "The effect of alkalization and fibre alignment on the mechanical and thermal properties of kenaf and hemp bast fibre composites: Part 1 – polyester resin matrix", Compos Sci Technol, 64: pp.1219.

[103] Higgins, G. H., V. Goldsmith, and A. N. Mukherjee, 1958, J. Polym. Sci., 32: pp.57.

[104] Tanaka, K., Minoshima, K., Grela, W. and Komai, K., 2002, "Characterization of the aramid/epoxy interfacial properties by means of pull-out test and influence of water absorption", Composites Science and Technology, 62: pp. 2169-2177.

[105] Lin, J.C., Chang, L.C., Nien, M.N. and Ho, H.L., 2006, "Mechanical behavior of various nano-particle filled composites at low-velocity impact", Comp Struct. 27: pp.30–36.

[106] Jayaraman, K., 2003, "Manufacturing sisal-polypropylene composites with minimum fiber degradation", Comp Sci Tech, 63: pp.367–74.

[107] Fujii, T., 1975, J. Jpn. Soc. Comp. Mater., **1,** 35 (1975).

[108] Joseph, P.V., Mathew, G., Joseph, K., Groeninckx G. and Thomas, S., 2003, "Dynamic mechanical properties of short sisal fiber reinforced polypropylene composites", Comp A ; 34: pp. 275–90.

[109] Sreenivasan, S., Iyer, P.B, and Krishna Iyer K.R., 1996, "Influence of delignification and alkali treatment on the fine structure of coir fibers (Cocos Nucifera)", J Mater Sci, 31: pp.721–726.

[110] Amontons, G., 1699, Mem. Acad. T. , Ser. A: pp 257-282.

[111] Petrov, N.P., 1893, "Friction in machines and the effect of the lubricant", Inzh. Ah, 1893, pp 71-140, Vol. 2; pp. 227-279.

[112] Tower, B., 1983, "First report on friction experiments", Proc., Inst. Mech. Eng., London, Nov: pp. 632-659.

[113] Reynolds, O., 1886, "On the theory of lubrication and its application to Mr. Beauchamp Tower's experiments", Plilos. Trans. T. Soc. London, Vol. 177, pp. 157-234.

[114] Holm, R., 1983, "The frictional force over the real area of Contact", Wiss. Vereoff. Siemens Werken, Vol. 17 (4), pp. 38-42.

[115] Peterson, M. B., 1990, "Advanced in tribo-materials-I Achievements in Tribology", Amer, Soc, Mech. Eng., Vol.1, New York; pp.91-109.

[116] Rigney, D.A., 1981, In: D.A. Rigney (Ed.), "Fundamentals of Friction and Wear of Materials", American Society for Metals, Metals Park, Ohio; pp.1–12.

[117] Ashby, M.F. and Lim, S.C., 1990, "Wear-mechanism maps", Scripta Metallurgical et Materialia, Vol.24: pp. 805-810.

[118] Wang, Y., Lei, T.C. and Gao, C.Q., 1990, "Influence of isothermal hardening on the sliding wear behaviour of 52100 bearing steel', Tribology International, Vol. 23(1): pp. 47-53.

[119] Lim, S. C., 1998, “Recent developments in wear mechanism Maps”, Tribology International Vol. 31, Nos 1–3, pp. 87–97.

[120] Eyre, L.S., 1976, “Wear Characteristics of metals”, Tribology International, October-1976, pp. 203-212.

[121] Dowson, 1985, “Wear oh where”, International Conference on wear of Materials, Vancouver Canada, April 14-18.

[122] Thwe M.M. and Liao, K., 2003, “Environment degradation of bamboo/glass fibre hybrid polypropylene composites”, J Mater Sci Lett, 38:pp.363–81.

[123] Blau, J., 1997, “Fifty years of research on the wear of metals”, Tribology International, Vol. 30(5): pp. 321-331.

[124] Barwell, F. T. and Strang, C. D., 1952, “Metallic Wear”, Proc. Roy. Soc. London, A, 212 (III): pp. 470-477.

[125] Archard, J.F., 1953, “Contact Rubbing of flat Surfaces”, J. Appl, Phys 24: pp. 981-988.

[126] Archard, J.F. and Hirst, W, 1957, “The Wear of Metal Under Unlubricated Conditions”, Proc. Roy. Soc. London, A, Vol. 238: pp 515-528.

[127] Kragelski, I. V., 1983, "Grundlagen der Berechnung von Reibung und VerschleiR”, Carl Hanser Verag. Miinchenu. Wien.

[128] Fleischer, G., 1973, “Energetische Methode der Bestimmung des VerschleiRes”, Schtnierungsrechnik 4(9): pp. 269-274.

[129] Gahr, K.H.Z., 1987, “Microstructure and wear of materials”, Tribology series 10, Elsevier Science Publishers.

[130] Stachowiak, G.W. and Batchelor, A.W., 1993, Engineering tribology. Amsterdam: Elsevier.

[131] Friedrich, K., 1986, “Friction and wear of polymer composites”, In: Friedrich K, editor. Composite materials series-1, Amsterdam: Elsevier; Chapter-8.

[132] Thorp, J.M., 1982, “Abrasive wear of some commercial polymers”, Tribol. Int., 15: pp.89–135.

[133] Budinski, K.G., 1997, “Abrasion resistance of plastics”, Wear; 203 (204): pp.302–309.

[134] Evans, D.C., and Lancaster, J.K., 1979. “The Wear of Polymers”, In: Scott, D. (Ed.), Treatise on Materials Science and Technology, New York, USA; Academic Press, 13, pp. 85—139.

[135] Unal, H., Sen, U. and Mimaroglu, A., 2005, “ Abrasive behaviour of polymeric

materials", Mater. Des. 26: pp.705–710.

[136] Unal, H., Sen, U. and Mimaroglu, A., 2004, "Dry Sliding Wear Characteristics of Some Industrial Polymers Against Steel Counter Face", Journal of Tribo, 37: pp.727–732.

[137] Shipway, P.H. and Ngao, N.K., 2003, "Microscale abrasive wear of polymeric materials", Wear; 255: pp.742–750.

[138] Harsha, A.P. and Tewari, U.S., 2003, "Two-body and three-body abrasive wear behaviour of polyaryletherketone composites", Polymer Testing; 22: pp. 403–418.

[139] Cirino, M., Pipes, R.B. and Friedrich, K., 1987, "The Abrasive Wear Behavior of Continuous Fiber Polymer Composites", J. Mater. Sci., 22: pp.2481–2492.

[140] Cirino, M., Friedrich, K. and Pipes, R.B., 1988, "Evaluation of Polymer Composites for Sliding and Abrasive Wear Application", Composites, 19: pp.383–392.

[141] Chand, N., Nayak, A. and Neogi, S., 2000, "Three-Body Abrasive Wear of Short Glass Fiber Polyester Composite", Wear, 242: pp.32–46.

[142] Bijwe, J., Logani, C.M. and Tewari, U.S., 1989, "Influence of fillers and fibre reinforcement on abrasive wear resistance of some polymeric composites", In: Proceeding of the International Conference on Wear of Materials, Denver, CO, USA, April 8–14, pp. 75–92.

[143] Liu, C., Ren, L., Arnell, R.D. and Tong, J., 1999, "Abrasive wear behavior of particle reinforced ultrahigh molecular weight polyethylene composites", Wear; 225–229: pp.199–204.

[144] Zhang, H., Zhang, Z., Guo, F., Jiang, W. and Liu W.M., 2009, "Study on the tribological behavior of hybrid PTFE/ cotton fabric composites filled with Sb_2O_3 and melaminecyanurate", Tribol. Int.; 42(7): pp.1061–1066.

[145] Hashmi, S.A.R., Dwivedi, U.K. and Chand, N., 2007, "Graphite modified cotton fiber reinforced polyester composites under sliding wear conditions, Wear; 262 (11–12): pp.1426–1432.

[146] Yousif, B.F. and El-Tayeb, N.S., 2007, "The effect of oil palm fibers as reinforcement on tribological performance of polyester composite", Surface Review and Letters (SRL); 14 (6): pp.1095–1102.

[147] Yousif, B.F., 2009, "Frictional and wear performance of polyester composites based on coir fibers",Proc IME J. J. Eng Tribol.;223(1): pp.51–9.

[148] Chin, C.W. and Yousif, B.F., 2009, "Potential of kenaf fibers as reinforcement for

tribological applications", Wear; 267: pp.1550–1557.

[149] Yousif, B.F., Lau, Saijod, T.W. and Mc-William, S., 2010, "Polyester composite based on betelnut fibre for tribological applications", Tribology International; 43: pp.503–511.

[150] Lai, W.L. and Mariatti, M., 2008, "The properties of woven betel palm (areca catechu) reinforced polyester composites", J. Reinf. Plast. Compos.; 27: pp.925-935.

[151] Dwivedi, U.K. and Chand, N., 2008, "Influence of Wood Flour Loading on Tribological Behavior of Epoxy Composites", Polymer Composites; 29: pp.1189-1192.

[152] Dwivedi, U. K., Ghosh, A., and Chand, N., 2007, "Abrasive wear behaviour of bamboo powder filled polyester composites," BioResources; 2(4): pp.693-698.

[153] Soda, N., 1975, "Wear of some F.F.C metals during unlubricated sliding part-1. Effects of load, velocity and atmospheric pressure on wear". Wear; 33: pp.1-16.

[154] Burwell, J.T. and Strang, C.D., 1953, 'Metallic wear', Proc.Soc (London), 212 A May: pp.470-477.

[155] Burwell, J.T., 1957, "Survey of possible wear mechanisms", Wear-1; 58: pp.119-141.

[156] Zumgahr, K.H., 1987, "Microstructure and wear of materials", Elsevier, Amsterdam.

[157] Ko, P.L., 1987, "Metallic wear-a review with special references to vibration-induced wear in power plant components", Tribology International, April,Vol.20, No.1: pp.66-78.

[158] Padmapriya S., Rai S., 2009, "Impact, Compression, Density, Void Content, and Weight Reduction Studies on Waste Silk Fabric/Epoxy Composites."Journal of Reinforced Plastics and Composite., 24, 15, pp. 1605-1610.

[159] Verma, A. P. and Sharma, P. C., 1992, "Abrasive Wear Behaviour of GRP Composite", The Journal of the Institute of Engineers (India) , Pt MC2,72, pp. 124.

[160] Sung, N.-H. and Suh, N. P., 1978, "Effect of fiber orientation on friction and wear of fiber reinforced polymeric composites", Wear; 53: pp.129-141.

[161] Lyhmn, C., 1987, "Tribological behaviour of unidirectional polypropylene sulfide carbon fiber reinforced laminate composites", Wear; 117: pp.147–59.

[162] Cirino, M., Friedrich, K. and Pipes, R. B., 1988, "The effect of fiber orientation on

the abrasive wear behavior of polymer composite materials," Wear; 121, pp.127-141.

[163] Vishwananth, B., Verma, A. P., Rao, V. S. K., 1993, "Effect of reinforcement on friction and wear of fabric reinforced polymer composites", Wear, 167, pp.93-99.

[164] Shim, H.H., Kwon, O.K., Youn, J.R., 1992, "Effects of fibre orientation and humidity on friction and wear properties of graphite fibre composites", Wear; 157: pp.141-149.

[165] K. Joseph, S. Varghese, G. Kalaprasad, S. Thomas, L. Prasannakumar, P. Koshy, and C. Pavithram, 1996, Eur. Polym. J., 32, pp. 1243.

[166] Z. Lu , K. Friedrich, W. Pannhorst, J. Heinz, 1993, "Wear and friction of a unidirectional carbon fiber-glass matrix composite against various counterparts", Wear**,** 162-164, pp. 1103-1113.

[167] Eleiche, A.M., Amin, G.M., 1986, "The effect of unidirectional cotton fibre reinforcement on the friction and wear characteristics of polyester", Wear, 112, pp.67.

[168] Chand, N. and Dwivedi, U.K., 2007, "High stress abrasive wear study on bamboo", Journal of Materials Processing Technology 183, pp. 155–159.

[169] Chand, N., Dwivedi, U.K. and Acharya, S.K., 2007, "Anisotropic abrasive wear behaviour of bamboo (Dentrocalamus strictus)", Wear, 262, pp. 1031–1037.

[170] Chand, N. and Dwivedi, U.K., 2007, "Influence of Fiber Orientation on High Stress Wear Behavior of Sisal Fiber-Reinforced Epoxy Composites", polymer composites, pp. 437-441.

[171] Chand, N. and Dwivedi, U.K., 2009, "Influence of Fibre Orientation on Friction and Sliding Wear Behaviour of Jute Fibre Reinforced Polyester Composite", Appl. Compos. Mater, 16: pp. 93–100.

[172] EI-Tayeb N.S.M. 2008, "Abrasive wear performance of untreated SCF reinforced polymer composite". Journal of Material Processing Technology, 206, pp.305-314.

[173] EI-Tayeb N.S.M. 2008, "A study on the potential of sugarcane fibers/polyster composite for tribological applications". Wear, 265, pp. 223-235.

[174] Finnie, I., 1995, "Some reflections on the past and future of erosion: Part-I", Wear; 186/187: pp.1-101.

[175] Meng, H. C. and Ludema, K. C., 1995, "Solid Particle Erosion Resistance of Ductile Wrought Super Alloys and Their Weld Overlay Coatings", ibid, 181–183: pp.443.

[176] Bitter, J.G.A., 1963, “A study of erosion phenomena”, Part I. Wear; 6: pp.5–21.

[177] Hutchings, I.M., Winter, R.E. and Field, J.E, 1976, “Solid particle erosion of metals: the removal of surface material by spherical projectiles”, Proc Roy Soc Lond, Ser A; 348: pp.379-392.

[178] J. Bijwe, M. Fahim, in: H.S. Nalwa (Ed.), Hand Book of Advanced Functional Molecules and Polymers, Gordon and Breach, London, Tokyo, Japan, 2000 (in press).

[179] Pool, K.V., Dharan, C.K.H. and Finnie, I., 1986, “Erosive wear of composite materials”, Wear; 107: pp.1-12.

[180] Kulkarni, S.M., Kishore, K., 2001, “Influence of matrix modification on the solid particle erosion of glass/epoxy composites”, Polymer and Polymer Composites;9: pp.25-30.

[181] Rajesh, J.J, Bijwe, J., Tewari, U.S. and Venkataraman, B., 2001, “Erosive wear behavior of various polyamides”, Wear; 249: pp.702 – 714.

[182] Friedrich K., 1986, Erosive wear of polymer surfaces by steel blasting. Journal of Material Science; 21 : pp. 3317–32.

[183] Kulkarni SM, Kishore., 2001, Influence of matrix modification on the solid particle erosion of glass/epoxy composites. Polymer and Polymer Composites; 9: pp. 25–30.

[184] Aglan HA, Chenock Jr TA. Erosion damage features of polyimide thermoset composites. SAMPEQ 1993; January :41–7.

[185] Roy M, Vishwanathan B, Sundararajan G., 1994, The solid particle erosion of polymer matrix composites. Wear; 171: pp. 149–61.

[186] Hager A, Friedrich K, Dzenis YA, Paipetis SA. Study of erosion wear of advanced polymer composites. In: Street K, editor. ICCM-10 Conference Proceedings, Whistler, BC, Canada. Cambridge (UK): Woodhead Publishing; 1995. p. 155–62.

[187] Tilly GP., 1969, Erosion caused by airborne particles. Wear, 14: pp.63–79.

[188] Tilly GP, Sage W., 1970, The interaction of particle and material behavior in erosion process. Wear; 16: pp.447–65.

[189] Zahavi J, Schmitt Jr GF., 1981, Solid particle erosion of reinforced composite materials. Wear; 71: pp.179–90.

[190] Tsiang TH., 1989, Sand erosion of fibre composites: testing and evaluation. In: Chamis CC, editor. Test methods for design allowable for fibrous composites. 2

ASTMSTP 1003. Philadelphia: American Society for Testing and Materials; p. 55–74.

[191] Mathias PJ, Wu W, Goretta KC, Routbort JL, Groppi DP, Karasek KR., 1989, Solid particle erosion of a graphite fibre reinforced bismaleimide polymer composite. Wear, 135: pp. 161–9.

[192] Brandsta¨ dter A, Goretta KC, Routbort RL, Groppi DP, Karasek KR., 1991, Solid particle erosion of bismaleimide polymers. Wear; 147: pp.155–64.

[193] Walley SM, Field JE, Scullion IM, Heukensfeldt Jansen FPM, Bell D. Dynamic strength properties and solid particle erosion behaviour of a range of polymers. In: Field JE, Daer JP, editors. 7th International Conference Proceedings, On Erosion by Liquid and Soild Impact. Cambridge (UK):: Cavendish Laboratory; 1984 [Paper 59].

[194] Walley SM, Field JE. The erosion and deformation of polyethylene by solid particle impact. Phil Trans Royal Soc (Lond) 1987;A 321:277–303.

[195] Walley SM, Field JE, Greengrass M., 1987, An impact and erosion study of PEEK. Wear; 114: pp. 59–71.

[196] Walley SM, Field JE, Yennadhiou P., 1984, Single solid particle impact erosion damage on polypropylene. Wear; 100: pp.263–80.

[197] Miyazaki N, Takeda N., 1993, Solid particle erosion of fibre reinforced plastics. Journal of Composite Materials; 27: pp. 21–31.

[198] Miyazaki N, Hamao T., 1994, Solid particle erosion of thermoplastic resins reinforced by short fibres. Journal of Composite Materials; 28: pp.871–83.

[199] Miyazaki N, Hamao T., 1996, Effect of interfacial strength on erosion behaviour of FRPs. Journal of Composite Materials; 30: pp.35– 50.

[200] Barkoula NM, Karger-Kocsis J., 2000, Solid particle erosion of unidirectional GF reinforced EP composites with different fibre/ matrix adhesion. Journal of Reinforced Plastics and Composites; 19: pp.1–12.

[201] Barkoula NM, Gremmels J, Karger-Kocsis J., 2001, Dependence of solid particle erosion on the cross-link density in an epoxy resin modified by hygrothermally decomposed polyurethane. Wear; 247: pp. 100–8.

[202] Karasek KR, Goretta KC, Helberg DA, Routbort JL., 1992, Erosion in bismaleimide polymers and bismaleimide polymer composites. Journal of Material Science Letters; 11: pp.1143–4.

[203] Rao P V, Buckley D H. , 1986 , Angular particle impingement studies of thermo

plastic materials at normal incidence. ASLE Trans; 29: pp.283–98.

[204] Rao PV, Young SG, Buckley DH. Solid spherical glass particle impingement studies of plastic materials. Report no. NASATP- 2161. National Aeronautics and Space Administration; 1983.

[205] Barkoula NM, Karger-Kocsis J., 2002, Effect of fibre content and relative fibre orientation on the solid particle erosion of GF/PP composites. Wear; 252: pp.80–7.

[206] Wang YQ,Huang LP, LiuWL, Li J., 1998, The blast erosion behaviour of ultrahigh molecular weight polyethylene.Wear; 218: pp. 128–33.

[207] Tong J, Ma Y, Chen D, Sun J, Ren L., 2005, Effects of vascular fiber content on abrasive wear of bamboo, Wear, 259: pp. 37-46.

[208] Hornsby PR, Hinrichsen E, Tarverdi K., 1997, Preparation and properties of polypropylene composites reinforced with wheat and flax straw fibers, part II. Analysis of composite microstructure and mechanical properties, J mater Sci., 32: pp. 1009-1015.

[209] Barkoula, N.M. and Karger-Kocsis, J., 2002, "Review-processes and influencing parameters of the solid particle erosion of polymers and their composites", J. Mater. Sci.; 37: pp. 3807–3820.

[210] Tewari, U.S., Harsha, A.P., Hager, A.M. and Friedrich, K., 2003, "Solid particle erosion of carbon fibre– and glass fibre–epoxy composites", Compos Sci Technol.; 63: pp.549–57.

[211] Bhushan, B., 1999, " Principles and applications of tribology",New York: Wiley.

[212] Harsha, A.P. and Thakre, A.A., 2007, "Investigation on solid particle erosion behaviour of polyetherimide and its composites", Wear; 262: pp.807–818.

[213] Bijwe, J., Indumathi, J., John, R.J. and Fahim, M., 2001, "Friction and wear behavior of polyetherimide composites in various wear modes", Wear; 249: pp.715–726.

[214] Bijwe, J., Indumathi, J. and Ghose, A.K., 2002, "On the abrasive wear behavior of fabric-reinforced polyetherimide composites", Wear; 253: pp.768–777.

[215] Ruff, A.W. and Ives, L.K., 1975, "Measurement of solid particle velocity in erosive wear", Wear; 35: pp.195–199.

[216] Sundararajan, G. and Roy, B.V., 1990, "Erosion efficiency– a new parameter to characterize the dominant erosion mechanism", Wear; 140: pp.369–381.

[217] Suresh, A. and Harsha, A.P., 2006, "Study of erosion efficiency of polymers and polymer composites", Polymer testing; 25: pp.188-196.

[218] Deo Chittaranjan and Acharya S.K., 2009, 'Solid Particle Erosion of Lantana-Camara Fiber Reinforced Polymer Matrix Composite.' Polymer-Plastic technology and Engineering, 48: pp.1084-1087.

[219] G.P. Tilly, W. Sage, 1970, The interaction of particle and material behaviour in erosion process, Wear, 16, pp. 447-465.

[220] Arjula S., Harsha A.P., Ghosh, M.K., 2008, Erosive wear of unidirectional carbon fibre reinforced polyerherimide composite, Materials letters, 62, pp. 3246-3249.

[221] Srivastava, V.K. and Pawar, A.G., 2006, "Solid particle erosion of glass fiber reinforced fly-ash filled epoxy resin composites", Composites Science and Technology; 66: pp.3021–3028.

[222] Sari, N. and Sinmazcelik, T., 2007, "Erosive wear behaviour of carbon fibre/polyetherimide composites under low particle speed", Materials Design; 28: pp.351–355.

[223] Myers, Raymond H., Khuri, Andre, I. and Carter, Walter H., Jr., 1989, "Response surface methodology: 1966-1988. Technometrics31(2): pp.137-153.

[224] Montgomery, D.C., 2005, "Design and Analysis of Experiments: Response surface method and designs", New Jersey: John Wiley and Sons, Inc.

[225] Sahin, Y. and Motorcu, A.R., 2005, "Surface roughness model for machining mild steel", Mater Des;26: pp.321–326.

[226] Noordin, M.Y., Venkatesh, V.C., Sharif, S., Elting, S. and Abdullah, A., 2004, "Application of response surface methodology in describing the performance of coated carbide tools when turning AISI 1045 steel", J Mater Process Technol.; 145: pp.46–58.

[227] Gunaraj, V. and Murugan, N., 1999, "Application of Response Surface Methodology for Predicting Weld Bead Quality in Submerged Arc Welding of Pipes", Journal of Materials Processing Technology; 88: pp.266-275.

[228] Lin, J. F. and Chou, C.C., 2002, "The Response Surface Method and the Analysis of Mild Oxidational Wear", Tribology International; 35: pp.771-785.

[229] Sagbas, A., Kahraman, F. and Esme, U., 2009, "Modeling and Predicting Abrasive Wear Behaviour Of Poly Oxy Methylenes Using Response Surface Methodolgy and Neural Networks", MetalurgiJa; 48 (2): pp.117-120.

[230] Khuri, A.I. and Cornell, J.A., 1987, "Response Surfaces. Designs and Analyses", Vol. 81 of Statistics, Textbooks and Monographs, Marcel Dekker, Inc. ASQC, New York.

[231] Box, G. and Hunter, J., 1957, “Multi-factor experimental designs for exploring response surfaces”, Ann. Math. Stat.; 21 (1): pp.195–241.

PUBLICATIONS

International Journal:

1. P.Mishra & Dr. S.K.Acharya. “Erosive wear behavior of red mud filled metal matrix composite.” International Journal of Reinforced plastics and Composites, Stanford University, USA, Volume 27, No. 2, Jan. 2008, pp.145-152.

2. P.Mishra & Dr. S.K.Acharya. “Weathering behavior of bagasse fiber reinforced polymer composite.” International Journal of Reinforced plastics and Composites, Stanford University, USA, Volume 27, No. 16-17, Nov. 2008, pp.1839-1846.

3. P.Mishra & Dr. S.K.Acharya. “The influence of fiber treatment on the performance of bagasse fiber reinforced polymer composite.” International Journal of Reinforced plastics and Composites, Stanford University, USA, Volume 28, No. 24, Dec. 2009, pp.3027-3036.

4. P.Mishra & Dr. S.K.Acharya. “Solid particle erosion of bagasse fiber reinforced epoxy composite.” International Journal of Physical Science, Volume 5, No.2, Feb. 2010, pp. 109-115.

5. Mishra Punyapriya and Acharya S.K. “Anisotropy abrasive wear behaviour of bagasse fiber reinforced polymer composite.” International Journal of Engineering, Science and Technology, Volume 2, No. 11, (2010): pp. 104-112.

6. Mishra Punyapriya and Acharya S.K. “Effect of fiber loading on the abrasive wear behaviour of bagasse fiber reinforced epoxy composite.” Journal of Tribology Research, Volume 1, No. 2, 2010. (Accepted for publication)

7. Mishra Punyapriya and Acharya S.K. “Effect of surface treatment on the mechanical properties of bagasse fiber reinforced polymer composite.” Journal of Bioresources. (Accepted for publication).

8. Mishra Punyapriya and Acharya S.K. “Study on dielectric properties of bagasse fiber reinforced epoxy composite.” Journal of Inventy. Vol 2, Issue 1, 2010.

National Journal

1. P.Mishra & Dr. S.K.Acharya. “Effect of environment on the mechanical properties of fly ash – jute – polymer Composite.” Indian Journal of Engineering and Material Science, Volume 15, No. 6, Dec. 2008, pp. 483-488.

International Conferences:

1. P.Mishra & Dr. S.K.Acharya. “The influence of fiber treatment on the performance of bagasse fiber reinforced polymer composite.” 52nd Congress of ISTAM-2007, 14-17 Dec. 2007, BNMIT, Bangalore, CM05, pp.90-91.

2. P.Mishra & Dr. S.K.Acharya. “Investigation on solid particle erosion behavior of bagasse fiber reinforced polymer composite.” ICIT 2008, 6-8 Nov. 2008, Scope convention Center, New Delhi, pp. 64.

3. P.Mishra & Dr. S.K.Acharya. “Erosive wear behavior of bagasse fiber reinforced polymer composite.” ICAT 2008, 3-5 Dec. 2008, NUS, Singapore, pp.109-111.

4. P.Mishra & Dr. S.K.Acharya. “Influence of impingement angle on the solid particle erosion behavior of bagasse fiber reinforced polymer composite.” 53rd Congress of ISTAM-2008, 27-30 Dec. 2008, Osmania University, Hyderabad, pp. 93.

5. P.Mishra & Dr. S.K.Acharya. “Micro structural and mechanical aspects of bagasse fiber reinforced epoxy composites at liquid nitrogen temperature.” 54th Congress of ISTAM-2009, 18-21 Dec. 2009, School of Applied Sciences, Netaji Subhas Institute of Technology, Sector-3, Dwarka, New Delhi, CM22, pp. 90.

6. P.Mishra & Dr. S.K.Acharya. “Effect of surface modification on the mechanical properties of bagasse fiber reinforced polymer composite.” ICRAME-2010, 8 & 9 April 2010, Noorul Islam University, Kanyakumari, pp.390.

7. P.Mishra & Dr. S.K.Acharya. “A study on the potential of bagasse fiber reinforced polymer composite for tribological applications.” ICIT 2010, 2-4 Dec. 2010, RDCIS, Ranchi.

8. P.Mishra & Dr. S.K.Acharya. “Statistical analysis for the abrasive wear behavior of bagasse fiber reinforced polymer composite.” AIML-11, 12-14 April 2011, Dubai.

National conference:

1. P.Mishra & Dr. S.K.Acharya. “Advances in vehicle suspension system.” 48th Technical Annual Session of Orissa State Center, Institute of Engineers (India), Bhubaneswar, 30th Jan 2007, pp.141-147.

2. P.Mishra & Dr. S.K.Acharya. “Weathering behavior of bagasse fiber polymer composite.” NCDC’07, 14-15 April 2007, NIT, Rourkela, pp. 232-240.

3. P.Mishra & Dr. S.K.Acharya. “Petri net- A tool for modeling and simulation in manufacturing system.” 50th Technical Annual Session of Orissa State Center, Institute of Engineers (India), Bhubaneswar, 8th Feb. 2009, pp.150-157.

4. P.Mishra & Dr. S.K.Acharya. “Wear behavior of bagasse fiber reinforced epoxy composites.” Technologia 2010, 24-25 Feb. 2010, MPCCET, Bhillai, C.G.

5. P.Mishra & Dr. S.K.Acharya. “Erosive wear of randomly distributed bagasse fiber reinforced polymer composite.” MR10, 7-8 May 2010, IIT, Bombay, pp.140.

BIBLIOGRAPHY

Mrs. Punyapriya Mishra is a faculty member in the Department of Mechanical Engineering, Veer Surendra Sai University of Technology, Burla, Orissa, India-768017. She did M.Tech. in Production Engineering from NIT, Rourkela. This dissertation is being submitted for the fulfillment of the Ph.D. degree. The contact address is:

Punyapriya Mishra
Department of Mechanical Engineering
Veer Surendra Sai University of Technology
Burla, Orissa, India-768017

C/O- Ar. Nihar Ranjan Debata
Main Road, Salipur
Cuttack – 754202
Ph.-09438436223
E-mail: priya.punya@gmail.com